SEDIMENT TRANSPORT IN PRISMATIC AND NONPRISMATIC CHANNELS

A Thesis Submitted

in Partial Fulfilment of the Requirements for the

Degree of

DOCTOR OF PHILOSOPHY

in

CIVIL ENGINEERING

by

VIJAY KAUSHIK

(Roll No.: 2K20/PHDCE/01)

Under the supervision of

PROF. VIJAY K. MINOCHA

Delhi Technological University

Department of Civil Engineering

DELHI TECHNOLOGICAL UNIVERSITY

(Formerly Delhi College of Engineering)

Shahbad Daulatpur, Main Bawana Road, Delhi-110042, India

February, 2025

ACKNOWLEDGEMENT

I would like to convey my gratitude to the individuals who have provided the greatest assistance to me during my research endeavours. I would like to express my sincere gratitude to my thesis advisor, Prof. Vijay K. Minocha, and Prof. Munendra Kumar, Professor in the Department of Civil Engineering at Delhi Technological University. Their unwavering patience, consistent encouragement, guidance, and support have been invaluable throughout this research journey. Without their assistance, the successful completion of this work would not have been achievable. Association with such supervisors and acquiring insights from their knowledge has been a privilege. I would like to express my gratitude to Dr. Bandita Naik, Professor in the Department of Civil Engineering at Methodist College of Engineering, Hyderabad, for her essential support during my research journey. I would like to express my profound appreciation to Mr. Anil Agnihotri, a laboratory technician, and Nitesh, a laboratory attendant, from the Department of Civil Engineering, for their invaluable assistance. I would like to extend my appreciation to my colleagues Saurabh Pujari, Rahul Kumar, Shailesh Kumar Gupta, Deepak Sharma, Rishabh Tyagi, and Dharmender Kumar for their assistance throughout my experimental work and their amicable discussions at various stages of the research endeavour. I would like to express my gratitude to my seniors, Dr. Sushant Kumar, Dr. Deepak Singh, Dr. Geeta Devi, Dr. Rahul Kumar Meena, Dr. Parvesh Kumar, Dr. Dinesh Kumar Reddy, and Dr. Inderjeet Singh, for their invaluable guidance, meticulous planning, valuable advice, and cooperative assistance throughout the different phases of this research.

I would like to express my profound thanks to Prof. K. C. Tiwari, the Head of the Civil Engineering Department, as well as all the faculty members for their invaluable assistance, useful suggestions, and kind collaboration throughout the research. Ultimately, I want to convey my deep affection and gratitude to my family for their unwavering encouragement and support, as they served as a steadfast pillar and a source of continuous inspiration over the years. Each of my family members has shown remarkable patience during this process and willingly given up their due time with a joyful attitude. Upon the completion of my Ph.D. study, I would like to express my gratitude to all those individuals who provided assistance, support, and encouragement during my research endeavour.

DELHI TECHNOLOGICAL UNIVERSITY
(Formerly Delhi College of Engineering)
Shahbad Daulatpur, Main Bawana Road, Delhi-42

CANDIDATE'S DECLARATION

I **Vijay Kaushik** hereby certify that the work which is being presented in the thesis entitled **Sediment transport in prismatic and nonprismatic channels** in partial fulfillment of the requirements for the award of the Degree of Doctor of Philosophy, submitted in the Department of **Civil Engineering**, Delhi Technological University is an authentic record of my own work carried out initially during the period from **25/08/2020** to **15/02/2024** under the supervision of **Prof. Munendra Kumar** and afterwards from **16/02/2024** under the supervision of **Prof. Vijay K. Minocha**.

The matter presented in the thesis has not been submitted by me for the award of any other degree of this or any other Institute.

Candidate's Signature

This is to certify that the student has incorporated all the corrections suggested by the examiners in the thesis and the statement made by the candidate is correct to the best of our knowledge.

Signature of Supervisor   **Signature of External Examiner**

DELHI TECHNOLOGICAL UNIVERSITY
(Formerly Delhi College of Engineering)
Shahbad Daulatpur, Main Bawana Road, Delhi-42

<u>CERTIFICATE BY THE SUPERVISOR(s)</u>

Certified that **<u>Vijay Kaushik</u>** (2K20/PHDCE/01) has carried out their search work presented in this thesis entitled **"<u>Sediment transport in prismatic and nonprismatic channels</u>"** for the award of **<u>Doctor of Philosophy</u>** from Department of Civil Engineering, Delhi Technological University, Delhi, under my supervision w.e.f. 16/02/2024, and prior to that supervised by Prof. Munendra Kumar. The thesis embodies results of original work, and studies are carried out by the student himself and the contents of the thesis do not form the basis for the award of any other degree to the candidate or to anybody else from this or any other University/Institution.

Signature

(**Prof. Vijay K. Minocha**)

(Professor)

(Department of Civil Engineering, DTU)

Date:

ABSTRACT

Understanding the hydraulic aspects of prismatic and nonprismatic reaches of a river channel are important for the design of flood control measures and channel improvement works. The floodplain geometry of a river system may alter over its length due to agricultural and development activities. This can result in the formation of a compound channel, which can either be converging or diverging. Obtaining precise and thorough field measurements in natural rivers under flood flow conditions is challenging. Hence, conducting laboratory experiments is crucial for enhancing the understanding of the flow dynamics in compound channels that include prismatic and nonprismatic floodplains. The investigation was carried out on a nonprismatic compound channel that consisted of a prismatic section followed by a converging section. The research examined five distinct relative flow depths (β), including 0.20, 0.30, 0.40, 0.50, and 0.60. Relative flow depth (β) is a dimensionless parameter and it is defined as the ratio of the overbank flow depth to the total flow depth. As the relative flow depth increases, a larger proportion of the water is found above the main channel, which can significantly affect the flow dynamics. The study conducted experiments on the following four different types of nonprismatic compound channels in a masonry flume: (i) a compound channel with smooth converging floodplains, (ii) a compound channel with rough converging floodplains, (iii) a compound channel with sediment in the main channel and smooth converging floodplains, (iv) a compound channel with sediment in the main channel and rough converging floodplains. The study examines different flow characteristics, including the stage-discharge relationship, the water surface profile, the energy slope, the flow resistance, the distribution of average velocity along the channel length, the depth-averaged velocity distribution at different sections, the boundary shear stress distribution, the rate of sediment transport, and the longitudinal bed profile. These characteristics are analyzed in both prismatic and nonprismatic sections of compound channels. In addition to the experimental investigation, the flow rate in nonprismatic compound channels was anticipated using the Gene Expression Programming (GEP) soft computing approach, based on geometric and flow variables.

The experimental findings revealed that the relationship between stage and discharge follows a power law in smooth and rough floodplains, both with and without sediment, respectively. In compound channels with rough floodplains, the water surface profile decreases as compared to smooth floodplains, due to head loss resulting from converging geometry and rough floodplains. The energy slope is nearly uniform in prismatic sections, whereas it rises in nonprismatic sections. The nonprismatic compound channel with rough floodplains experiences lower velocities, decreasing by up to 5.5% and 16% compared to the nonprismatic compound channel with smooth floodplains, without and with sediment, respectively. Shear stress is significantly higher in nonprismatic compound channels with rough floodplains, increasing by up to 70% and 94% compared to smooth floodplains, without and with sediment, respectively. Additionally, sediment transport rates are up to 10% higher in nonprismatic compound channels with smooth floodplains than in those with rough floodplains. The longitudinal bed profile of nonprismatic compound channels falls within the ripples and dunes category. Sediment deposition occurs in the first half of the converging section, while sediment degradation takes place in the latter half. Manning's roughness coefficient decreases with increasing longitudinal distance in compound channels with smooth and rough floodplains, without sediment, due to flow acceleration caused by the converging channel geometry. Conversely, in sediment-laden compound channels with smooth and rough floodplains, Manning's roughness coefficient increases along the longitudinal distance due to additional resistance from sediment transport. The roughness coefficient in nonprismatic compound channels with rough floodplains is up to 7% higher in the absence of sediment and up to 20% higher in sediment-laden conditions compared to smooth floodplains.

Using GEP, discharge models were developed based on the experimental dataset from this study and validated with data from previous research. Statistical analysis assured that the proposed GEP model (M7), which incorporates factors such as width ratio, relative flow depth, converging angle, relative distance, Froude number, Manning's roughness coefficient, and floodplain shear force, outperforms other GEP models, theoretical approaches, and existing methodologies for predicting discharge in nonprismatic compound channels. The model demonstrates superior performance across various statistical measures (R^2 = 0.990, RMSE = 0.094, MAPE = 3.511, SI = 0.043, AIC = -632.347). Furthermore, the study proposed a unique equation derived through GEP for predicting discharge in nonprismatic compound channels. The effectiveness of this

equation was validated using real-world data from the River Main in Northern Ireland. Statistical evaluation (R^2 = 0.959, RMSE = 2.633, MAE = 2.337, MAPE = 10.467) assures the reliability of the proposed GEP-based equation for forecasting discharge in nonprismatic river systems.

LIST OF PUBLICATIONS

❖ Kaushik, V., and M. Kumar. 2023. "Sustainable gene expression programming model for shear stress prediction in nonprismatic compound channels." *Sustainable Energy Technologies and Assessments*, 57: 103229. (IF: 7.1)
https://doi.org/10.1016/j.seta.2023.103229

❖ Kaushik, V., and M. Kumar. 2023. "Assessment of water surface profile in nonprismatic compound channels using machine learning techniques." *Water Supply*, 23 (1): 356–378. (IF: 1.9)
https://doi.org/10.2166/ws.2022.430

❖ Kaushik, V., and M. Kumar. 2024. "Prediction of shear stress distribution in compound channel with smooth converging floodplains." *Journal of Hydrology and Hydromechanics*, 72 (2): 170–184. (IF: 2.3)
https://doi.org/10.2478/johh-2024-0004

❖ Naik, B., V. Kaushik, and M. Kumar. 2022. "Water surface profile in converging compound channel using gene expression programming." *Water Supply*, 22 (5): 5221–5236. (IF: 1.9)
https://doi.org/10.2166/ws.2022.172

❖ Kaushik, V., M. Kumar, B. Naik, and A. Parsaie. 2023. "Modeling of water surface profile in non-prismatic compound channels." *Water Practice and Technology*, 18 (9): 2151–2167. (IF: 1.6)
https://doi.org/10.2166/wpt.2023.142

❖ Kaushik, V., B. Naik, M. Kumar, and V. K. Minocha. 2024. "Prediction of the flow resistance in non-prismatic compound channels." *Water Practice and Technology*, 19 (5): 1822–1835. (IF: 1.6)
https://doi.org/10.2166/wpt.2024.117

❖ Kaushik, V., M. Kumar, and B. Naik. 2024. "Numerical Simulation of Flow Characteristics in Nonprismatic Compound Channels." *Water Practice and Technology*, 19 (7): 2532–2550. (IF: 1.6)
https://doi.org/10.2166/wpt.2024.153

❖ Kaushik, V., and M. Kumar. 2023. "Water surface profile prediction in non-prismatic compound channel using support vector machine (SVM)." *AI In Civil Engineering*, 2 (1).

https://doi.org/10.1007/s43503-023-00015-1

❖ Kumar, R., V. Kaushik, and M. Kumar. 2023. "Application of Gene Expression Programming in Computation of Flow Resistance in Compound Channel with Converging Floodplains." *Civil Engineering and Architecture*, 11 (5): 2719–2730. https://doi.org/10.13189/cea.2023.110535

❖ Kaushik, V., and M. Kumar. 2024a. "A Review of Different Approaches for Boundary Shear Stress Assessment in Prismatic Channels." *Lecture Notes in Civil Engineering*, 117–129. https://doi.org/10.1007/978-981-99-3557-4_10

International Conferences

❖ Kaushik, V., and M. Kumar. "Water Surface Profile Prediction in Nonprismatic Compound Channels Using Support Vector Machine (SVM)." *International Conference on Advances in Civil Engineering*, held on 20-22 December 2022, organized by Technology Research and Innovation Centre, India and hosted by LSKBJ College of Engineering, Chanwad, Nashik, India.

❖ Kaushik, V., and M. Kumar. "A Review of Different Approaches for Boundary Shear Stress Assessment in Prismatic Channels." *1st International Conference on Innovations in Smart and Sustainable Infrastructure (ISSI-2022)*, held on 23-25 August 2022, organized by Civil Engineering Department, School of Technology, Pandit Deendayal Energy University, Gandhinagar, India.

❖ Kaushik, V., M. Kumar, and B. Naik. "A Review on Bed Morphology in Compound Channels: Processes, Patterns, and Implications." *28th International Conference on Hydraulics, Water Resources, River and Coastal Engineering (HYDRO 2023 International)*, held on 21st to 23rd December 2023, organized by Department of Civil Engineering, National Institute of Technology, Warangal, India.

TABLE OF CONTENTS

LIST OF TABLES

LIST OF FIGURES

LIST OF SYMBOLS

B = total width of compound channel

b = width of the main channel

h = height of the main channel

H = flow depth

α = width ratio (B/b)

β = relative flow depth [(H – h)/H]

γ = differential roughness (n_{fp}/n_{mc})

δ = aspect ratio (b/h)

θ = converging angle

X_r = relative distance (x/L)

L = converging length

x = distance between two consecutive sections

D_{50} = mean bed size

S_o = longitudinal bed slope

S_e = energy slope

Q_r = discharge ratio (Q/Q_b)

Q = discharge at any depth

Q_b = bankfull discharge

F_r = Froude number

R_e = Reynolds number

n = Manning's roughness coefficient

S_{fp} = floodplain shear force

f = Darcy-Weisbach friction factor

λ = eddy viscosity

Γ = secondary flow

C = Chezy's coefficient

Q_{th} = theoretical discharge

Q_a = actual discharge

C_d = coefficient of discharge for the triangular notch

θ = crest angle of the triangular notch

H_c = head over the crest of the notch

U_d = depth-averaged velocity

u_i, U, v = point longitudinal velocity

Δh_i = depth associated with the local velocity

E = energy at any section

V or V_{avg} = average velocity of cross section

Δp = pressure difference

ρ = density of water

A = flow area

ΔA = flow area associated to point longitudinal velocity

E_L = energy loss

l = distance between two sections

R = hydraulic radius

g = acceleration due to gravity

α^* = kinetic energy correction factor

τ_b = boundary shear stress

τ_o = bed shear stress

d = external diameter of the pitot-static tube

ν = kinematic viscosity of the liquid

x^*, y^* = non-dimensional parameters

G_s = sediment transport rate

q = amount of sediment collected

t = duration of sediment collection

a = actual values

p = predicted values

$\bar{a}$ = mean of actual values

$\bar{p}$ = mean of predicted values

N = number of datasets

k = number of variables

A_{mc} = main channel flow area

A_{fp} = floodplain flow area

P_{mc} = wetted perimeter of main channel

P_{fp} = wetted perimeter of floodplain

n_{mc} = Manning's roughness coefficient of main channel

n_{fp} = Manning's roughness coefficient of floodplain

X_{mc} = proportionate length of interface to be included in main channel perimeter

X_{fp} = proportionate length of interface to be excluded in floodplain perimeter

LIST OF ABBREVIATIONS

1D = one dimensional

2D = two dimensional

3D = three dimensional

DCM = Divided channel method

LES = Large eddy simulation

UK = United Kingdom

FCF = Flood channel facility

PTV = Particle tracking velocimetry

RANS = Reynolds-averaged Navier-Stokes model

EDM = Exchange discharge model

CFD = Computational fluid dynamics

SKM = Shiono Knight method

ANN = Artificial neural networks

FFBP = Feed forward back-propagation

COHM = Coherence method

SCM = Single channel method

MDCM = Modified divided channel method

ANFIS = Adaptive network fuzzy interference system

TKE = Turbulent kinetic energy

RBF = Radian basis neural network

MLP = Multilayer perceptron

ECM = Energy concept method

WDCM = Weighted divided channel method

BPNN = Back-propagation neural network

GEP = Gene expression programming

CCNPF = Compound open channels with nonprismatic floodplains

MARS = Multivariate adaptive regression splines

GMDH-NN = Group method of data handling neural network

MLPNN = Multilayer perceptron neural networks

RSS = Reynolds shear stress

AIM = Anisotropic invariant map

SVM = Support vector machines

NF-GMDH = Neuro-fuzzy group method of data handling

LDA = Laser doppler anemometer

DPM = Discrete phase model

ML = Machine learning

PS = Prismatic section

NPS = Nonprismatic sections

ADV = Acoustic doppler velocimeter

SNR = Sound to noise ratio

ET = Expression tree

HDCM = Horizontal divided channel method

VDCM = Vertical divided channel method

DDCM = Diagonal divided channel method

GEA = Gene expression algorithm

CHAPTER 1

INTRODUCTION

1.1 General

Overbank flows are extremely recurrent as well as expensive catastrophes resulting from worldwide climate alterations. Over the last several decades, there has been a substantial rise in the frequency of recorded floods, with an average annual increase of 7.4% (Scheuren et al. 2008). Rivers have emerged as a significant cause of disputes worldwide due to the scarcity of accessible freshwater supplies (Cunge and Erlich 1999). To ensure the continued survival of increasing numbers of people around the globe, it is essential to efficiently regulate the limited water resources that waterways furnish. The aforementioned concerns possess the main impetus for investigating and comprehending the various phenomena associated with streams in overbank flow conditions.

Throughout history, several advanced human societies have emerged in close proximity to rivers due to the presence of floodplains. These floodplains have enticed humanity with their potential for agriculture, transportation, domestic usage, irrigation, industrial activities, and renewable energy sources. Due to population pressure over the last centuries and the subsequent rise in river use, bigger towns have emerged on river floodplains and coastal areas. Currently, over half of the global population resides within a 65 km radius of coastal areas, and over 65% of all cities are located directly on the shore. The trend of urban migration is expected to rise, and in some nations, individuals have little alternative but to reside in vulnerable regions (Knight and Shamseldin 2005). Consequently, the occurrence of floods has resulted in a rise in both human casualties and financial burdens. There are primarily two causes that might lead to flooding. Artificial causes, which include things like failure of dams, bank embankment plummets, riverbank contravention, alterations to the utilization of land, and insufficient management of trash, are the first aspects to consider. The additional aspect is natural causes, which includes precipitation, landslides, storm surges, rising groundwater levels, and warming temperatures. Fluvial flooding, urban flooding, and coastal flooding are the three kinds of inundation that may be distinguished from one another. In the event that a river's depth is greater than its bankfull level, flooding might occur. The insufficient drainage that happens via metropolitan waterways and pipeline infrastructure is often the trigger of floods in metropolitan areas. In the event that coastal barriers are breached,

high tide levels are achieved, and breakwaters are damaged as a result of abnormal wave conditions, flooding along the coast will occur. The collection of flood data and the use of flow modeling are crucial for the advancement of civilization. In order to forecast, regulate, and optimize the use of rivers and open channels, it is often necessary to evaluate several flow characteristics in a laboratory setting. As a result, models should be created that can predict floods and analyze the movement of water in a river. These models should capable of predicting both in-bank and overbank flow situations, as well as analyzing both prismatic and nonprismatic parts of a real river stream.

1.2 Flow in compound channels

A channel that maintains a consistent cross-sectional form, size, and bottom slope is referred to as a prismatic channel. The majority of artificial channels are prismatic channels that extend across large distances. The rectangle, trapezoid, triangle, and circle are often used geometric forms in artificial conduits. Most natural channels have different cross-sections, making them nonprismatic. A compound channel is a channel configuration consisting of a primary deep segment plus one or two floodplains that accommodate high-volume water flows. The primary conduit transports the arid weather discharge, and during the rainy season, the discharge may overflow the boundaries of the primary conduit into the neighboring floodplains. The bulk of natural rivers have compound portions. A compound section is sometimes referred to as a composite or complex or two-stage channel. Both the primary waterway and the area of flooding have considerably different hydraulic attributes, especially with regard to the form of the waterway and the degree of roughness of the channel topography. In many cases, the floodplains have roughness traits that are far more extensive and varied. It is essential to take into consideration these aspects in order to solve environmentally conscious, and engineering issues. Because of this, it is of the utmost importance to investigate the behavior of flow in rivers when they are experiencing overbank flow scenarios. This is because there is a substantial variation in velocity between the primary stream channel and flood zones.

The flow in the compound channel under the condition of water flowing in both the main and floodplains is inherently complex. The velocity of flow in the floodplain is reduced compared to the main channel owing to the relatively shallower water depth and increased bed roughness. The primary flow in the channel will interact with the flow in the floodplains, resulting in significant momentum exchange at the interface.

Additionally, there will be intricate interaction with the boundaries at the junction, resulting in the formation of many sets of vortices that cause the development of turbulence. The interconnections between the main channel flow and the floodplain flows are quite intricate. Fig. 1.1 depicts a conceptual representation of the interaction situation. This graphic illustrates many noteworthy flow characteristics occurring at the confluence of the main and flood bank flows. The existence of swirling forms at the junction of the primary waterway and the flood zone is one of the most important aspects. These structures have a vertical axis that extends up to the water surface. This vortex set is thought to be accountable for the transfer of momentum between the primary and shallow water currents. Furthermore, the channel segment exhibits helical secondary flows in the longitudinal stream direction at different corners. The secondary flows exhibit varying directions at various corners and have a role in altering the boundary shear stress.

During a flood, when the flow exceeds the normal channel capacity, there is a notable escalation in the intricacy of flow dynamics, even in straight sections of the river. The disparity in speed between the primary channel and the floodplain flows may create powerful lateral shear layers, resulting in the formation of extensive turbulent patterns, namely massive planform vortices, as shown by Sellin (1964), Ikeda et al. (2001), and Bousmar and Zech (2002). In order to effectively regulate flooding, one of the most important responsibilities of a stream scientist is to make predictions about the stage-discharge relationships. When the two-stage waterway flow exceeds its usual limitations, the capacity of the waterway to convey water is affected by the transfer of momentum between its primary path and flooded areas that are located in the vicinity. One of the effects of the momentum shift at the interface is that it reduces the capacity of the primary channel to transport water while simultaneously enhancing the capacity of the floodplain for releasing water, particularly in situations when the depth of flow is low. The momentum shift causes energy redistribution, slowing flow in the main channel while increasing velocity in the floodplain, enhancing its water-carrying capacity. As a result, the overall ability of the entire channel to carry water is reduced. The intricacy of the issue is further heightened by addressing a compound channel with nonprismatic floodplains, sometimes referred to as a nonprismatic compound channel. Nonprismatic floodplains may take the form of converging, diverging, or skew types. In a compound channel with converging floodplains, the narrowing of the floodplain geometry causes water on the floodplain to flow over water in the primary waterway. This leads to more contact and exchange of momentum between the two flows. The additional transfer of

momentum should also be taken into account when modeling the flow. The hydraulic characteristics of two-stage channels, which include prismatic and nonprismatic floodplains, play an important part in the process of flood prediction in streams as well as the creation of overflow protection methods and diversion channels that are both economical. For the purpose of gaining a better knowledge of the mechanics of compound channel flow with prismatic and nonprismatic floodplains, it is necessary to conduct investigations in both the field and the laboratory. Nevertheless, it is difficult to get adequately precise and all-encompassing field data in natural rivers during periods of high-water flow. In order to get a better understanding of the influence that overbank flows have on hydraulic behavior in the composite waterway, it is necessary to carry out laboratory experiments. This is true for both prismatic and nonprismatic flood zones. Establishing the correlation between the depth of the water and the flow rate in prismatic compound channels has been accomplished via the development of a number of different methods. These include a 1D model created by Ackers (1991, 1992), which utilizes a large-scale FCF at HR Wallingford, and a 2D model developed by Shiono and Knight (1988) that is based on an analytical solution of the depth-averaged Navier-Stokes equations. Nevertheless, these approaches were primarily designed to simulate consistent flow in prismatic compound channels and proved to be ineffective in accurately predicting flow behavior in nonprismatic compound channels. This study investigates flow characteristics in nonprismatic compound channels with converging floodplains and formulates predictive flow models for application in such channel configurations.
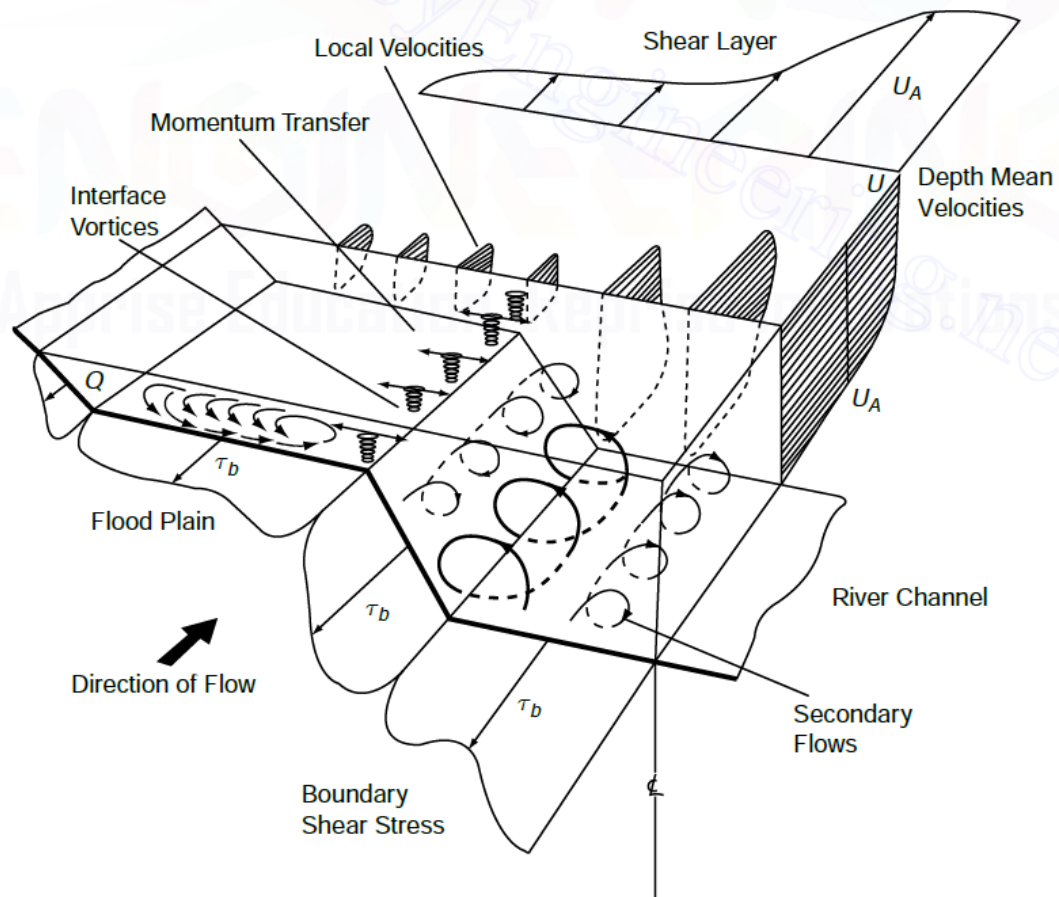
Fig. 1.1 Conceptual model of interaction of flows in flood bank and main channel (Subramanya 2015)

1.3 Sediment transport

The accumulation of sediment has wide-ranging effects on several environmental factors, including soil erosion, water quality, water supply, flood management, river regulation, reservoir longevity, groundwater levels, irrigation, navigation, fishing, and tourism. As a result, it has garnered growing interest from both the general public and engineers. Erosion of the soil in an area of rivers is a major contributor to the deterioration of the natural environment, as well as the decrease in the production of crops. Furthermore, it permanently renders farmland unproductive by diminishing the fertility and productivity of the soil. Moreover, the accumulation of silt in river systems causes an increase in the water level during flood events. Consequently, it gives rise to a range of biological and environmental issues and exacerbates flood catastrophes, both via the floodwaters themselves and the silt they transport. Conversely, the act of scouring river channels results in a decrease in water level, leading to issues with water supply and transportation, as well as posing a danger to the safety of river training structures.

Sediment in water has dual impacts on water quality and the ecosystem, which are diametrically opposed. One benefit of sediment particles in water, particularly the smaller ones, is their ability to absorb certain contaminants, so enhancing water quality to some extent. However, sediment also serves as the primary contaminant, a carrier, and an accumulation of other harmful substances. These substances include pesticides, leftovers, assimilated phosphate and nitrogen, organic compounds, pathogenic microbes, and infections. It has an impact on the purity, clarity, and quality of water. Sediment transport in compound channels pertains to the transportation of various types of sediment (such as sand, silt, and gravel) inside river channels that have a complicated shape. Compound channels are influenced by many crucial elements that affect sediment flow: (WMO 2003)

- Flow Distribution: The existence of several channels in a complex system results in fluctuations in the speed and depth of flow. A substantial influence on the movement of particles is exerted by the arrangement of flow among the primary waterway and flooding zones. This, in turn, has an effect on the patterns of sediment deposition and erosion.

- Channel morphology: It refers to the form and geometry of the compound channel, which has a significant impact on sediment movement. Diverse flow patterns and sediment transport dynamics may be influenced by the presence of ripples, dunes, bars, and other objects.

- Sediment Characteristics: The composition, dimensions, and arrangement of sediment particles in the compound channel have an impact on their transportation. Large particles tend to settle faster, whereas little particles might be transported over longer distances downstream.

- Hydraulic interactions: These refer to the interactions of primary waterway flow and flow in neighboring floodplain regions. These interactions may result in intricate patterns of sediment movement. Flow interchange between the main channel and floodplains may lead to silt accumulation during periods of low flow and erosion during periods of strong flow.

- Vegetation Impact: Vegetation in floodplain regions may influence sediment transport by altering flow patterns, stabilizing banks, and facilitating sediment entrapment. Vegetation may serve as either a stabilizing or destabilizing element, depending on its density and qualities.

1.3.1 River sediment and flood disasters

The relationship between river sediment and flood catastrophes is intricately intertwined, as the transportation of sediment plays a crucial role in the functioning of river systems and may amplify the intensity of flood occurrences. Rivers inherently transport silt downstream as an inherent aspect of their natural cycles. The sediment consists of various particle sizes, ranging from small silt to larger sand and gravel. Sediment movement is affected by variables such as the speed of the flow, the shape of the channel, and the properties of the sediment. Rivers have heightened flow rates during floods, which may augment their ability to move materials, resulting in elevated sediment loads. During flood occurrences, rivers may undergo augmented sediment deposition as a result of the heightened flow velocities. This might result in aggradation, a phenomenon in which sediments gradually build on the riverbed, causing an increase in the height of the bed. Aggradation diminishes the channel's capacity to transport water, thereby increasing the likelihood of flooding by limiting the river's capability to handle larger amounts of flow. Severe floods may cause substantial changes to the physical structure of river systems. Sediment accumulation may modify the form and measurements of the channel, impacting its capacity to effectively transport water in future flood occurrences. Alterations in the physical shape of a channel may result in channel avulsion, which is when a river changes its path. This has the potential to create hazards for both infrastructure and communities situated beside the riverbanks. Riverbank erosion may be caused by an excessive amount of silt carried by floods. The erosion of riverbanks by water containing silt may undermine the stability of nearby infrastructure such as buildings, roads, and bridges. Riverbank erosion may further result in the expansion of the river channel, therefore exerting a greater impact on flood dynamics. The deposition of sediment on floodplains during floods may impact the operation of agricultural fields, urban areas, and natural ecosystems located on or near the floodplains. Although a certain amount of sediment deposition is normal and may enhance the fertility of the soil, an excessive amount of sedimentation might impede the floodplain's capacity to absorb and disperse floods.

As a consequence of the enormous subsidence of soil that occurs in the river basin, a huge quantity of silt is introduced into the Yellow River and accumulates in the lower portions of the river. The height of the stream's bed rises by about five to ten centimeters per year as a direct consequence of this. Zhengzhou City, which serves as the capital of

Henan Province, is located on an elevated river bed in comparison to the topography that surrounds it, which results in the formation of a river that is referred to as a suspended river. The watersheds of the Haihe and Huaihe Rivers are separated by the river pathway, which serves as the boundary between them. The floods would have the greatest possible effect on a region that is 250,000 km^2 in size, stretching from the north of Tianjin City to the south of the Huaihe River, in the event that the waterway barriers in the lower reaches were to fail. Within China, this region is considered to be among the most economically prosperous regions. According to estimates, the greatest population that might be affected by floods is around 100 million individuals.

1.3.2 Conveyance capacity of rivers

The deposits of silt and the erosion that occurs inside the stream channel both contribute to the fluctuation of a river's ability to convey water. An intricate waterway channel configuration may be seen in the Lower Yellow River. This arrangement includes a principal channel as well as floodplains, and the overall width of the river can range anywhere from 10 to 20 km. The areas subject to flooding are inhabited by approximately 1.5 million people, while the cultivated farmlands span an area that is equivalent to 0.22 million hectares. With 85% of the sediment being deposited in the principal pathway, the intermediate and low floods are purposefully kept to the primary waterways rather than the secondary waterways. Hence, the capacity of the primary waterway diminishes considerably, a phenomenon referred to as river channel shrinkage. The flow areas of the primary waterway of the Lower Yellow River saw a drop of about 27% from May 1986 to May 1994. This decline occurred over 36 cross-sections of the river's course. The amount of water that is present underneath the flow output of 3000 m^3/s rises by 0.12 to 0.15 m after each year. In order to reduce the bankfull discharge, the range was reduced to between 2800 and 3700 m^3/s. There has been a substantial rise in the frequency of flow events over floodplains in recent years. In 1996, the flood flow at Huayuankou Station in Zhengzhou City was only 7860 m^3/s, much lower than the 22300 m^3/s recorded in 1958. However, the flood level reached a height of 94.73 m, the highest ever recorded, which was 0.91 m higher than the flood stage in 1958. The flooded area in the floodplain covered around 250,000 hectares, impacting a total of 1.07 million people. The precise amount of the loss was around US$ 800 million.

1.3.3 Fluvial process and channel instability

The fluvial events happen in both horizontal and vertical perspectives, and they have a significant influence on the behavior and equilibrium of rivers. This is especially true for large rivers, which play significant roles in the long-term growth of a nation's economy, ecology, and environment. It's possible that fluvial processes might either lead to or aggravate disasters. An important illustration of this is the flood that occurred in China's Middle Yangtze River in the year 1998. Rivers and lakes come together to create a river-lake system in the middle portions of the Yangtze River. These sections include the Jinjiang River, which is often referred to as the Middle Yangtze River, as well as Dongting Lake and other lakes. During periods of flooding, a portion of the water is sent to Dongting Lake via three interconnected river channels, which helps to reduce the amount of floodwater flowing through the Jinjiang River channel at its height. Nevertheless, the ability of the channels to transport materials has greatly diminished as a result of silt accumulation in the downstream sections of the three interconnected channels. In the past, the Lower Jinjiang River had the features of a conventional meander river, which included a total of twelve curves that were very noticeable. Both Zhongzhouzi and Shangchewan were purposefully divided from one another in the years 1967 and 1969, respectively, but Shatanzi was organically differentiated. As a result of the stream's three turns, the length of the river was reduced by 81 km in the year 1972. As a direct result of this, the slope of the bed, the discharge, and the capacity to convey debris also experienced a surge. This resulted in a drop in the percentage of flow entering Dongting Lake in comparison to the amount of flow that was still present in the primary waterway, which ultimately triggered the Lower Jinjiang River degradation.

The eroded silt deposits traveled downstream from Luoshan to Wuhan City and prompted a rise in the flood level therein. This occurred as a consequence of the aforementioned. In the flood of 1931, Dongting Lake received 50.4% of the highest amount of water flow, which was 66700 m^3/s, from the three rivers that link to it. Out of this, 28.4%, equivalent to 18970 m^3/s, was contributed by the Ouchi River. In 1998, the Ouchi River provided a discharge of just 6000 m^3/s, which accounted for 10% of the overall peak flow. The yearly flow volume given to Dongting Lake between 1951 and 1958 was 146 billion m^3. However, there was a decline in the amount of water to 69.7 billion m^3 from 1981 to 1994. This resulted in an increase of 76.3 billion m^3 of water flowing through Lower Jinjiang, which considerably worsened flood catastrophes. In spite of the fact that the

peak flood in 1998 was 61500 m^3/s, which was lower than the peak flood in 1954, which was 66800 m^3/s, the overbank flow heights at the stations in the intermediate reaches were the greatest they have ever been registered. The size and storage capacity of Dongting Lake has drastically decreased due to the accumulation of silt and the conversion of the lake into farmland to accommodate the growing population. This significantly diminishes its regulating function during periods of flooding in the Yangtze River. The flow rate shifted to the storage zones while flooding occurred in the year 1998 was just about 10 billion m^3, but in 1954 it was 102.3 million m^3. One significant factor contributed to the record high stage of the 1998 floods.

1.3.4 Safety of training works

When compared to the flow velocity upstream and downstream, the flow velocity may be greater in the area of training constructions such as bridges, grooves, levees, embankments, etc. associated with training. Specifically, this is due to the fact that the geometry of the structures narrows the flow's width, which ultimately results in a surge in velocity. As a consequence of this, the erosion of streams in close proximity to structures is a common occurrence that might potentially endanger the protection of the structures as well as the operations that are being trained. In addition, fatalities may occur if the expected washout is not precise throughout the conceptualization stage of the project.

1.3.5 Sediment deposits by floods

Floods exhibit significantly elevated silt concentrations compared to anticipated water flows. Hence, assessments of flood damage should include the ecological degradation caused by silt accumulation and the substantial expenses associated with its removal. Flooding has resulted in the formation of close to forty alluvial fans along the two banks of the Yellow River. The fans' sediment contains a significant proportion of tiny particles that are very susceptible to wind erosion. As a result, certain locations lose their certification. In August 1982, around 400 million m^3 of floodwater were sent to the Dongping detention basin, while roughly 5 million m^3 of material, mostly consisting of sand, were held back. As a result, a total of 425 hectares of agricultural land were destroyed due to the accumulation of silt.

1.3.6 Variation of groundwater levels

It is primarily because of the deposition of silt in the waterways that the flow elevations in the stream have increased. The recharge of river water into the groundwater in nearby regions may lead to an increase in groundwater levels along the river banks, which may result in the occurrence of farming salinity or other environmental issues. The water level in the Lower Yellow River often exceeds the surrounding land surface by a vertical distance of 3 to 5 m. Approximately 49,800 tons of salt are yearly replenished into the groundwater via the lateral filtration of river flow. The groundwater level reaches 0.6 to 0.7 m at a distance of 0.5 km from the river channel, leading to significant salt issues in the adjacent river regions.

1.4 Objectives of the study

The use of experimental and computational analysis is the principal means by which this study intends to accomplish its primary purpose, which is to acquire insight into the flow features in nonprismatic two-stage channels with converging floodplains. The aims of this research are:

- ❖ To study the flow characteristics in nonprismatic compound channels.
- ❖ To study the effect of sediment transport in nonprismatic compound channels.
- ❖ To analyze the effect of floodplain roughness on flow resistance in nonprismatic compound channels.
- ❖ To optimize the flow rate in nonprismatic compound channels with the help of a soft computing method (Gene Expression Programming).

1.5 Organization of the thesis

This thesis has five chapters, one of which is the introduction chapter. Chapter II provides a comprehensive analysis of pertinent literature that discusses the flow dynamics and sediment transport in two-stage channels with prismatic and nonprismatic floodplains. Chapter III provides a comprehensive account of the experimental setup and process for the compound channel, as well as the methods used for the analysis. Chapter IV provides an examination and discourse on the outcomes derived from experimental and computational investigations. The last chapter includes the synopsis and deductions of the investigation. Chapter V also contains the suggestions for further research.

CHAPTER 2

REVIEW OF LITERATURE

2.1 General

This study is dedicated to a thorough examination of the existing literature that discusses different features of prismatic and nonprismatic composite waterways. The subsequent sections delineate the previous research conducted in the domain of flow and sediment transport in composite channels, including both prismatic and nonprismatic planforms. The literature study was conducted with consideration for the purpose and goals of the current research. An attempt was made to analyze and examine the research conducted by previous scholars on different topics, such as the velocity distribution and distribution of wall tractive stresses in waterways with various shapes and patterns, the factors causing dissipation of energy in nonprismatic compound channel flows, models for predicting average velocity and boundary shear, stage-discharge relationships for different scenarios, sediment transport rate, and bed morphology. Studies were conducted to obtain an understanding of the concerns and challenges in the field using analytical, experimental, and computational methodologies. The research conducted by scientists and investigators from both historical and contemporary periods was acknowledged.

2.2 Flow and sediment transport in compound channels

Year	Authors	Research Focus	Methodology	Key Findings
1964	Sellin	Kinematics effect and vortex formation at waterway confluences	Controlled tests in a research facility; visual evidence from experiments	Demonstrated the presence of vortices at the confluence of the main waterway and riverbank; velocity was higher in isolated conditions than in interactive scenarios.

1965	Zhelezny akov	Momentum transmission between primary waterway and flood zones	Laboratory experiments and field tests	Showed momentum transfer led to reduced total flow rate when flood depth slightly exceeded bank-full level.
1971	Ghosh and Jena	Boundary shear distribution in two-stage channels with varying roughness	Experimental study on smooth and rough edges	Investigated the influence of roughness and flow levels on drag force distribution across the waterway.
1975	Myers and Elsawy	Momentum transfer and shear stress distribution at main channel-floodplain junction	Experimental analysis	Found shear stress decreased by 22% in the main channel but increased by 260% in the flood zones; identified erosion and scouring zones.
1977	James and Brown	Effects of floodplain convergence angles on flow resistance	Experimental studies with different convergence angles	Higher convergence angles correlated with increased flow resistance; velocity increased on converging floodplains but decreased on wider ones.
1979	Rajaratn am and Ahmadi	Flow interaction in straight channels with symmetrical floodplains	Experimental analysis	Indicated longitudinal momentum transfer from the main channel to floodplains, increasing flood zone shear stress while

				decreasing it in the main waterway.
1982	Wormlea ton et al.	Discharge calculation methods in compound channels	Controlled experiments using DCM for discharge calculations	Introduced an apparent shear stress ratio for accurate discharge estimation; horizontal and diagonal separations provided better estimates than vertical division.
1983	Knight and Demetrio u	Discharge and shear force distribution in composite conduits	Experimental trials in straight, symmetrical composite conduits	Provided equations for shear force fractions and flow distribution; found apparent shear force increased with wider floodplains and shallower depths.
1984	Knight and Hamed	Influence of bed roughness on lateral momentum transfer	Experimental study with six bed roughness types	Analyzed six bed roughness types; computed shear force proportions using various interface planes and dimensional parameters.
1985	Wormlea ton and Hadjipan os	Flow distribution accuracy in composite waterways	Experimental and analytical study on flow distribution	Found total discharge calculations were reliable, but floodplain flow was underestimated and main channel flow overestimated.

1987	Myers	Velocity and discharge ratios in composite channels	Theoretical analysis with mathematical modeling	Showed velocity and discharge ratios depended on channel geometry rather than bed slope; traditional methods overestimated cross-section capacity at shallow depths.
1990	Stephenson and Kolovopoulos	Discharge calculation methods in composite channels	Comparative analysis of four different approaches	Evaluated four approaches, concluding that their 'area technique' was the most effective for discharge estimation.
1990	Elliott and Sellin	Crossflow interaction in asymmetrical conduits	Experimental study analyzing momentum transfer equations	Found that crossflow distorted velocity distribution and boundary shear stress, altering forces across the cross-section.
1990	Myers and Brennan	Impact of momentum transfer on compound channel capacity	Analytical and experimental study on resistance factors	Demonstrated that momentum transfer influenced resistance in compound channels and highlighted potential errors in simplified analysis approaches.
1988, 1991	Shiono and Knight	Water behavior in straight open channels with	Developed an analytical model for velocity and shear stress	Derived equations for shear layers using a dimensionless eddy viscosity model;

		complex cross sections	prediction; extended to various channel shapes using linear elements	incorporated turbulence effects and secondary flows.
1992, 1993a, 1993b	Ackers	Impact of riverbank connection on composite waterway hydraulics	Developed formulas and validated them through experimental testing	Proposed a parameter linking primary waterway flow conditions to flood zone hydraulics; confirmed with diverse channel geometries.
1993	Garcia and Niño	Formation and evolution of sediment bars in straight and meandering channels	Experimental study with laboratory tests and theoretical modeling	Identified height, wavelength, and migration patterns of alternating bars; theoretical predictions matched experimental observations.
1995	Cokljat and Younis	Application of Reynolds stress model to open channel flows	Numerical simulation approach	Found strong agreement between model predictions and observed data for rectangular and complex conduits.
1995	Thomas and Williams	LES modeling of steady, uniform flow in trapezoidal compound channels	Numerical modeling and comparison with experimental data	Analyzed tractive stress, velocity distribution, and secondary currents; compared LES results with empirical findings.

1997	Myers and Lyness	Influence of discharge on bed roughness in compound channels	Experimental study on discharge ratios	Showed that discharge capacity depends on channel geometry rather than bed slope; lateral bed gradient influenced flow dynamics.
1997	Salvetti et al.	LES of uniform flow in compound channels	LES analysis with high Reynolds number	Found high consistency between simulated tractive stresses, secondary movement, and observed data.
1998	Pang	Flow distribution and energy loss in two-stage straight composite channels	Experimental investigation of isolated and interactive flow conditions	Demonstrated that Manning's roughness coefficient influences energy loss; variations in 'n' values linked to differences in flow depth.
1998	Lyness et al.	Hydraulic properties of overbank flows in meandering channels	Experimental study at UK FCF	Found that valley-direction flow velocity was higher on floodplains than in the main channel when relative depth exceeded 0.2.
1999	Bousmar and Zech	1D modeling of flow rate in compound channels	Theoretical model with turbulence-based analysis	Proposed a model for momentum transfer across junctions using velocity gradients and mass exchange;

				validated with natural data.
1999	Myers et al.	Resistance coefficients in compound channels	Laboratory and field studies	Found that roughness coefficients in mobile bed channels increased with depth due to dune formation; floodplain roughness influenced channel flow.
2000	Thornton et al.	Apparent shear stress at main channel-floodplain junctions	Experimental study with turbulence-based evaluation	Developed empirical equations for apparent shear stress, considering bed tractive stress, flow velocity, depth, and vegetation obstruction.
2001	Myers et al.	Flow correlations in channels with different floodplain roughness	Experimental and mathematical modeling	Showed logarithmic velocity-discharge ratios in experiments, but linear in natural streams.
2001	Knight and Brown	Resistance variations in compound channels	Experimental trials	Identified complex relationships between flow depth, discharge, and bed shapes.
2001	Cassells et al.	Flow capacity forecasting in composite channels	Laboratory models with fixed beds	Determined that WDCM was the most accurate method for discharge prediction.

2002	Bathurst et al.	Sediment deposition patterns in flumes	Experimental studies	Found channel shape significantly influences sediment deposition, with maximum accumulation near meander bends.
2002	Atabay and Knight	Stage-discharge equation for symmetrical channels	Experimental data analysis	Established empirical relationships for flow depth and rate based on floodplain width.
2002	Bousmar and Zech	Turbulent structures in compound channels	Experimental and numerical analysis	Determined vortex wavelengths and momentum shifts using unsteady RANS modeling.
2003	Ozbek and Cebe	Shear stress and discharge in composite channels	Experimental study	Found diagonal method most effective for shear stress calculations.
2004	Tominaga and Knight	Secondary flow impact on momentum transfer	Numerical simulation	Identified linear momentum transfer, with high shear stress in riverbanks.
2004	Bousmar and Zech	Water movement in converging compound channels	Experimental study with EDM method	Found strong correlation between measured and estimated water profiles.
2005	Knight and Shamseldin	CFD modeling of open-channel flow	Numerical simulation	Examined turbulence models, identifying variations in shear stress.

2005	Atabay et al.	Sediment transport and flow rate in multi-section channels	Laboratory experiments	Verified Ackers' sediment transport predictions and developed empirical relationships.
2006	Tang and Knight	Impact of floodplain irregularities on sediment transport	Experimental study with mobile sand bed (d_{50}=0.88 mm)	Identified quasi-equilibrium state in the riverbed affecting sediment transport rate.
2006	Atabay and Knight	Conveyance capacity, flow distribution, and sediment movement	Empirical study, COHM and WDCM model comparison	Found WDCM accurate for uniform roughness, but COHM more useful for mobile boundary cases.
2006	Karamis heva et al.	Sediment transport prediction models	Large-scale and small-scale flume experiments	Yang sediment transport formula provided best estimates.
2006a	Proust et al.	Flow in nonprismatic composite channels	Experimental study with varying convergence angles	Found significant mass transfer and head loss at 22° convergence angle.
2006b	Proust et al.	Flow characteristics in asymmetric floodplains	Experimental and numerical study (1D and 2D models)	Model accurately predicted flow elevations but had higher errors in flow rate distribution.
2006	Rezaei	Flow transfer in nonprismatic channels	Laboratory experiments in converging floodplains	Identified increased momentum transfer due to varying floodplain shapes.

2008	Cater and Williams	LES simulation of turbulent flows in compound channels	Numerical modeling and experimental validation	Found high stress at the bed surface in floodplain regions.
2008	Khatua	Shear stress distribution model for composite channels	Laboratory experiments in straight channels	Developed novel model for boundary shear and discharge prediction.
2008	Tang and Knight	Shear stress distribution in overbank flows	Analytical modeling with Navier-Stokes equations	Provided reliable velocity and stress estimates validated by experimental data.
2009	Rezaei and Knight	Modified SKM for nonprismatic channels	Numerical modeling	Incorporated convergence by replacing bottom gradient with energy gradient.
2009	Shiono et al.	Influence of floodplain roughness on sediment transport	Laboratory experiments with LDA device and digital photogrammetry	Identified secondary flow cells affecting bed morphology.
2010	Chunhong et al.	Flow and sediment transport dynamics	Experimental study, mathematical modeling	Developed formulations for lateral eddy viscosity and sediment diffusion.
2010	Fraselle et al.	Sediment transfer in overbank floods	Flume experiments with movable and rigid beds	Found strong dependence on water depth and floodplain roughness.

2010	Beaman	Hydraulic effects on in-bank and overbank flows	Numerical simulations using LES	Used calibrated variables to estimate flow characteristics.
2010	Gandhi et al.	Velocity profiles in real fluid flows	ADV experiments, CFD simulations	Found deviations from ideal velocity profiles due to bed curvature effects.
2010	Khatua et al.	Apparent shear stress in composite channels	Empirical research in rectangular channels	Developed approach to estimate proportional wall shear in flood zones.
2010	Moreta and Martin-Vide	Shear stress interaction at the main channel-floodplain junction	Mathematical modeling, experimental validation	Derived a formula using velocity gradient and apparent frictional coefficient.
2010	Panda	ANN-based discharge prediction	ANN modeling with empirical data	ANN outperformed existing models in discharge estimation.
2010	Chlebek et al.	Flow classification in compound channels	Experimental study	Observed increased head loss and large velocity/shear stress disparities.
2010	Proust et al.	Energy dissipation in two-stage channels	Thermodynamic approach	Found identical energy slope across cross-section but different slopes for main channel and flood zone.
2010	Rezaei and Knight	Flow distribution in converging compound channels	Laboratory experiments	Found linear discharge increase at low flow depths but non-linear at higher depths.

2011a	Sahu et al.	Forecasting flow rates in straight compound open channels using neural networks	Applied ANN and compared with traditional models (COHM, SCM, DCM, EDM)	ANN exhibited the lowest mean absolute percentage error.
2011b	Sahu et al.	Velocity prediction in meandering waterways	Used ANN with backpropagation	Considered location and flow depth as inputs, with velocity as the output.
2012	Khatua et al.	Stage-discharge correlation in compound channels	Developed MDCM based on apparent shear stress and interaction length	Improved correlation in channels with higher width ratios.
2012	Khazaee and Mohammadiun	Flow distribution analysis in open channels	Utilized 3D and two-phase CFD models	Identified variations in water depth and mass flow rate based on aspect ratios and inclination angles.
2012	Kara et al.	Depth-averaged streamwise velocity analysis	Compared LES-based velocity with SKM analytical solutions	Found that calibrating lateral eddy viscosity coefficient (λ) and secondary current parameter (Γ) is necessary for accurate predictions.
2012	Sahu et al.	Entry length estimation in low Reynolds number pipe flow	Developed ANFIS model using CFD-generated datasets	Optimized model with ideal membership function distributions.
2012	Ali et al.	Sediment transport capacity analysis	Investigated impact of unit discharge, mean velocity, and slope gradient	Found slope gradient had the greatest impact due to increased tangential

				component of gravity. Developed empirical transport capacity equation.
2013	Jumain et al.	Sediment transport and river roughness analysis	Studied sedimentation and erosion effects	Found that velocity variations in main channels significantly alter bed arrangements.
2013	Conway et al.	Stage-discharge relationship prediction	Proposed an enhanced 3D CFD technique with resistance coefficients	Improved upon k-ε turbulence closure and validated using UK FCF data.
2013	Xie et al.	Flow simulation in composite waterways	Used LES models	Examined velocity distributions, turbulence intensities, wall shear stress, and secondary flow structures. Found chaotic flow near walls and significant horizontal momentum transfer.
2013	Yonesi et al.	Effect of floodplain roughness on overbank flow	Analyzed velocity distribution, discharge percentage, friction factors, and turbulence intensities under various conditions	Studied different roughness conditions and divergence angles, showing impact on secondary flow and turbulence intensities.

2014	Mohanty and Khatua	Zonal variation of friction factor in compound waterways	Proposed a novel approach for estimating overall and individual discharges in floodplain and primary channels	Accurately predicted component outflows in flume and river datasets.
2014	Zhang et al.	Sediment movement and river bed changes	Developed a 2D numerical model incorporating hydrodynamic, sedimentological, and bed deformation equations	Simulated sediment accumulation in the Three Gorges Reservoir for 70 years.
2015	Minatti	Simulation of complex natural channels	Applied Shallow Water-Exner model using finite volume framework	Modeled both liquid and solid phase dynamics with a path-conservative method.
2015	Filonovich	RANS model evaluation for river flow simulations	Used CFD-based simulations on straight rectangular and trapezoidal composite waterways	Analyzed secondary current effects and model performance.
2015	Fernandes et al.	Momentum exchange in composite waterways	Compared seven approaches with experimental datasets	Found that traditional methods were less effective than those incorporating momentum exchange mechanisms.

2016	Devi and Khatua	Momentum shift in primary and floodplain interface	Applied SKM analytical solution with key parameters	Identified variations in boundary friction factor and shear layer width.
2016	Parsaie et al.	Discharge prediction in compound open channels	Compared SCM, COHM, DCM, and RBF neural network	Found DCM more accurate, with MLP outperforming RBF and analytical methods.
2016	Naik and Khatua	Shear stress distribution in composite waterways	Conducted laboratory experiments and formulated novel shear stress equation	Developed a predictive equation based on geometric and hydraulic parameters.
2016	Jumain et al.	Flow and sediment transport in mobile-bed channels	Investigated flow resistance, vorticity, bed shape, and sediment transport	Found significant increases in Darcy-Weisbach friction factor with higher relative depths.
2016	Västilä et al.	Vegetation impact on flow and sediment processes	Conducted a two-year field study in a two-stage channel	Demonstrated vegetation control on sediment deposition through cross-sectional blockage factor.
2016	Gamal	Corrugated bed effects on sediment transport	Used LES modeling on different bed configurations	Showed that sediment transport increases with bed corrugation amplitude.

2017	Tang	Developed a new model integrating ECM and WDCM to improve flow forecast accuracy	Comparison with experimental and literature data	New model outperforms ECM, WDCM, and DCM, reducing mean relative error to ~5%
2017a	Naik and Khatua	Multivariable regression model for water surface profile in nonprismatic channels	Laboratory experiments, nonlinear regression	High conformity between model predictions and experimental/other researchers' data
2017b	Naik et al.	Empirical study on prismatic and nonprismatic waterways under overbank flow	Formulated equations for tractive stress distribution, validated with natural river data	Reliable stage-discharge correlation predictions for waterways with low width ratios
2017c	Naik et al.	Velocity distribution prediction in converging compound channels	3D CFD modeling, ANSYS-Fluent simulations, ANN trained with BPNN	ANN models demonstrate high accuracy compared to experimental flume data
2018	Khuntia et al.	ANN model for boundary shear stress distribution in straight composite conduits	BPNN trained with width ratio, Reynolds number, etc., error analysis validation	BPNN provides robust nonlinear mapping, improving prediction range
2018	Das and Khatua	Resistance properties in nonprismatic compound channels	Laboratory experiments, multivariable regression model	Proposed model outperforms other methods in Manning's 'n' estimation
2018	Mohanta and Patra	CFD validation for open channel flow simulations	Volume of fluid approach, finite volume method	Strong correlation with experimental data, accurate

				secondary circulation predictions
2018a	Naik et al.	ANN-based boundary shear and velocity prediction in two-stage channels	ANN model trained with variable shape/flow conditions, error analysis	High precision in boundary shear and velocity forecasts
2018b	Naik et al.	Energy dissipation study in converging channels	Multivariable regression model for energy slope prediction	Superior discharge capacity prediction in converging channels
2019	Das et al.	GEP-based flow discharge estimation in nonprismatic channels	Comparative review of analytical and empirical methods, GEP modeling	GEP model outperforms traditional methods, achieving $R^2 > 0.80$ and MAPE < 15%
2020	Wu et al.	Flow properties and sediment bed morphology in a prolonged channel with a uniform sediment layer.	Experimental approach using a controlled laboratory flume with a sediment bed (grain size = 0.5 mm). Observed flow and sediment bed characteristics.	Significant differences in flow features and bed geometry were observed between complex waterways formed by two isolated channels and conventional complex channels.
2021	Lu et al.	Analytical modeling of bed shear stress and bed-load transport in vegetated flows.	Derived an analytical method based on the phenomenological theory of turbulence; validated results by	The model effectively estimated bed shear stress and transport rates in vegetated flows, demonstrating its applicability for

			comparing bed-load transport rates with and without vegetation.	uniform and patchy vegetation.
2021	Fernandes	Flow dynamics in compound channels, emphasizing apparent shear stress.	Developed a conceptual model incorporating apparent shear stress; validated through real-world data and experimental calibration.	The proposed model improved Manning's roughness coefficient estimation and refined stage-discharge predictions in complex streams.
2022	Prasad et al.	Shear force distribution in compound channels with varying roughness.	Conducted experiments on smooth and rough bed conditions; employed a genetic algorithm model with K-Fold cross-validation for predictive analysis.	The genetic algorithm outperformed existing models in shear force prediction, showing improved accuracy with reduced mean absolute percentage error.
2022	Yonesi et al.	Discharge prediction in CCNPF using machine learning models.	Applied MARS and GMDH models; compared results with MLPNN using statistical error indices.	Identified key hydraulic and geometric parameters influencing discharge; models demonstrated high accuracy in flow estimation.

2022	Naik et al.	Water surface profile prediction in compound channels with converging floodplains using GEP.	Utilized experimental datasets from previous studies; formulated a new mathematical relationship incorporating nondimensional variables.	The developed model closely aligned with experimental and literature data, providing reliable predictions of water surface profiles.
2022	Branß et al.	Evolution and development of fluvial levees in trained inland river sections.	Conducted a literature review, synthesizing existing research on bedforms, vegetation, and sediment interactions; supplemented with findings from flume studies.	Demonstrated the role of bedforms and vegetation in levee formation and evolution, influencing hydraulics and sediment suspension.
2022	Wang et al.	Critical flow velocity determination for sediment transport in vegetated channels.	Developed a novel equation based on force balance principles; validated with empirical data from literature.	The equation showed strong correlation with experimental data, indicating that vegetation density significantly affects sediment transport thresholds.

2022	Selim et al.	Sediment transport dynamics in composite channels with diverging floodplains using CFD.	Used ANSYS-Fluent for CFD simulations; analyzed sediment transport under different conditions.	Smaller sediment particles reduced longitudinal flow velocity; increased sediment discharge decreased turbulence, especially in expanding floodplains.
2023	Mir and Patel	Forecasting roughness using ML models	ML models (Random Forest, Additional Trees Regression, Extreme Gradient Boosting, Lasso Regression), Sensitivity Analysis, Pearson's coefficient, Taylor's Diagram, Box Plots, K-fold Cross-validation	Random Forest, Additional Trees, and XGBoost performed exceptionally; Lasso Regression showed moderate accuracy. Energy grade line was the most influential factor in roughness prediction.
2023	Zeng and Li	Turbulent dynamics forecasting using LES technique	LES modeling, flow simulations	Demonstrated intricate turbulent patterns due to eddy movements, emphasizing differences between prismatic and nonprismatic channels.

2023	Khattab et al.	Flow discharge analysis in compound channels	Experimental study, Dimensional Analysis, ANFIS prediction	High concordance between empirical and computational techniques in predicting output.
2023	Barman and Kumar	Influence of vegetation on flow characteristics in complex channels	AIM analysis, velocity and turbulence measurements	Revealed greater RSS and TKE variations in floodplain slopes with increased vegetation.
2023	Rahim et al.	Impact of emergent stiff vegetation on turbulence in nonprismatic flooding areas	Experimental study, velocity distribution analysis	Identified drag force as the primary influence on velocity distribution; strong secondary currents and shear stress fluctuations at channel boundaries.
2023	Mohseni and Naseri	Prediction of water surface profile in vegetated floodplains	ANN, SVM, Regression Models	SVM outperformed ANN and regression models; relative discharge and depth were key influencing parameters.
2023	Singh et al.	Examination of turbulent flow characteristics in two-stage channels	LES modeling, Depth-averaged velocity analysis	Identified impact of vortical structures on momentum exchange in floodplains.
2023	Bijanvand et al.	Water surface elevation forecasting in compound channels	Soft Computing Models (MLPNN, GMDH, NF-GMDH, SVM)	SVM performed best; sigmoid and radial tangent functions were optimal for activation and kernel functions.

2023	Gadissa et al.	Velocity and shear stress distribution modeling in channels with varying floodplain widths	Depth-averaged velocity models, Shear stress distribution analysis	Confirmed model effectiveness in predicting velocity and shear stress; shear forces showed varied influence across channel sections.
2023	Mihani and Rezaei	Overbank flow in converging, sloped floodplains	Experimental study, Velocity and wall tractive stress measurements	Higher velocity and wall shear stress at the end of convergent sections; velocity increased more than twice over transition sections.
2023a	Kaushik and Kumar	Shear stress distribution in nonprismatic compound channels	Shear force modeling using GEP	Proposed a novel equation for floodplain shear force estimation, outperforming past approaches.
2023b	Kaushik and Kumar	Water surface profile prediction using ML	GEP, ANN, SVM, Statistical Analysis	ANN exhibited the highest accuracy; introduced a GEP-based equation for predicting water surface profiles.
2023	Kaushik et al.	HEC-RAS calibration for predicting water surface profiles	Experimental validation using HEC-RAS models	HEC-RAS models effectively predicted water surface profiles with minimal discrepancies.

2024	Kaushik and Kumar	ML-based shear force prediction in floodplains	GEP, ANN, SVM	ANN outperformed GEP and SVM; study used high-quality experimental datasets.
2024a	Kaushik et al.	Flow resistance estimation in nonprismatic channels	SVM for Manning's roughness coefficient prediction	Strong correlation between SVM-predicted roughness coefficients and experimental data.
2024b	Kaushik et al.	Numerical simulations of flow characteristics in nonprismatic channels	HEC-RAS modeling, experimental validation	HEC-RAS simulated velocity and shear stress distributions; strong agreement noted between experimental and simulated data.

The above table presents a chronological review of key studies, highlighting the research focus, methodologies employed, and key findings. Early research primarily concentrated on fundamental hydrodynamic principles, while later studies integrated numerical models and machine learning techniques to improve predictive accuracy. Some of the most relevant papers with chronologically are presented below for quick review.

Zheleznyakov (1965) examined momentum transmission between primary waterways and flood zones, concluding that momentum transfer led to a reduced total flow rate when the flood depth slightly exceeded the bank-full level. Ghosh and Jena (1971) explored boundary shear distribution in two-stage channels with varying roughness, identifying how flow levels and roughness impact drag forces. Myers and Elsawy (1975) studied momentum transfer at the main channel-floodplain junction and found that shear stress decreased in the main channel but increased significantly in flood zones, leading to erosion and scouring. James and Brown (1977) investigated the effects of floodplain convergence angles on flow resistance, revealing that higher convergence angles resulted in increased flow resistance. Knight and Hamed (1984) analyzed bed roughness effects,

showing that roughness influenced lateral momentum transfer. Wormleaton and Hadjipanos (1985) refined flow distribution accuracy in composite waterways.

In the late 1980s and early 1990s, Myers (1987) and Elliott and Sellin (1990) focused on velocity and discharge ratios, with Myers demonstrating that traditional methods often overestimated cross-section capacity. Shiono and Knight (1988, 1991) developed an analytical model predicting velocity and shear stress in complex channels, incorporating turbulence effects. Garcia and Niño (1993) explored sediment bar formation, while Cokljat and Younis (1995) applied the Reynolds stress model to open channel flows, validating its effectiveness. Thomas and Williams (1995) and Salvetti et al. (1997) contributed to LES modeling for uniform flow, improving tractive stress and velocity distribution predictions. Pang (1998) analyzed energy loss in two-stage straight composite channels, confirming Manning's roughness coefficient's influence.

By 2000, Bousmar and Zech (1999, 2002) focused on turbulence-based models, while Myers et al. (2001) correlated flow properties with different floodplain roughness levels. Cassells et al. (2001) determined WDCM to be the most accurate discharge prediction method. Atabay and Knight (2002) introduced stage-discharge equations for symmetrical channels. From 2005 onwards, research increasingly relied on computational techniques. Knight and Shamseldin (2005) examined turbulence models using CFD, while Atabay et al. (2006) studied sediment transport in multi-section channels. Proust et al. (2006a, 2006b) analyzed nonprismatic channels and asymmetric floodplains, respectively, finding significant mass transfer effects. Rezaei and Knight (2009) modified the SKM model for nonprismatic channels, improving accuracy by incorporating energy gradients.

In the 2010s, Panda (2010) introduced ANN-based discharge predictions, demonstrating superior accuracy over traditional models. Sahu et al. (2011) and Khatua et al. (2012) refined ANN velocity and shear stress models. Conway et al. (2013) proposed enhanced 3D CFD techniques, improving k-ε turbulence closure. Xie et al. (2013) used LES models to simulate flow in composite waterways, identifying flow patterns. Mohanty and Khatua (2014) analyzed zonal friction factor variations, accurately predicting discharges in floodplain and main channels. The late 2010s and early 2020s saw rapid adoption of machine learning techniques. Das et al. (2019) applied GEP for discharge estimation, surpassing traditional empirical methods. Lu et al. (2021) developed an analytical model

for vegetated flows, estimating bed shear stress and transport rates. Fernandes (2021) introduced a conceptual model refining Manning's roughness coefficient estimation.

In recent years, research has focused on advanced computational techniques. Prasad et al. (2022) employed genetic algorithms for shear force prediction, outperforming existing models. Naik et al. (2022) applied GEP for water surface profile prediction, closely aligning with experimental data. Singh et al. (2023) and Mihani and Rezaei (2023) used LES techniques to analyze turbulent flow structures, providing insights into momentum exchange. Gadissa et al. (2023) developed depth-averaged velocity and shear stress distribution models, confirming their effectiveness in predicting flow patterns. Kaushik and Kumar (2023a, 2023b) employed machine learning for shear force and water surface profile predictions, respectively, with ANN models outperforming traditional techniques. Kaushik et al. (2024a, 2024b) calibrated HEC-RAS models, effectively predicting water surface profile, velocity and shear stress distributions with minimal discrepancies.

Despite significant advancements, several research gaps persist in the study of flow and sediment transport in compound channels. A major challenge remains the integration of real-time monitoring data with predictive models to enhance accuracy in flood forecasting and sediment transport predictions. Additionally, most studies have focused on straight and symmetrical channels, leaving a gap in understanding flow behaviours in highly irregular and natural waterways. The impact of climate change on compound channels, particularly in terms of altered flood patterns and sediment yield, also requires further exploration. Moreover, while machine learning and computational models have improved predictive capabilities, their application to dynamic, large-scale river systems remains limited. There is also a need for interdisciplinary research combining hydrodynamics, ecology, and geomorphology to address the complex interactions between sediment transport, vegetation, and human activities. Addressing these gaps will be crucial in advancing sustainable water resource management and flood risk mitigation strategies. The literature on flow and sediment transport in compound channels has evolved from early experimental observations to sophisticated numerical modeling and machine learning applications. Over the decades, researchers have refined discharge estimation methods, improved turbulence modeling techniques, and incorporated environmental variables to enhance prediction accuracy. The integration of artificial intelligence, advanced CFD simulations, and ecological considerations has propelled

hydraulic research into a new era, ensuring more reliable and adaptive solutions for water resource management. Out of the above gaps, this study aims to fill some of the research gaps as mentioned below.

2.3 Literature gaps

❖ Studies have been carried out on nonprismatic compound channels with smooth floodplains, but limited research was available on nonprismatic compound channels with rough floodplains.

❖ Research has been conducted on sediment transport effect on flow characteristics in compound channels with prismatic floodplains.

❖ The flow resistance in compound channels has been studied thoroughly but the effect of floodplain roughness on flow resistance in nonprismatic compound channels has received less attention and must be the scope for future research.

❖ There has been a lack of research conducted on the computation of flow rate in compound channels utilizing soft computing approaches. Therefore, the future focus of research will be on using soft computing methods to estimate the flow rate in nonprismatic compound channels.

2.4 Conclusion

The earlier studies focused only on the examination of flow characteristics in a prismatic composite channel, specifically for cases of uniform and steady flow. There has been little research conducted on nonprismatic compound channels, which have significant practical uses. Therefore, it is vital to improve existing approaches or create other methods that have a stronger theoretical foundation, higher accuracy, applicability to real-world scenarios, and are simpler to employ in computer programs. Scientists have conducted experiments on certain physical models of nonprismatic compound channels. However, they have not taken into account the actual characteristics of rivers, such as sediment movement and rugged floodplains, which need to be taken into consideration. Hence, the primary objective of the present study is to examine the flow properties in nonprismatic composite waterways, both with and without sediment, in addition to smooth and rough converging floodplains. The objective is to develop a comprehensive computational model for estimating flow rate in nonprismatic compound channels and then validate it using experimental data from prior investigations.

CHAPTER 3

METHODOLOGY

3.1 Experimental setup/procedure

The experiments were carried out in the Hydraulics laboratory situated in the Department of Civil Engineering at Delhi Technological University in Delhi, India. The trials were carried out in a masonry flume with dimensions of 12 m in length, 1.0 m in width, and 0.8 m in depth. A complex cross-section was built in a masonry flume using brick masonry. The main channel has a width of 0.5 m and a depth of 0.25 m (Fig. 3.1). The geometric attributes of a two-stage channel in terms of its depth are depicted in Fig. 3.1. The converging stretch of the channel was constructed using brick masonry in order to achieve a converging angle of $\theta = 4°$. A top view of an experimental setup that consists of both prismatic and nonprismatic parts of a compound channel has been represented in Fig. 3.2. The compound channel consists of a prismatic component that extends over a distance of 6 m, a nonprismatic section that extends over a distance of 3.6 m, and the remaining section is the downstream section. NPS1 and NPS5 denote the commencement and termination segments of the converging section. NPS3 denotes the central segment of the converging section. The NPS2 functions as an intermediary segment situated between NPS1 and NPS3. NPS4 functions as an intermediary segment situated between NPS3 and NPS5.

The study conducted experiments on four different nonprismatic compound channels in a masonry flume. These channels included a nonprismatic compound channel with smooth floodplains, a nonprismatic compound channel with rough floodplains, a nonprismatic compound channel with sediment and smooth floodplains, and a nonprismatic compound channel with sediment and rough floodplains (Fig. 3.3). The width ratio ranges from 1.0 to 2.0, while the relative flow depth varies between 0.20 and 0.60. The measured flow rate ranges from 0.02 to 0.22 cubic meters per second for a nonprismatic compound channel without sediment and from 0.01 to 0.055 cubic meters per second with sediment. The channel profile, illustrating its rectangular geometry, is shown in Fig. 3.1. The experimental stretch refers to a 3.6 m segment within the converging section of the nonprismatic compound channel. The top width of the composite waterway is 1.0 m before convergence and 0.5 m after convergence, resulting

in a converging angle of 4°.The overhead view of the nonprismatic cross-sections obtained from Rezaei (2006), Naik and Khatua (2016), and the present channel are shown in Fig. 3.4. The floodplains were smoothened using cement mortar placed with a trowel finish, while roughness was created by randomly depositing aggregates of 10 - 20 mm in size throughout the length of the floodplains. The sediment used was Yamuna sand, obtained from the nearby area, with a specific gravity of 2.62 and a mean particle size (D_{50}) of 0.80 mm (as shown in grain size distribution curve in Fig. 3.5). The sediment was positioned inside the main channel at a depth of 0.15 m. It was found that the composite waterway possessed a bed inclination of 0.001 in the longitudinal direction, which indicated the presence of subcritical flow. Utilizing observations collected from in-bank and over-bank flows in the flood zones and the primary waterway, a computation of Manning's roughness coefficient was carried out. The experimental channel is supplied with water from a subterranean reservoir and then transferred to an overhead tank by the system. The water from the canal is collected in a volumetric tank equipped with a V-notch. The V-notch was properly adjusted to accurately quantify the flow rate from the experimental channel. It facilitates the water's descent back into the sump positioned underneath. A sluice gate was installed at the end of the flume to control the water level and ensure a uniform flow depth throughout its entire length. For each instance of a nonprismatic compound channel, five distinct relative flow depths β (ratio of overbank flow depth to the flow depth) are examined, namely 0.20, 0.30, 0.40, 0.50, and 0.60. Flow metrics, including the connection between stage and discharge, the profile of the water surface, the slope of energy, the resistance to flow, the distribution of velocity, and the distribution of shear stress, were measured for each run in both the prismatic section and different nonprismatic portions as seen in Fig. 3.2. The sediment transport rate and longitudinal bed profile were evaluated for each run after establishing a level bed at the beginning of each run. Velocity and shear stress distributions were recorded at an interval of 2.5 cm vertically and 10 cm horizontally, respectively, across the width of the channel, specifically at the grid locations shown in Fig. 3.1.
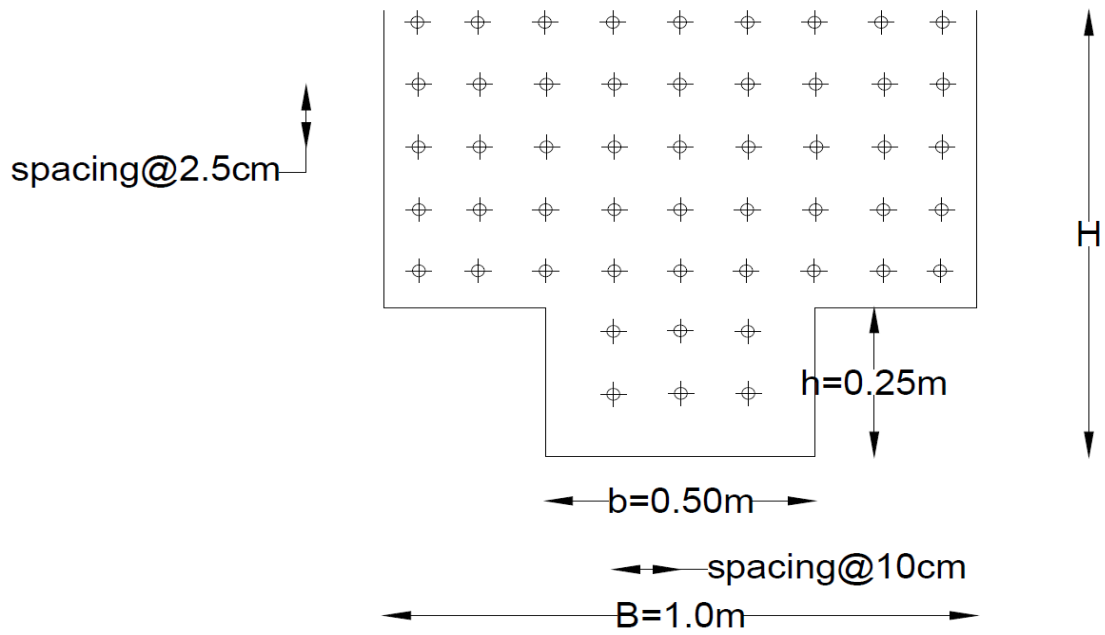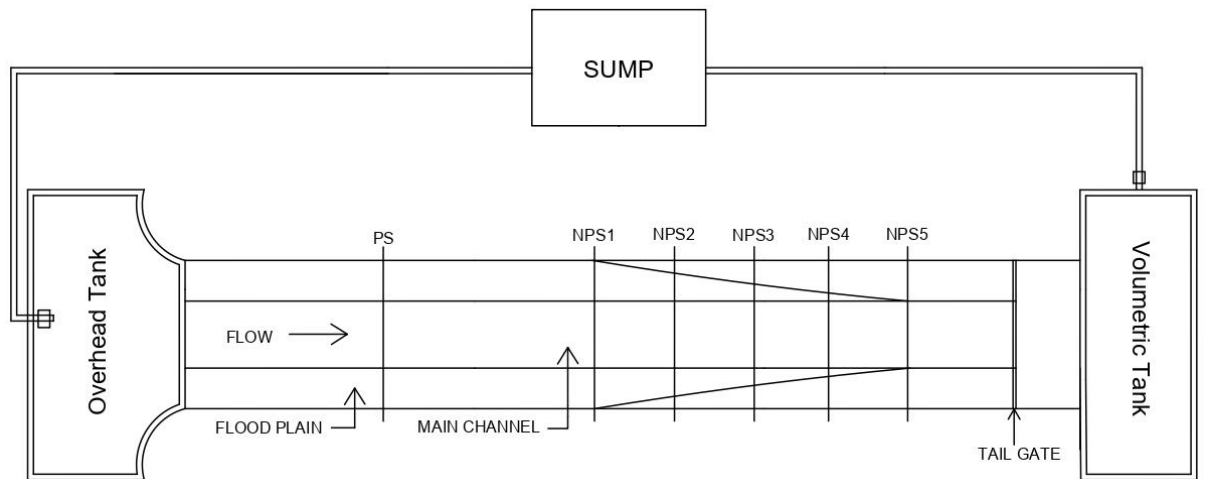
Fig. 3.1 Compound channel cross-section

Fig. 3.2 Experimental setup

Compound channel with smooth converging floodplains

Compound channel with rough converging floodplains

Compound channel with sediment in main channel and smooth converging floodplains

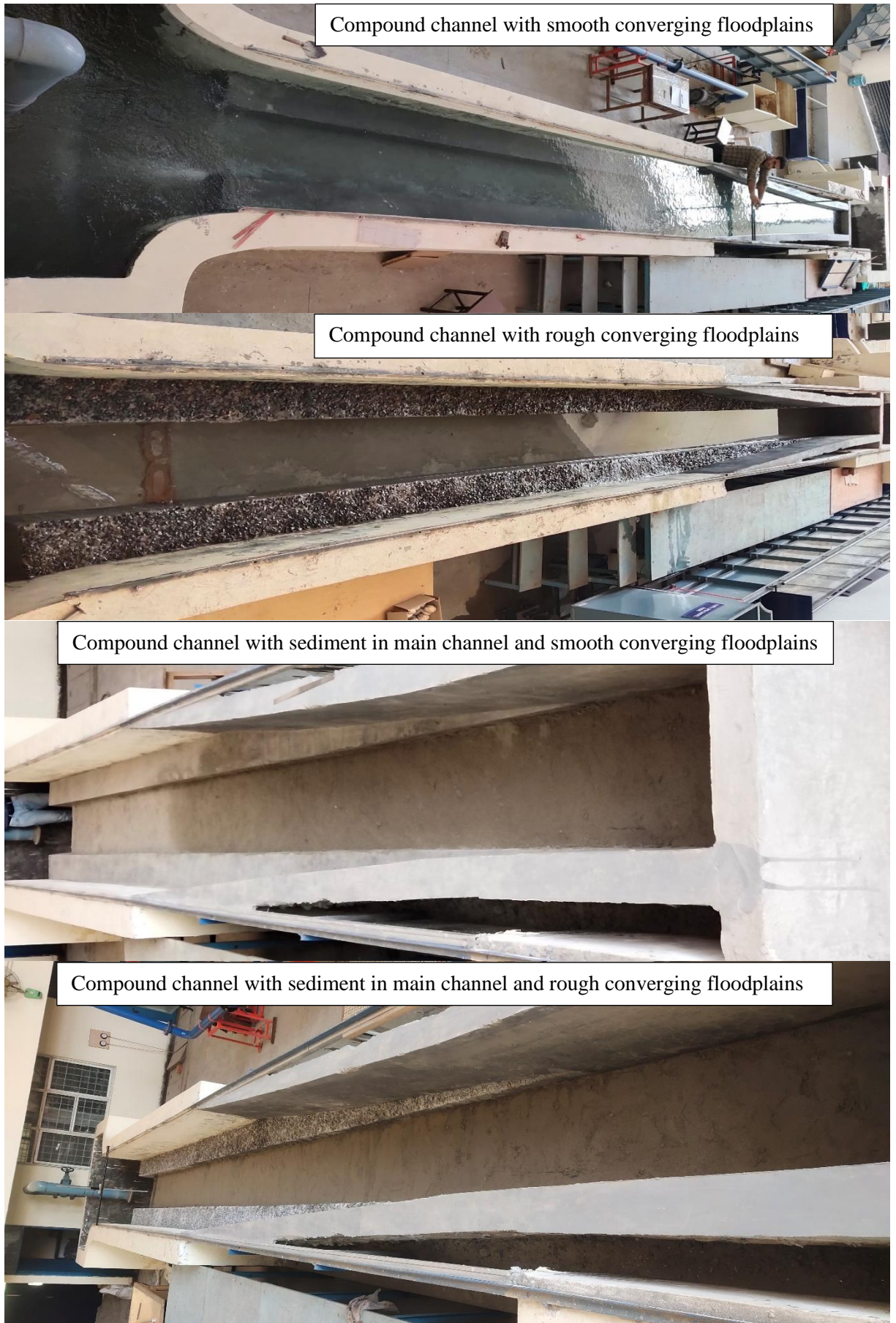Compound channel with sediment in main channel and rough converging floodplains
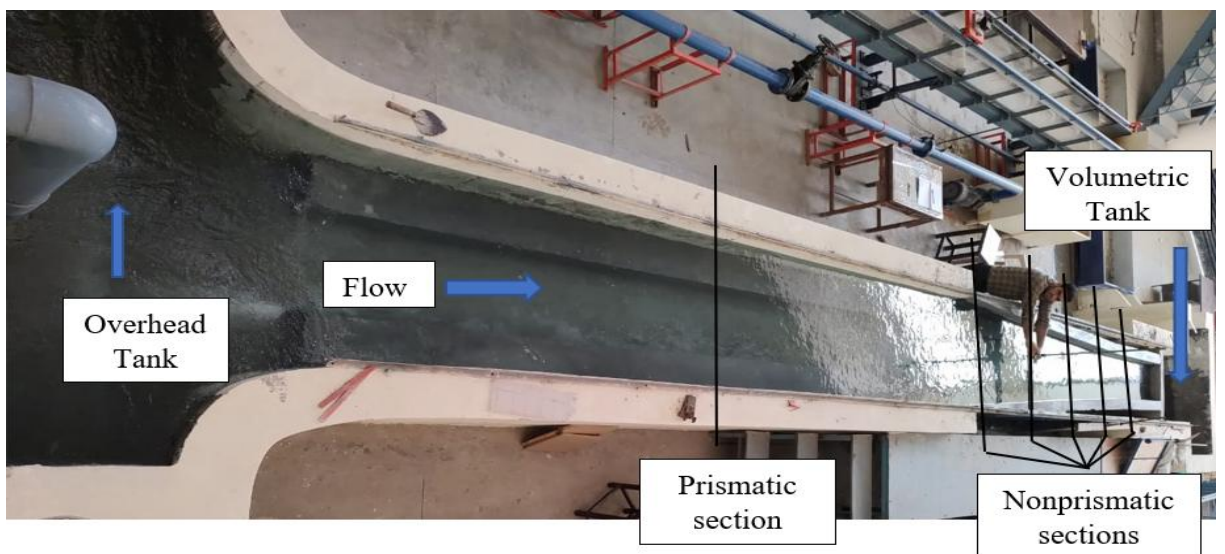
Fig. 3.3 Different nonprismatic compound channels
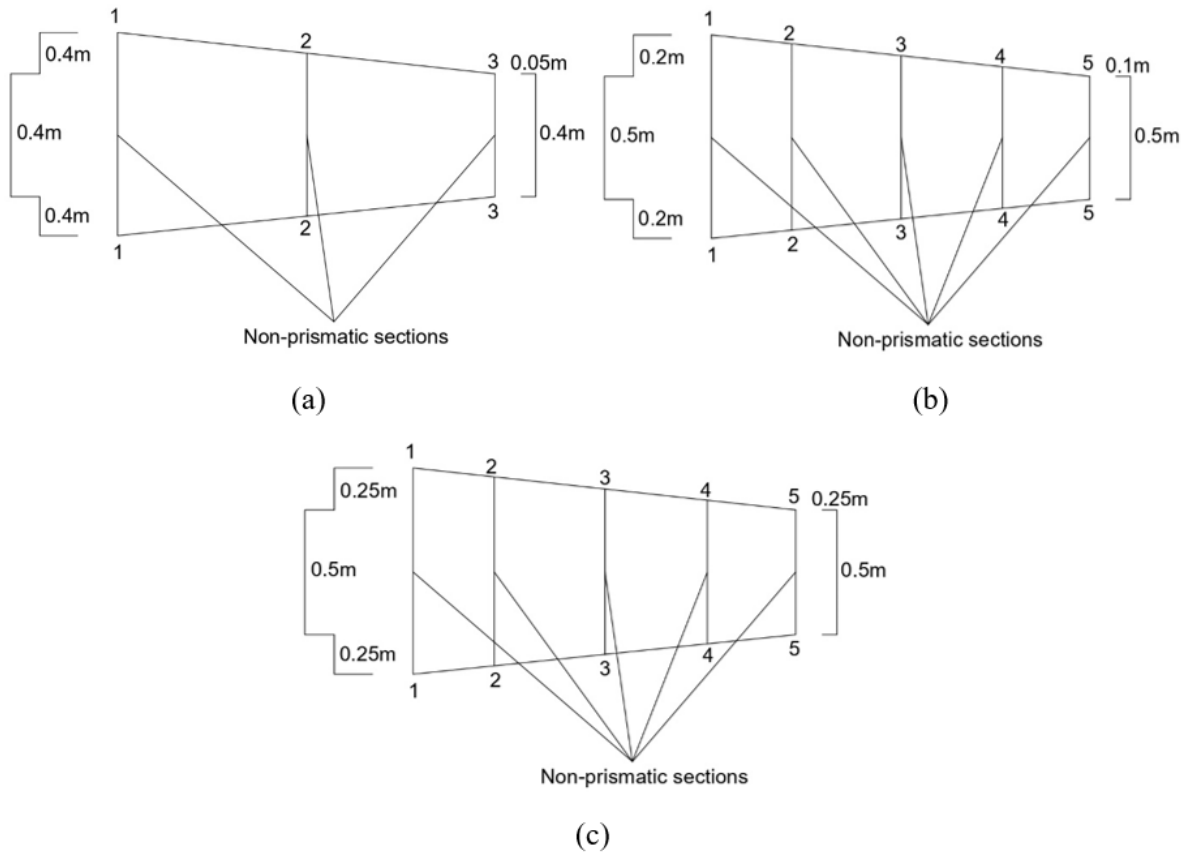
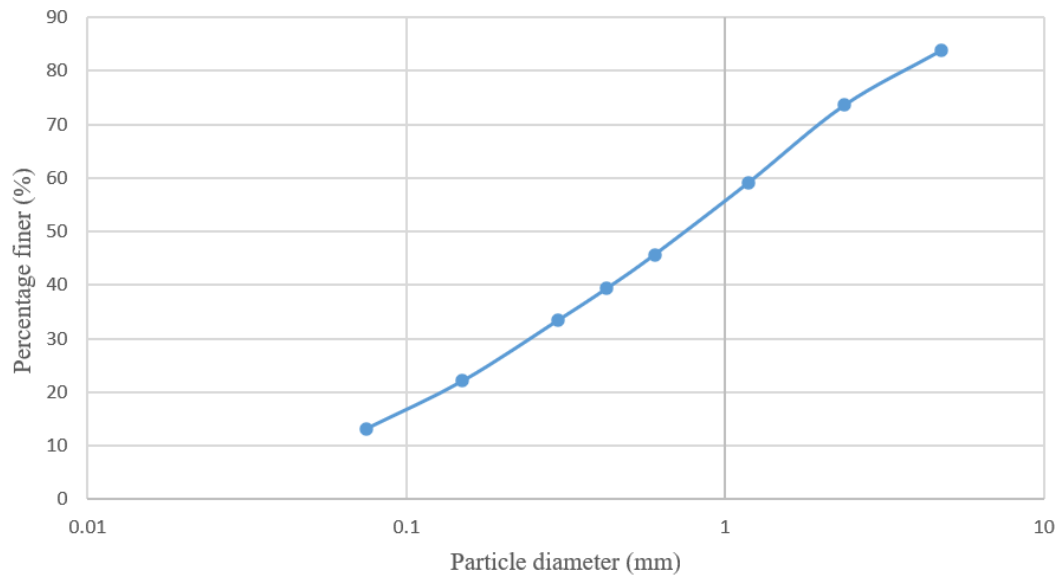Fig. 3.4 Nonprismatic sections of (a) Rezaei (2006) (b) Naik and Khatua (2016) (c) Present channel

Fig. 3.5 Grain size distribution curve

3.2 Measurement of discharge

A tank that is situated above the study's waterway is the destination of the water that is transported by the process from subterranean storage. A volumetric tank that is situated at the end of the channel and is equipped with a V-notch is where the water that is collected from the waterway is stored. After that, it is sent back to the sump that is situated below. The V-notch was calibrated to measure the flow rate from the experimental channel. The equation used to estimate the theoretical discharge for a V-notch is:

$$Q_{th} = \frac{8}{15}\sqrt{2g}\tan\frac{\theta}{2}\,H_c^{5/2} \qquad (3.1)$$

$$C_d = \frac{Q_a}{Q_{th}} \qquad (3.2)$$

$$Q_a = \frac{8}{15}C_d\sqrt{2g}\,tan\frac{\theta}{2}\,H_c^{5/2} \qquad (3.3)$$

The coefficient of discharge was determined to be 0.595 after calibrating the V-notch. Consequently, the equation mentioned above has been altered and used for the purpose of measuring discharge.

$$Q_a = \frac{8}{15}\times 0.595\times\sqrt{2\times 9.81}\,tan\frac{90}{2}\,H_c^{5/2}$$

$$Q_a = 1.406 H_c^{5/2} \qquad (3.4)$$

Where Q_{th} is theoretical discharge (m³/s), Q_a is actual discharge (m³/s), C_d is coefficient of discharge for the triangular notch (dimensionless), θ is crest angle of the triangular notch (degree) and H_c is head over the crest of the notch (m).

The duration of water accumulation in the measuring tanks is subject to variation based on the rate of flow, with a shorter interval seen for a higher discharge rate. Therefore, any change in the average elevation of water in the storage unit during the specified period is noted. The rate of flow for each test run in the experimental waterway is determined by calculating the volume of flow gathered in the measuring tank, which has an area of 2.154 m², along with the corresponding collection time. The discharge obtained by the use of a triangle notch technique is compared to the volumetric discharge, and the findings demonstrate a deviation within a range of ±3 percent.

3.3 Measurement of flow depth

In order to get an accurate measurement of the water surface elevations, a point gauge with an accuracy of 0.1mm was used. Additionally, the point gauge was positioned on the measuring device platform (Fig 3.6). When the water level was measured, it was

documented at intervals of 1.0m in the prismatic portion and 0.3m in the converging portion of the channel, respectively.
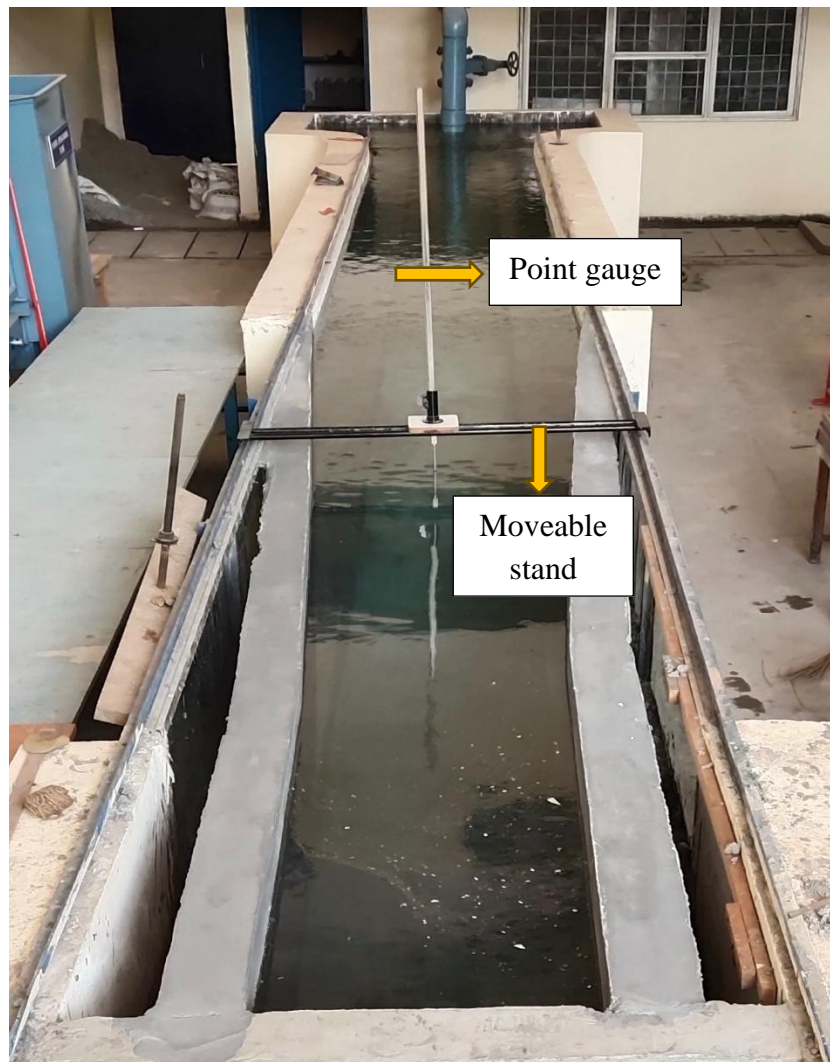

Fig. 3.6 Point gauge

3.4 Measurement of velocity

The Son-Tek micro ADV is employed to measure the velocity at every grid point of the channel sections as shown in Fig. 3.1. The ADV instrument is specifically intended to measure the velocity components at a single location with a high frequency and accuracy. Measurements are conducted by assessing the velocity of particles inside a distant sample volume using the Doppler shift phenomenon. ADV functions based on the notion of Doppler shift. This notion is shown by a straightforward scenario: when you are positioned at a railroad crossing and a train emits a loud sound from its horn while

passing, you perceive the sound at a higher frequency as the train gets closer, and then at a lower frequency as it moves away. As the train approaches, the sound waves emitted by the horn undergo compression, resulting in a higher frequency. Consequently, you experience the sound at a higher pitch. As the train departs, the compression of sound waves ceases, resulting in the perception of a lower-pitched and lower-frequency sound. The ADV is the optimum instrument for laboratory investigation due to its higher acoustic frequency of 16 MHz. The ADV, together with its software package, was used to identify 3D velocity data at various places on the established grids of channel cross-sections. The observations obtained through the sensor were gathered at the processing unit of ADV. For the purpose of assembling 3D velocity data, the application suite makes use of the computer as an interface. The sensor records several velocity measurements per minute at each location. In the following phase, the application that was deployed will be utilized to carry out statistical computations for every depth of flow to capture the averages of point velocities. Each one of the flow velocities is broken down into three different aspects that are mutually perpendicular to one another: "tangential, radial, and vertical". These components are then measured at a depth of 5 cm below the tip of the instrument. This significantly reduces the amount of disruption that is brought about by the stream of fluid and makes it feasible to carry out observations in very close distance to the surface.

ADV has a number of remarkable qualities, such as the capacity to detect velocity along all three axes, significant rates of specimen up to 50 Hz, a tiny collecting volume of less than 0.1 cm³, and the capability to manage minimal flow while maintaining little optimum dispersion. It encompasses a large velocity assortment, from 1 mm/s to 2.5 m/s, and operates particularly well in low-discharge circumstances. It also gives great precision, up to 1% of the determined variety, and it includes an extensive array of dimensions. In addition to this, it does not need to be recalibrated and is assisted by an entirely thorough application. In order to get a favorable outcome from the ADV, the selection and collection of data were conducted according to the parameters of SNR and correlation coefficients, respectively. If the SNR is below 15dB and the correlation is less than 70%, it is recommended to ignore the detected velocity regardless of the direction. In this study, the ADV was set to a sampling frequency of 25 Hz with a measurement duration of 1 minute per point, yielding 1500 velocity samples per location. To improve data accuracy, a signal-to-noise ratio (SNR) threshold of 12 dB was applied for

denoising, while despiking techniques were used to eliminate erroneous data points, ensuring the reliability of the velocity measurements. Additionally, the velocities observed are affected by the particles that are in motion alongside the water, contributing to a more accurate result. Nevertheless, the ADV is unable to measure the velocity within a range of 50 mm from the bed and free surface. In order to address the issue of limited length, a pitot-static tube with a diameter of 5 mm is used alongside a digital manometer with a precision of 0.12 mm. This setup is used to get velocity measurements at a specific spot inside the upper and lower 50 mm regions, spanning from the free surface to the bed, throughout the channel. The equation is utilized for this purpose:

$$v = \sqrt{\left(\frac{2\Delta P}{\rho}\right)} \qquad (3.5)$$

Where v is point longitudinal velocity (m/s), Δp is pressure difference (KPa) and ρ is density of water (Kg/m^3).

In order to ensure that there are no air pockets present within a pitot-static tube, the extended PVC conduit, or the pressure measurement device, it is necessary to thoroughly inspect these instruments before beginning any measurements. It was necessary to have a steady flow of water going from the end of the pitot tube that was immersed in the waterway to the digital manometer to accomplish this requirement. For the purpose of ensuring precise estimation of the difference in pressure, the pitot tube tip was maintained in a fixed position at every point on the grid. This was done so as to minimize variations in the pressure difference readings. The pitot-static tube and ADV, together with its data processing device, used for measuring velocity are depicted in Fig. 3.7.
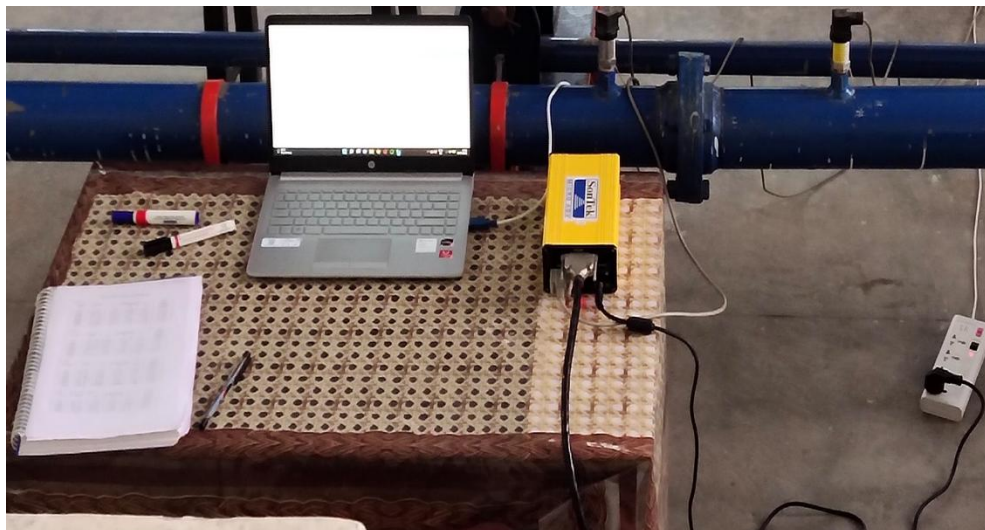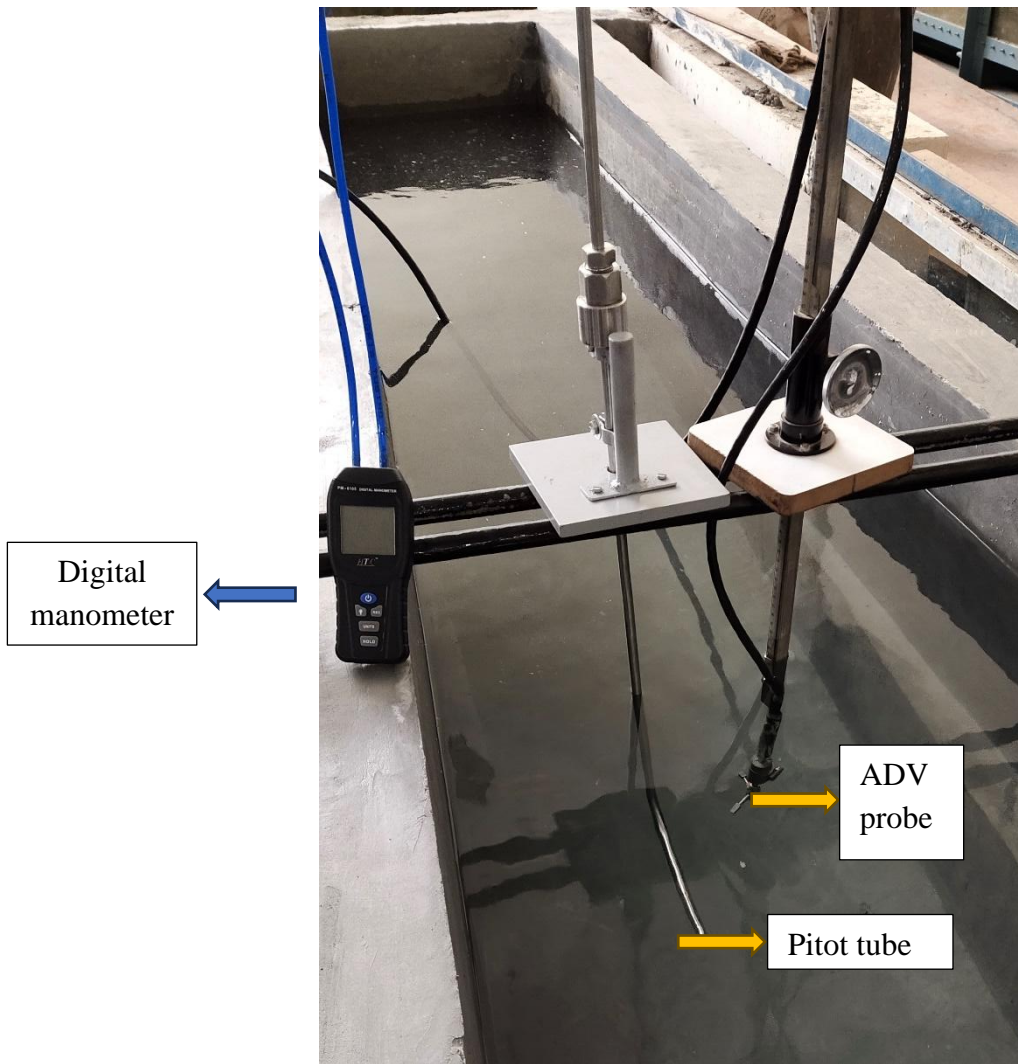
Fig. 3.7 Pitot tube and ADV along with data processing arrangement

3.5 Measurement of depth-averaged velocity

The observations of velocity were computationally averaged over the depth, which contributed to the production of the flow rate per unit width of the channel. Next, the depth-averaged velocity was calculated by dividing this value by the depth of the local flow inside the area. The equation that is used to calculate the depth-averaged velocity, which is indicated by the U_d, is as follows:

$$U_d = \frac{1}{H}\sum u_i \Delta h_i \tag{3.6}$$

Where U_d is depth-averaged velocity (m/s), H is flow depth (m), u_i is point longitudinal velocity (m/s) and Δh_i is depth associated with the local velocity (m).

The traditional velocity distribution and the depth-averaged velocity in an open channel flow are shown in Fig 3.8. The average flow velocity at different depths and the stress exerted on the channel boundaries are important factors in simulating the flow of a compound channel. These characteristics must be measured accurately to calculate their distribution over the flow section, taking into account different flow depths, and to estimate flow rate.
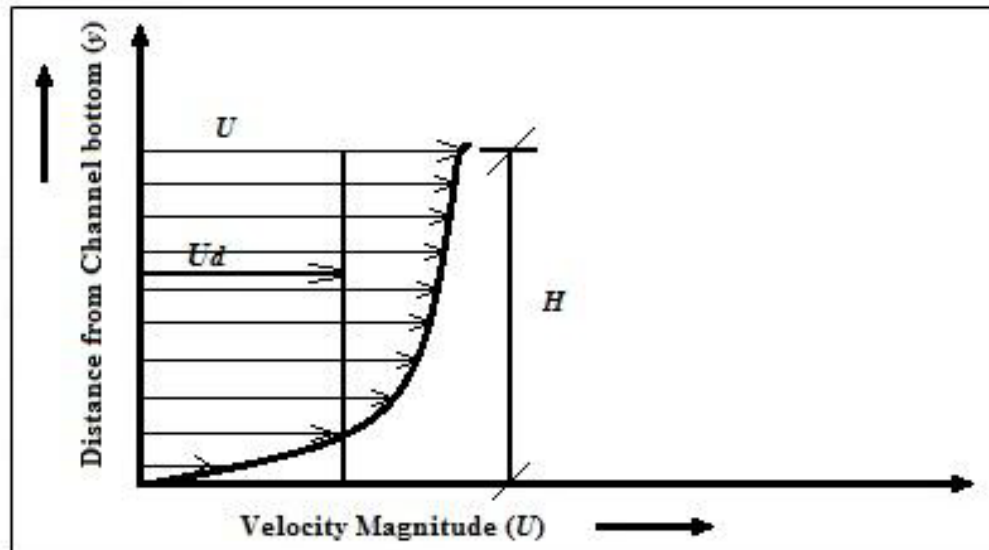
Fig. 3.8 Distribution of velocity in waterway

3.6 Measurement of energy slope

It is feasible for flowing streams to undergo an alteration from a uniform flow to a nonuniform flow as a result of differences in their cross-sectional dimensions. Given

these conditions, the hydrodynamic assessment becomes more complicated than it would be in the case of a simple flow that is consistent. One of the most important aspects of river engineering study is figuring out how much energy is lost in a channel that takes up a composite shape. The equation provided has been used to compute the energy dissipation at every cross-section of the converging section.

$$E_1 = H_1 + \frac{\alpha_1^* V_1^2}{2g} \tag{3.7}$$

$$E_2 = H_2 + \frac{\alpha_2^* V_2^2}{2g} \tag{3.8}$$

$$E_L = E_1 - E_2 \tag{3.9}$$

$$S_e = \frac{E_L}{l} \tag{3.10}$$

Where α^* is the kinetic energy correction factor, computed using:

$$\alpha^* = \frac{\sum v^3 \Delta A}{V^3 A} \tag{3.11}$$

Where E is energy at a section (m), H is flow depth at a section (m), V is average velocity of cross section (m/s), g is acceleration due to gravity (m/s^2), S_e is energy slope (dimensionless), E_L is energy loss (m), l is distance between two sections (m), A is flow area (m^2), v is point longitudinal velocity (m/s) and ΔA is flow area associated to point longitudinal velocity (m^2).

3.7 Measurement of flow resistance

The presence of flow resistance in open channel flow is crucial for ensuring the stability of channels, regulating sediment movement, facilitating energy dissipation, and enabling the design of efficient water conveyance systems. Engineers and hydrologists must meticulously evaluate flow resistance while analyzing and designing open channels for diverse purposes to guarantee optimal functionality. The roughness of the channel segment of a river that has been flooded varies in a horizontal direction across the extent of the wetted perimeter. Calculating the composite roughness is required in order to determine the discharge potential of a compound waterway. The composite roughness for a compound channel is determined using the equation (Rezaei 2006):

$$n = \frac{AR^{2/3}\sqrt{S_e}}{Q} \tag{3.12}$$

$$n = \frac{R^{1/6}}{C} = \sqrt{\frac{8g}{f}} \tag{3.13}$$

Where n is Manning's roughness coefficient, A is flow area (m^2), R is hydraulic radius (m), S_e is energy slope (dimensionless), Q is flow over the section (m^3/s), g is acceleration due to gravity (m/s^2), C is Chezy's coefficient ($m^{1/2}$/s) and f is Darcy-Weisbach friction factor (dimensionless).

3.8 Measurement of boundary shear stress

The pitot-static tube method was used to measure the boundary shear stress (τ_b) over the wetted perimeter of the flow section, which includes both the main channel and the floodplains, in the whole compound section. In order to determine the effect that the momentum shift at the interface between the principal passageway and the floodplains has on the dispersion of wall tractive stress across the width of the channel. In addition, specified locations situated on the grid boundaries were used for nonprismatic compound channels (as seen in Figure 3.1) in order to estimate the flow resistance or skin friction involved. The prior values acquired on the boundary points for velocity measurement were used to calculate the boundary shear stress using Patel's calibration technique (Patel 1965). "According to Patel's research in 1965, the discrepancy in static and stagnation pressure readings (Δp) between the static and dynamic holes of a tube submerged in the boundary layer of a flowing liquid may be used to indirectly estimate the point boundary shear stress along the solid boundary." Patel (1965) proposed many mathematical connections for calculating the boundary shear stress in open channel flow. These relationships are as follows:

$$x^* = \log_{10}\left(\frac{\Delta p d^2}{4\rho v^2}\right) \tag{3.14}$$

$$y^* = 0.5x^* + 0.037 \quad \text{for } 0 < y^* < 1.5 \text{ and } 0 < x^* < 2.9 \tag{3.15}$$

$$y^* = 0.8287 - 0.1381x^* + 0.1437x^{*2} - 0.0060x^{*3} \text{ for } 1.5 < y^* < 3.5 \text{ and } 2.9 < x^* < 5.6 \tag{3.16}$$

$$y^* = \log_{10}\left(\frac{\tau_b d^2}{4\rho v^2}\right) \tag{3.17}$$

Where d is external diameter of the pitot-static tube (mm), v is kinematic viscosity of the liquid (m^2/s), Δp is pressure difference (KPa), ρ is density of water (Kg/m^3), x^*, y^* are non-dimensional parameters and τ_b is boundary shear stress (N/m^2).

As a consequence of this, the equations that were presented earlier were assessed via a process of trial and error, and one of the appropriate equations was chosen to compute the tractive stresses at the border, taking into consideration an assortment of x* numbers.

Following that, the evaluations of tractive stress were included over the whole depth in order to ascertain the average shear stress that was sustained by the compound section.

3.9 Measurement of sediment transport rate and bed profile

The sediment transport rate was calculated by measuring the quantity of material collected in a volumetric tank and sediment trap located downstream of the channel, for a certain period, at a specified flow rate. The weight of the sediment collected is ascertained by the use of the evaporation technique. Following the water that was on top of the wet sediment specimen is drained out, the specimen is transferred to a dish and then heated in an oven at a temperature that is slightly below the boiling point. This process continues until all of the noticeable wetness is removed. After that, the temperature of the oven is raised to 105°C and that temperature is kept there for a period of two hours. In the event that the specimen contains dissolved solids that are more than two percent of its total weight, the concentration of these solids needs to be tested separately in the water that was first used. When calculating the sediment concentration, it is necessary to deduct the amount of dissolved solids from the weight of the dried sediment. Prior to use, the exact dry weight of the evaporation dish is often measured with precision. It is essential to conduct regular checks throughout everyday operations to prevent any potential errors. During each run, the quantity of sediment carried is accumulated in the tank over a certain period, and the sediment transport rate (G_s) is determined using the following formula:

$$G_s = \frac{q}{t} = \frac{amount\ of\ sediment\ collected\ (g)}{Duration\ of\ sediment\ collection\ (sec)} \tag{3.18}$$

The morphology of an alluvial stream bed varies in response to variations in flow conditions. Ripples are formed on the bed of sand-bedded rivers as sediment particles are mobilized. As flow conditions alter, many types of bed shapes emerge, including dunes, flat beds, and sand waves. Varying bed shapes exhibit distinct levels of roughness, which in turn alters the resistance to flow and therefore impacts the flow and sediment movement. Fluvial streams exhibit variations in bed structure and resistance, which are the primary features that need further investigation. The longitudinal bed profile was measured at regular intervals of 0.3 m in the longitudinal direction using a point gauge. The ripple bed shape of a nonprismatic compound channel with both smooth and rough floodplains is illustrated in Fig. 3.9.
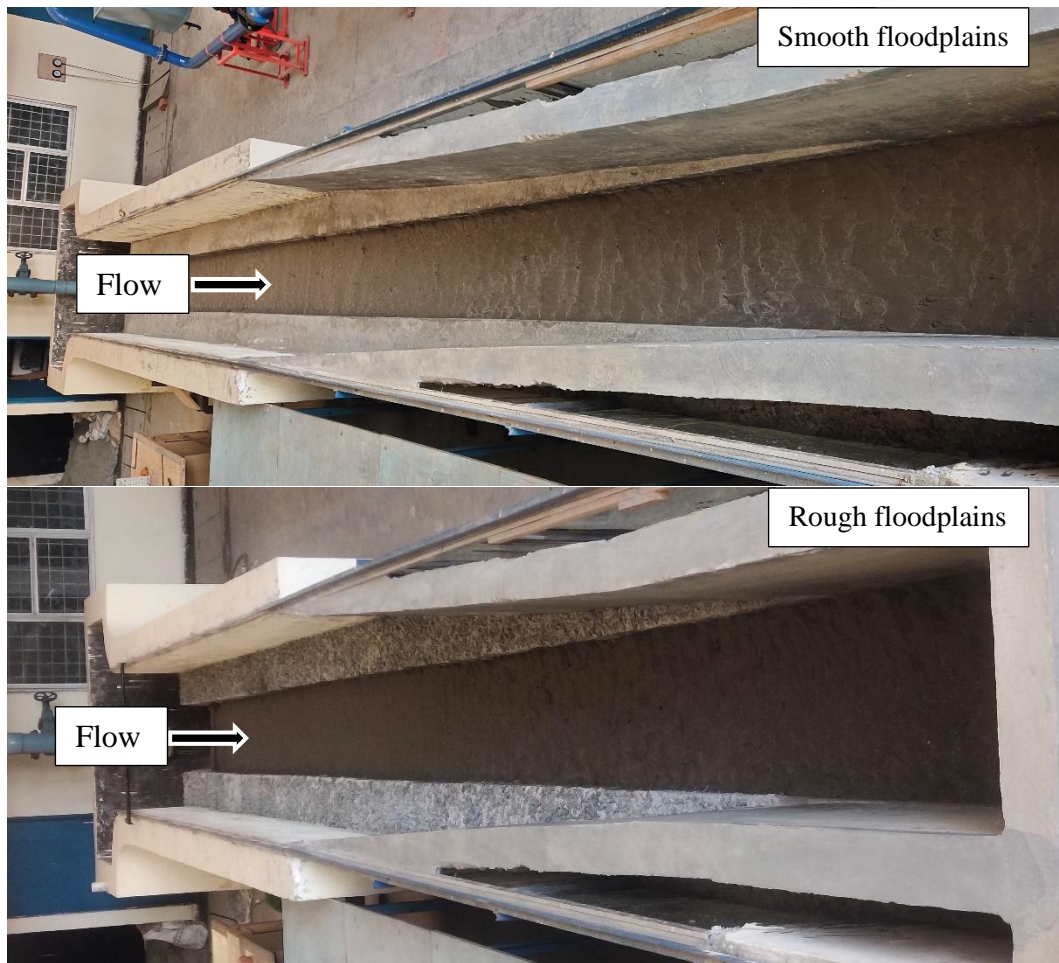
Fig. 3.9 Bed form for nonprismatic compound channel with smooth and rough floodplains

3.10 Computational analysis

3.10.1 General

Computation refers to the systematic transformation of input data into a desired output format via the application of certain control actions. In the context of computing, the term "antecedent" refers to the input, whereas the term "consequent" refers to the result. A mapping function is a process that transforms the input from one form to another form, producing the required output by implementing certain control actions. Computing may be classified into two distinct categories: hard computing and soft computing. Hard computing is a computational technique where we use pre-existing mathematical procedures to instruct the computer to solve certain problems, resulting in an accurate output value. An exemplary instance of hard computing involves a numerical issue. Soft computing is a methodology used to solve complicated issues when the output results are

imprecise or fuzzy. One key characteristic of soft computing is its adaptability, ensuring that any changes in the environment do not disrupt the current process. Soft computing is a field that relies on several approaches including fuzzy logic, genetic algorithms, artificial neural networks, machine learning, and expert systems (Ibrahim 2016). The following are the features of soft computing:

- The reason mathematical modeling is not necessary to address any given issue.
- When solving a problem with one input, it provides several answers over time.
- It employs biologically inspired approaches including genetics, evolution, particle swarming, and the human nervous system.
- Characterized by adaptability

Genetic algorithms are components of artificial intelligence and fuzzy computing that are primarily used to address diverse optimization challenges found in practical applications. The fundamental concept behind a genetic algorithm is to emulate the process of natural selection in order to identify an optimal solution for a certain application. A genetic algorithm is a machine learning model that is derived from the evolutionary process seen in nature. Genetic algorithms are effective tools for solving intricate search issues often encountered in engineering applications. For instance, they may explore a range of designs and components to identify the optimal combination that will provide a superior and more cost-effective design. Genetic algorithms are being used in several domains including climatology, biomedical engineering, code-breaking, control engineering, game theory, electronic design, and automated manufacturing and design (Ibrahim 2016).

The fundamental operations in genetic algorithms are:

- Initialization involves the creation of an initial population by a random process.
- Evaluation involves assessing each member of the population and determining the fitness of people based on their level of conformity to the desired standards.
- Selection refers to the process of choosing just those that meet the required criteria.
- Crossover is a process in which new people are generated by merging the most favorable characteristics of the current individuals. Ultimately, the goal is to produce persons that closely align with the required criteria. The procedure is iterated from the second stage until a termination condition is ultimately achieved.

3.10.2 Gene expression programming (GEP)

Utilizing GEP, a computational methodology, facilitates the development of computer programs with the ability to solve intricate problems. Cândida Ferreira, a PhD candidate at the University of Coimbra in Portugal, was the one who originally proposed the idea in 1992 as a component of her dissertation assignment. GEP is an evolutionary method used in computer programming to generate computer programs or models. These computer programs are intricate hierarchical arrangements that acquire knowledge and adjust by changing their dimensions, forms, and composition, like a living thing. Similar to live organisms, the computer programs of GEP are similarly stored in straightforward linear chromosomes of a set length. Therefore, GEP is a system that involves the relationship between genotype and phenotype. It utilizes a basic genome to store and pass on genetic information, while also having a sophisticated phenotype to interact with the environment and adjust accordingly.

Evolutionary algorithms use a group of people, choose individuals based on their fitness, and add genetic diversity via one or more genetic operators. GEP is a member of the evolutionary algorithms family and has strong connections to genetic algorithms and genetic programming. It acquired the linear chromosomes of a set length from genetic algorithms and the expressive parse trees of different sizes and forms from genetic programming. Within the framework of GEP, the linear chromosomes function as the genetic makeup or genotype, while the parse trees serve as the observable characteristics or phenotype, thereby establishing a genotype/phenotype system. The genotype/phenotype system is polygenic, meaning it encodes numerous parse trees in each chromosome. Consequently, the computer programs developed by GEP consist of several parse trees. Due to their origin from gene expression, these parse trees are referred to as expression trees (ET) in GEP. The benefits of a system such as GEP are evident from its inherent nature, but it is crucial to highlight the most significant advantages. Initially, the chromosomes are simple structures: they are linear, condensed, relatively petite, and can be easily modified genetically (duplicated, altered, combined, transferred, etc.). Secondly, the ETs are solely determined by their individual chromosomes. They are the creatures that undergo selection and, according to their fitness, are chosen to reproduce with alterations. During the process of reproduction, it is the chromosomes of the people that undergo reproduction with modifications and are passed on to the next

generation, not the extraterrestrials. Due to these characteristics, GEP is very adaptable and significantly outperforms the current evolutionary approaches.

The flowchart of a gene expression algorithm (GEA) is shown in Fig. 3.10. The method starts by randomly generating the chromosomes of the starting population. Next, the chromosomes undergo expression, and the fitness of each individual is assessed. Subsequently, individuals are chosen based on their suitability to reproduce with alterations, resulting in offspring with novel characteristics. The individuals of this next generation undergo a similar developmental process, which includes the expression of their genomes, exposure to the selection environment, and reproduction with modifications. Until an outcome is found, the method is repeated until a specific amount of iterations has passed, whichever comes first. Reproduction encompasses both the process of copying genetic material and the activity of genetic operators that generate genetic variation. Replication involves the duplication and transmission of the genome to the next generation. Replication alone is insufficient to create variation. Genetic variation is only introduced into the population via the activity of the remaining operators. These operations stochastically pick the chromosomes that will undergo modification.

In GEP, a chromosome may undergo modification by one or more operators simultaneously, or it may remain unmodified. GEP genes consist of a distinct head and tail. The head of the symbol includes representations of both functions and terminals, whereas the tail solely contains terminals. Hence, distinct sets of letters are present in separate sections of a gene. GEP chromosomes often consist of many genes that are of identical length. For each issue or run, the selection is made for the number of genes and the length of the head. Every gene encodes a subunit of an ET, and these subunits interact with each other to build a more intricate multi-subunit ET. Within the realm of nature, the phenotype exhibits various degrees of intricacy, with the highest amount of complexity residing in the organism as a whole. However, it is important to note that tRNAs, proteins, ribosomes, cells, and other similar components are all outcomes of gene expression, and they are all ultimately determined by the genetic information stored in the genome. Regardless of the situation, the process of expressing genetic information always begins with transcription, which is the creation of RNA. In the case of protein genes, this is followed by translation, which is the creation of proteins. An important use of GEP is symbolic regression or function discovery, which aims to discover an

expression that performs well for all fitness situations within a certain margin of error from the right value.

In some mathematical applications, using minor relative or absolute mistakes might be advantageous for uncovering an optimal solution. However, when the range of selection is too limited, populations undergo delayed evolution and become unable to discover an accurate answer. Conversely, if the selection range is expanded, a multitude of solutions with high fitness may emerge, although being far from optimal. Through the processes of natural selection and chance in the game of roulette, some people are chosen to reproduce with changes in their genetic makeup. This leads to the essential diversity of genes, which ultimately enables evolution to occur throughout time. With the exception of replication, which involves the precise copying of genomes from all chosen people, all other operators randomly choose chromosomes to undergo certain modifications. However, with the exception of mutation, each operator is prohibited from altering a chromosome more than once. For example, when the transposition rate is set at 0.7, a random selection is made from a pool of 10 distinct chromosomes, with seven of them being picked. In GEP, a chromosome may be selected by zero or more genetic operators that introduce diversity in the population. This characteristic also sets GEP apart from GP, since it ensures that an entity is never updated by more than one operator simultaneously. Therefore, under the GEP framework, the genetic operators undergo several alterations throughout reproduction, resulting in children that are very distinct from their parents.

Replication, although essential, is the least captivating process since it does not independently contribute to genetic variation. Replication, in conjunction with selection, is alone responsible for inducing genetic drift. Based on the principles of fitness and chance in the game of roulette, chromosomes are accurately replicated in the next generation. The more physically fit a person is, the greater the likelihood of producing a larger number of children. Therefore, during replication, the genomes of the chosen people are duplicated a number of times according to the result of the roulette. The roulette wheel is rotated an equal number of times as there are persons in the population, consistently preserving the population size. Genetic mutations have the potential to manifest at any location within the chromosome. Nevertheless, it is essential to maintain the structural integrity of chromosomes. In the heads of the symbols, every symbol has the ability to transform into another symbol, whether it is a function or a terminal.

However, in the tails, terminals can only transform into other terminals. By maintaining the structural arrangement of chromosomes, all the offspring resulting from mutation possess structurally accurate programming. Point mutations in a gene's sequence may either cause a tiny alteration in the protein's structure or have no effect at all. These neutral mutations are rather common, such as mutations in introns or mutations that result in the same amino acid owing to the redundancy of the genetic code. While neutral mutations, such as those occurring in noncoding areas, sometimes occur, a mutation in the coding sequence of a gene has a far greater impact, often leading to a dramatic alteration of the resulting organism. The transposable elements of GEP are genomic segments capable of being mobilized and translocated to different locations within the chromosome. Within the field of genetics and evolutionary biology, the term GEP refers to the phenomenon of transposable elements, which may be classified into three distinct categories. (1) Brief pieces containing a functional or terminal element that move to the beginning of genes, save for the root (known as insertion sequence elements or IS elements). (2) Brief fragments with a function located at the beginning that move to the core of genes (core IS elements or CIS elements). (3) Whole genes that relocate to the start of chromosomes. The presence of IS and RIS elements is a residue of the developmental progression of GEP.

Initially, the earliest GEA used single-gene chromosomes, rendering a gene with a terminal at the root practically useless. The introduction of multigenic chromosomes retained this characteristic since these operators play a crucial role in comprehending the processes of genetic variation and evolvability. All RIS components are selected from sequences of the heads based on their purpose. In this process, a point is selected at random at the beginning of the sequence, and the gene is examined in the direction of its end until a function is discovered. This function serves as the initial location of the RIS element. If no functions are detected, it remains inactive. Within the GEP framework, recombination may occur in three distinct forms: one-point recombination, two-point recombination, and gene recombination. Regardless of the situation, two parent chromosomes are selected at random and joined together to exchange genetic material. During one-point recombination, the chromosomes undergo a process where they exchange genetic material at a randomly selected place, resulting in the formation of two daughter chromosomes. In two-point recombination, the chromosomes undergo pairing, and the two places of recombination are selected at random. The genetic material located

between the recombination points is subsequently swapped between the two chromosomes, resulting in the creation of two new daughter chromosomes. Two-point recombination possesses a higher capacity for transformation compared to one-point recombination. It is particularly valuable for developing solutions to more intricate problems, particularly when employing multigenic chromosomes consisting of multiple genes. It is important to mention that this operator lacks the ability to generate new genes. Instead, it produces persons that are composed of diverse combinations of already existing genes. When gene recombination is the only source of genetic variety, solving increasingly complicated issues requires extremely large beginning populations to ensure a sufficient diversity of genes. Nevertheless, the innovative potential of GEP relies not only on the recombination of genes or building blocks but also on the continuous generation of new genetic material. (Ferreira 2001)
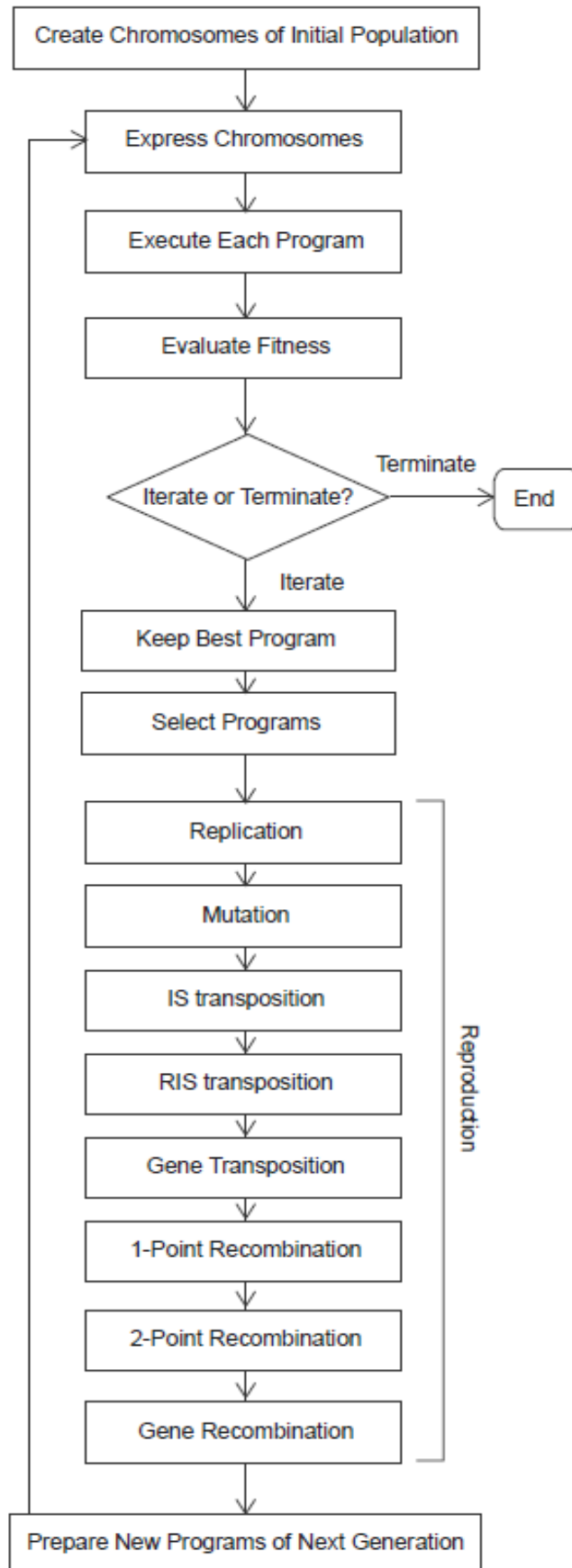
Fig. 3.10 Flowchart of a gene expression algorithm (Ferreira 2001)

3.10.3 Model formation

Several researchers have conducted calculations to evaluate the flow rate of compound open channels. Theoretical methods, such as the single channel method (SCM), use equation (3.19) for the computation of the discharge. By using this method, the cross-section of the composite waterway is considered to be an integrated component. There is no difference in the mathematical structure between basic and complex systems. The assessment of flow potential is the principal limitation of the SCM. This is especially true in situations when the flow levels in the primary waterway increase, which results in overflowing in flooded areas that are located close to the primary waterway. Therefore, when the wetted perimeter is increased in contrast to the wetted area, the predicted discharge is lower than the discharge that was observed. In addition, the rate of release that is predicted by SCM is ultimately fewer than the values that are really in existence. An alternative method is the divided channel method (DCM), which uses equation (3.20) to compute the discharge. This approach involves doing independent assessments of the flow in each individual portion. Hence, the aggregate discharge in the compound section may be ascertained by adding together the discharges of each subsection. The approach is classified into three distinct categories: horizontal divided channel method (HDCM), vertical divided channel method (VDCM), and diagonal divided channel method (DDCM). The categorization is determined by the orientation of the dividing line, which may be either horizontal, vertical, or diagonal. The line is delineated from the junction of the primary waterway and zones of flooding, as seen in Fig. 3.11. Das et al. (2019) proposed a new equation (3.21) using the GEP approach to analyze the flow rate in nonprismatic compound channels. Naik et al. (2017b) devised a mathematical equation (3.22) to predict the rate of flow in compound channels with converging floodplains.

$$Q = \frac{1}{n} A R^{2/3} \sqrt{S_o} \tag{3.19}$$

$$Q = \sum_{i=1}^{N} \frac{A_i R_i^{2/3}}{n_i} \sqrt{S_o} \tag{3.20}$$

$$\left(\frac{Q}{Q_b}\right) = -0.076 \times \beta F_r^{-1} + R_r^{-S_o} + \left(\frac{\beta}{F_r}\right)^{R_r^{S_o}} \tag{3.21}$$

$$Q = \frac{\sqrt{S_o}}{n_{mc}} A_{mc}^{5/3} (P_{mc} + X_{mc})^{-2/3} + \frac{\sqrt{S_o}}{n_{fp}} A_{fp}^{5/3} \left(P_{fp} + X_{fp}\right)^{-2/3} \tag{3.22}$$

Where,

$$X_{mc} = P_{mc} \left[\frac{100}{(100 - \% S_{fp})} \left(\frac{A_{mc}}{A} - 1\right) \right] \tag{3.23}$$

$$X_{fp} = P_{fp}\left[\frac{100}{\%S_{fp}}\left(\frac{A_{mc}}{A} - 1\right) + 1\right] \tag{3.24}$$

$$\%S_{fp} = 18.505 + 62.140(\beta)^{0.631} - 24.42(X_r) + 1.38(\theta) \tag{3.25}$$

Where Q is discharge at any depth (m³/s), A is flow area (m²), R is hydraulic radius (m), S_o is longitudinal bed slope (dimensionless), n is Manning's roughness coefficient (dimensionless), Q_b is bankfull discharge (m³/s), β is relative flow depth (dimensionless), F_r is Froude number (dimensionless), R_r is Reynolds number (dimensionless), A_{mc} is main channel flow area (m²), A_{fp} is floodplain flow area (m²), P_{mc} is wetted perimeter of main channel (m), P_{fp} is wetted perimeter of floodplain (m), n_{mc} is Manning's roughness coefficient of main channel (dimensionless), n_{fp} is Manning's roughness coefficient of floodplain (dimensionless), X_{mc} is proportionate length of interface to be included in main channel perimeter (m), X_{fp} is proportionate length of interface to be excluded in floodplain perimeter (m), S_{fp} is floodplain shear force expressed as percent of total shear force (percent), θ is converging angle (degree) and X_r is relative distance (dimensionless).
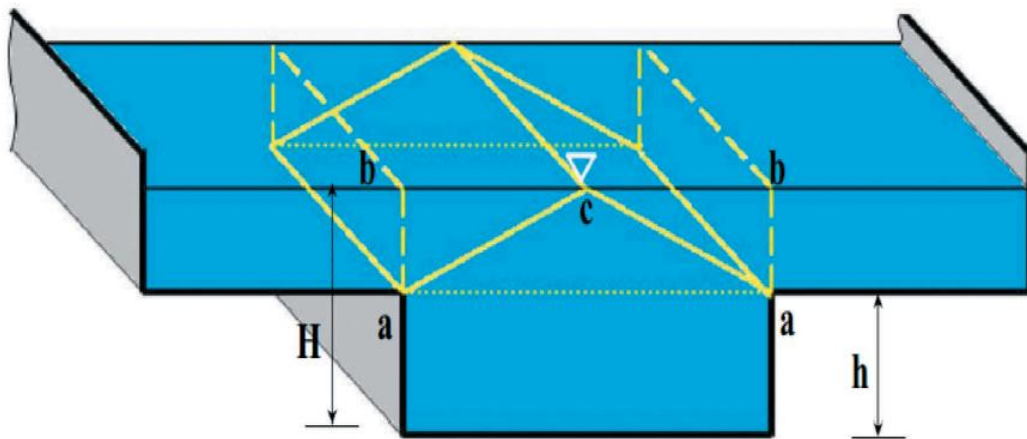
Fig. 3.11 Types of separating boundaries between the primary waterway and floodplains (Das et al. 2019)

The discharge in a compound channel with non-uniform cross-section is affected by several factors, such as the width ratio (α) (ratio of the total channel width to the main channel width), the relative depth of flow (β) (ratio of the overbank flow depth to the overall flow depth), the differential roughness (γ) (ratio of Manning's roughness coefficient for the floodplains to that for the main channel), the aspect ratio (δ) (ratio of the main channel width to its depth), the converging angle (θ), the relative distance (X_r) (ratio of the distance between two converging sections to the length of a converging section), the average size of particles (D_{50}), the longitudinal bed slope (S_o), the energy

slope (S_e), the Froude number (F_r) (ratio of inertial forces to gravitational forces), the Reynolds number (R_e) (ratio of inertial forces to viscous forces), Manning's roughness coefficient (n), and the floodplain shear force (S_{fp}) (expressed as percentage of total shear force). A comprehensive selection of parameters is meticulously made to ensure that the ultimate model equation may be efficiently applied to a wide variety of channels.

Discharge ratio (Q_r) is a dimensionless parameter that represents the ratio of discharge at any given depth to the bankfull discharge. The required equation for discharge ratio may be formulated as:

$$Q_r = F(\alpha, \beta, \gamma, \delta, \theta, X_r, D_{50}, S_o, S_e, F_r, R_e, n, S_{fp}) \tag{3.26}$$

The variables selection for different model formations for the prediction of discharge in nonprismatic compound channels is done on the basis of two criteria: first, correlation among the parameters and second, gamma test.

Based on the correlation among the parameters (correlation matrix as shown in Table 3.1), three models were formed with variables ranging from 7 to 8 and they are:

C1: $\quad Q_r = F(\alpha, \gamma, \theta, S_o, F_r, R_e, S_{fp})$

C2: $\quad Q_r = F(\alpha, \gamma, \theta, S_o, S_e, F_r, R_e, S_{fp})$

C3: $\quad Q_r = F(\alpha, \gamma, \theta, S_o, F_r, R_e, n, S_{fp})$

In order to determine the optimal input combination, a trial-and-error approach must be conducted. The gamma test offers valuable insights for identifying the optimal input variables to build a dependable and seamless model. Additionally, it minimizes the amount of labor needed to create models by taking into account all possible input combinations. The Gamma test is a non-parametric test that computes a test statistic by measuring the average squared differences between observed and predicted outcomes, assuming a Gamma distribution. This is usually done using chi-square or maximum likelihood estimation techniques. Using the gamma test, over 20 models were created which resulted in gamma values ranging from 0.15 to 0.002. Models with gamma values below 0.05 were chosen for study, with the number of variables ranging from 13 to 4. The selected models are as follows:

M1: $Q_r = F(\alpha, \beta, \gamma, \delta, \theta, X_r, D_{50}, S_o, S_e, F_r, R_e, n, S_{fp})$

M2: $Q_r = F(\alpha, \beta, \gamma, \delta, \theta, X_r, S_o, S_e, F_r, R_e, n, S_{fp})$

M3: $Q_r = F(\alpha, \beta, \gamma, \delta, \theta, X_r, S_e, F_r, R_e, n, S_{fp})$

M4: $Q_r = F(\alpha, \beta, \gamma, \theta, X_r, S_e, F_r, R_e, n, S_{fp})$

M5: $Q_r = F(\alpha, \beta, \gamma, \theta, X_r, S_e, F_r, n, S_{fp})$

M6: $Q_r = F(\alpha, \beta, \theta, X_r, S_e, F_r, n, S_{fp})$

M7: $Q_r = F(\alpha, \beta, \theta, X_r, F_r, n, S_{fp})$

M8: $Q_r = F(\alpha, \beta, \theta, X_r, n, S_{fp})$

M9: $Q_r = F(\alpha, \beta, \theta, X_r, S_{fp})$

M10: $Q_r = F(\alpha, \beta, \theta, S_{fp})$

In this research, a modeling technique is used where the desired value is represented as Q_r, and the independent components are considered as input variables, as stated in equation (3.26). The model's structure was constructed using the four fundamental arithmetic operators ($+, -, \times, /$) in conjunction with GeneXproTools 5.0 (2014). Multiple models were developed using high-quality experimental datasets, which included three distinct types of converging compound channels from Naik and Khatua (2016), three sets of converging compound channel data from Rezaei (2006), and data from the current study (specifics of the datasets can be found in Table 3.2). The current work used the data for training the models, whereas two additional datasets from prior studies were included for testing and validation purposes. The characteristics of the different GEP models are shown in Table 3.3. An example of a function of fitness that was used in this investigation was the root-mean-squared error (RMSE), which is abbreviated as E_i. Through the use of an equation that was developed from an expression tree, the fitness (f_i) was computed. This equation took into account the total number of mistakes that were produced with respect to the target value. The approach of genetic component integration included the use of the addition technique.

Table 3.1 Correlation matrix

	α	β	γ	δ	θ	X_r	D_{50}	S_o	S_e	F_r	R_e	n	S_{fp}	Q_r
α	1.000	0.030	5.0E-17	-4.7E-17	0.000	-0.985	-7.8E-18	-2.9E-15	-0.544	-0.075	-0.134	0.054	0.573	0.024
β	0.030	1.000	-2.3E-01	2.7E-01	0.000	-0.031	2.7E-01	1.4E-15	-0.482	-0.656	0.176	0.677	0.825	0.902
γ	0.000	-0.233	1.0E+00	-8.6E-01	0.000	0.000	-8.6E-01	-1.8E-15	0.461	0.735	0.728	-0.594	-0.194	-0.304
δ	0.000	0.271	-8.6E-01	1.0E+00	0.000	0.000	1.0E+00	0.0E+00	-0.426	-0.809	-0.850	0.764	0.226	0.362
θ	0.000	0.000	0.0E+00	0.0E+00	1.000	0.000	0.0E+00	0.0E+00	0.000	0.000	0.000	0.000	0.000	0.000
X_r	-0.985	-0.031	-8.3E-18	0.0E+00	0.000	1.000	5.7E-18	0.0E+00	0.568	0.098	0.138	-0.035	-0.582	-0.024
D_{50}	0.000	0.271	-8.6E-01	1.0E+00	0.000	0.000	1.0E+00	-2.3E-15	-0.426	-0.809	-0.850	0.764	0.226	0.362
S_o	0.000	0.000	-1.8E-15	0.0E+00	0.000	0.000	-2.3E-15	1.0E+00	0.000	0.000	0.000	0.000	0.000	0.000
S_e	-0.544	-0.482	4.6E-01	-4.3E-01	0.000	0.568	-4.3E-01	3.0E-15	1.000	0.644	0.274	-0.354	-0.710	-0.457
F_r	-0.075	-0.656	7.4E-01	-8.1E-01	0.000	0.098	-8.1E-01	4.1E-16	0.644	1.000	0.455	-0.798	-0.599	-0.618
R_e	-0.134	0.176	7.3E-01	-8.5E-01	0.000	0.138	-8.5E-01	7.1E-16	0.274	0.455	1.000	-0.463	0.065	-0.003
n	0.054	0.677	-5.9E-01	7.6E-01	0.000	-0.035	7.6E-01	3.9E-17	-0.354	-0.798	-0.463	1.000	0.570	0.698
S_{fp}	0.573	0.825	-1.9E-01	2.3E-01	0.000	-0.582	2.3E-01	3.8E-15	-0.710	-0.599	0.065	0.570	1.000	0.713
Q_r	0.024	0.902	-3.0E-01	3.6E-01	0.000	-0.024	3.6E-01	-2.8E-16	-0.457	-0.618	-0.003	0.698	0.713	1.000

Table 3.2 Statistical characteristics of the dataset used in the study

Verified test channel	Type of channel	Cross-sectional geometry	Range	α	β	γ	δ	θ	X_r	D_{50}	S_o	S_e	F_r	R_e	n	S_{fp}	Q_r
Rezaei (2006) channel	Converging (without sediment)	Rectangular	Minimum	1.000	0.146	1.000	7.96	1.91	0.000	0.00	0.0020	0.00018	0.194	24488.34	0.01132	25.948	1.300
			Maximum	3.000	0.505	1.000	7.96	11.31	1.000	0.00	0.0020	0.00256	0.793	172686.28	0.01290	74.432	3.960
			Average	2.153	0.344	1.000	7.96	5.35	0.378	0.00	0.0020	0.00125	0.491	64196.43	0.01186	47.968	2.125
			Median	2.250	0.358	1.000	7.96	3.81	0.375	0.00	0.0020	0.00119	0.483	55468.17	0.01181	47.724	1.800
			Standard Deviation	0.603	0.108	0.000	0.00	3.85	0.258	0.00	0.0000	0.00065	0.147	29796.90	0.00375	9.758	0.758
Naik and Khatua (2016) channel	Converging (without sediment)	Rectangular	Minimum	1.000	0.029	1.000	5.00	5.00	0.000	0.00	0.0011	0.0007	0.407	93481.72	0.01130	7.658	0.976
			Maximum	1.800	0.329	1.000	5.00	12.38	1.000	0.00	0.0011	0.00167	0.630	234238.2	0.01185	66.124	2.002
			Average	1.389	0.212	1.000	5.00	7.70	0.514	0.00	0.0011	0.00123	0.557	156871.6	0.01147	39.581	1.452
			Median	1.379	0.219	1.000	5.00	5.00	0.529	0.00	0.0011	0.00122	0.559	155095.2	0.01144	40.083	1.451
			Standard Deviation	0.252	0.071	0.000	0.00	2.96	0.315	0.00	0.0000	0.0002	0.049	31628.44	0.00125	11.837	0.238
Present channel	Converging (without sediment)	Rectangular	Minimum	0.840	0.053	1.000	2.00	4.00	0.000	0.00	0.0010	0.00023	0.208	177368.6	0.00893	9.303	1.062
			Maximum	2.000	0.599	1.545	2.00	4.00	1.000	0.00	0.0010	0.0015	0.482	603135.5	0.02182	69.001	3.024
			Average	1.481	0.335	1.273	2.00	4.00	0.500	0.00	0.0010	0.0008	0.344	383708	0.01447	41.636	1.798
			Median	1.500	0.339	1.273	2.00	4.00	0.500	0.00	0.0010	0.00085	0.346	368213.9	0.01426	42.901	1.616
			Standard Deviation	0.343	0.182	0.273	0.00	0.00	0.313	0.00	0.0000	0.00034	0.065	123268.8	0.00303	14.085	0.647
Present channel	Converging (with sediment)	Rectangular	Minimum	0.840	0.159	0.440	5.00	4.00	0.000	0.80	0.0010	0.00017	0.099	28577.57	0.01157	19.130	1.243
			Maximum	2.000	0.598	0.680	5.00	4.00	1.000	0.80	0.0010	0.00099	0.264	159492	0.03383	68.989	3.439
			Average	1.481	0.385	0.560	5.00	4.00	0.500	0.80	0.0010	0.00055	0.203	74741.38	0.02281	45.168	2.098
			Median	1.500	0.388	0.560	5.00	4.00	0.500	0.80	0.0010	0.00053	0.211	68129.47	0.02251	45.265	1.896
			Standard Deviation	0.343	0.151	0.120	0.00	0.00	0.313	0.00	0.0000	0.00021	0.036	32436.25	0.00428	11.764	0.729

Table 3.3 Selection standards and attributes for the GEP models

Attribute Description	C1	C2	C3	M1	M2	M3	M4	M5	M6	M7	M8	M9	M10
Set of function	$+,-,\times,/$	$+,-,\times,/$	$+,-,\times,/$	$+,-,\times,/$	$+,-,\times,/$	$+,-,\times,/$	$+,-,\times,/$	$+,-,\times,/$	$+,-,\times,/$	$+,-,\times,/$	$+,-,\times,/$	$+,-,\times,/$	$+,-,\times,/$
Chromosomes number	30	30	30	30	30	30	30	30	30	30	30	30	30
Head size	8	8	10	12	12	12	10	10	8	8	8	8	10
Number of genes	3	3	4	6	6	6	4	4	3	3	3	3	3
Size of gene	26	26	32	38	38	40	32	34	26	26	28	30	28
Linking Function	Addition	Addition	Addition	Addition	Addition	Addition	Addition	Addition	Addition	Addition	Addition	Addition	Addition
Fitness Function	RMSE	RMSE	RMSE	RMSE	RMSE	RMSE	RMSE	RMSE	RMSE	RMSE	RMSE	RMSE	RMSE
Size of program	45	47	64	104	112	114	62	60	45	45	43	49	41
Literals	15	15	24	40	44	47	23	26	19	15	16	19	9
Number of Generations	1233711	1173740	760039	162013	687396	647142	645192	596737	691550	711214	511813	426182	440418
Constants per Gene	10	11	10	10	10	10	10	10	10	10	10	10	10
Data Type	Floating-point	Floating-point	Floating-point	Floating-point	Floating-point	Floating-point	Floating-point	Floating-point	Floating-point	Floating-point	Floating-point	Floating-point	Floating-point
Mutation	0.00138	0.00138	0.00138	0.00138	0.00138	0.00138	0.00138	0.00138	0.00138	0.00138	0.00138	0.00138	0.00138
Inversion	0.00546	0.00546	0.00546	0.00546	0.00546	0.00546	0.00546	0.00546	0.00546	0.00546	0.00546	0.00546	0.00546
Gene recombination rate	0.00277	0.00277	0.00277	0.00277	0.00277	0.00277	0.00277	0.00277	0.00277	0.00277	0.00277	0.00277	0.00277

3.11 Statistical measures

Diverse error analysis methodologies were used to assess the precision of the GEP models. "The identified metrics encompassed the coefficient of determination (R²), root mean square error (RMSE), mean absolute percentage error (MAPE), scatter index (SI), and the Akaike Information Criterion (AIC)." The applicable formulae were used to calculate these measures:

$$R^2 = \frac{\sum_{i=1}^{N}(a_i-\bar{a})^2\,(p_i-\bar{p})^2}{\sum_{i=1}^{N}(a_i-\bar{a})^2\;\sum_{i=1}^{N}(p_i-\bar{p})^2} \tag{3.27}$$

$$RMSE = \sqrt{\frac{1}{N}\sum_{i=1}^{N}(p_i-a_i)^2} \tag{3.28}$$

$$MAPE(\%) = \frac{1}{N}\sum_{i=1}^{N}\left(\frac{|p_i-a_i|}{a_i}\times 100\right) \tag{3.29}$$

$$SI = \sqrt{\frac{\sum_{i=1}^{N}[(p_i-\bar{p})-(a_i-\bar{a})]^2}{\sum_{i=1}^{N}a_i^2}} \tag{3.30}$$

$$AIC = N\log\left(\frac{1}{N}\sum_{i=1}^{N}(p_i-a_i)^2\right)+2k \tag{3.31}$$

Where a is actual values, p is predicted values, $\bar{a}$ is mean of actual values, $\bar{p}$ is mean of predicted values, N is number of datasets and k is number of variables.

CHAPTER 4

RESULTS AND DISCUSSIONS

This chapter of the thesis outlines the experimental findings concerning various scenarios of nonprismatic compound channels. The experiments focused on a specific type of nonprismatic compound channel characterized by a converging floodplain angle of 4°, a converging length of 3.6 m, and varying width ratios from 2 to 5. Tests were conducted on each nonprismatic compound channel under five distinct overbank flow conditions, with relative flow depths (β) of 0.20, 0.30, 0.40, 0.50, and 0.60. Relative flow depth (β) is a dimensionless parameter and it is defined as the ratio of the overbank flow depth to the total flow depth. As the relative flow depth increases, a larger proportion of the water is found above the main channel, which can significantly affect the flow dynamics. This dimensionless parameter allows for a comparison across different channel designs and conditions, making it an essential factor in the analysis and design of compound channels. The primary objectives of these experiments were to analyze (i) stage-discharge relationships, (ii) water surface profiles, (iii) depth-averaged velocity distribution, (iv) longitudinal changes in average velocities, (v) distribution of tractive stresses at the walls, and (vi) energy losses at different nonprismatic sections of the compound channel. The study of these flow characteristics in compound channels is crucial for accurately predicting water behavior during varying flow conditions, such as floods. Stage-discharge relationships and water surface profiles help in estimating discharge rates and managing flood risks, while depth-averaged velocity distribution and longitudinal changes in velocity are key to understanding flow patterns and sediment transport. The distribution of boundary shear stress aids in assessing erosion potential and channel stability, and analyzing energy losses is vital for optimizing hydraulic designs and improving the efficiency of water conveyance systems. This knowledge ensures better water management, infrastructure planning, and environmental protection.

The flow rate in a nonprismatic compound channel with converging floodplains was predicted using Gene Expression Programming (GEP), taking into account both geometric and flow variables, based on the experimental data. The generated models for estimating the flow rate in nonprismatic compound channels were evaluated by statistical goodness of fit tests, which included comparing the proposed approach with theoretical methodologies and previously developed approaches from other researchers.

4.1 Flow characteristics in nonprismatic compound channels without sediment

The stage-discharge relationship for the prismatic section (PS) and nonprismatic sections (NPS) of the compound channel with smooth and rough floodplains are represented in Fig. 4.1 and 4.2. The flow depth rises as the discharge increases linearly up to the bankfull depth. However, there is a minor fall in increment beyond bankfull depth due to interaction and additional momentum transfer between the primary waterway and floodplains. The flow depth reduces for the same discharge in the converging section from NPS1 to NPS5 as a result of the converging geometry of the channel which leads to flow acceleration. A similar trend has been observed for nonprismatic compound channels with rough floodplains. However, for the same discharge, depth in nonprismatic compound channels with rough floodplains is less when compared to smooth floodplains. This is due to the increased resistance to flow in a compound channel with rough floodplains. In a rough floodplain, the irregularities and roughness of the floodplain disrupt the flow, causing more energy losses through friction. As a result, the water in a rough floodplain will need to accelerate to overcome these losses, which leads to a decrease in flow depth compared to a smooth floodplain where the flow encounters less resistance and can maintain a higher depth for the same discharge. For both in-bank and over-bank flow in prismatic and nonprismatic sections, it has been discovered that a power function is the line of progression that provides the appropriate fitting.

For various relative flow depths ranging from 0.20 to 0.60, the water surface profile along the longitudinal distance of the nonprismatic compound channel for both smooth and rough floodplains are illustrated in Fig. 4.3. Remarkably, the water surface profile in the prismatic section of the compound channel remains consistent. However, in the converging section of the channel, the water level (M$_2$ profile) decreases due to the converging geometry of the channel, resulting in increased flow acceleration, particularly during the latter half of the transition. In the portion of the waterway that is located downstream, the flow is almost consistent, with a few minor sways. The nonprismatic compound channel with smooth and rough floodplains exhibits a drop in flow depth ranging from 3.5 to 4.5 percent and 4 to 5 percent, respectively.

The variation in energy slope with respect to longitudinal distance for various relative depths in a nonprismatic compound channels with smooth and rough floodplains is shown in Fig. 4.4. As the longitudinal distance rises, there is a corresponding increase in

the energy slope due to an upsurge in energy loss. The converging geometry of the section results in a progressive rise until the midpoint, followed by a sudden increase in the latter half of the section, causing flow acceleration. In regard to rough floodplains, it has been shown that the energy slope is greater in comparison to smooth floodplains. This may be attributed to the increased loss of head resulting from the channel shape and roughness of the floodplains. The energy slope in a nonprismatic compound channel with rough floodplains, compared to smooth floodplains, increased by 4.34%, 8.08%, 10.91%, 13.55%, and 15.15% for prismatic sections, and by 51.27%, 51.37%, 51.32%, 51.31%, and 51.41% for nonprismatic sections, respectively, for relative depths of 0.20, 0.30, 0.40, 0.50, and 0.60.

The variations in average velocity over the longitudinal distance for varying relative flow depths in a nonprismatic compound channel with smooth and rough floodplains are shown in Fig. 4.5. The research findings indicate that there is an upward trend of the average velocity along the longitudinal distance of the channel. The prismatic segment exhibited a uniform variation, however, the nonprismatic sections had a considerable spike, which may be attributed to the constriction in the shape of the channel. In the case of smooth floodplains, the increase in velocity was seen up to 2.27%, 1.40%, 0.82%, 0.50%, and 0.30% in the prismatic part, and 15.00%, 23.26%, 31.00%, 38.23%, and 42.28% in the nonprismatic section, respectively, at relative depths of 0.20, 0.30, 0.40, 0.50, and 0.60. A similar pattern has been seen in the case of compound channels including rough floodplains. In the case of rough floodplains, the increase in velocity was seen up to 2.23%, 1.48%, 0.92%, 0.50%, and 0.29% in the prismatic portion, and 12.92%, 19.56%, 26.06%, 32.10%, and 35.63% in the nonprismatic portions, respectively, at relative depths of 0.20, 0.30, 0.40, 0.50, and 0.60. In compound channels with rough floodplains, the velocity is lesser as compared to smooth floodplains due to the presence of irregularities on the floodplain surface thereby creating frictional resistance, which tends to slow down the flow. The decrease in velocity is seen up to 2.56%, 3.75%, 4.50%, 5.07%, and 5.50% at relative depths of 0.20, 0.30, 0.40, 0.50, and 0.60, respectively, compared to smooth floodplains.

The depth-averaged velocity distribution over the cross-section for different relative depths at the prismatic and various nonprismatic sections for compound channels with smooth and rough floodplains are represented in Fig. 4.6 and 4.7. The position Y (on x-axis) represents the width of the channel section over which distribution is presented. As

a consequence of these figures, it has been determined that the distribution of depth-averaged velocity is fairly uniform in all segments and that they steadily grow from PS to NPS5. The primary waterway velocity is higher than the velocity in the floodplains, and it progressively rises in the downstream direction owing to the flow acceleration from the converging geometry of the channel. At the higher relative depths, the increase in the center line velocity is found to be more as the flow progresses downstream. The velocity in the floodplains decreases and reaches to minimum at the channel boundaries at lower relative depths. While, at higher relative depths, velocity increases in the interface region of the primary waterway and flooding zones due to the shift of momentum from the primary waterway to floodplains and then, reaches to minimum at the floodplain ends.
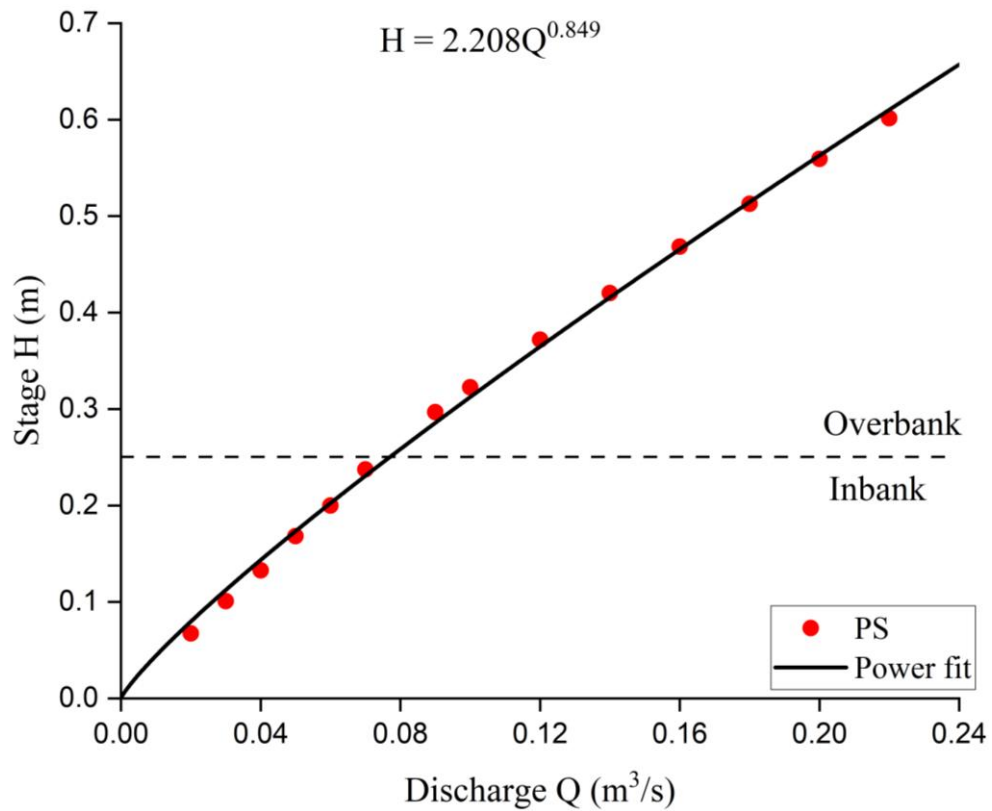
(a)
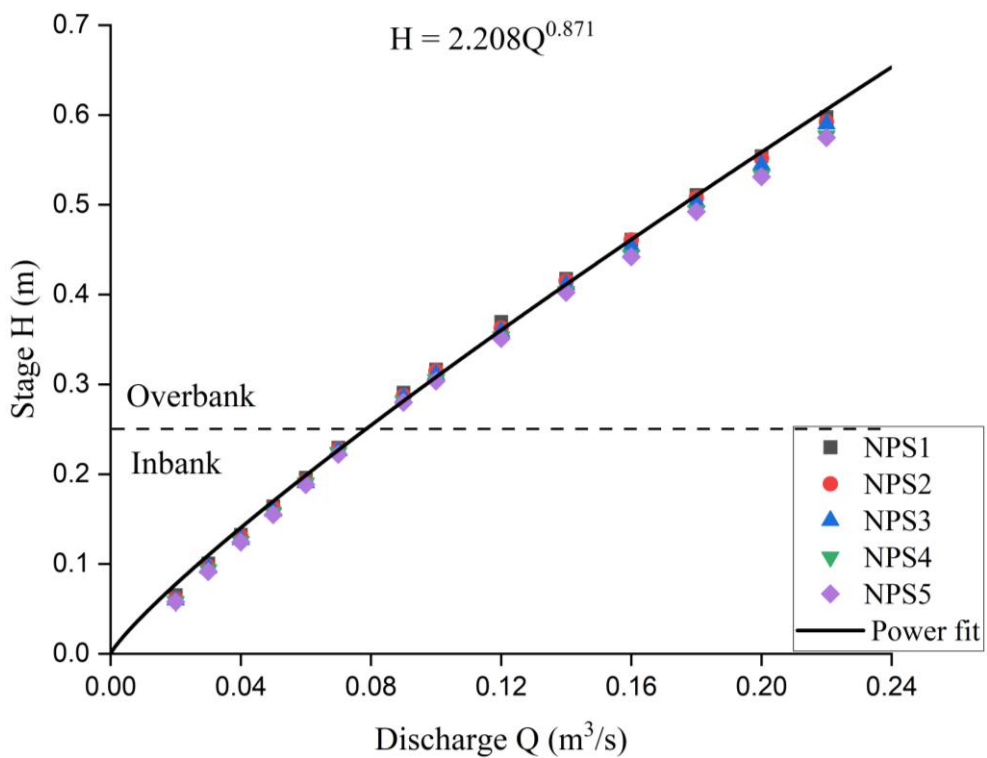
(b)

Fig. 4.1 Stage-discharge relationship for (a) prismatic section and (b) nonprismatic sections of the compound channel with **smooth floodplains**

$$H = 2.208Q^{0.865}$$

(a)

$$H = 2.208Q^{0.895}$$
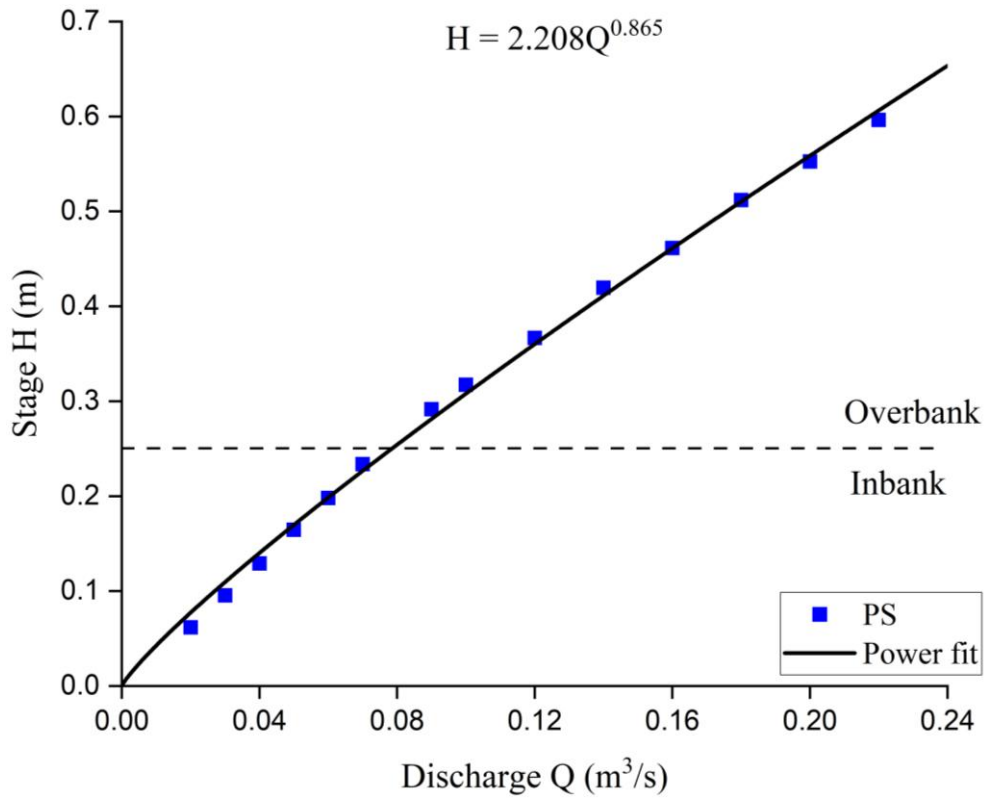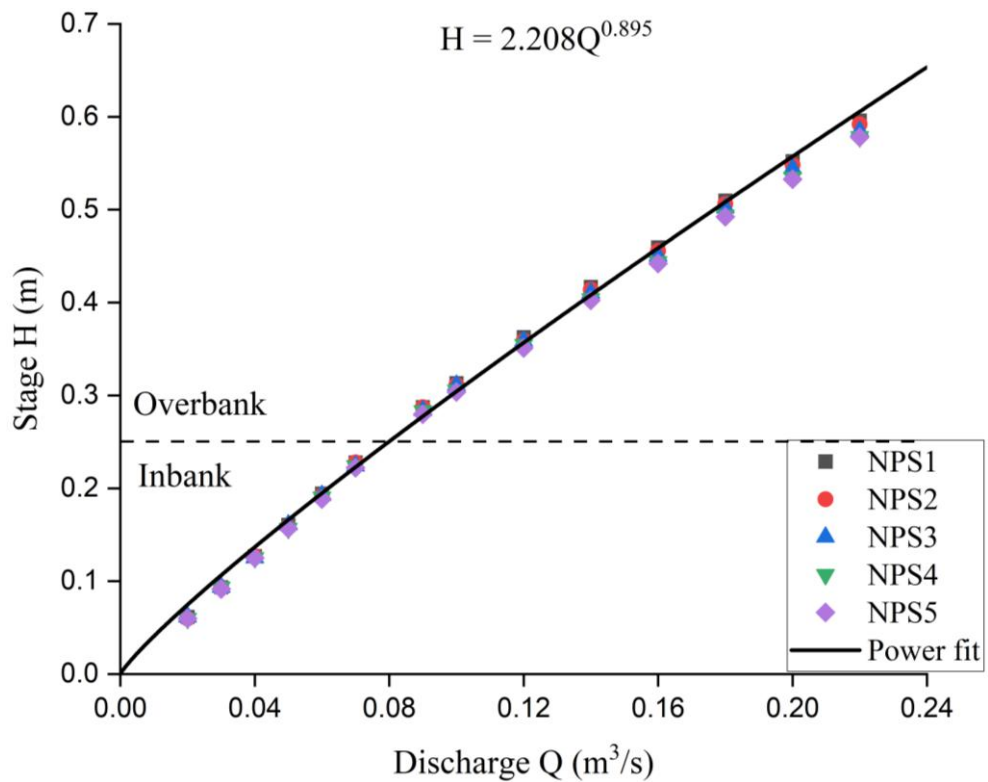
(b)

Fig. 4.2 Stage-discharge relationship for (a) prismatic section and (b) nonprismatic sections of the compound channel with **rough floodplains**
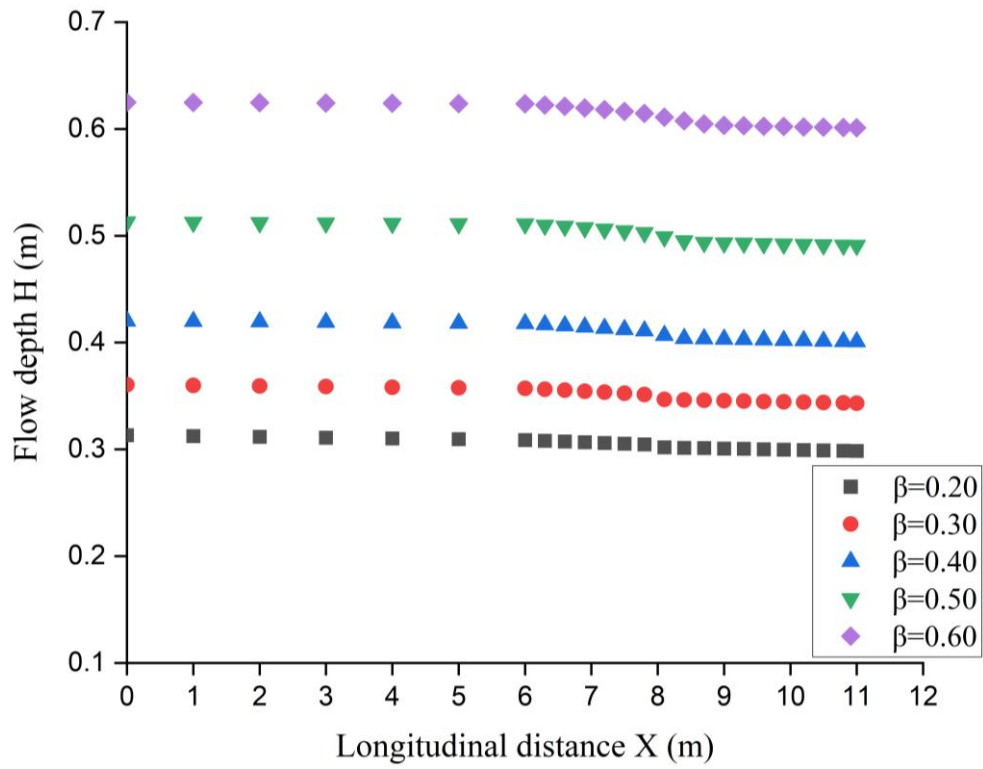
(a)
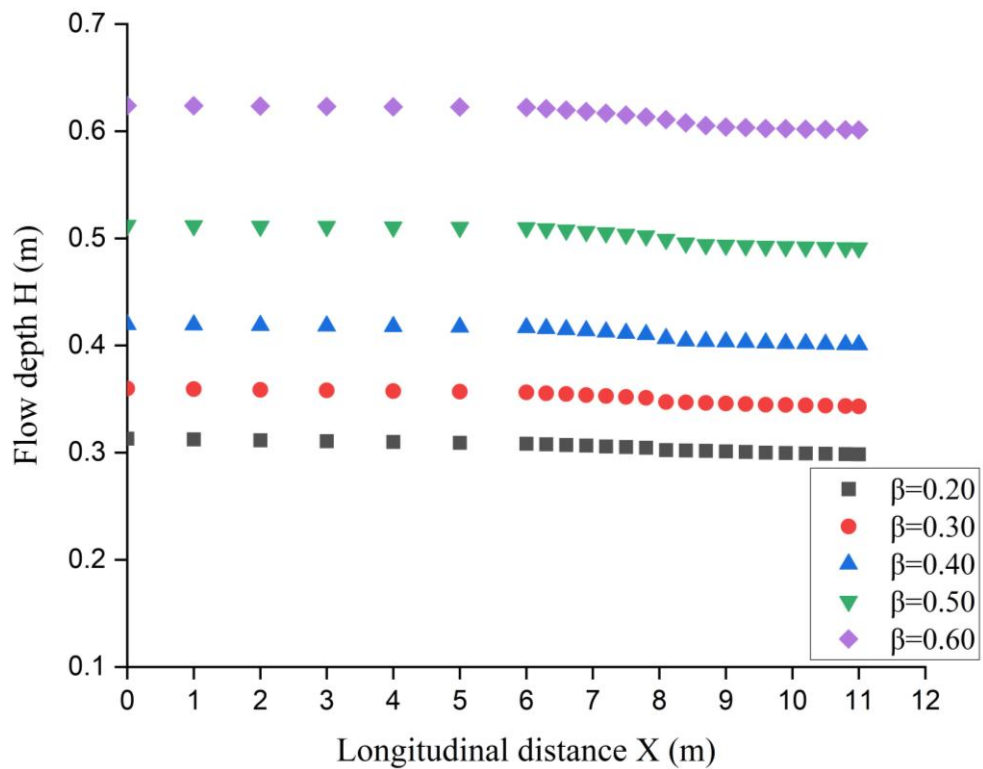
(b)

Fig. 4.3 Water surface profile for nonprismatic compound channel with (a) smooth floodplains and (b) rough floodplains
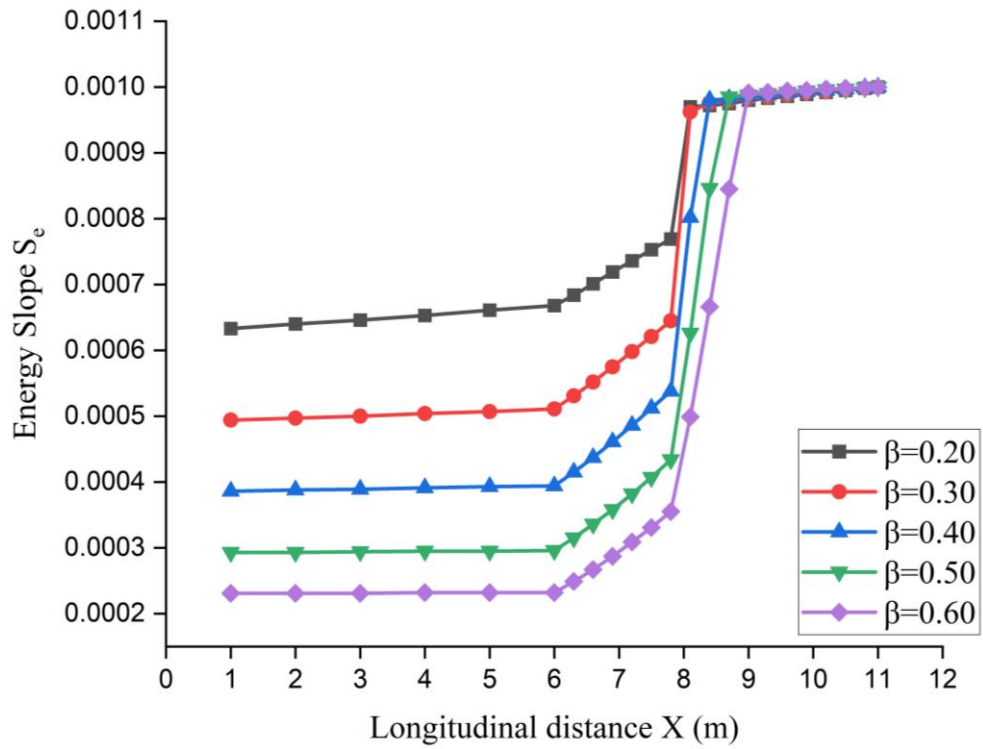
(a)
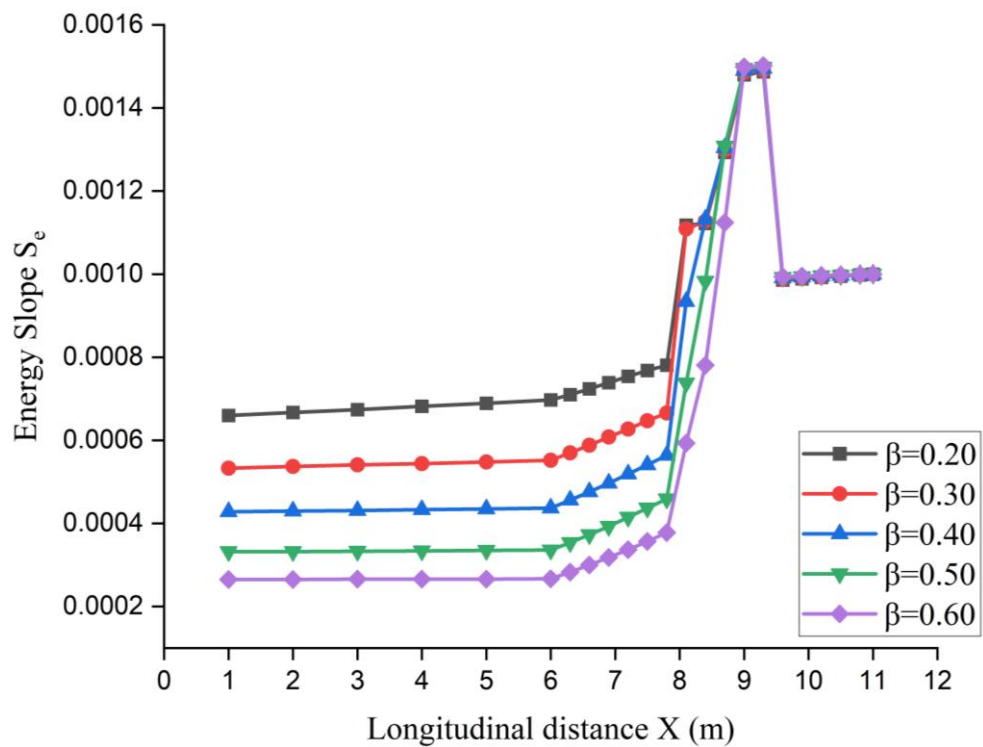
(b)

Fig. 4.4 Variation of energy slope with longitudinal distance in nonprismatic compound channel with (a) smooth floodplains and (b) rough floodplains
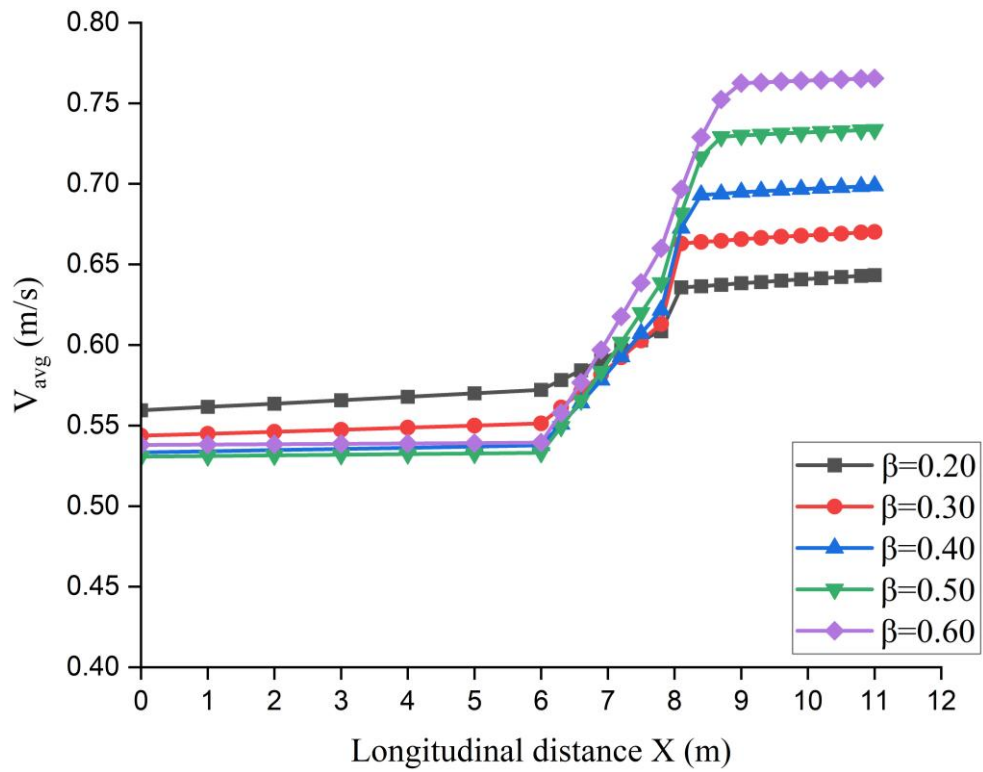
(a)
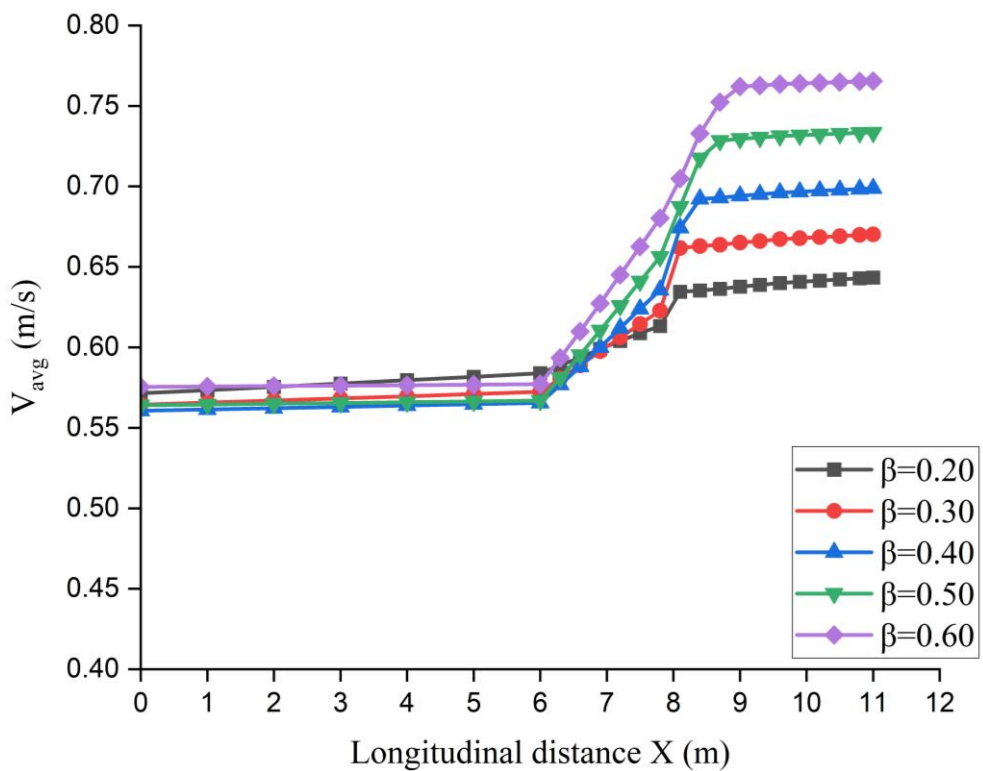
(b)

Fig. 4.5 Variation of average velocity along the longitudinal distance for nonprismatic compound channel with (a) smooth floodplains and (b) rough floodplains

β = 0.20

β = 0.30
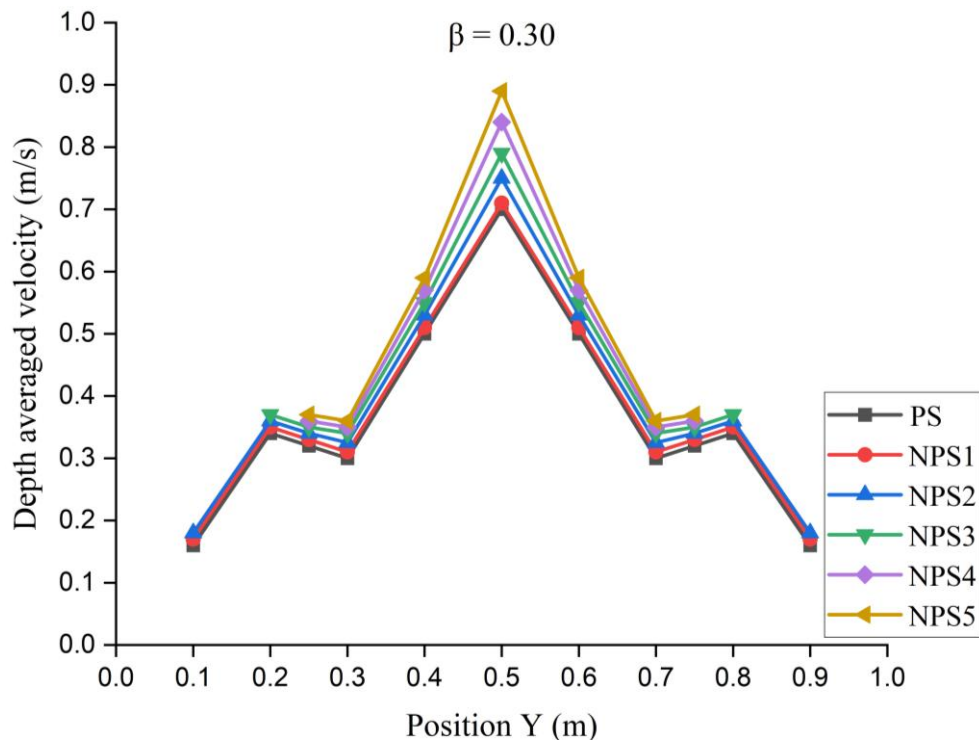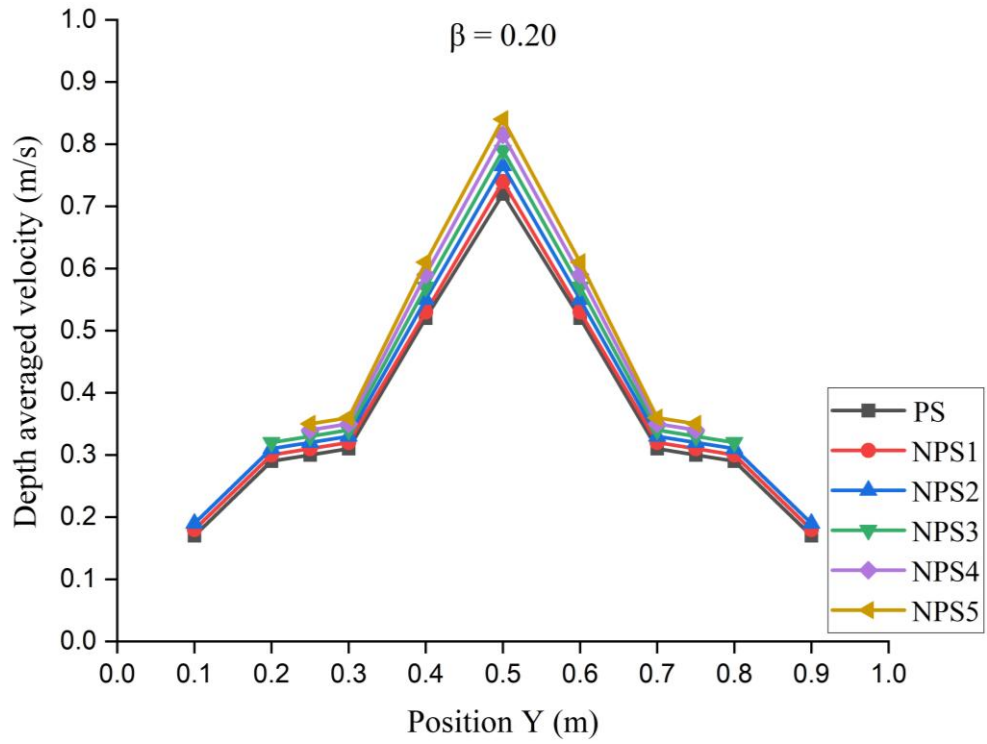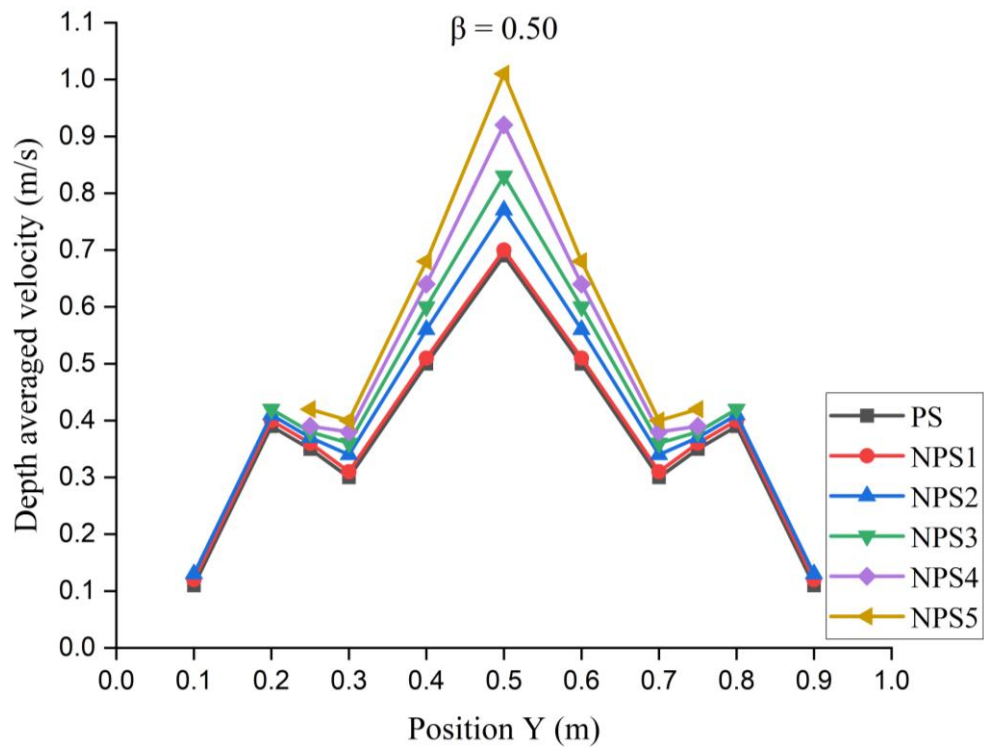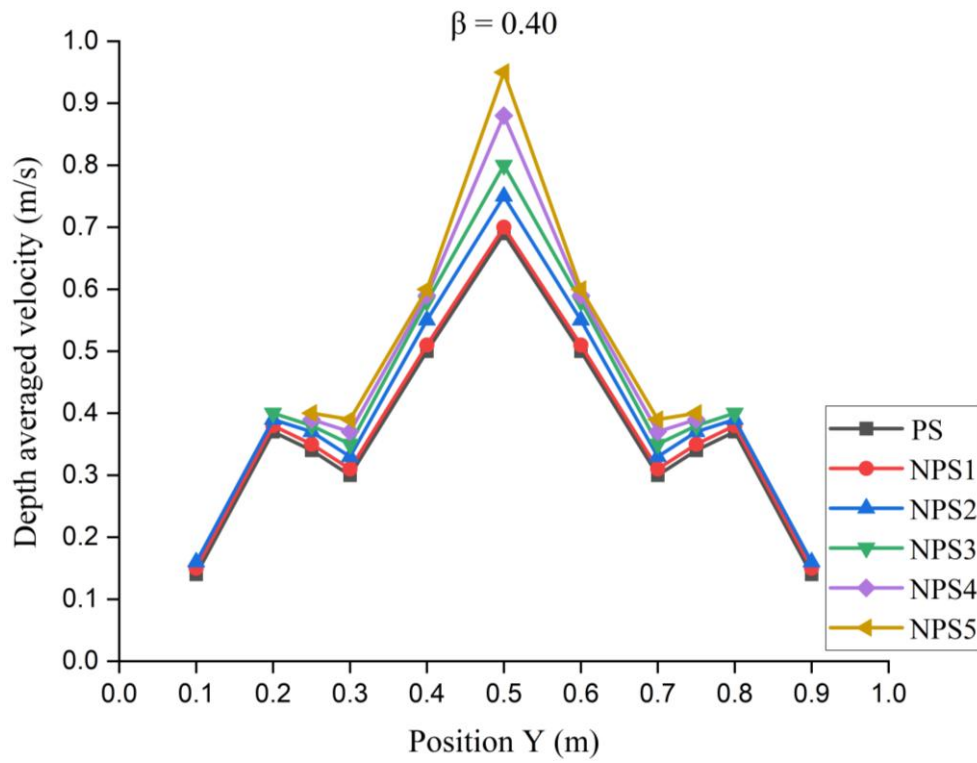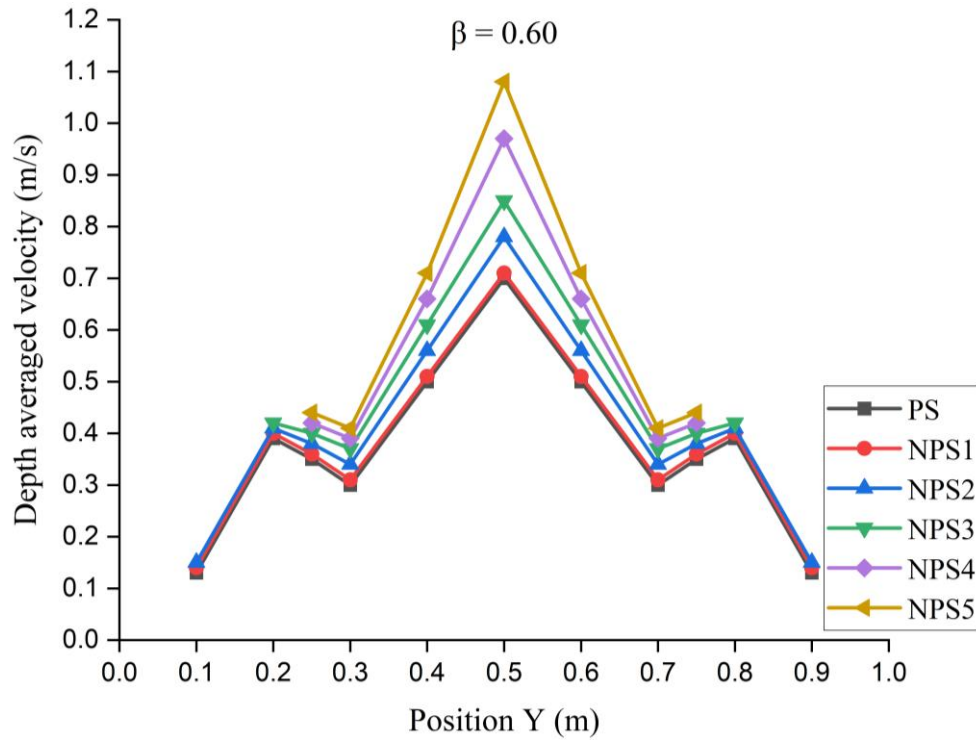
Fig. 4.6 Depth averaged velocity distribution for different relative flow depths in nonprismatic compound channel with **smooth floodplains**
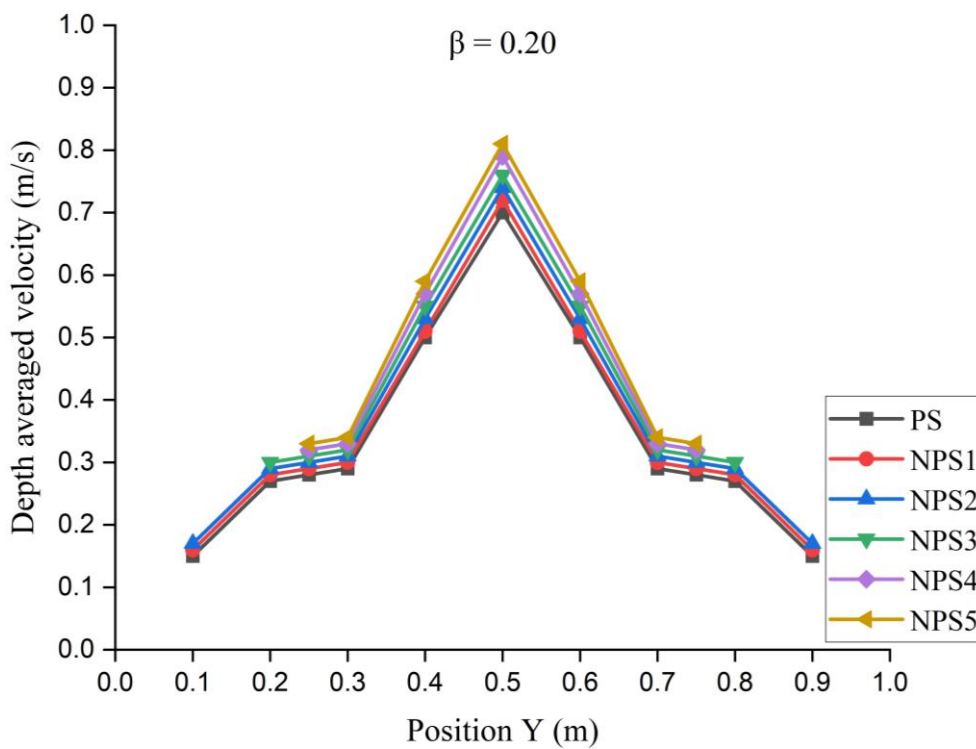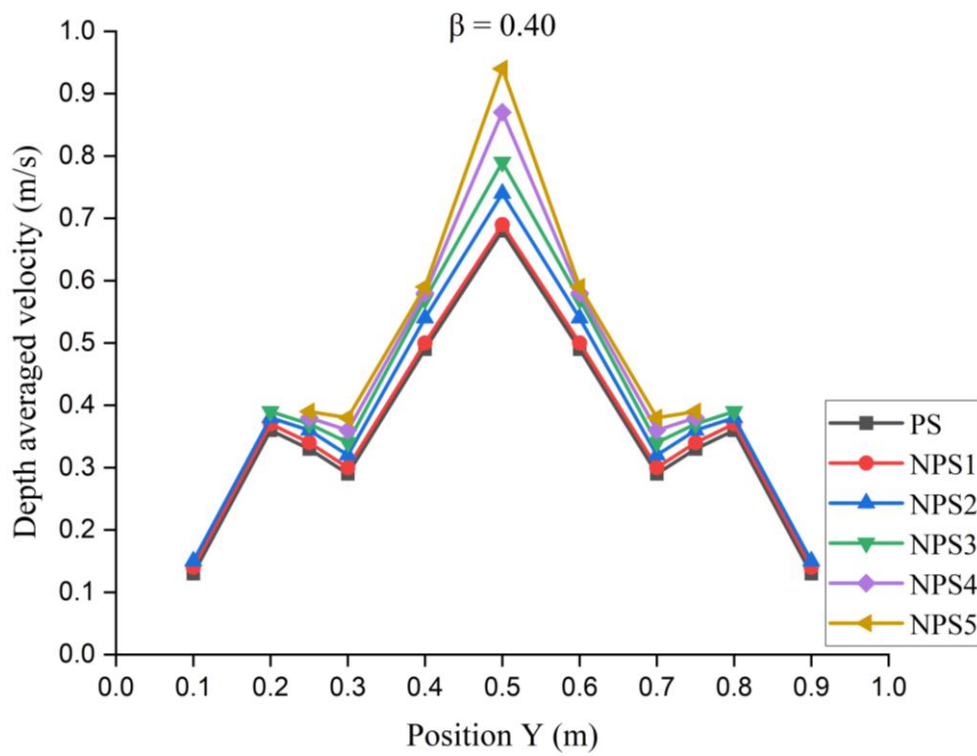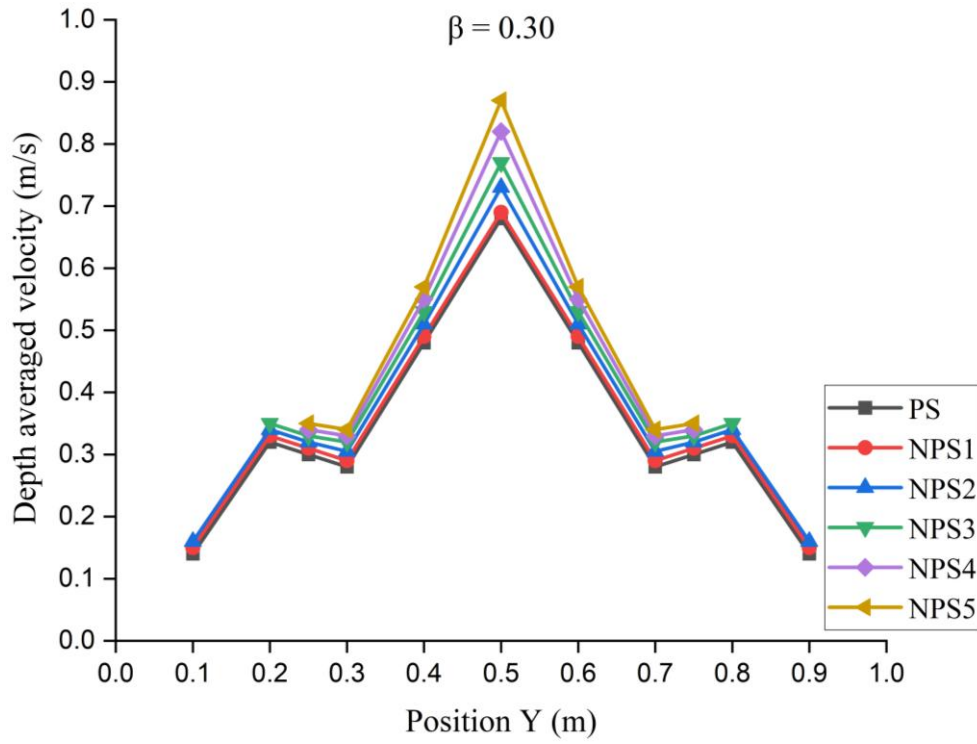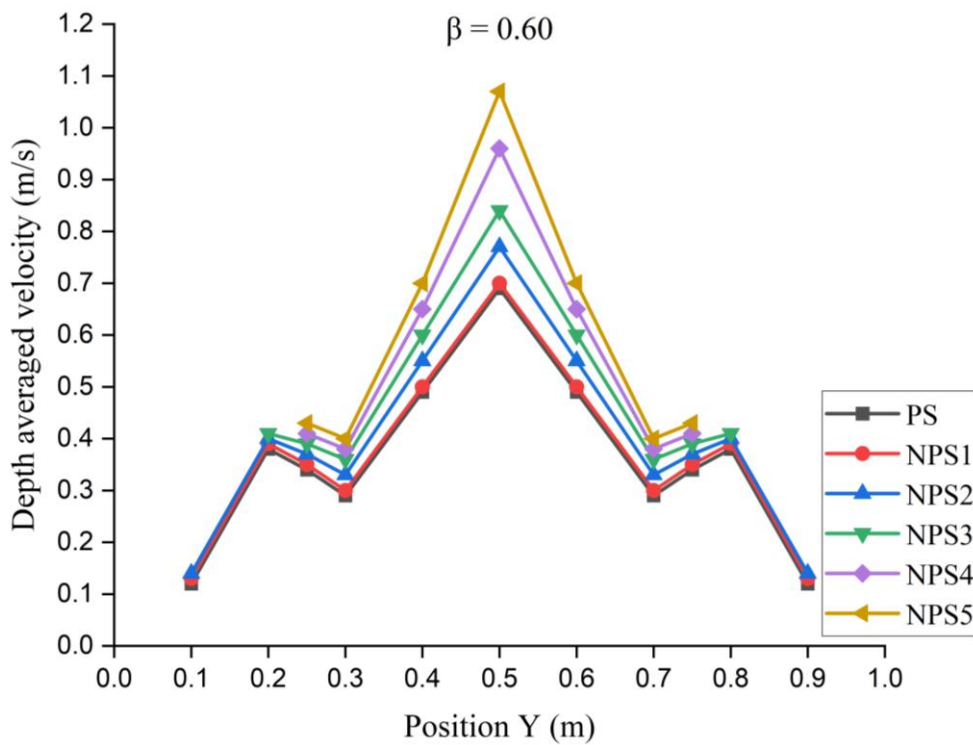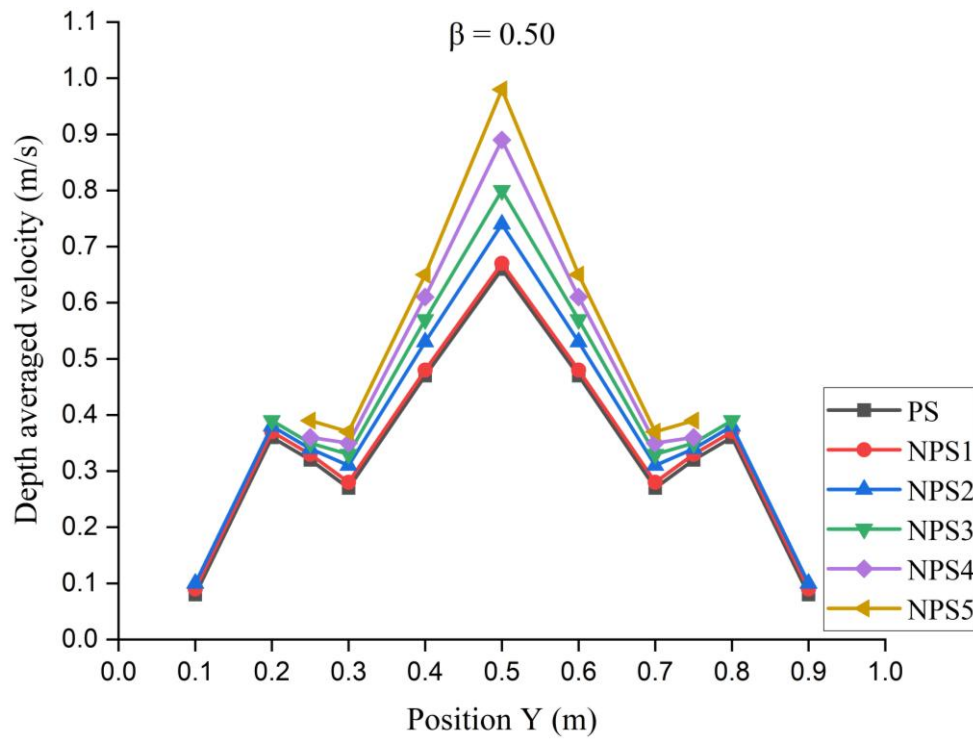
Fig. 4.7 Depth averaged velocity distribution for different relative flow depths in nonprismatic compound channel with **rough floodplains**

In a nonprismatic compound channel with smooth and rough floodplains, the fluctuation of average shear stress throughout the longitudinal distance for different relative flow depths ranging from 0.20 to 0.60 is shown in Figure 4.8. It has been found that there is a rise in shear stress throughout the longitudinal distance in the initial segment of the convergent portion of the waterway. Additionally, in the latter half of this section, there is a sudden rise in shear caused by the convergence of the channel's geometry, resulting in more frictional resistance to flow. The shear stress in the channel exhibits an increase in magnitude as the longitudinal distance progresses. This increase is mostly attributed to the rise in relative depth, with greater relative depths seeing a more pronounced effect. The primary driver behind this phenomenon is the shift of momentum from the primary waterway to the flooding zones. In the case of smooth floodplains, the increase in shear was seen up to 5.21%, 2.30%, 2.53%, 1.37%, and 0.50% in the prismatic part, and 39.58%, 63.22%, 91.14%, 121.92%, and 143.66% in the nonprismatic sections, respectively, at relative depths of 0.20, 0.30, 0.40, 0.50, and 0.60. In the case of rough floodplains, the increase in shear was seen up to 5.00%, 3.22%, 1.13%, 1.21%, and 2.47% in the prismatic portion, and 124.02%, 155.91%, 187.50%, 228.92%, and 258.02% in the nonprismatic portions, respectively, at relative depths of 0.20, 0.30, 0.40, 0.50, and 0.60. In compound channels with rough floodplains, the shear is higher as compared to smooth floodplains due to the presence of irregularities on the floodplain surface which creates frictional resistance. The increase in shear is seen up to 69.69%, 70.00%, 68.66%, 69.56%, and 68.60% at relative depths of 0.20, 0.30, 0.40, 0.50, and 0.60, respectively, compared to smooth floodplains.

The depth-averaged distribution of boundary shear stress across the width of the nonprismatic compound channel with smooth and rough floodplains for relative flow depth of 0.60 are depicted in Fig. 4.9. The distribution of boundary shear stress exhibits symmetry and expands progressively from NPS1 to NPS5. The highest value of wall tractive stress is seen near the center of the main channel, and this value rises as the flow transitions from a prismatic portion to a nonprismatic segment. This increase in boundary shear stress may be attributed to the boundary resistance resulting from the converging shape of the channel. The magnitude of the boundary shear stress diminishes as it approaches the floodplain interface across all sections. At lower relative depths, in close proximity to the junction of the primary waterway and flooding zones, the shear stress at the wall experiences a rapid fall, followed by a gradual decrease until reaching a

minimum at both ends of the floodplain. At elevated relative flow depth, in close proximity to the junction of the primary waterway and floodplains, there is a rapid decline in shear stress. This is followed by a gradual increase towards the center of both floodplains and subsequently a decrease towards the boundaries of the channel. In these compound channel arrangements, this pattern emerges as a result of the shift of momentum from the flood zones to the primary waterway and vice-versa. In compound channels, momentum exchange between the main channel and the floodplain is controlled by a combination of hydraulic and geometric factors. This includes the channel's shape and slope, the relative flow depths, the velocity distribution and the associated shear stresses at the interface. Surface roughness on both the main channel and floodplain also plays a crucial role, as it influences turbulence and energy dissipation, thereby affecting how momentum is transferred. Collectively, these elements dictate the efficiency and characteristics of momentum transfer in compound channels.
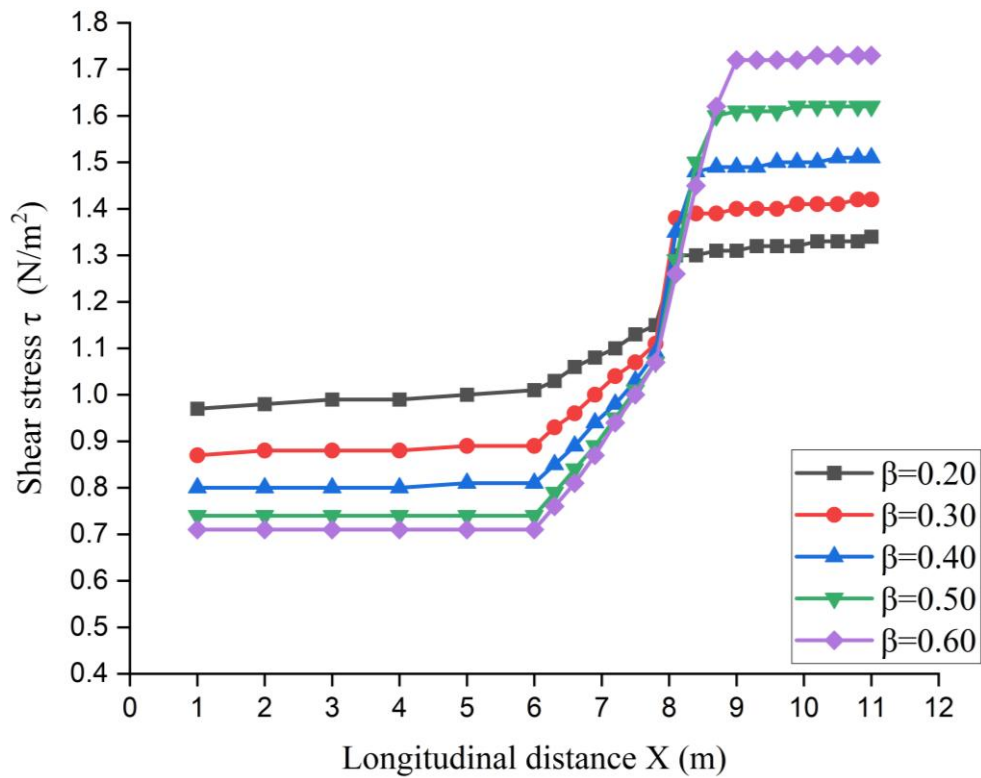
(a)
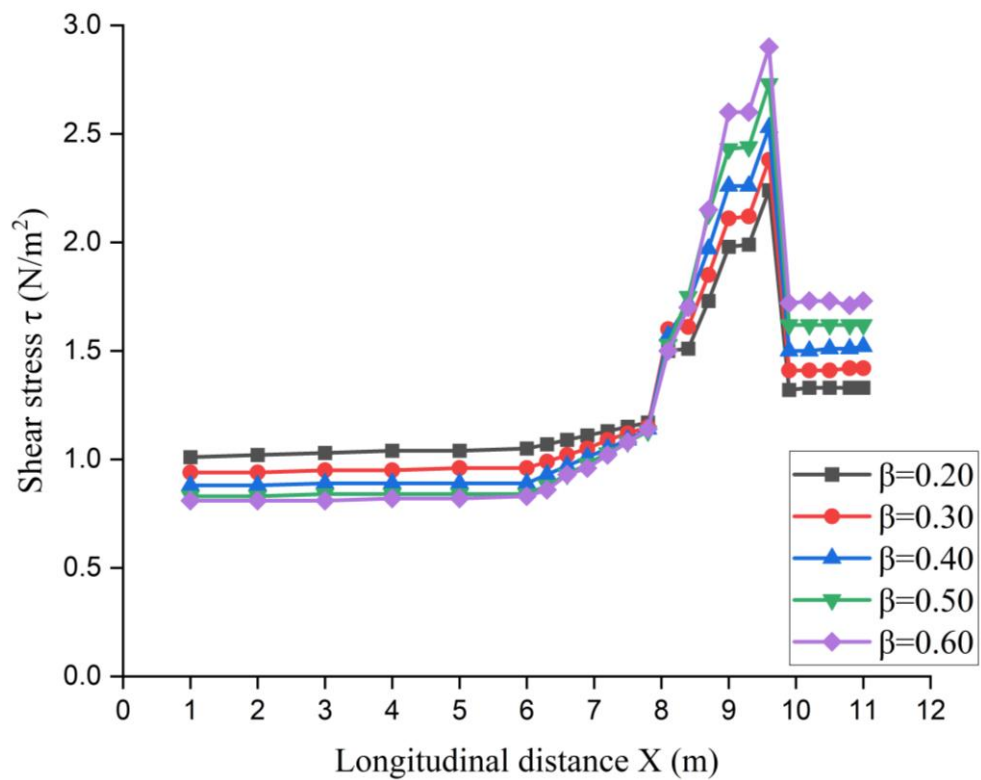
(b)

Fig. 4.8 Variation of shear stress along the longitudinal distance of the nonprismatic compound channel with (a) smooth and (b) rough floodplains
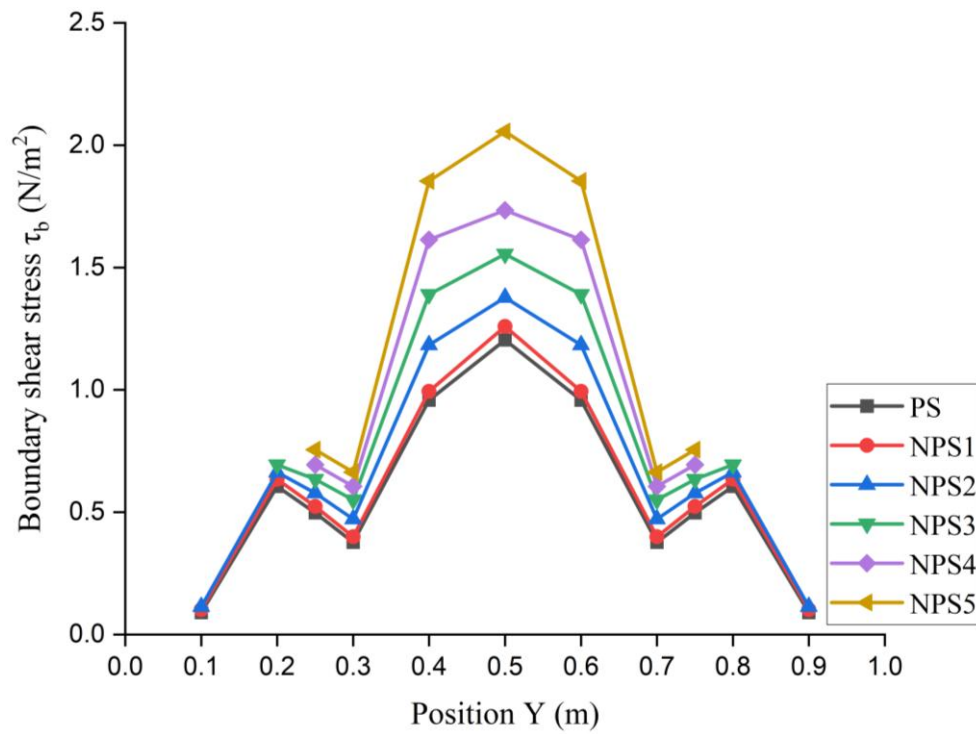
(a)
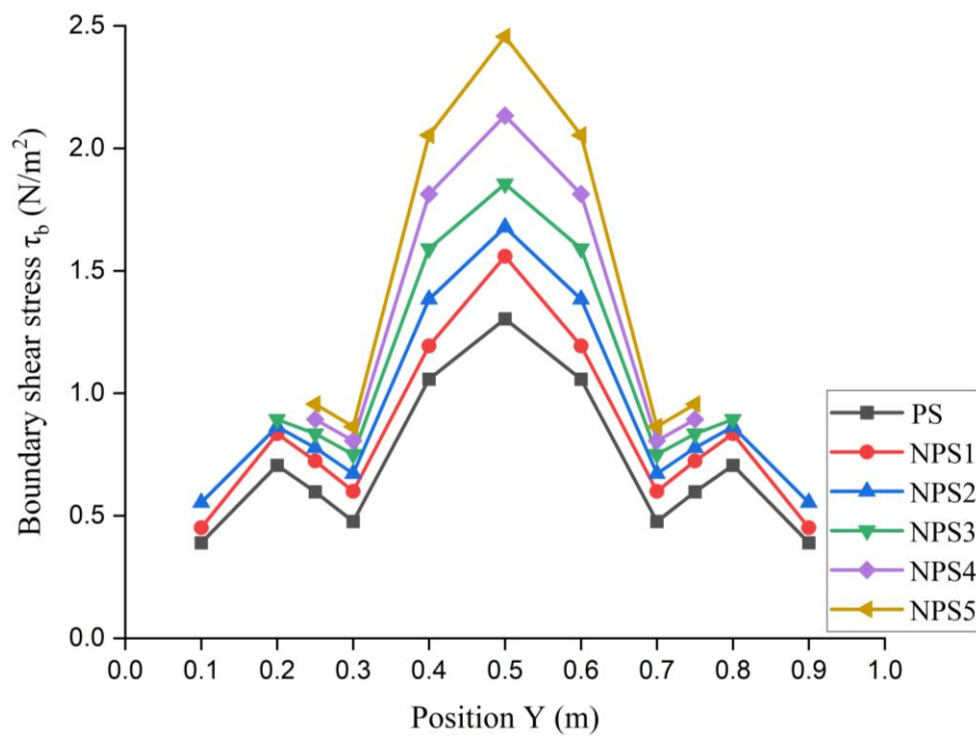
(b)

Fig. 4.9 Distribution of boundary shear stress across the width of nonprismatic compound channel with (a) smooth and (b) rough floodplains

4.2 Flow characteristics in nonprismatic compound channels with sediment

The stage-discharge relationship for the prismatic section (PS) and nonprismatic sections (NPS) of the nonprismatic compound channel with sediment in the main channel and with smooth and rough floodplains are represented in Fig. 4.10 and 4.11. The flow depth rises as the discharge increases. However, there is a fall in increment beyond bankfull depth due to interaction and additional momentum transfer between the primary waterway and floodplains. Due to the convergence of the geometry, flow depth reduces for the same discharge in the converging section from NPS1 to NPS5. A similar trend has been observed for nonprismatic compound channels with rough floodplains. However, for the same discharge, depth in nonprismatic compound channels with rough floodplains is less when compared to smooth floodplains. In a rough floodplain and sediment bed, the irregularities and roughness of the floodplain and bed disrupt the flow, causing more energy losses through friction. As a result, the water in a rough floodplain will need to accelerate to overcome these losses, which leads to a decrease in flow depth compared to a smooth floodplain where the flow encounters less resistance and can maintain a higher depth for the same discharge. For both in-bank and over-bank flow in prismatic and nonprismatic sections, it has been discovered that a power function is the line of progression that provides a suitable approximation.

The variation in energy slope with respect to longitudinal distance is shown for various relative depths in a nonprismatic compound channel with sediment in the main channel and smooth and rough floodplains are shown in Fig. 4.12. As the longitudinal distance rises, there is a corresponding increase in the energy slope due to an upsurge in energy loss. This may be attributed to sediment deposition which can lead to an increase in energy slope as flow is impeded, causing water to spread out and lose energy. Conversely, sediment erosion can result in a decrease in energy slope as flow accelerates through the channel. These variations highlight the complex interplay between flow dynamics and sediment transport processes. In regard to rough floodplains, it has been shown that the energy slope is greater in comparison to smooth floodplains. This may be attributed to the increased loss of head resulting from the channel bed and roughness of the floodplains. The energy slope in a nonprismatic compound channel with rough floodplains increased by 9.80%, 18.50%, 27.35%, 35.60%, and 42.09% for prismatic sections, and by 55.98%, 55.81%, 55.78%, 56.05%, and 56.22% for nonprismatic sections, respectively, for relative depths of 0.20, 0.30, 0.40, 0.50, and 0.60.
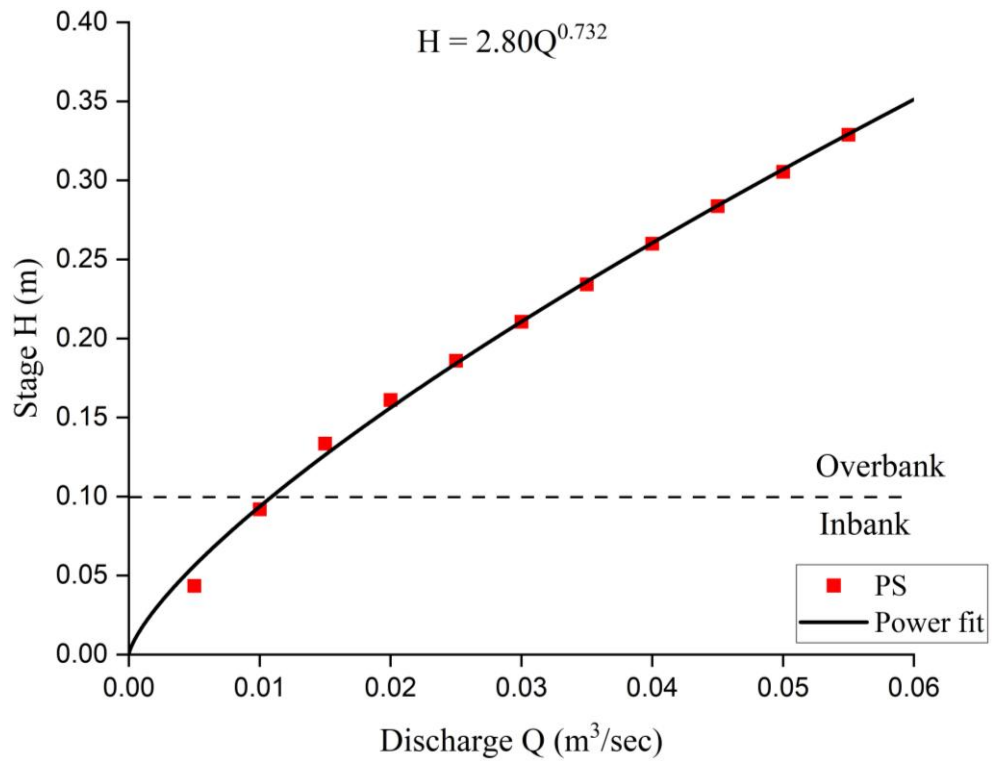
(a)
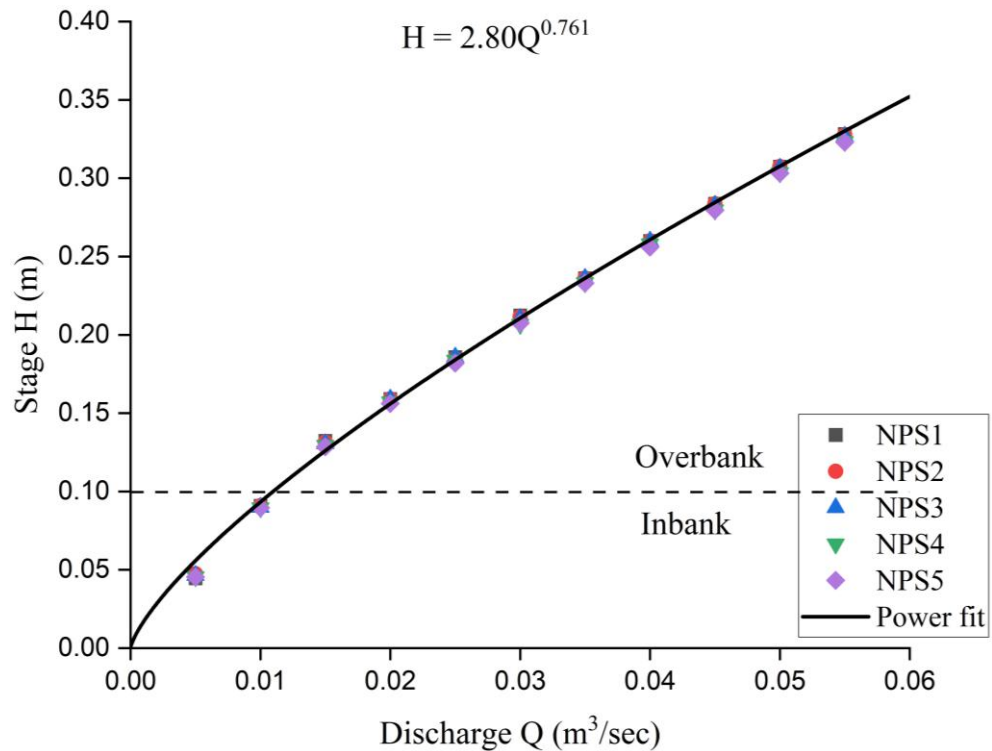
(b)

Fig. 4.10 Stage-discharge relationship for (a) prismatic section and (b) nonprismatic sections of the compound channel with sediment and **smooth floodplains**
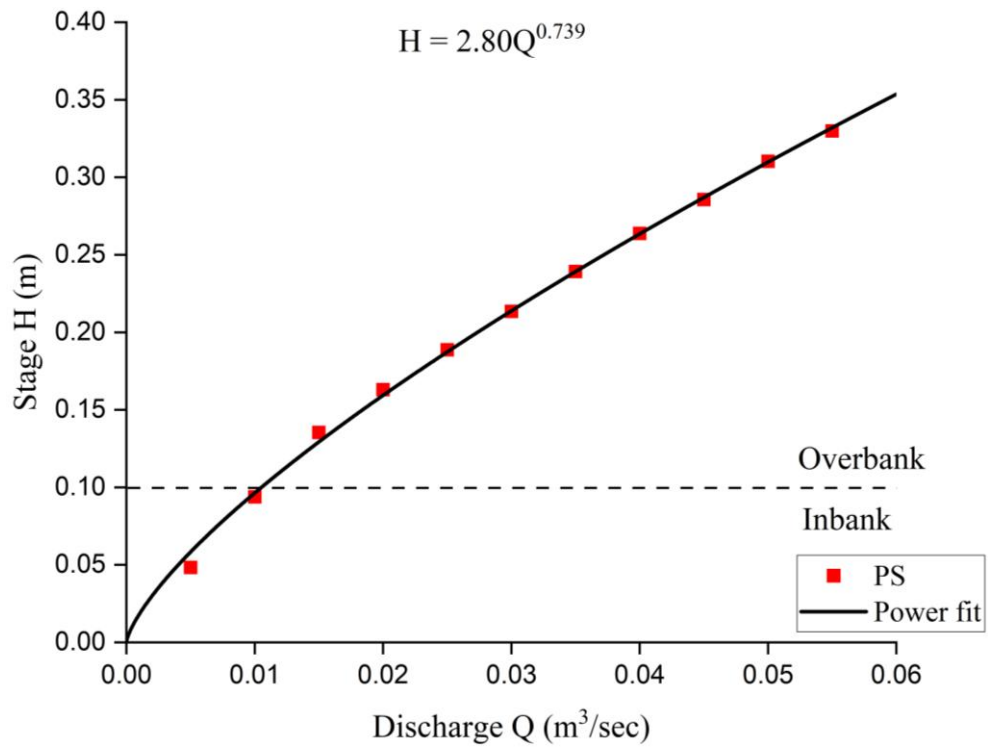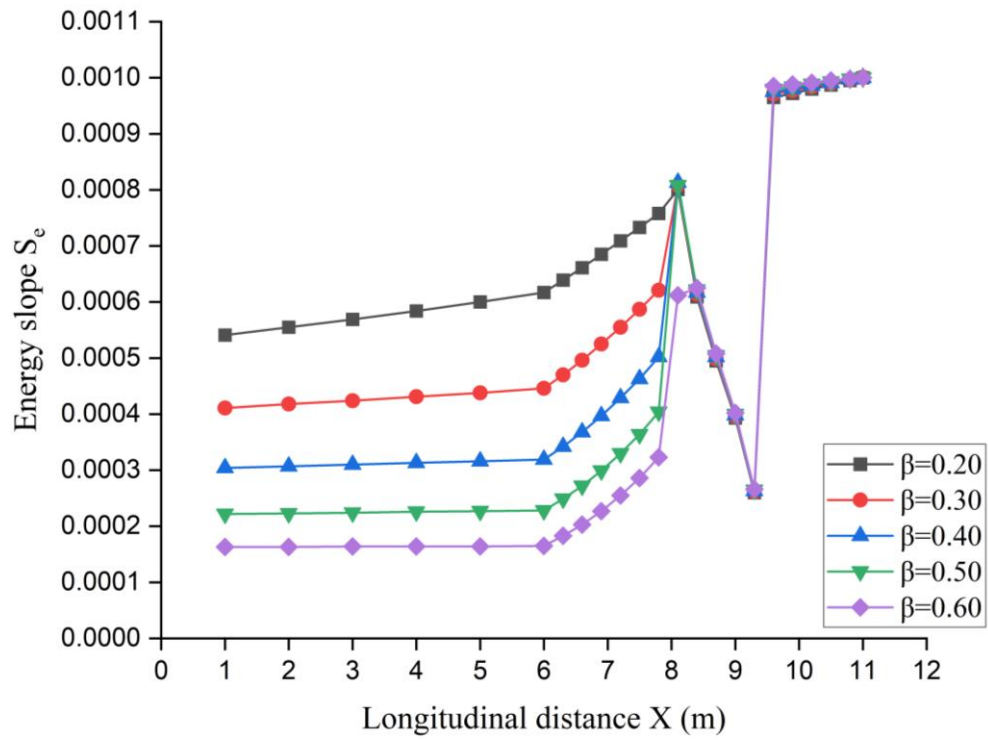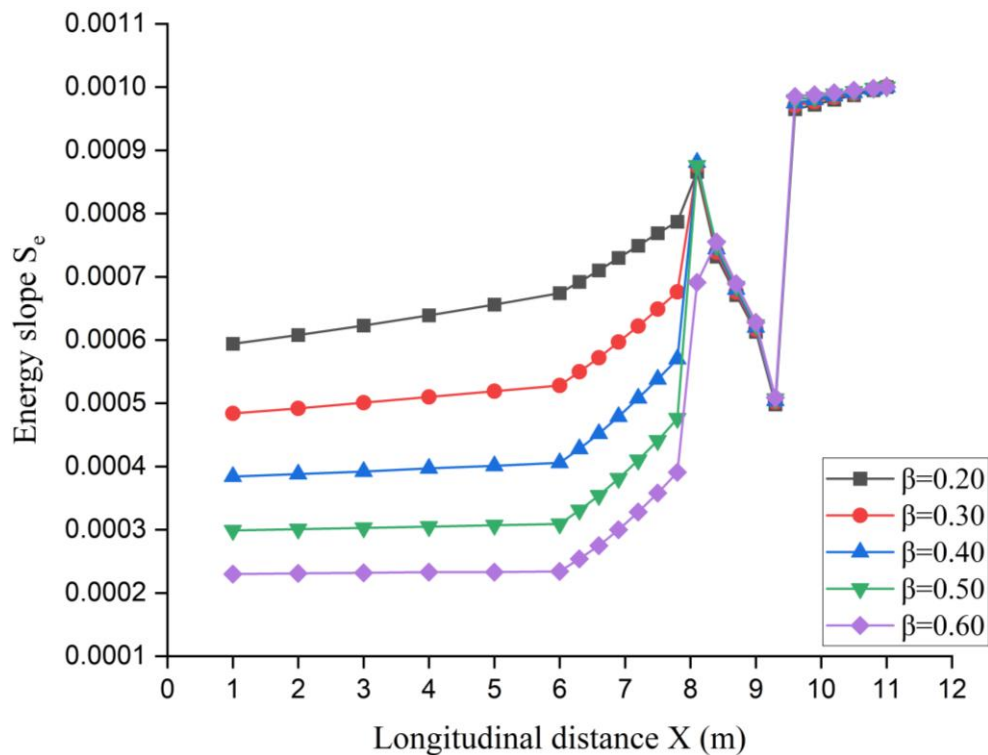
(a)
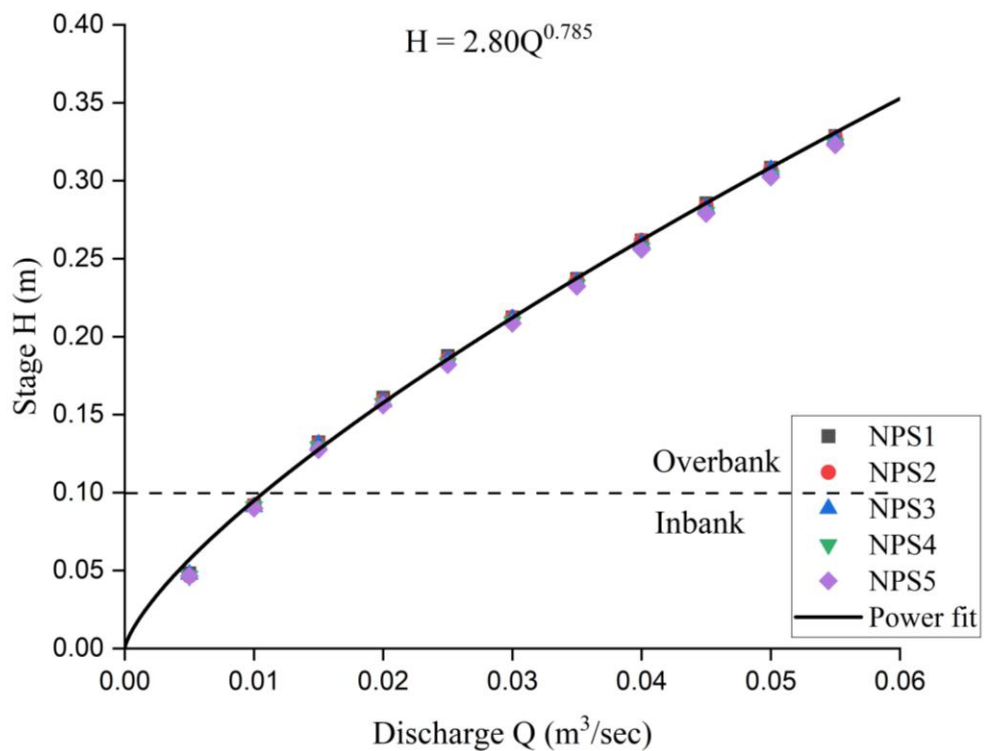
(b)

Fig. 4.11 Stage-discharge relationship for (a) prismatic section and (b) nonprismatic sections of the compound channel with sediment and **rough floodplains**
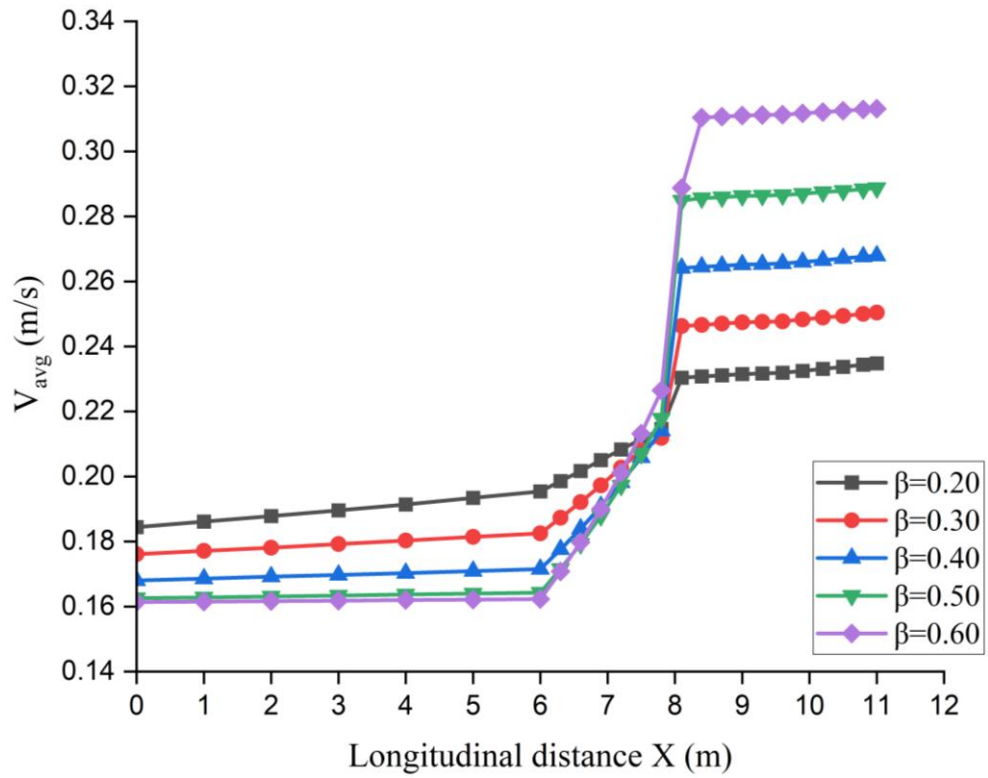
(a)

(b)

Fig. 4.12 Variation of energy slope with longitudinal distance in nonprismatic compound channel with sediment and (a) smooth floodplains (b) rough floodplains

The variations in average velocity over the longitudinal distance for varying relative flow depths in a nonprismatic compound channel with sediment and smooth and rough floodplains are shown in Figure 4.13. The research findings indicate that there is an upward trend of the average velocity along the longitudinal distance of the channel. The prismatic segment exhibited a minor rise, however, the nonprismatic sections had a considerable spike, which may be attributed to the constriction in the shape of the channel. In the case of smooth floodplains, the increase in velocity was seen up to 7.70%, 6.36%, 5.71%, 5.54%, and 5.82% in the prismatic part, and 26.08%, 41.01%, 58.33%, 76.51%, and 93.12% in the nonprismatic section, respectively, at relative depths of 0.20, 0.30, 0.40, 0.50, and 0.60. A similar pattern has been seen in the case of nonprismatic compound channels including rough floodplains. In the case of rough floodplains, the increase in velocity was seen up to 6.70%, 5.73%, 5.06%, 4.76%, and 4.83% in the prismatic portion, and 19.91%, 29.46%, 40.37%, 51.77%, and 62.01% in the nonprismatic portions, respectively, at relative depths of 0.20, 0.30, 0.40, 0.50, and 0.60. In compound channels with rough floodplains, the velocity is lesser as compared to smooth floodplains due to the presence of irregularities on the floodplain surface and sediment creates frictional resistance, which tends to slow down the flow. The decrease in velocity is seen up to 4.90%, 8.25%, 11.55%, 14.25%, and 16.27% at relative depths of 0.20, 0.30, 0.40, 0.50, and 0.60, respectively, compared to smooth floodplains.

The depth-averaged velocity distribution over the cross-section for different relative flow depths at the prismatic section and various nonprismatic sections for compound channels with sediment in the main channel and smooth and rough floodplains are depicted in Fig. 4.14 and 4.15. The position Y (on x-axis) represents the width of the channel section over which distribution is presented. As a result of these figures, it has been determined that the depth-averaged velocity patterns are fairly uniform in all segments and that they steadily grow from PS to NPS5. Because of the narrowing shape of the channel, the velocity in the primary waterway is found to be higher than that in the floodplains, and it gradually increases in the direction of the downstream flow. This is because the flow acceleration is caused by the structure of the channel. The velocity increases in the interface region of the primary waterway and floodplains and then, reaches a minimum at the floodplain ends. At the interface, the difference in flow depth and channel geometry creates a shear layer, resulting in complex flow patterns and turbulence. Sediment transport and deposition further influence this region, as the varying flow velocities can

cause differential sediment movement. This interaction enhances the mixing of flow from the primary waterway and the zones of flooding, accelerating the velocity in the interfacial region of the compound channel. Additionally, the presence of sediment can alter the channel's roughness and flow resistance, further contributing to the increased velocity in this transitional zone.
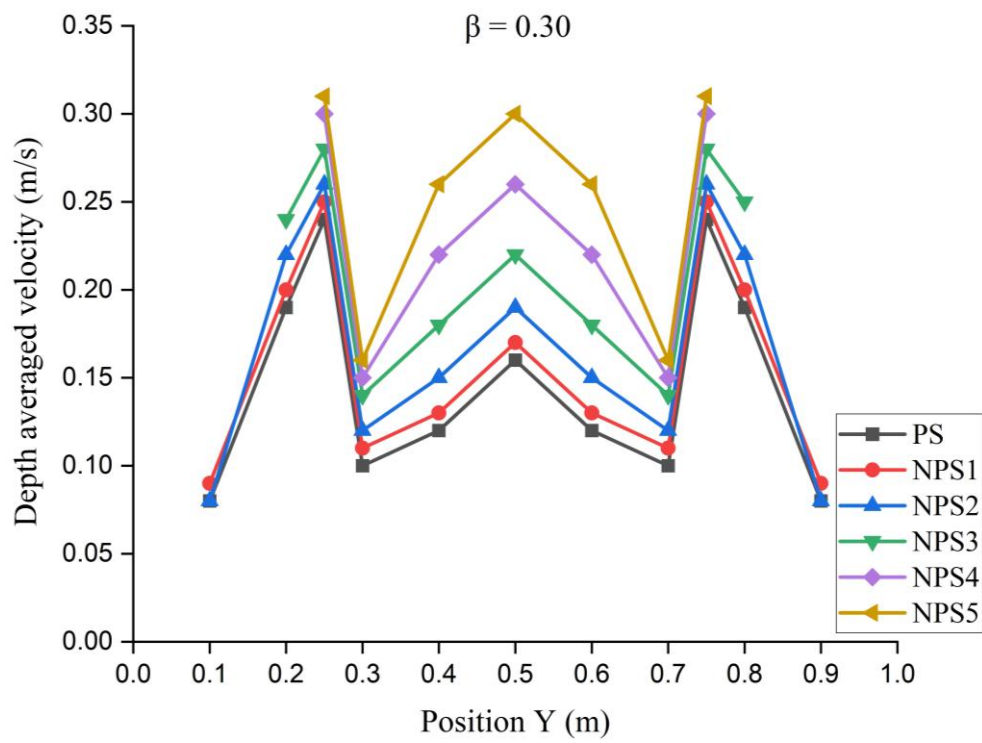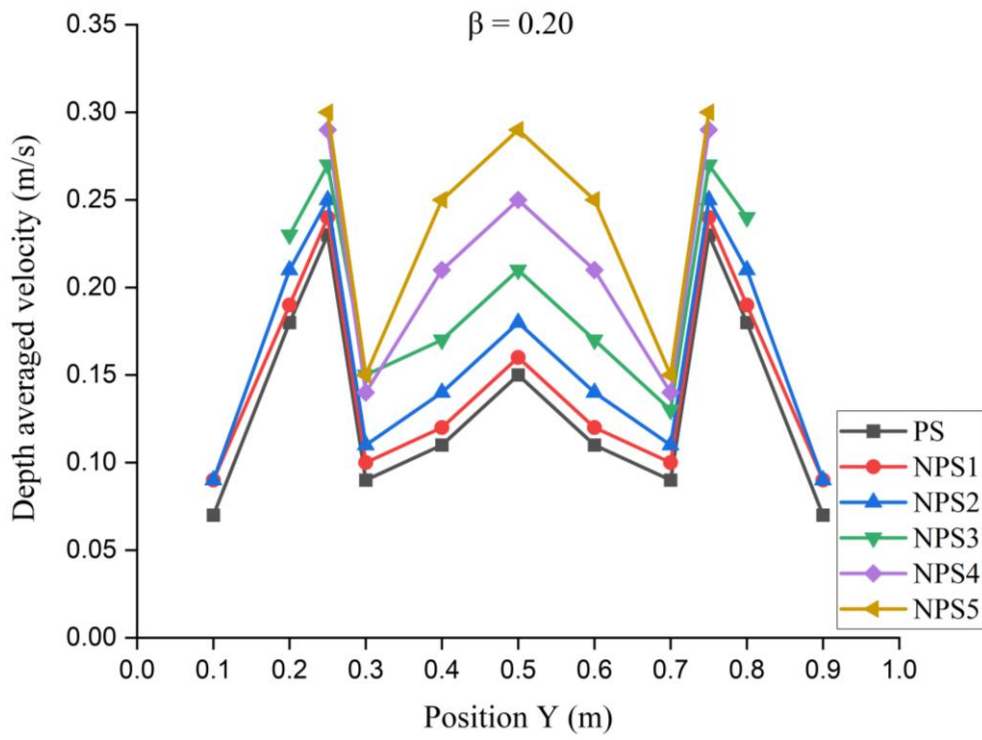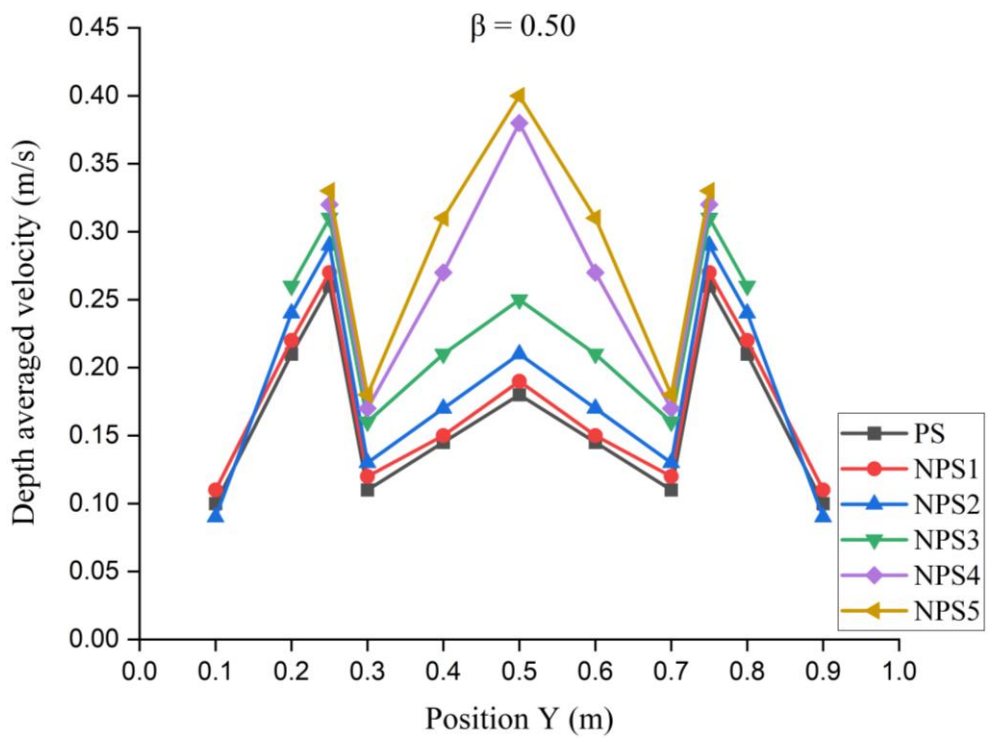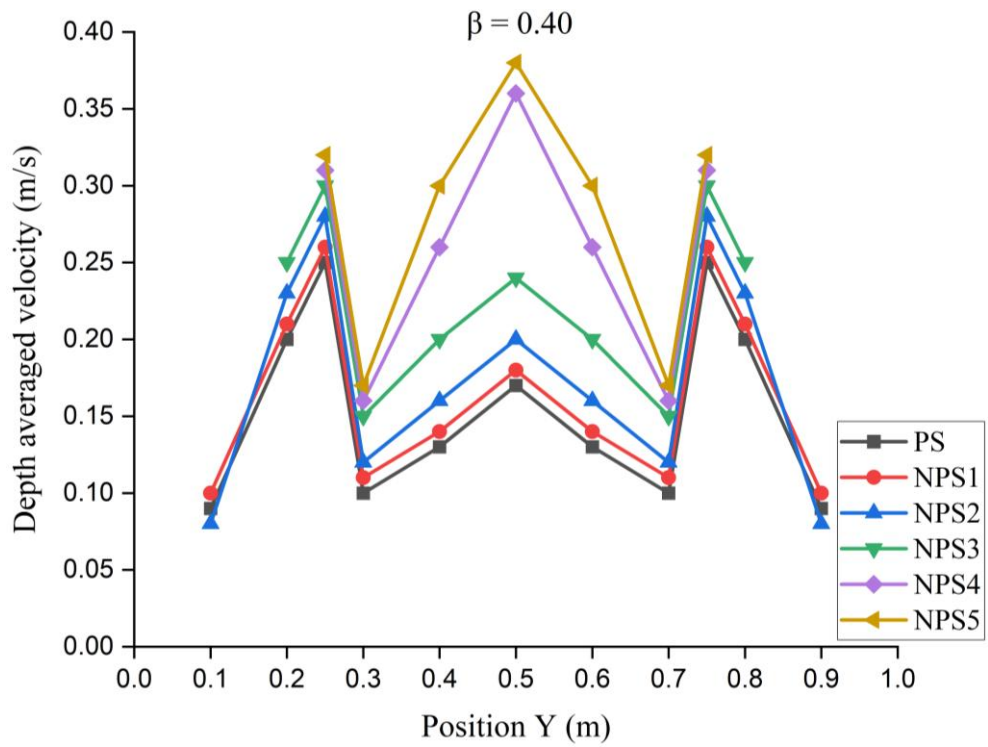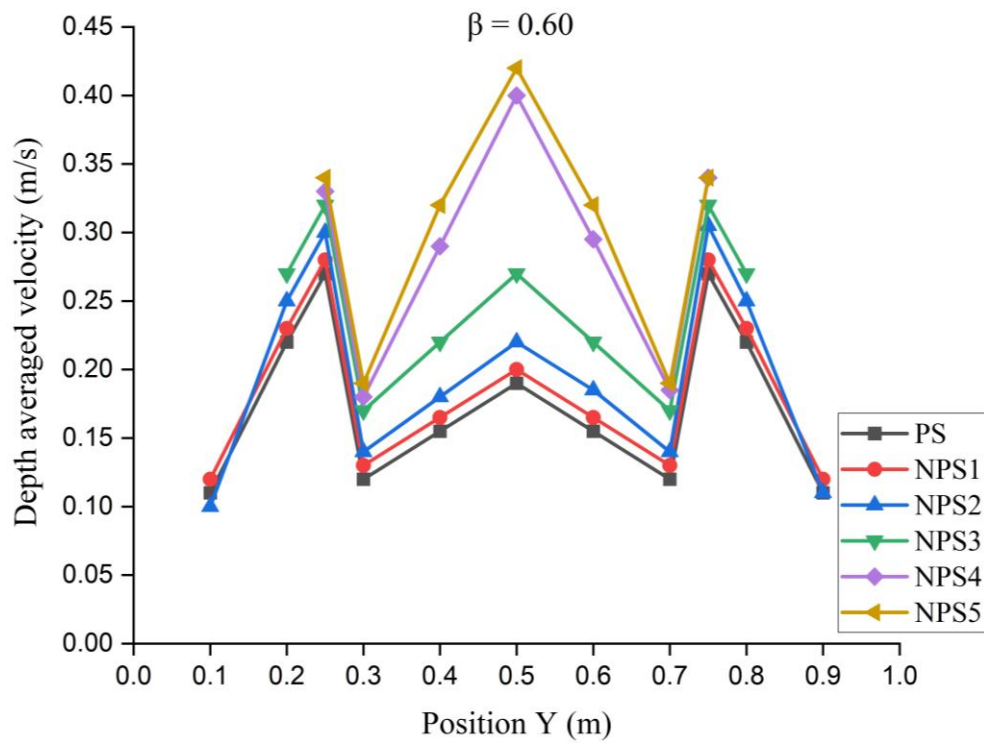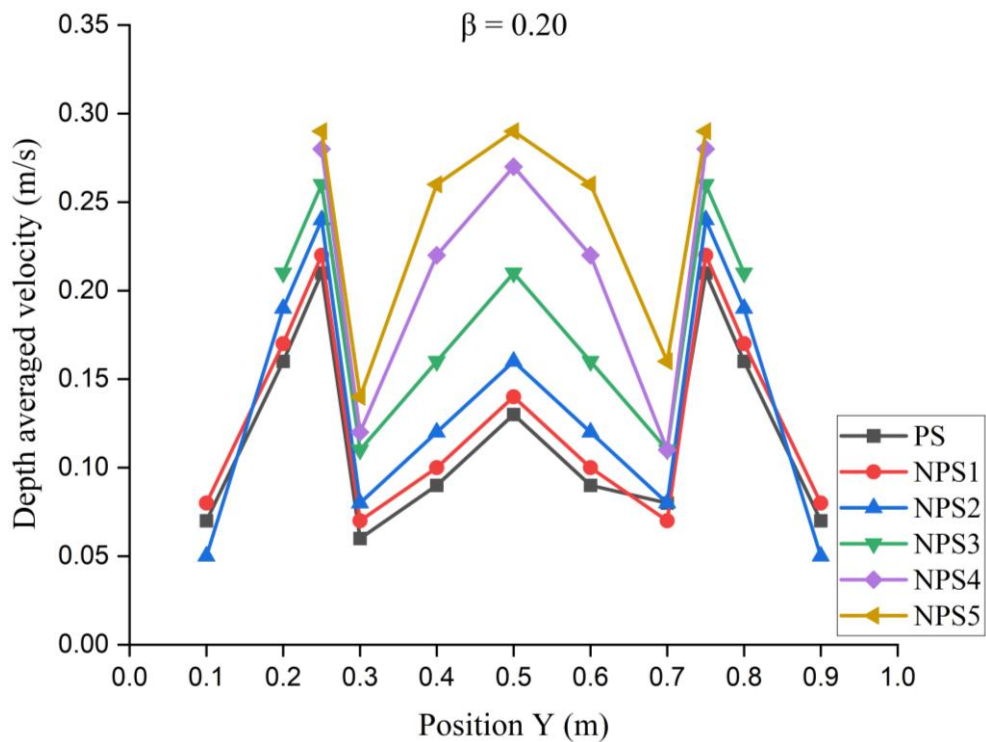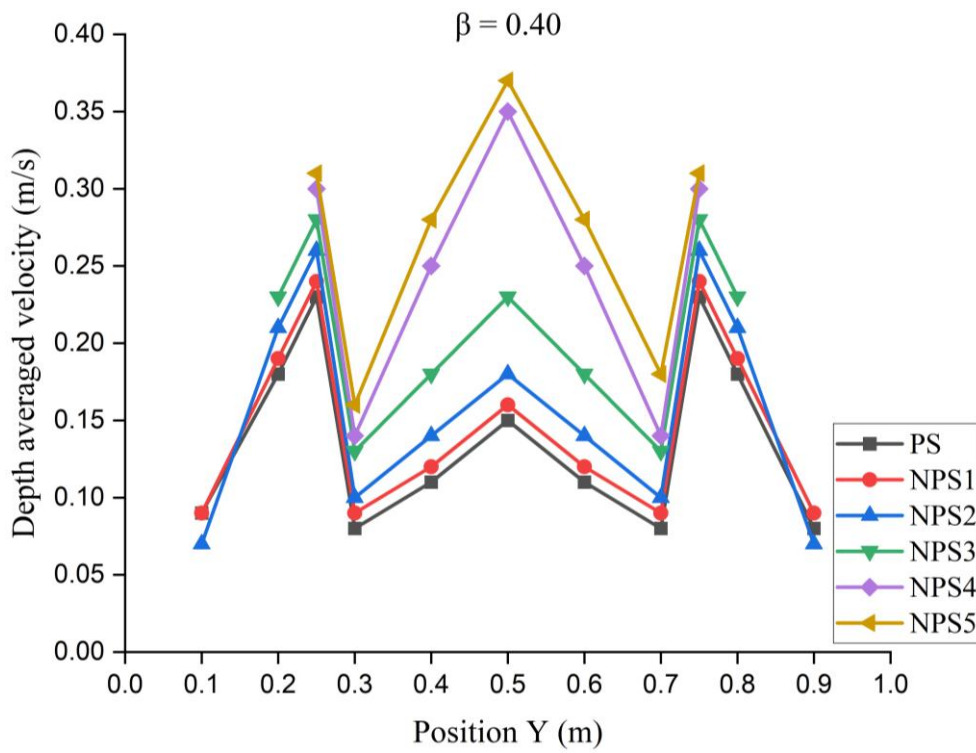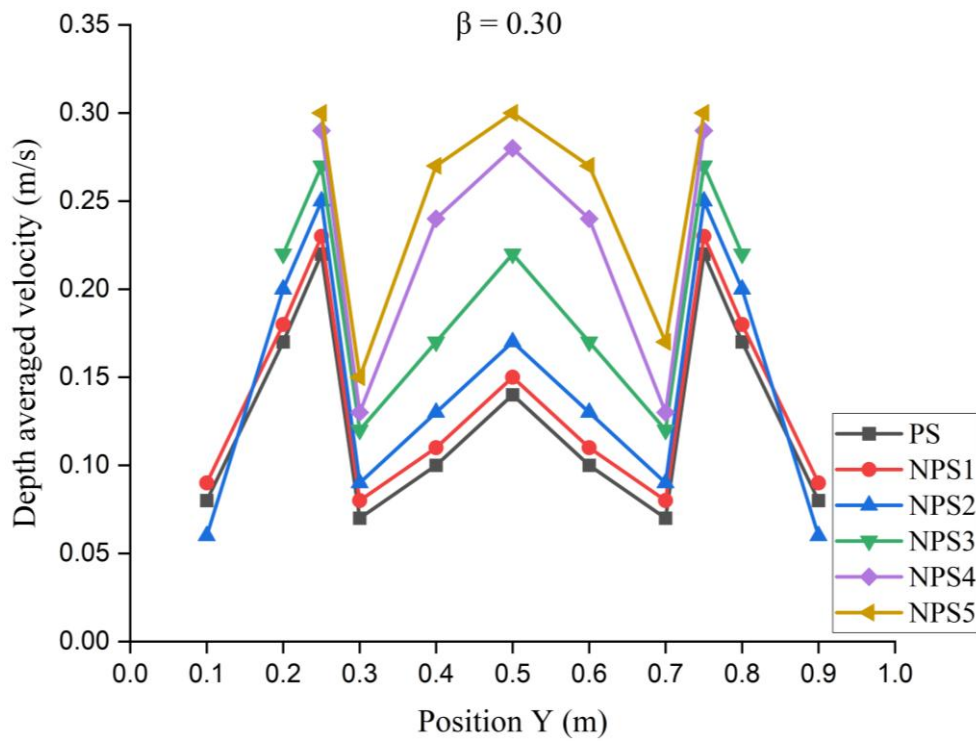
(a)
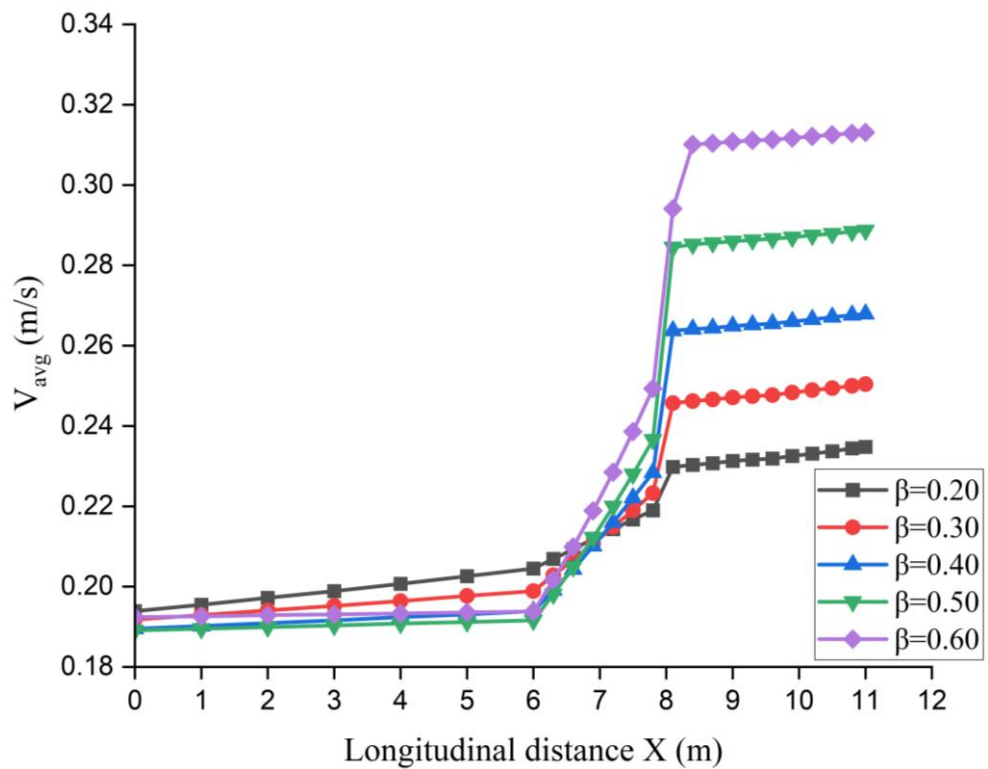
(b)

Fig. 4.13 Variation of average velocity along the longitudinal distance for nonprismatic compound channel with sediment and (a) smooth floodplains (b) rough floodplains

β = 0.20

β = 0.30

β = 0.40

β = 0.50

Fig. 4.14 Depth averaged velocity distribution in nonprismatic compound channel with sediment and smooth floodplains for various relative flow depths

β = 0.30

β = 0.40
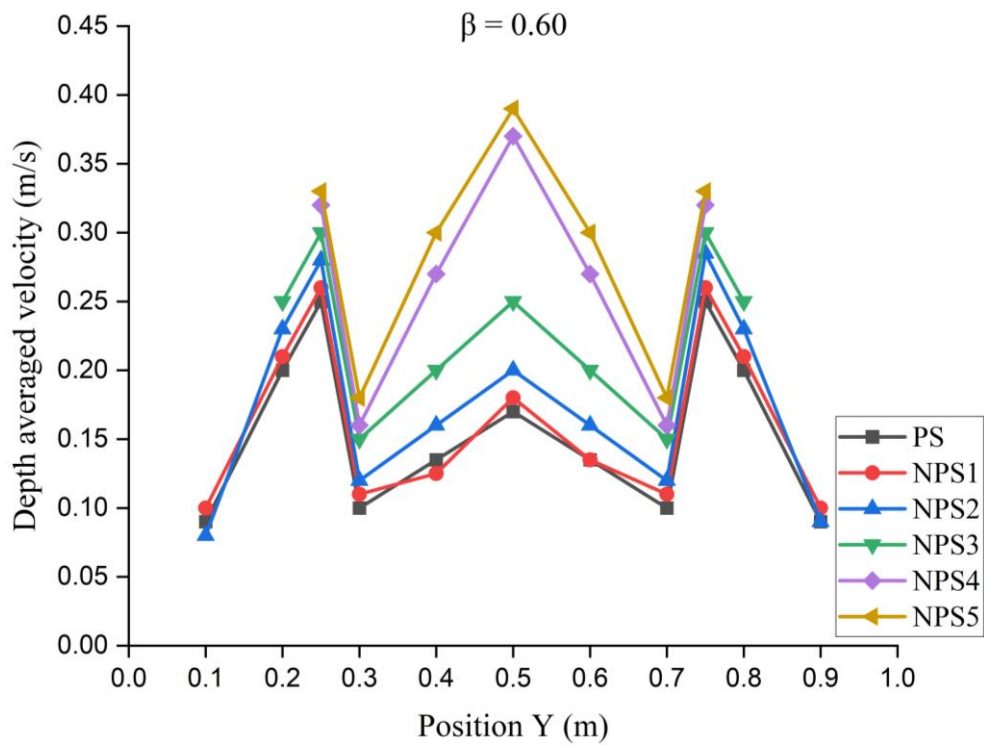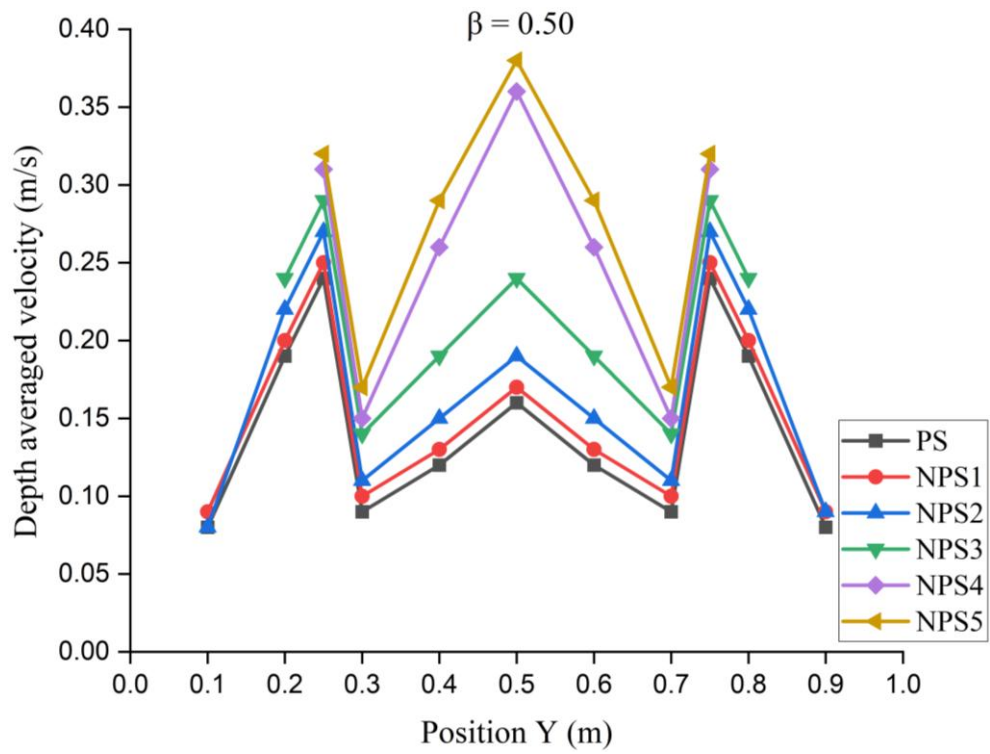
Fig. 4.15 Depth averaged velocity distribution in nonprismatic compound channel with sediment and rough floodplains for various relative flow depths

The variation of bed shear stress along the longitudinal distance for various relative depths (range from 0.20 to 0.60) in a nonprismatic compound channel with sediment and smooth and rough floodplains is shown in Fig. 4.16. Initially, bed shear stress exhibits a linear increase with longitudinal distance until reaching the prismatic section. However, in the early part of the convergent zone, a sharp rise in bed shear stress is observed due to the narrowing of the channel, which intensifies flow concentration and bed tractive forces. As the channel continues to converge, a subsequent reduction in shear stress occurs, primarily due to the acceleration of flow within the constricted section. This reduction is attributed to the redistribution of flow energy and the realignment of velocity gradients in response to the changing geometry. Overall, the magnitude of bed shear stress tends to increase with longitudinal distance, with the effect becoming more pronounced at higher relative depths. This is because greater relative depths contribute to increased flow intensity, thereby amplifying shear forces acting on the bed. In nonprismatic compound channels with rough floodplains, the bed shear is higher as compared to smooth floodplains due to the presence of irregularities on the floodplain surface and sediment in the main channel, creating frictional resistance. The increase in bed shear is seen up to 85.72%, 91.30%, 92.00%, 92.86%, and 93.75% at relative depths of 0.20, 0.30, 0.40, 0.50, and 0.60, respectively, compared to smooth floodplains.

The distribution of depth-averaged shear stress at the boundaries across the width of the nonprismatic composite waterway with sediment and smooth and rough floodplains are depicted in Fig. 4.17. The figure includes both prismatic and nonprismatic cross-sections and the relative flow depth β is set at 0.60. The distribution of boundary shear stress exhibits symmetry and expands progressively from NPS1 to NPS5. The largest value of wall tractive stress is seen at the interface of the primary waterway and flooding zones, and this value rises as the flow transitions from a prismatic portion to a nonprismatic segment. The magnitude of the boundary shear stress diminishes as it approaches the floodplain interface across all sections. In the vicinity of the junction of the primary waterway and zones of flooding, there is a rapid rise in shear stress values. This is followed by a gradual decrease towards the boundaries of the channel. This pattern arises due to the abrupt change in flow characteristics and turbulence generated at the interface. A large velocity gradient is experienced in this location as a result of the interaction. The shear stress increases as the flow transitions between these two areas, leading to higher energy dissipation and turbulence.
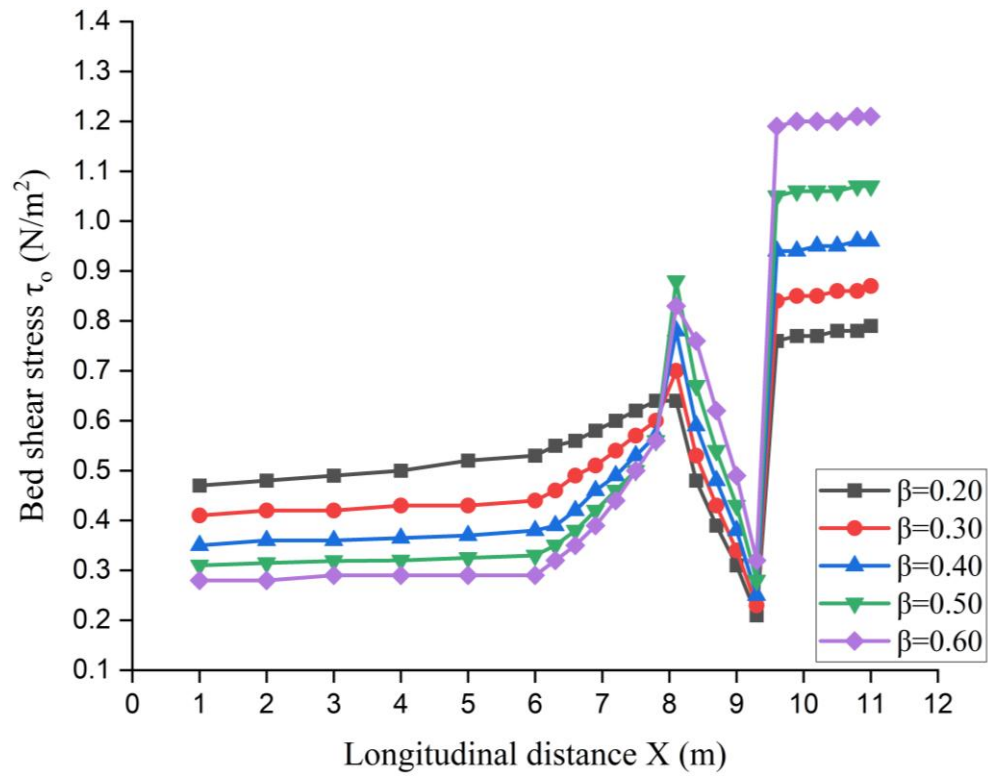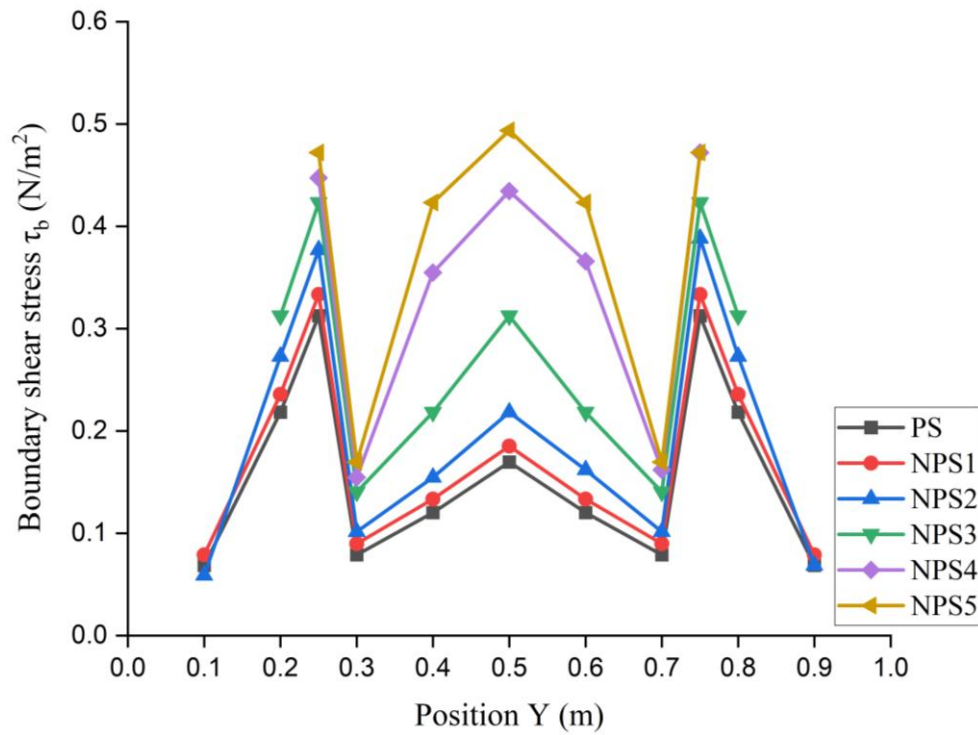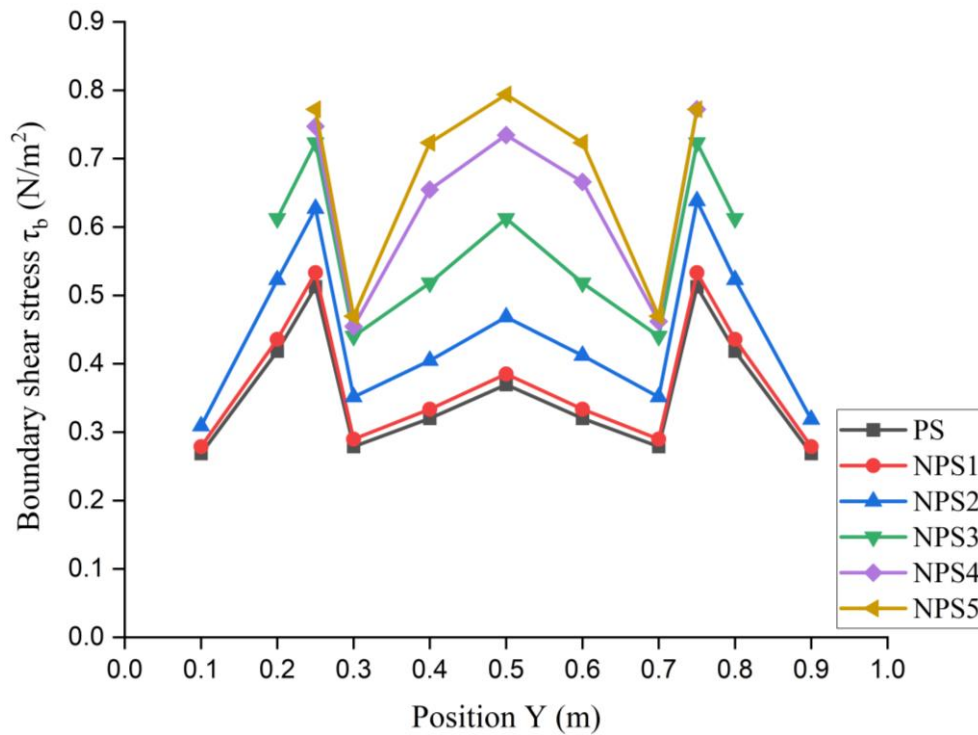
(a)
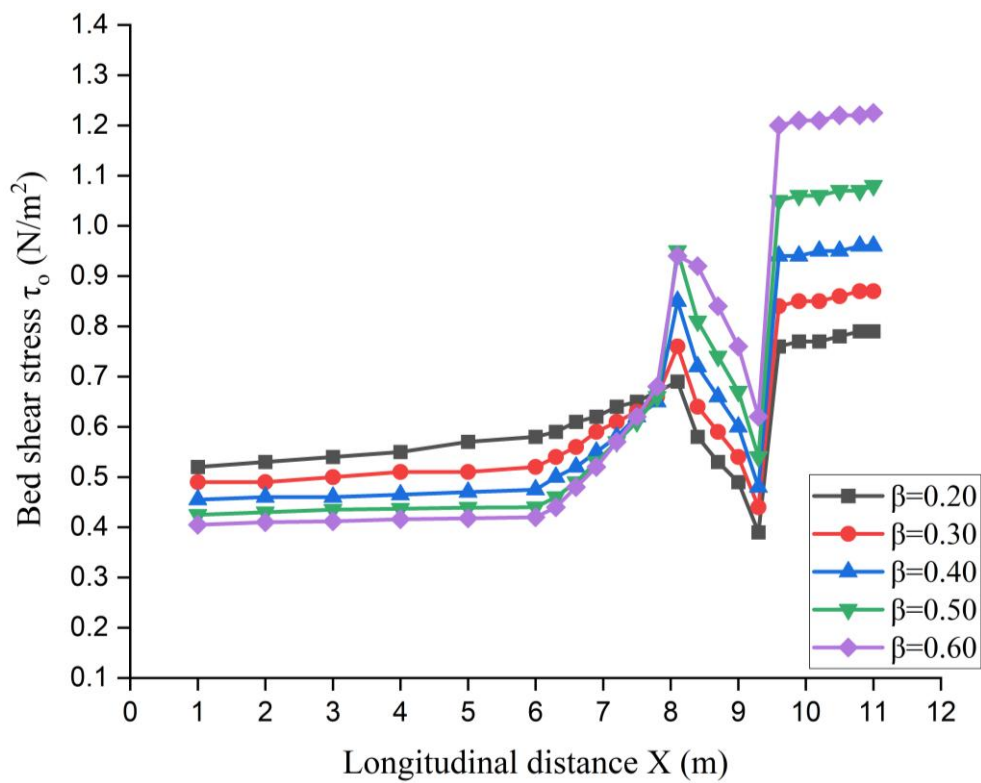
(b)

Fig. 4.16 Variation of bed shear stress along the longitudinal distance of the nonprismatic compound channel with sediment and (a) smooth floodplains (b) rough floodplains

(a)

(b)

Fig. 4.17 Distribution of boundary shear stress across the width of nonprismatic compound channel with sediment and (a) smooth and (b) rough floodplains

The variation of sediment transport rate with the discharge for nonprismatic compound channels with smooth and rough floodplains is represented in Fig. 4.18. It is observed that the sediment transport rate increases as the discharge increases in overbank flow conditions. The combination of higher flow velocities expanded flow area, and increased turbulence results in a greater sediment transport rate as discharge increases during overbank flow conditions. Increasing floodplain roughness is seen to depress the sediment transport rate further, arising from the increase in flow depth and reduction in bed shear stress within the main channel. This study compares its findings to prior research conducted on prismatic compound channels. Notably, sediment transport rates in nonprismatic compound channels with converging floodplains exceed those reported by Atabay et al. (2005) and Tang and Knight (2006), who examined sediment analysis in prismatic compound channels with similar bed conditions and induced roughness using wire mesh with varying spacings on floodplains, respectively.

Garde and Rangaraju (1985) considered a parameter $S^* = \frac{S_o}{[(\gamma_s - \gamma)/\gamma]}$ and R/d to predict the type of bed forms. The various bed form phases can be expressed as:

For plane bed with no motion: $\qquad$ S* ≤ 0.05 (R/d)$^{-1}$

For ripples and dunes: $\qquad$ 0.05 (R/d)$^{-1}$ ≤ S* ≤ 0.014 (R/d)$^{-0.46}$

For transition: $\qquad$ 0.014. (R/d)$^{-046}$ ≤ S* ≤ 0.059 (R/d)$^{-0.54}$

For Antidunes: $\qquad$ S* ≥ 0.059 (R/d)$^{-0.54}$

Where S^* is dimensionless parameter, S_o is longitudinal bed slope (dimensionless), γ is unit weight of water (KN/m^3), γ_s is unit weight of the sediment particle (KN/m^3), R is hydraulic radius (m) and d is diameter the sediment particle (m).

Since, 0.05 (R/d)$^{-1}$ ≤ S* ≤ 0.014 (R/d)$^{-0.46}$, the bed form is of ripples and dunes category in both nonprismatic compound channels with smooth and rough floodplains.

The longitudinal bed profile along the middle line of the primary passageway of a nonprismatic compound channel is illustrated in Fig. 4.19. The profile is shown for various relative flow depths, including both smooth and rough floodplains. The bed level first lowers then increases, and finally degrades up to the commencement of the converging portion owing to an increase in velocity. The bed deposition occurs in the first portion of the converging section and subsequently in the latter portion of the converging section, as a result of increased flow velocity, there is a drop in the amount of sediment accumulation. As the channel converges, the flow velocity causes sediment

to settle and deposit in the first half of the section. However, as the flow continues to narrow, the velocity increases sharply, enhancing the shear stress on the bed. This increased tractive stress in the latter half of the portion leads to entrainment and transportation of sediment, resulting in degradation. Thus, the dynamic interplay of flow velocities drives the pattern of sediment deposition followed by degradation in a channel.
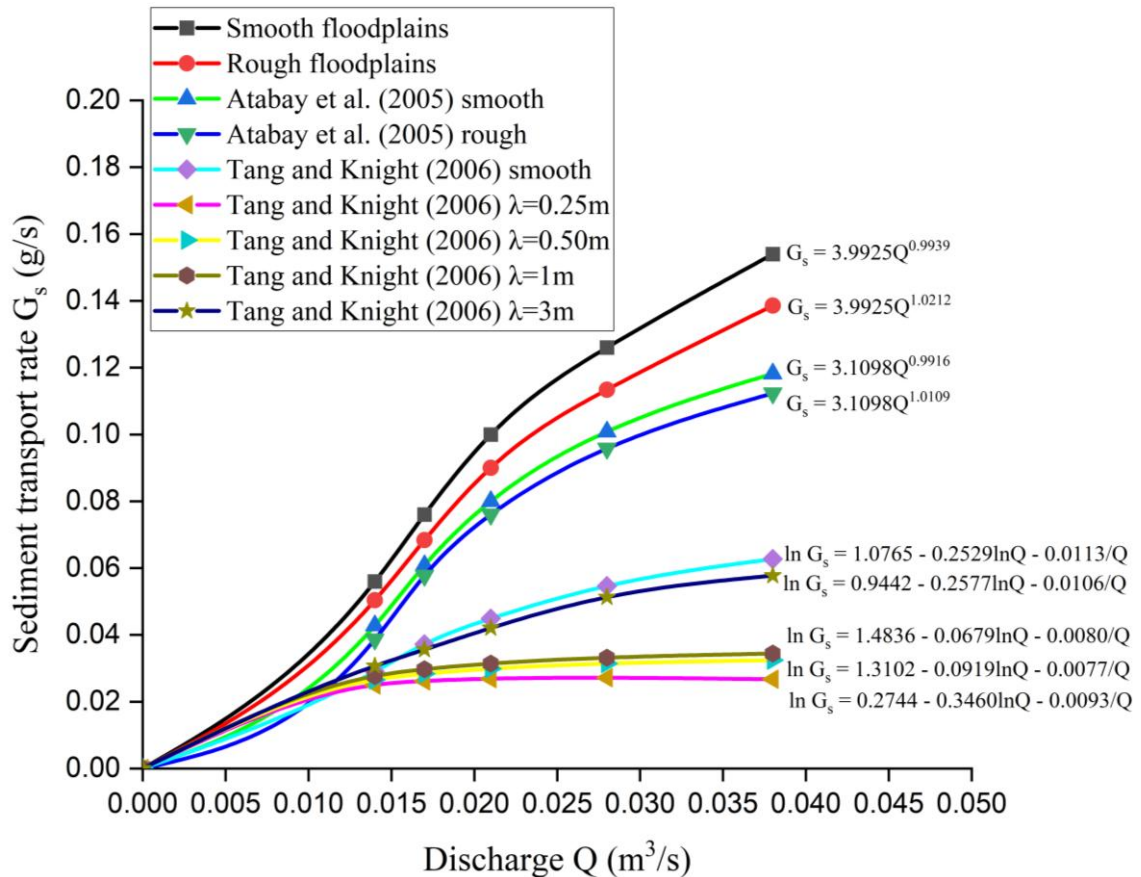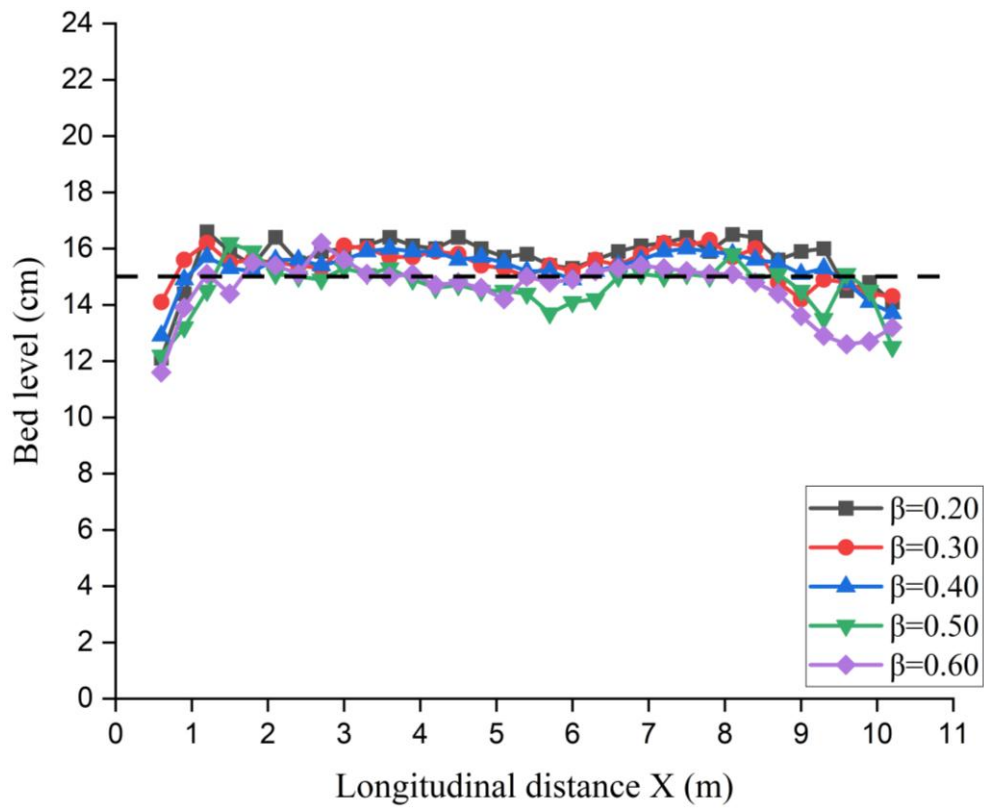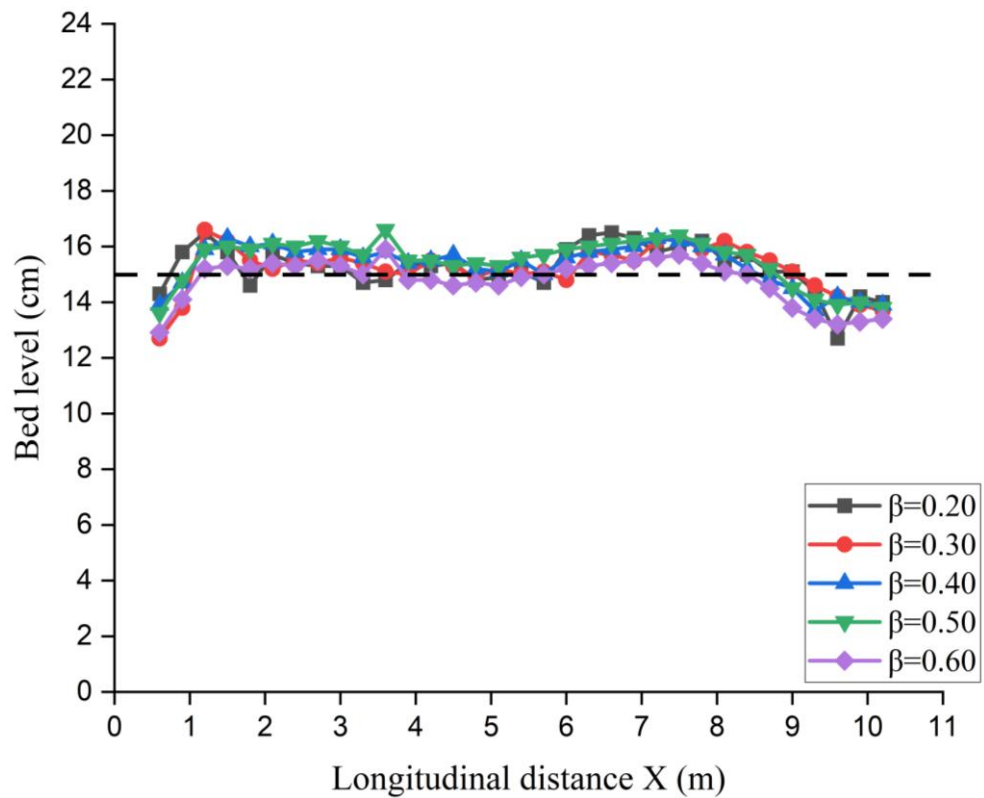

Fig. 4.18 Variation of sediment transport rate with discharge in nonprismatic compound channels
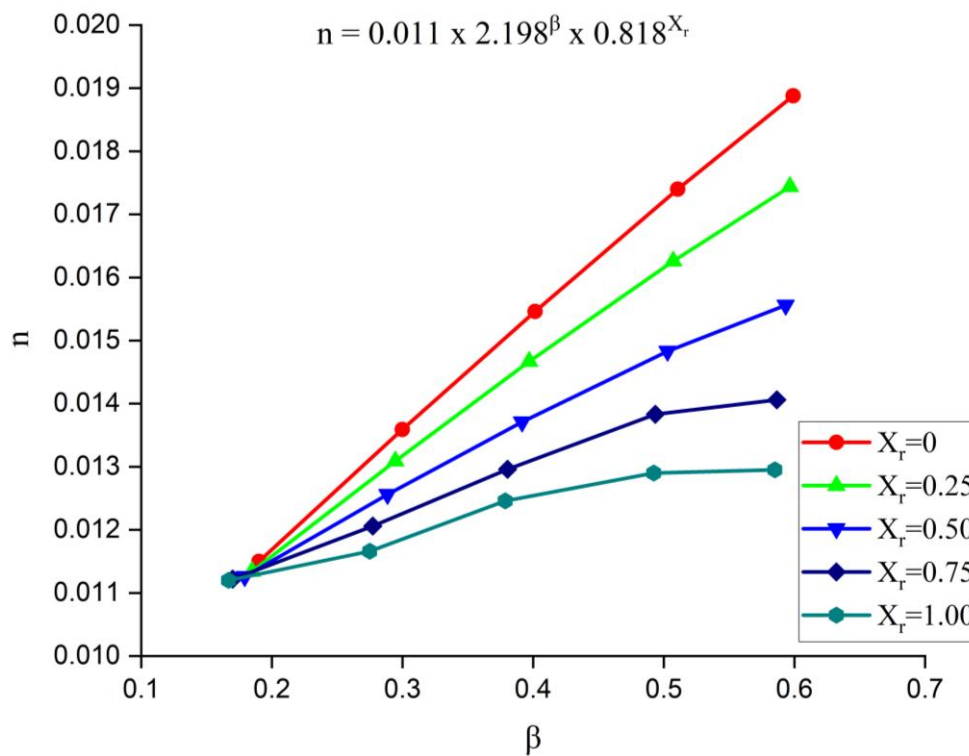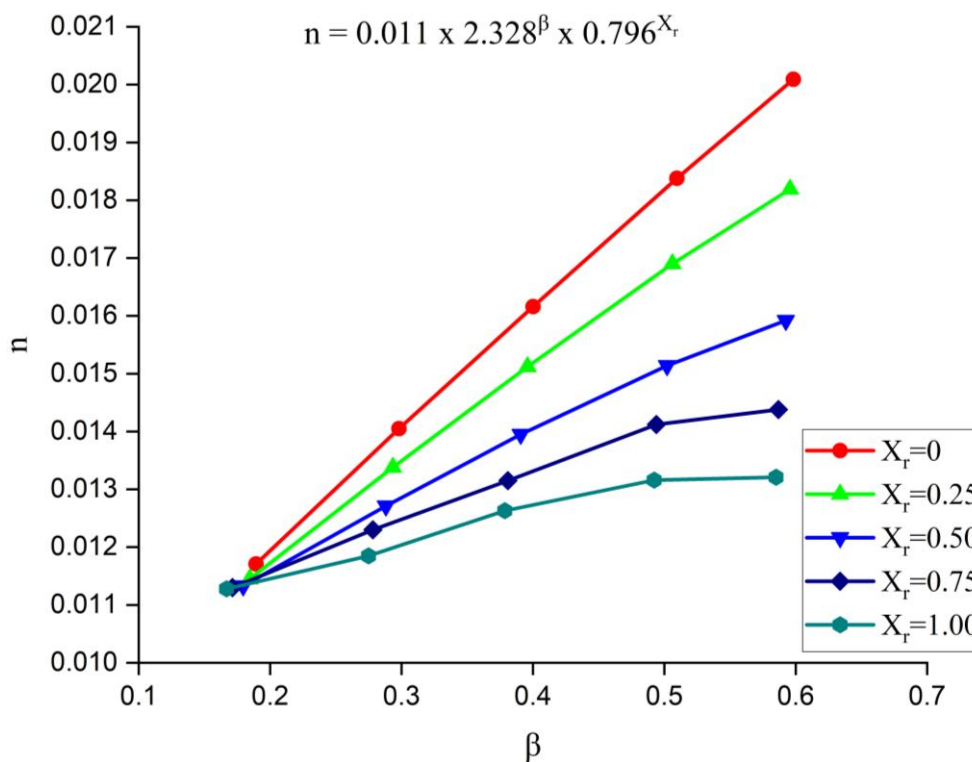
(a)

(b)

Fig. 4.19 Bed profile along the center of the nonprismatic compound channels with (a) smooth floodplains and (b) rough floodplains

4.3 Flow resistance in nonprismatic compound channels

The Manning's roughness coefficient (n) variations with the relative flow depth (β) for different nonprismatic sections in a nonprismatic compound channels with smooth and rough floodplains are represented in Fig. 4.20. The x-axis represents the relative flow depth (β), while the y-axis indicates Manning's n, which measures flow resistance. Relative distance (X_r) values represent different sections of the converging segment as follows: $X_r = 0$ corresponds to NPS1, marking the beginning of the converging section, $X_r = 0.25$ corresponds to NPS2, an intermediary segment between NPS1 and NPS3, $X_r = 0.50$ corresponds to NPS3, which represents the central section of the converging segment, $X_r = 0.75$ corresponds to NPS4, an intermediary segment between NPS3 and NPS5, $X_r = 1.00$ corresponds to NPS5, marking the end of the converging section. In nonprismatic compound channels having both smooth and rough floodplains, the values of 'n' exhibit an upward trend as the relative flow depth rises. As the depth of the flow rises, a greater portion of the flow makes contact with both the channel bed and the floodplains. The augmented contact area results in heightened frictional resistance between the water in motion and the boundaries of the channel. Furthermore, the interaction between the main channel and the floodplains contributes to changes in flow resistance, as momentum exchange occurs between these regions. This effect is more pronounced in rough floodplains, where additional surface irregularities intensify turbulence. In the case of smooth floodplains, Manning's n tends to be lower as the surface offers less frictional resistance, whereas rough floodplains exhibit higher values due to increased turbulence and energy dissipation. As the flow progresses through nonprismatic parts, the 'n' values fall owing to the converging geometry of the channel, resulting in flow acceleration. The compound channel with smooth and rough floodplains exhibits an increase in 'n' values with relative flow depth was up to 64.17%, 53.79%, 38.19%, 25.31%, 15.62%, and 71.56%, 58.86%, 40.52%, 27.26%, and 17.11% for relative distance $X_r = 0$, 0.25, 0.50, 0.75 and 1.00, respectively. In comparison to compound channels with smooth floodplains, rough floodplains exhibit more resistance to flow. The observed increase in 'n' values were up to 6.41%, 4.31%, 2.31%, 2.28%, and 2.01% for relative distance $X_r = 0$, 0.25, 0.50, 0.75 and 1.00, respectively.
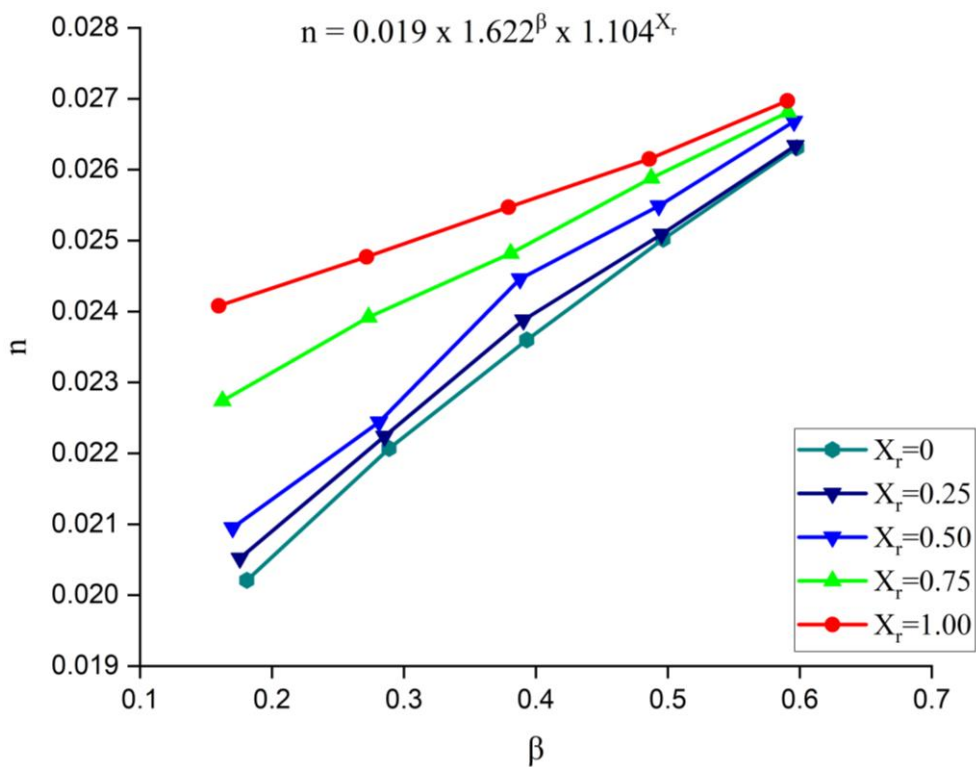
$$n = 0.011 \times 2.198^{\beta} \times 0.818^{X_r}$$

(a)

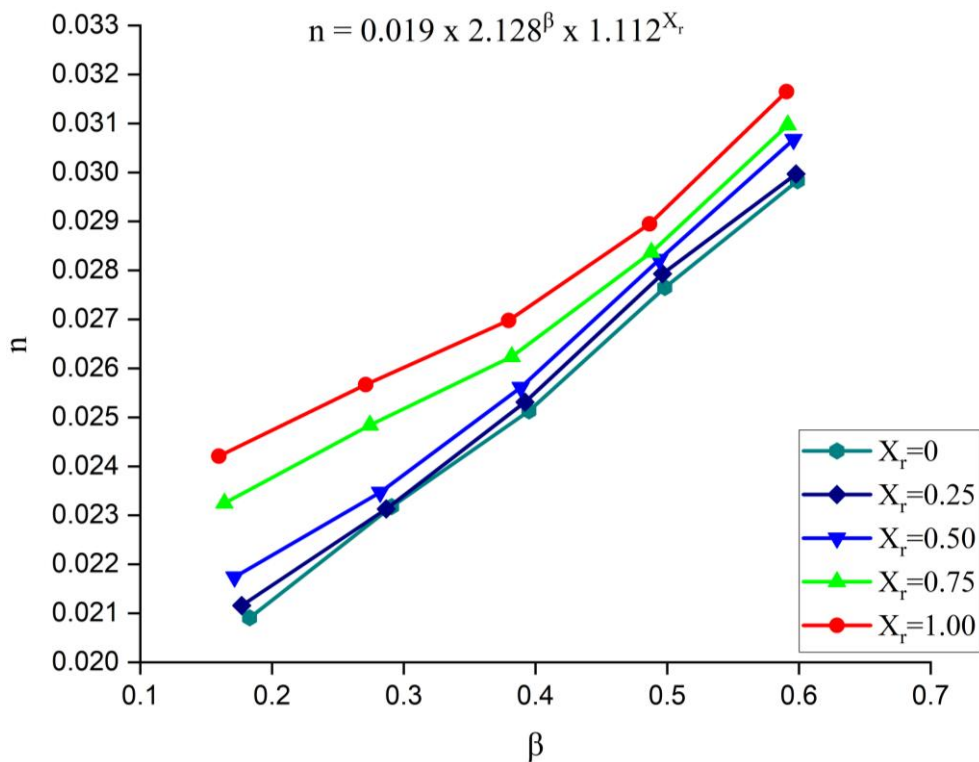$$n = 0.011 \times 2.328^{\beta} \times 0.796^{X_r}$$

(b)

Fig. 4.20 Variation of Manning's roughness coefficient with the relative flow depth for nonprismatic compound channel with (a) smooth floodplains (b) rough floodplains

The relationship between Manning's roughness coefficient (n) and relative flow depth (β) for various nonprismatic sections in a nonprismatic compound channels with sediment bed, including both smooth and rough floodplains is illustrated in Fig. 4.21. The x-axis represents the relative flow depth (β), while the y-axis indicates Manning's n, which measures flow resistance. X_r values represent different sections of the converging segment as follows: $X_r = 0$ corresponds to NPS1, marking the beginning of the converging section, $X_r = 0.25$ corresponds to NPS2, an intermediary segment between NPS1 and NPS3, $X_r = 0.50$ corresponds to NPS3, which represents the central section of the converging segment, $X_r = 0.75$ corresponds to NPS4, an intermediary segment between NPS3 and NPS5, $X_r = 1.00$ corresponds to NPS5, marking the end of the converging section. In nonprismatic compound channels having both smooth and rough floodplains, the values of 'n' exhibit an upward trend as the relative flow depth rises throughout the sections. As the flow traverses nonprismatic regions of the compound channel, the values of 'n' exhibit a rise with increasing depth. The presence of rough floodplains and sediment beds in overbank flows leads to increased flow resistance. This is mainly because the increased surface area contact between the water and the uneven surfaces improves the frictional resistance. The presence of friction, along with turbulent mixing resulting from surface roughness, disperses the energy of the flow and decelerates the water's motion. Moreover, the existence of obstacles and irregularities in the course of the flow amplifies the distance of travel, hence increasing resistance. The presence of shear stress at the interface, as well as the processes of sediment transport, together contribute to the hindrance of flow, resulting in an increase in total resistance. The compound channel with smooth and rough floodplains exhibits a rise in 'n' values with relative flow depth up to 30.18%, 28.36%, 27.35%, 17.89%, 12.05%, and 42.66%, 41.63%, 41.08%, 33.20%, and 30.73% for relative distance $X_r = 0$, 0.25, 0.50, 0.75 and 1.00, respectively. The increase in 'n' values in rough floodplains was found up to 13.38%, 13.78%, 14.96%, 15.52%, and 17.35% for relative distance $X_r = 0$, 0.25, 0.50, 0.75, and 1.00, respectively, as compared to compound channel with smooth floodplains. Table 4.1 summarizes the effects of various factors on Manning's n in compound channels, both without and with sediment, respectively.

.

(a)

(b)

Fig. 4.21 Variation of Manning's roughness coefficient with the relative flow depth for nonprismatic compound channel with sediment and (a) smooth floodplains (b) rough floodplains

Table 4.1 Effect of various factors on Manning's n in compound channels with and without sediment

| Factor	Effect on Manning's n (compound channel without sediment)	Effect on Manning's n (compound channel with sediment)
Floodplain Roughness	Rough floodplains increase Manning's n as compared to smooth floodplains.	Rough floodplains increase Manning's n as compared to smooth floodplains, with additional resistance due to sediment accumulation.
Channel Geometry	As flow progresses through the converging section, Manning's n decreases due to reduced resistance.	As flow progresses through the converging section, Manning's n increases due to sediment-induced resistance.
Relative Flow Depth	Manning's n increases as relative depth increases.	Manning's n increases as relative depth increases.
Sediment Presence	Not applicable	Sediment accumulation modifies flow paths, increases turbulence, and raises Manning's n.

4.4 Flow rate estimation using GEP

The scatter plots comparing the anticipated and observed values of Q_r for several GEP models (C1 to C3) and (M1 to M10) throughout the training and testing/validation stages are depicted in Fig. 4.22 and 4.23. The closeness of the values to the line indicating high agreement provides strong evidence of the predictive accuracy of the created GEP models. When comparing all models, it is evident that the predictions from model (M7) are closer to the best-fitting line than those of the other models. Therefore, it can be inferred that the GEP model (M7) has the best degree of agreement with the experimental data.

In order to evaluate the performance of the GEP models, statistical goodness of fit tests were used. These evaluations included R^2, RMSE, MAPE, SI, and AIC metrics. The metrics for the training and validation stages for models based on the gamma test are shown in Tables 4.2 and 4.3. The tables demonstrate and validate that the GEP model (M7) outperforms other GEP models. The statistical results show that the GEP model (M7) had the best R^2 (0.990), lowest RMSE (0.0855), lowest MAPE (3.3225), lowest SI (0.0405), and lowest AIC (-658.672) throughout the training phase. In the validation phase, the GEP model (M7) demonstrates the best R^2 (0.990), lowest RMSE (0.0942), lowest MAPE (3.5108), lowest SI (0.0427), and lowest AIC (-632.347).

The statistical analysis for the training and validation stages for models based on correlation among the variables are shown in Tables 4.4 and 4.5. The tables demonstrate that the GEP model (C3) outperforms other GEP models (C1 and C2). The statistical results show that the GEP model (C3) had the best R^2 (0.872), lowest RMSE (0.3268), lowest MAPE (11.6407), lowest SI (0.1507), and lowest AIC (-289.960) throughout the training phase. In the validation phase, the GEP model (C3) demonstrates the best R^2 (0.846), lowest RMSE (0.3487), lowest MAPE (12.1658), lowest SI (0.1638), and lowest AIC (-272.216). When comparing these models (C1 to C3) with the GEP model (M7) using the gamma test, it is validated that the model (M7) performs better than all the other models and demonstrates the highest level of agreement with the experimental data.
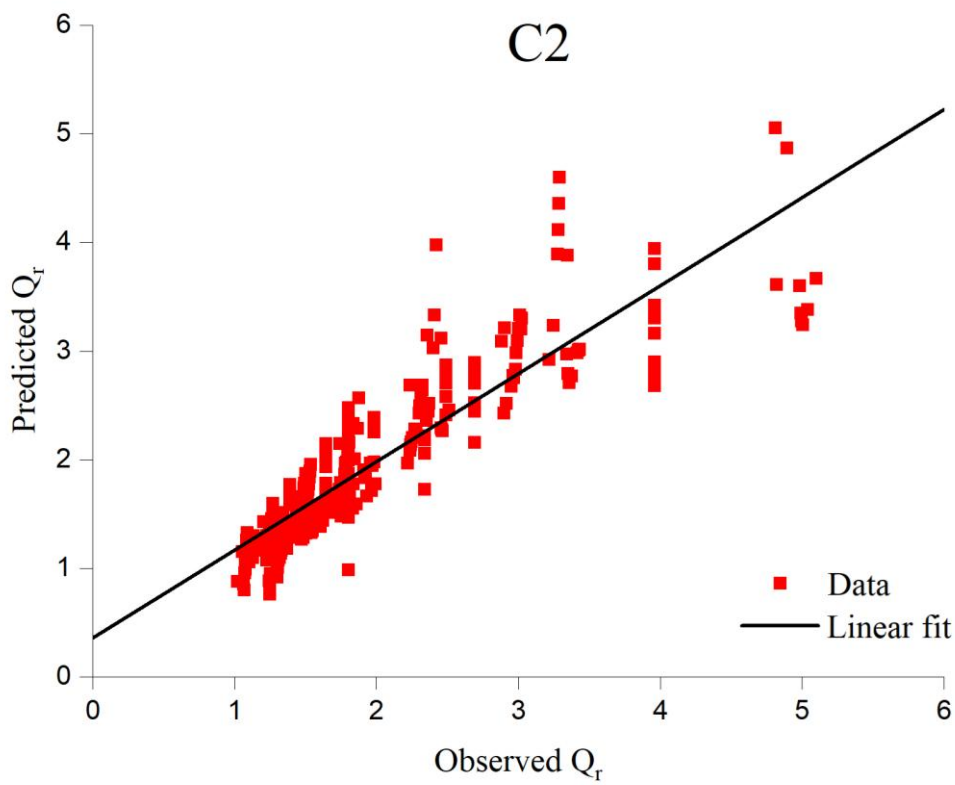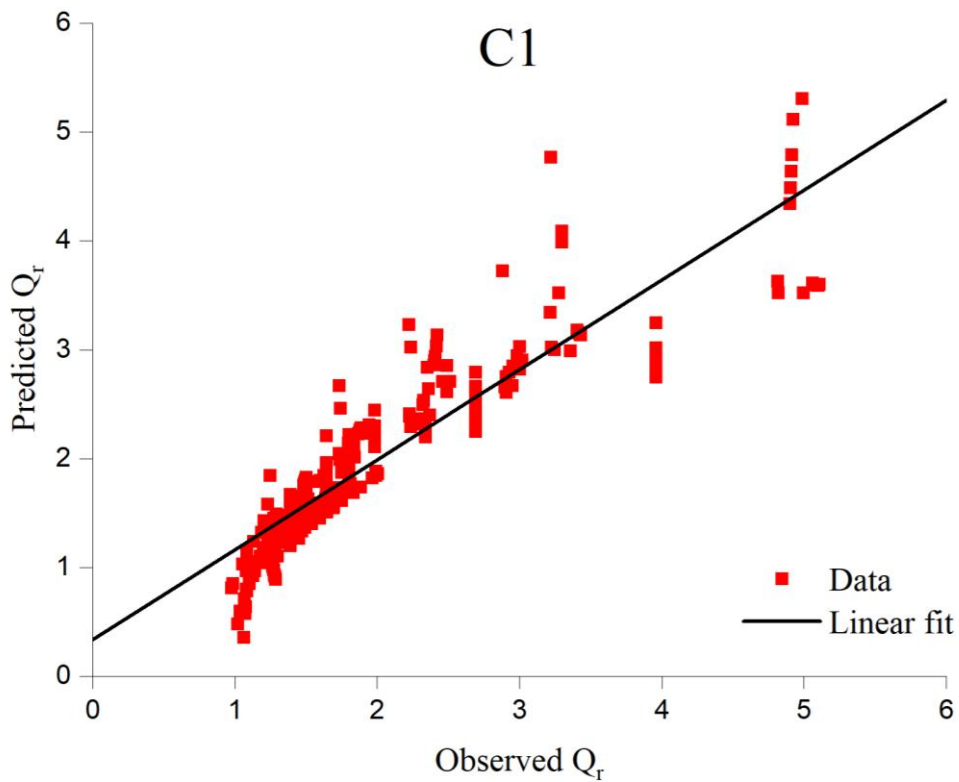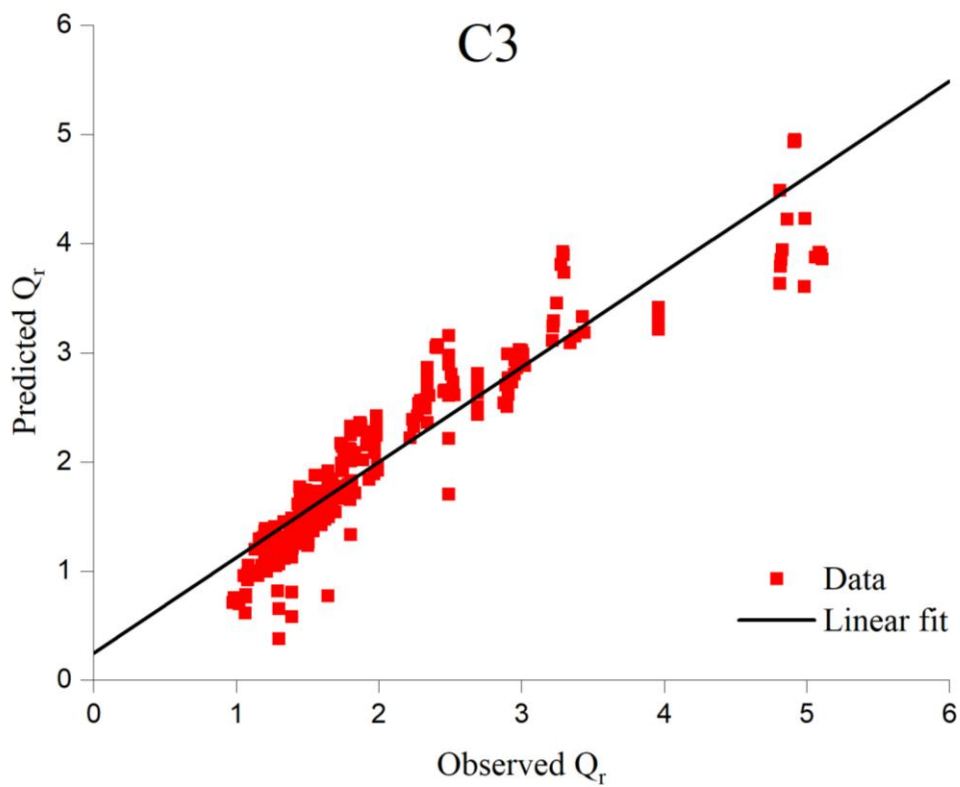
(a)
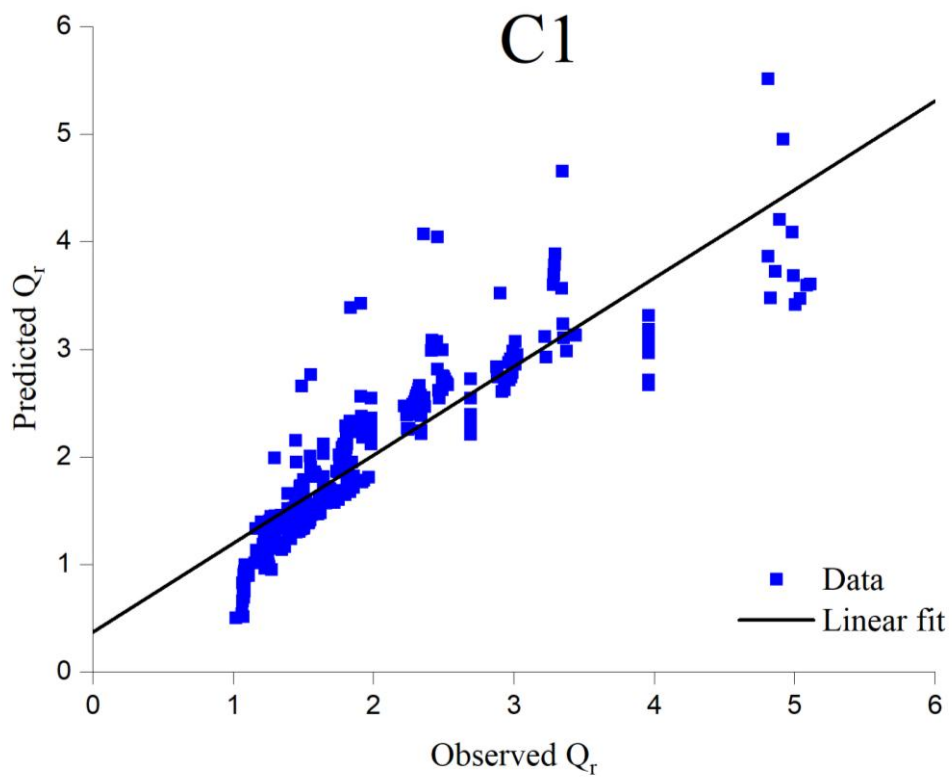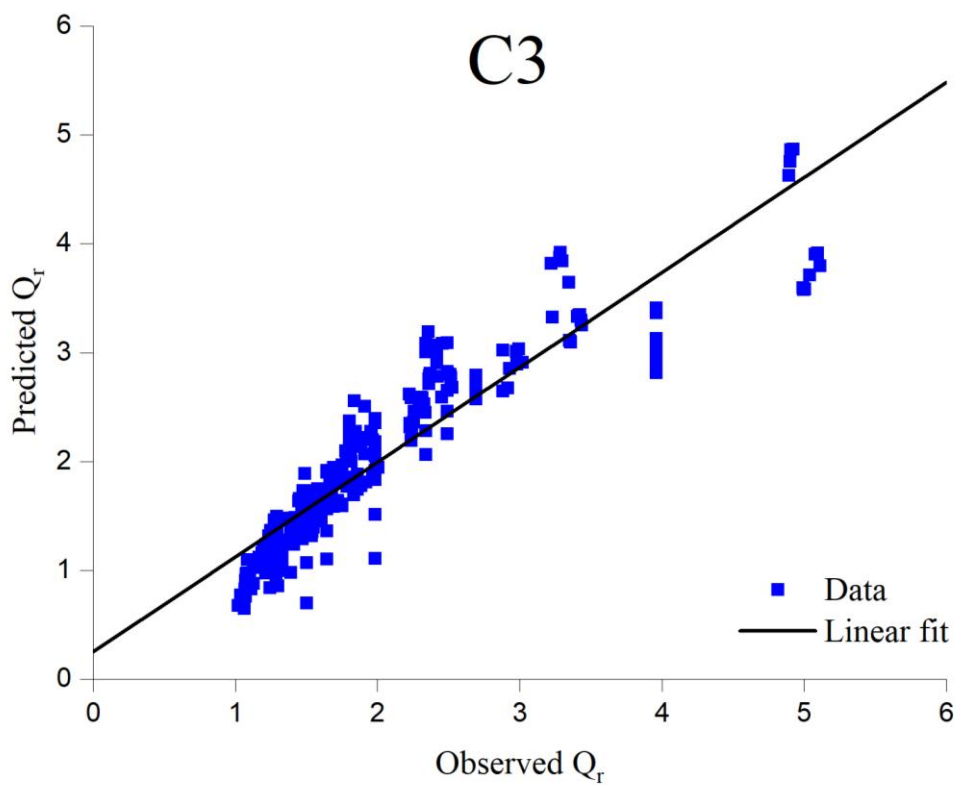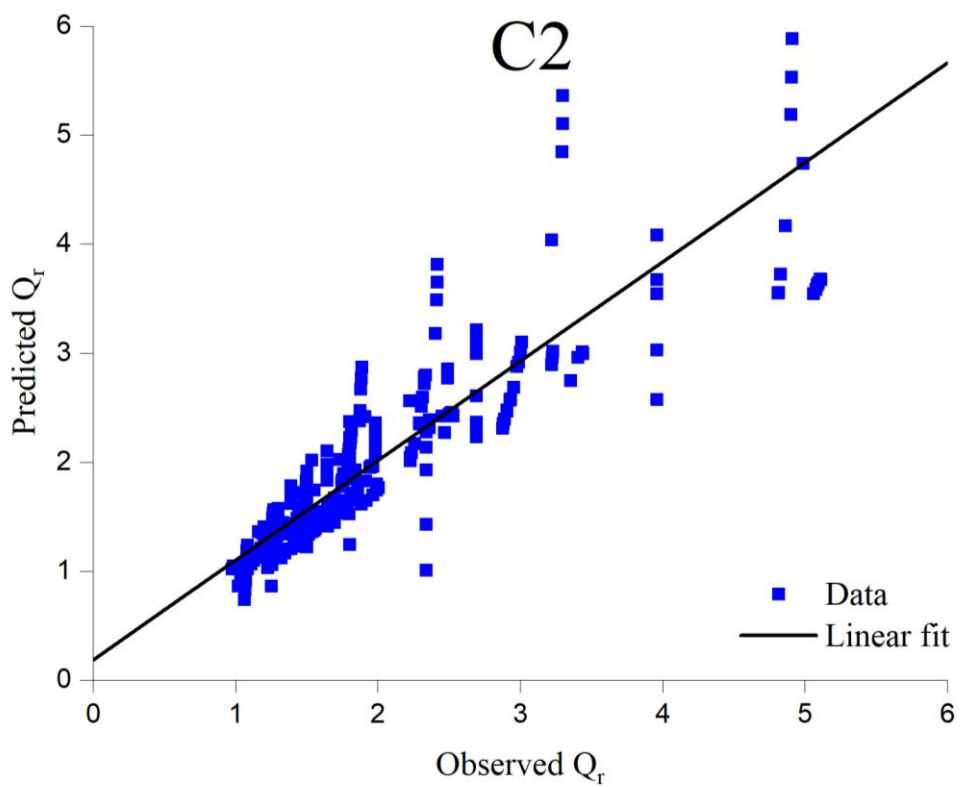
(b)

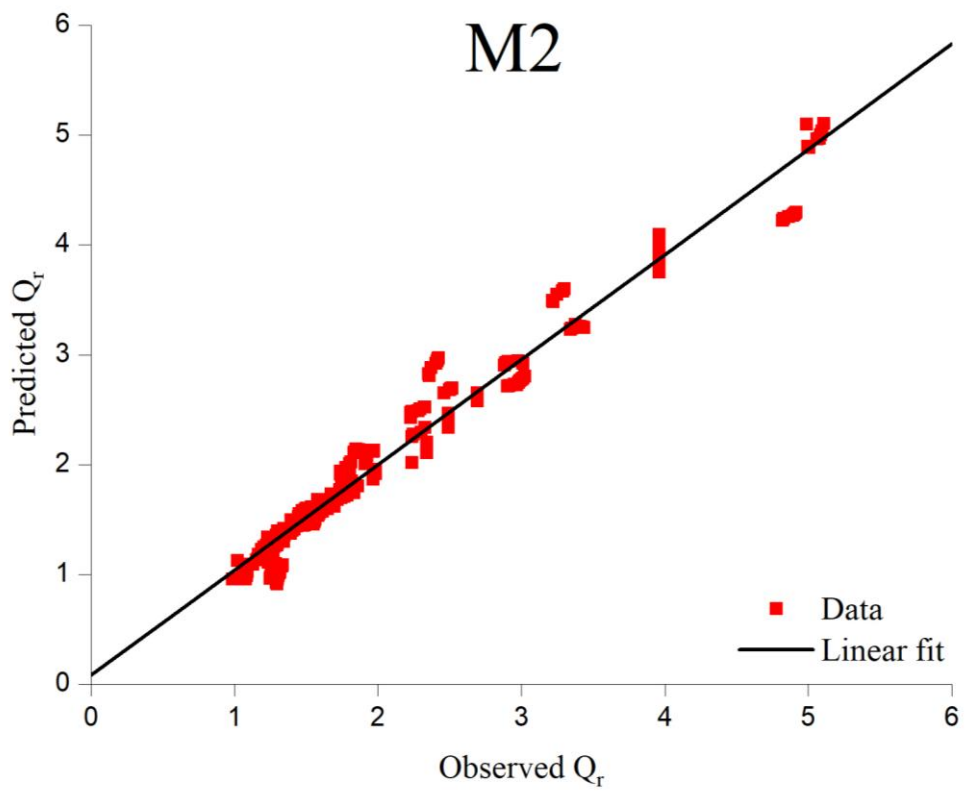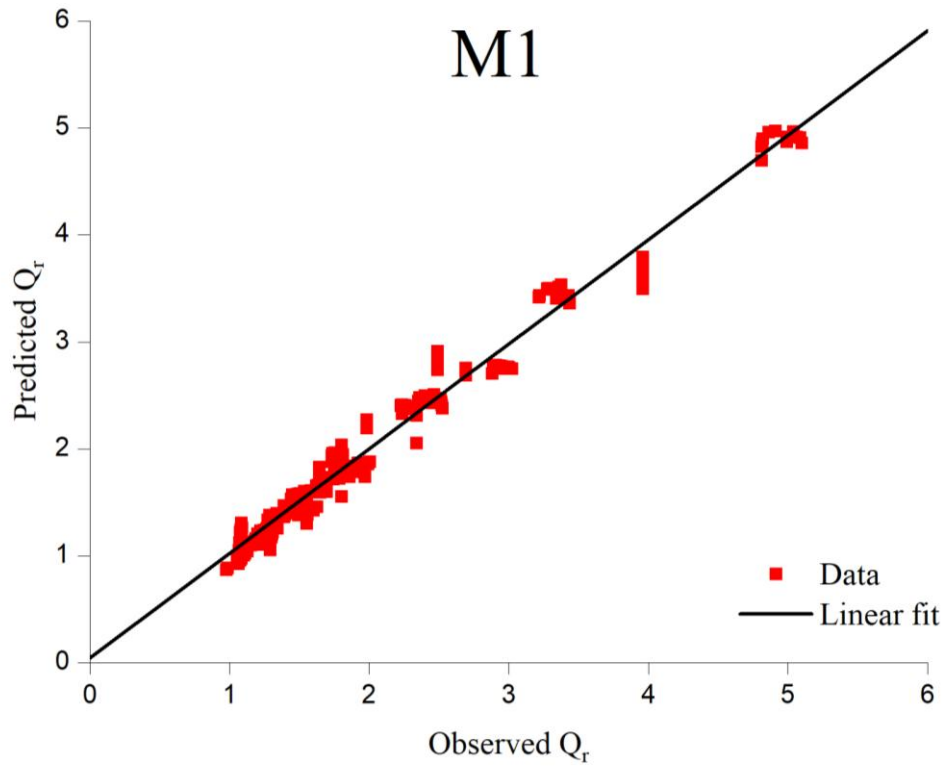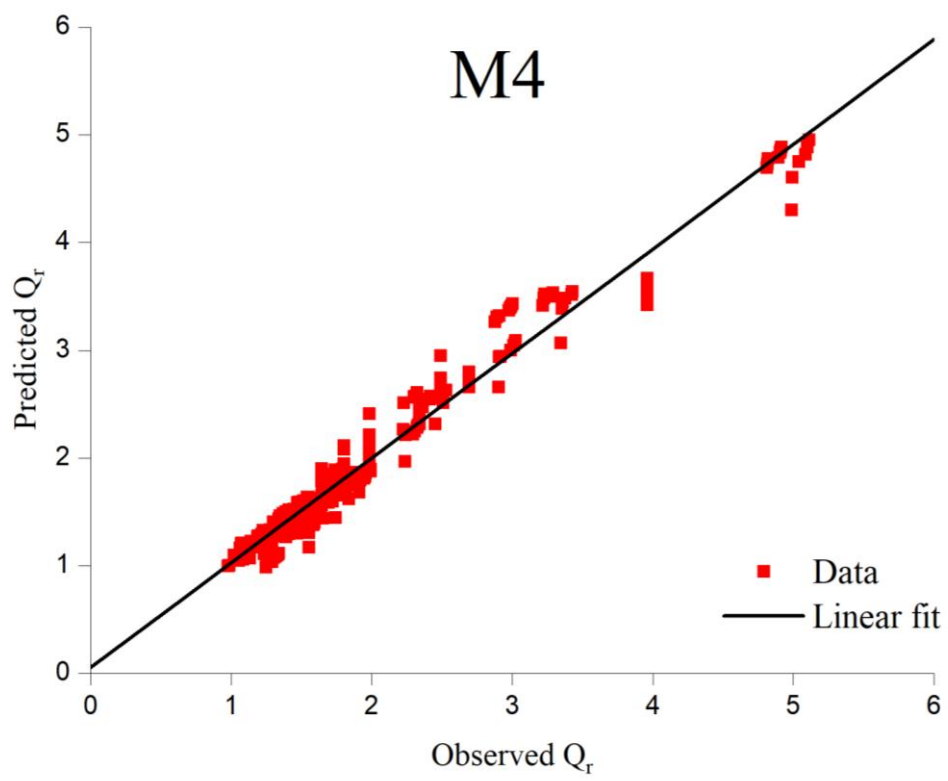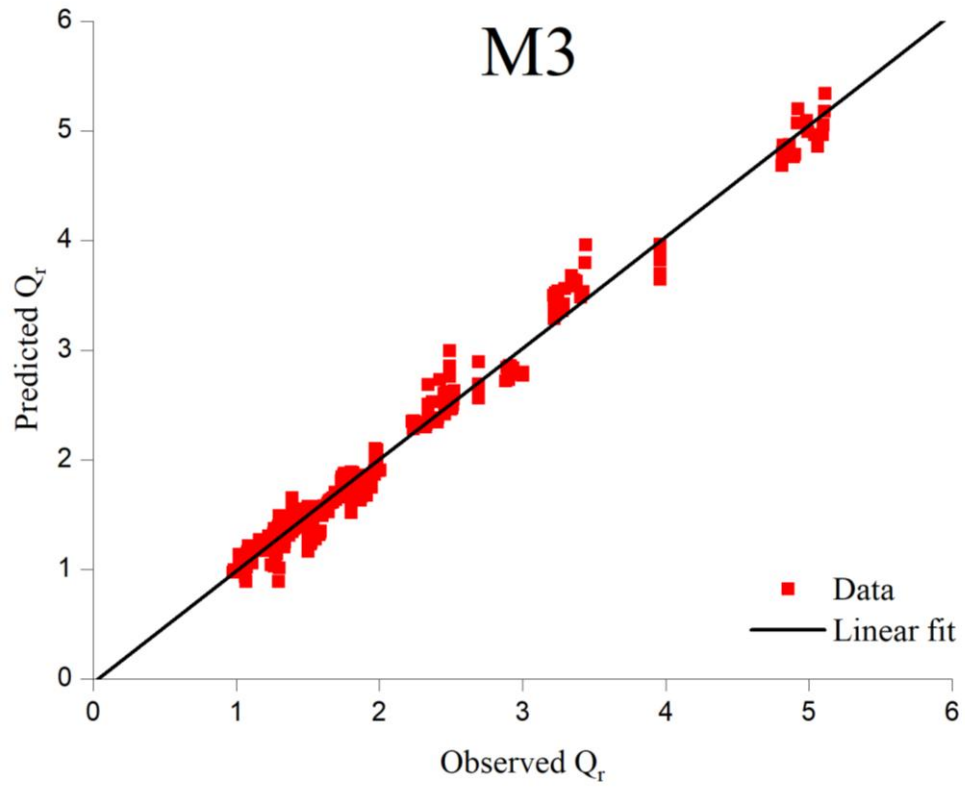Fig. 4.22 Scatter plots of observed and predicted Q_r for models (C1 to C3) in (a) the training phase (b) the validation phase
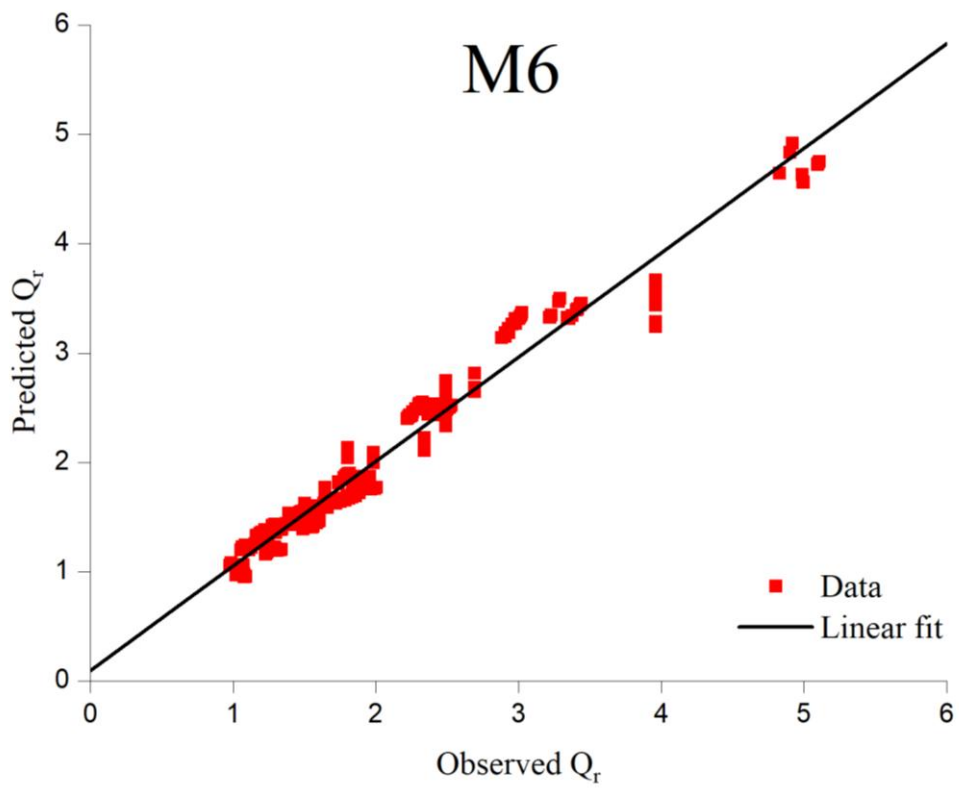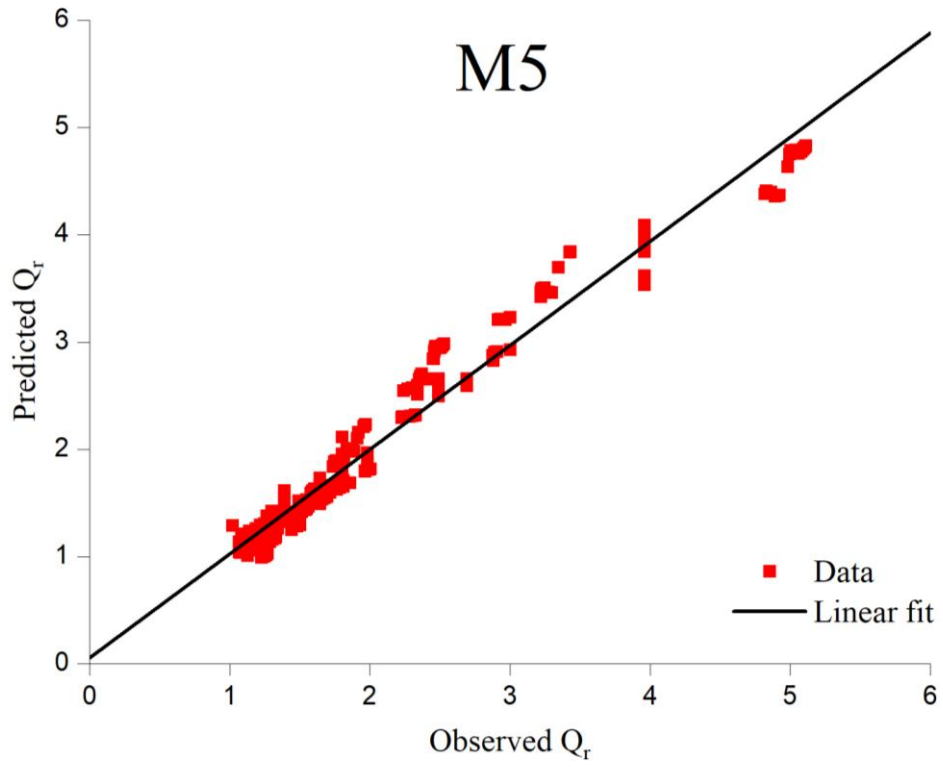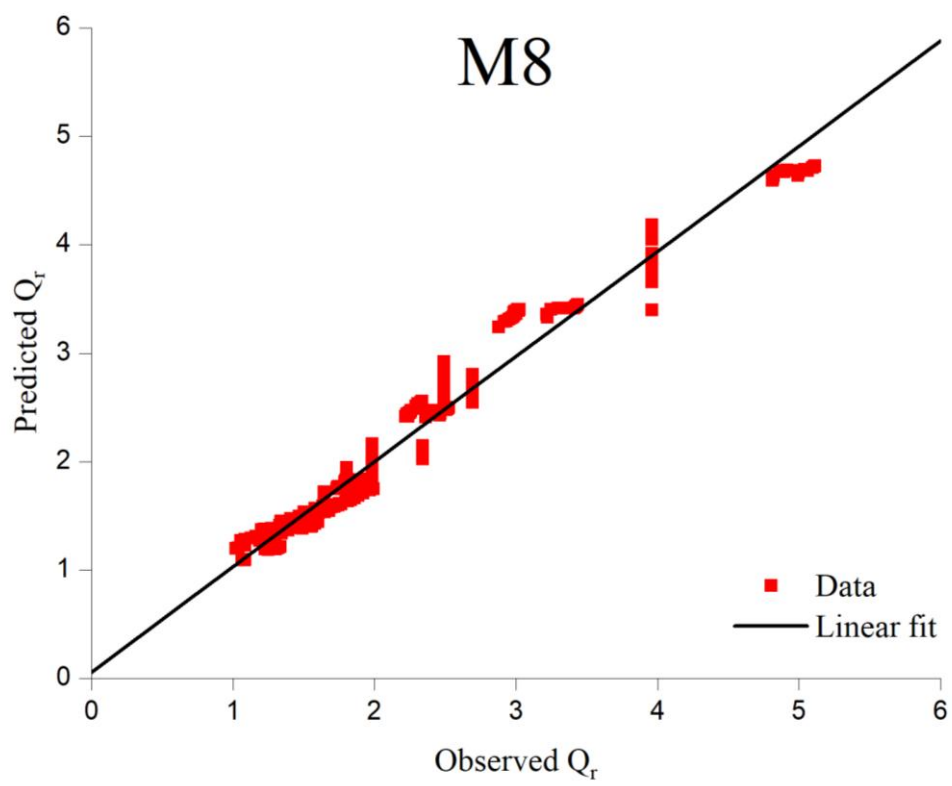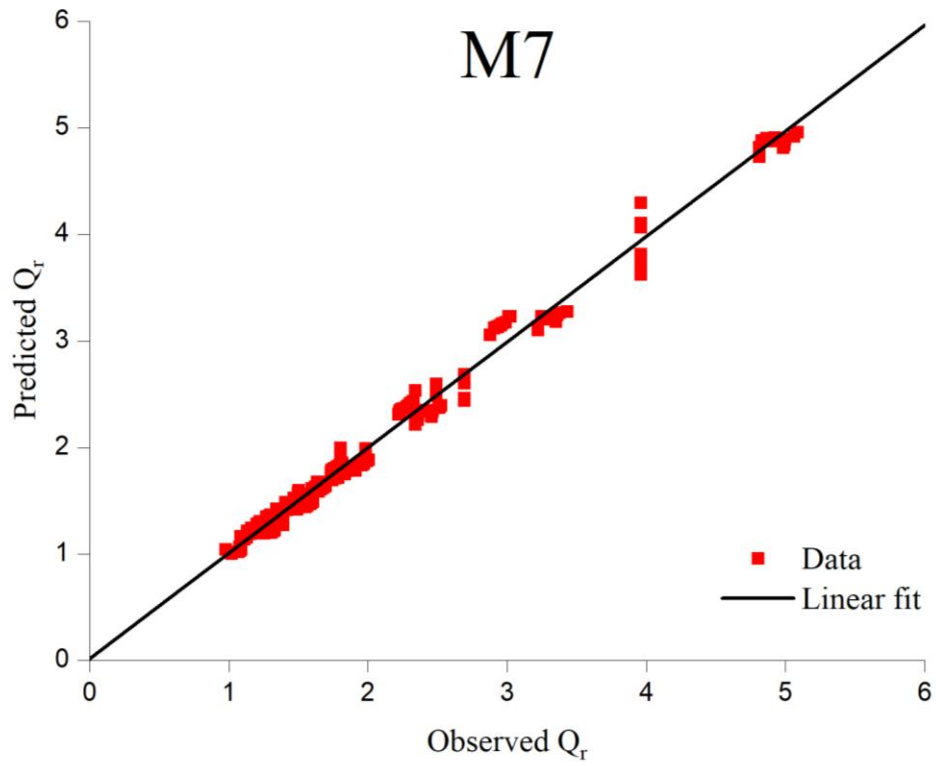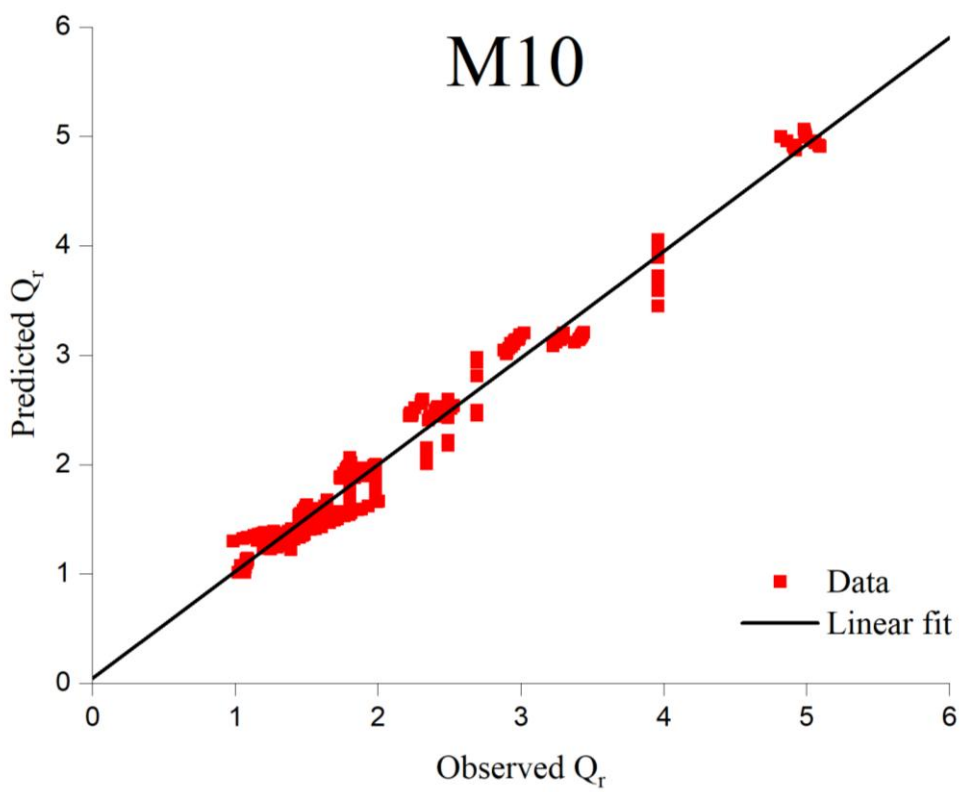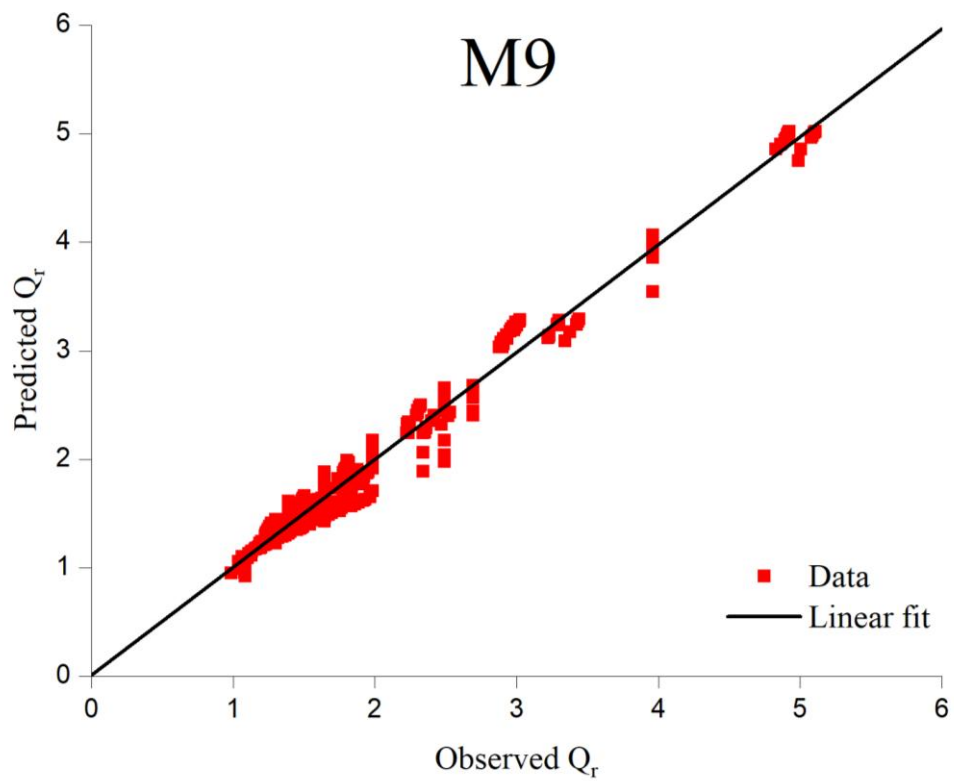
(a)
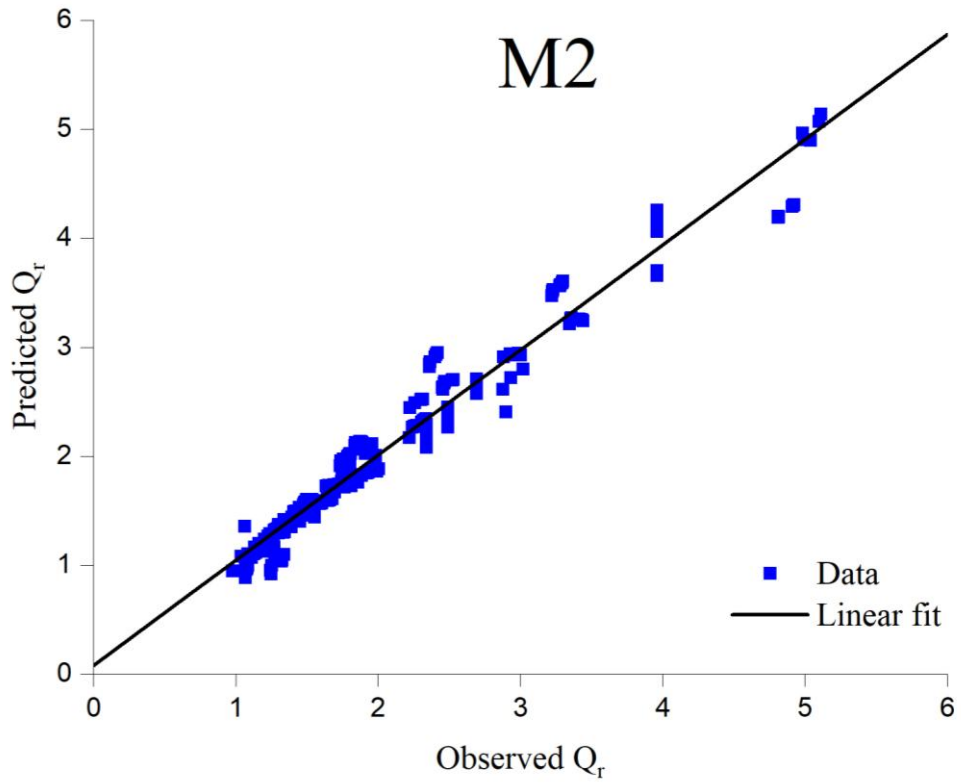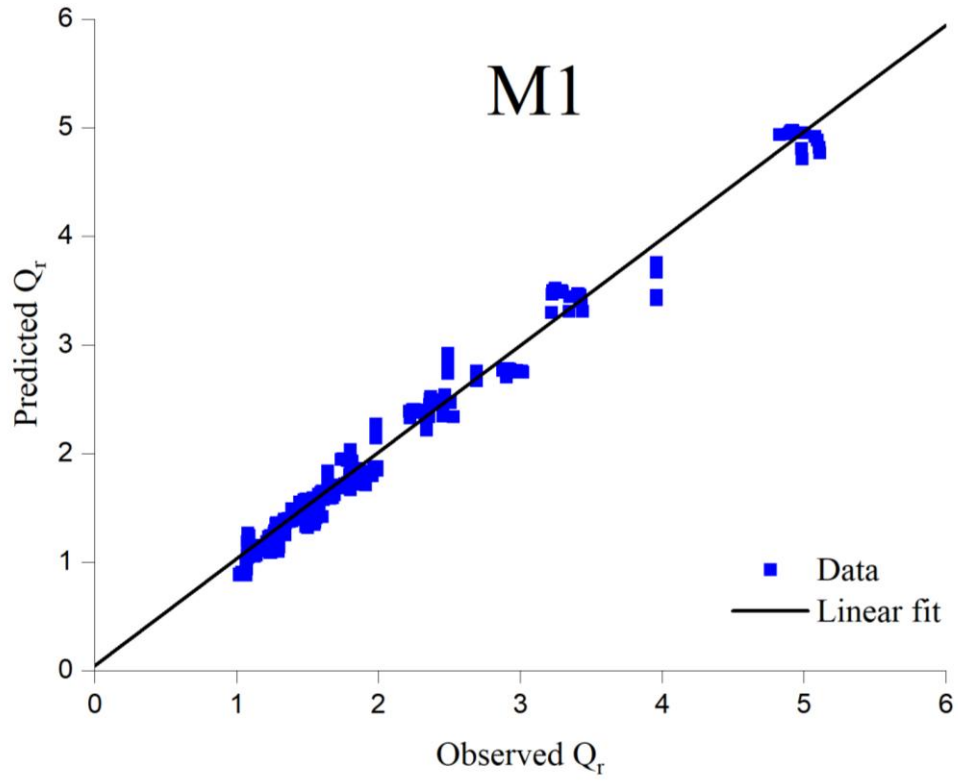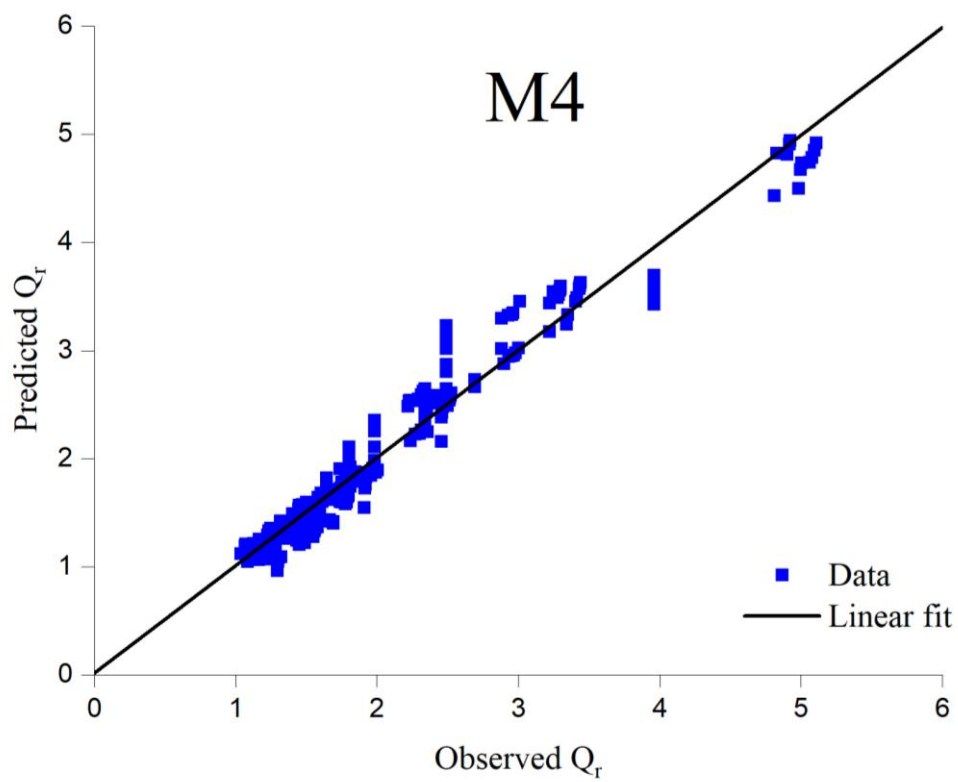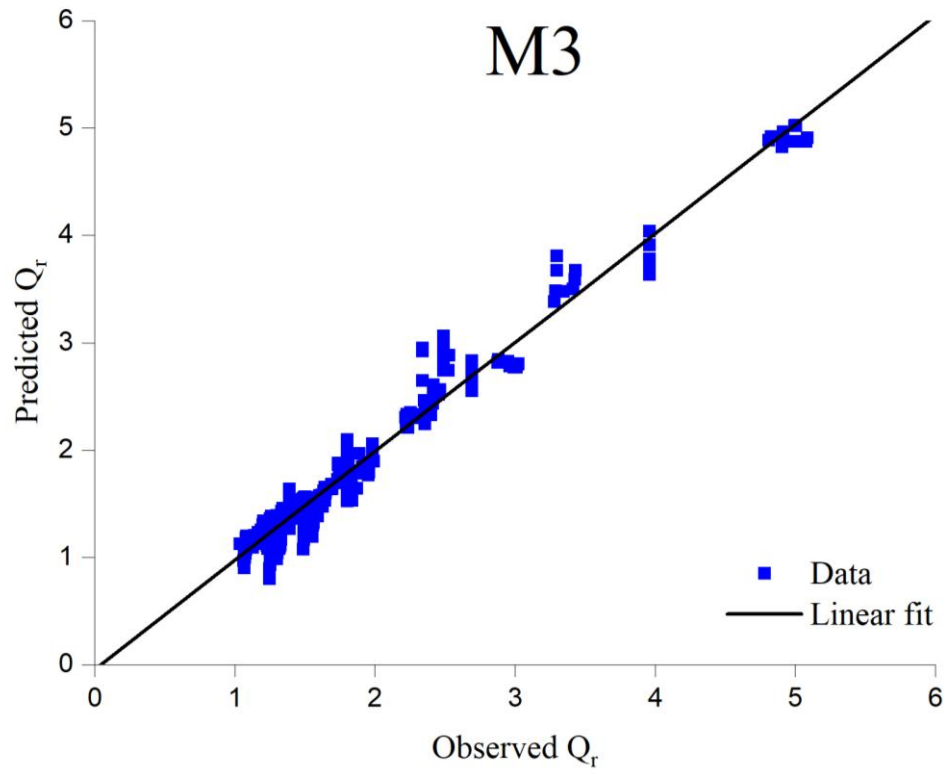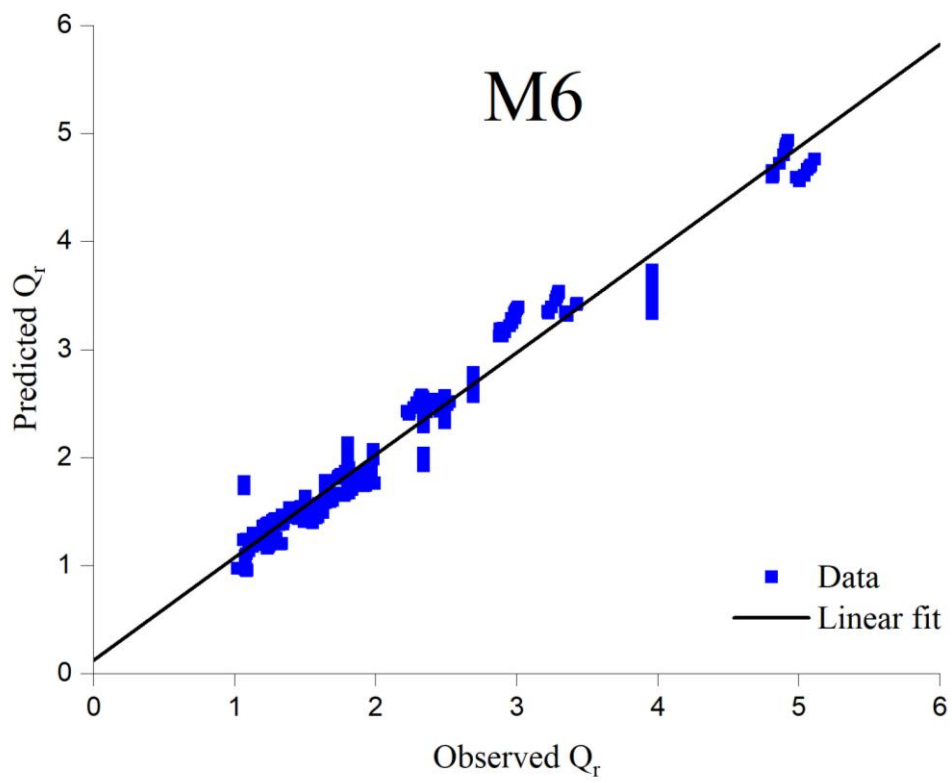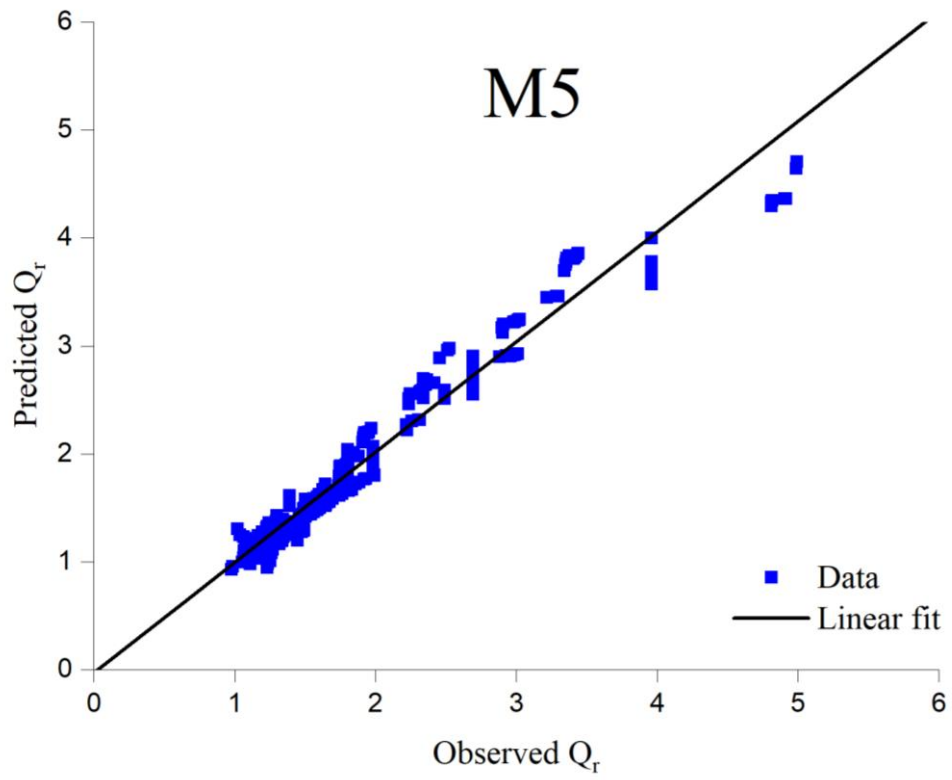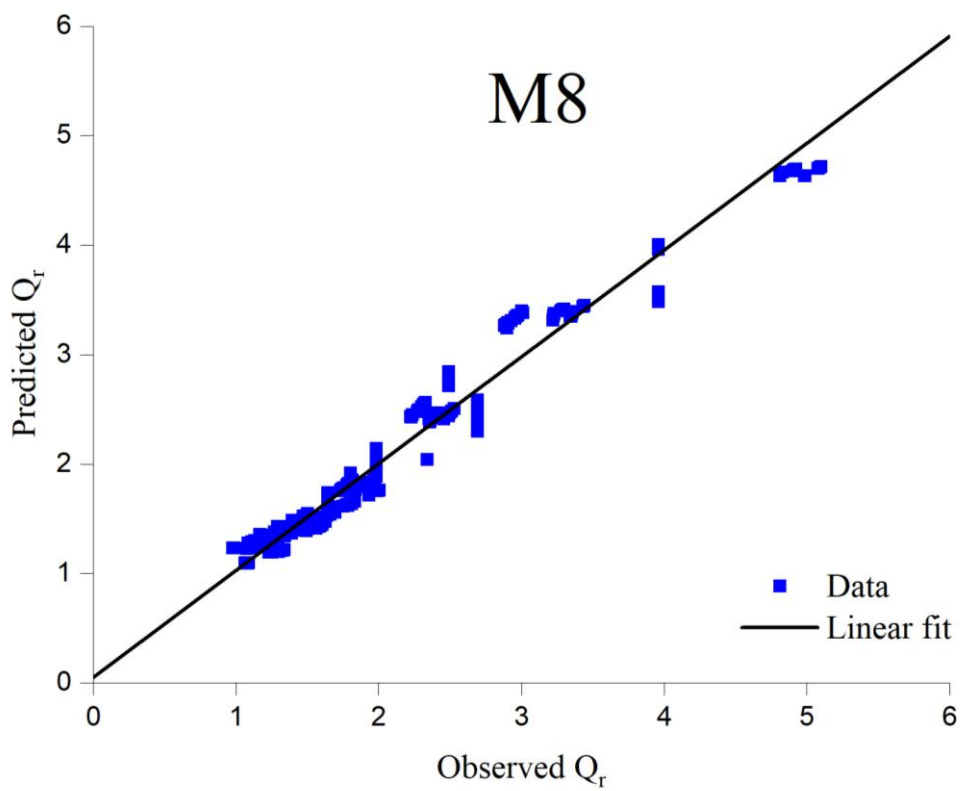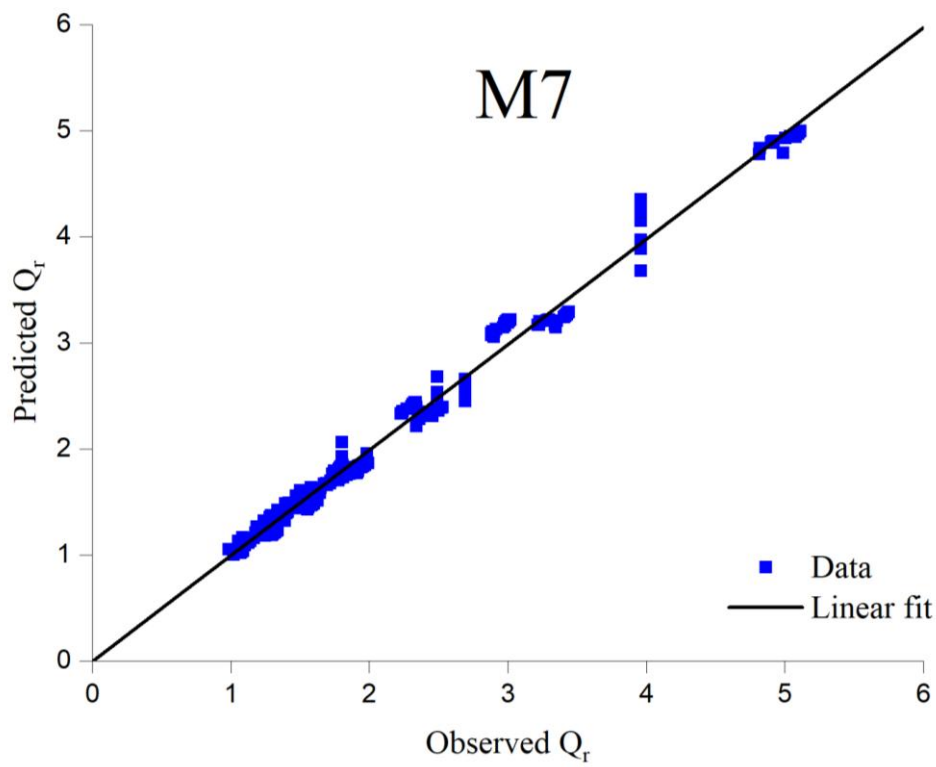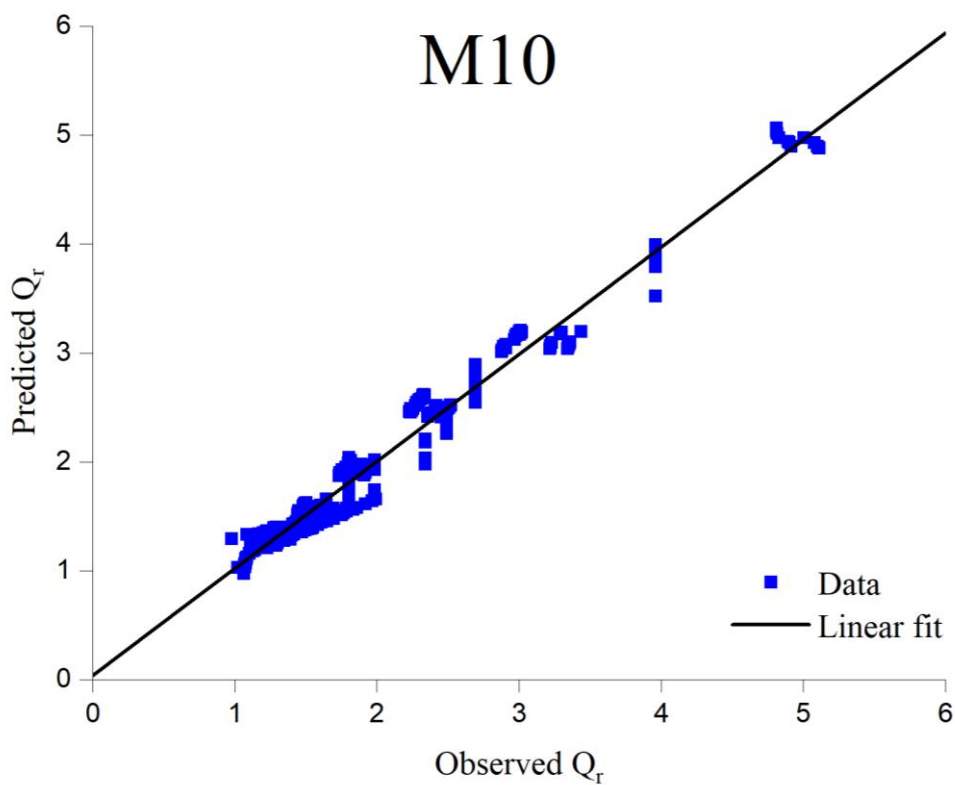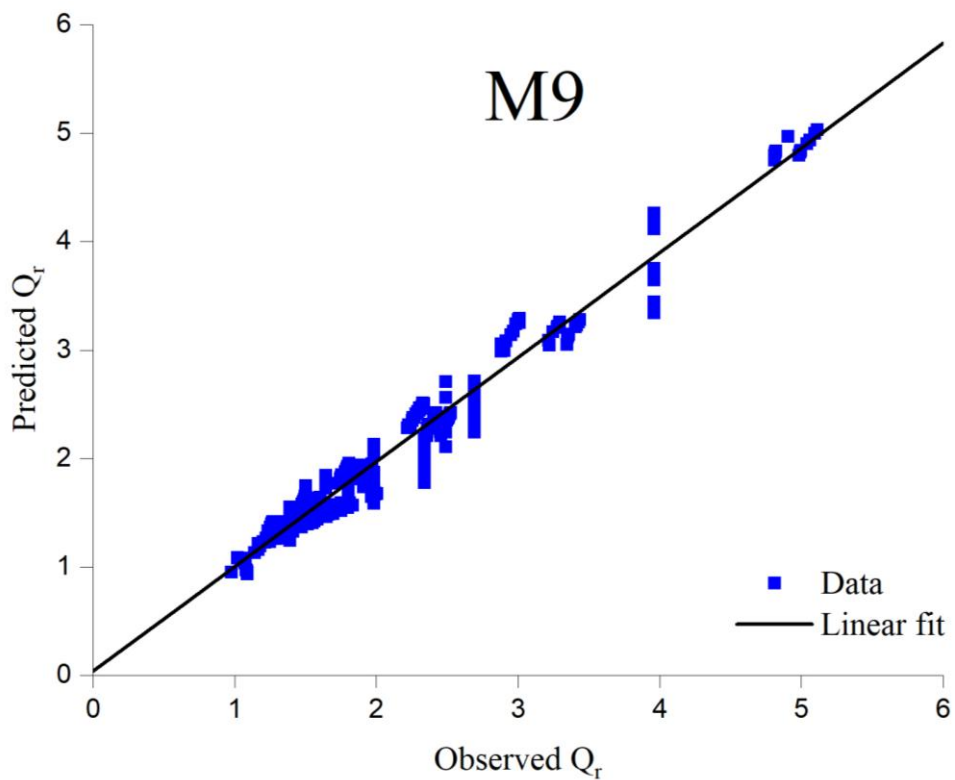
(b)

Fig. 4.23 Scatter plots of observed and predicted Q_r for models (M1 to M10) in (a) the training phase (b) the validation phase

Where,

Based on the correlation among the parameters, three models were formed and they are:

C1: $\quad Q_r = F(\alpha, \gamma, \theta, S_o, F_r, R_e, S_{fp})$

C2: $\quad Q_r = F(\alpha, \gamma, \theta, S_o, S_e, F_r, R_e, S_{fp})$

C3: $\quad Q_r = F(\alpha, \gamma, \theta, S_o, F_r, R_e, n, S_{fp})$

Based on gamma test, ten models were chosen for study and they are:

M1: $\quad Q_r = F(\alpha, \beta, \gamma, \delta, \theta, X_r, D_{50}, S_o, S_e, F_r, R_e, n, S_{fp})$

M2: $\quad Q_r = F(\alpha, \beta, \gamma, \delta, \theta, X_r, S_o, S_e, F_r, R_e, n, S_{fp})$

M3: $\quad Q_r = F(\alpha, \beta, \gamma, \delta, \theta, X_r, S_e, F_r, R_e, n, S_{fp})$

M4: $\quad Q_r = F(\alpha, \beta, \gamma, \theta, X_r, S_e, F_r, R_e, n, S_{fp})$

M5: $\quad Q_r = F(\alpha, \beta, \gamma, \theta, X_r, S_e, F_r, n, S_{fp})$

M6: $\quad Q_r = F(\alpha, \beta, \theta, X_r, S_e, F_r, n, S_{fp})$

M7: $\quad Q_r = F(\alpha, \beta, \theta, X_r, F_r, n, S_{fp})$

M8: $\quad Q_r = F(\alpha, \beta, \theta, X_r, n, S_{fp})$

M9: $\quad Q_r = F(\alpha, \beta, \theta, X_r, S_{fp})$

M10: $\quad Q_r = F(\alpha, \beta, \theta, S_{fp})$

Table 4.2 Statistical analysis of discharge for various models (M1 to M10) in the training phase

Parameters	M1	M2	M3	M4	M5	M6	M7	M8	M9	M10
R^2	0.979	0.966	0.981	0.967	0.964	0.968	0.990	0.973	0.981	0.977
RMSE	0.1299	0.1718	0.1335	0.1649	0.1868	0.1517	0.0855	0.1547	0.1277	0.1397
MAPE	5.3191	5.7012	5.1647	6.4771	7.1386	5.7534	3.3225	5.5786	5.1189	5.6731
SI	0.0614	0.0794	0.0602	0.0771	0.0833	0.0725	0.0405	0.0702	0.0602	0.0636
AIC	-532.444	-458.009	-528.891	-473.058	-440.975	-500.046	-658.672	-498.662	-553.184	-530.455

Table 4.3 Statistical analysis of predicted discharge for various models (M1 to M10) in the testing/validation phase

Parameters	M1	M2	M3	M4	M5	M6	M7	Simplified M7	M8	M9	M10
R^2	0.977	0.963	0.968	0.961	0.957	0.972	0.990	0.985	0.972	0.971	0.973
RMSE	0.1364	0.1668	0.1583	0.1789	0.1739	0.1639	0.0942	0.1266	0.1455	0.1536	0.1439
MAPE	5.2694	5.3665	6.3251	7.0484	6.8495	6.2826	3.5108	3.9159	5.2983	5.9132	6.2327
SI	0.0622	0.0779	0.0759	0.0828	0.0845	0.0733	0.0427	0.0529	0.0695	0.0690	0.0684
AIC	-519.012	-466.079	-482.347	-448.887	-460.674	-478.832	-632.347	-568.115	-515.304	-502.614	-522.413

Table 4.4 Statistical analysis of discharge for various models (C1 to C3) in the training phase

Parameters	C1	C2	C3	M7
R^2	0.830	0.793	0.872	0.990
RMSE	0.3756	0.3886	0.3268	0.0855
MAPE	11.7960	11.9703	11.6407	3.3225
SI	0.1753	0.1837	0.1507	0.0405
AIC	-253.907	-242.615	-289.960	-658.672

Table 4.5 Statistical analysis of predicted discharge for various models (C1 to C3) in the testing/validation phase

Parameters	C1	C2	C3	M7
R^2	0.782	0.784	0.846	0.990
RMSE	0.4164	0.4603	0.3487	0.0942
MAPE	13.0639	12.8234	12.1658	3.5108
SI	0.1929	0.2108	0.1638	0.0427
AIC	-225.668	-196.254	-272.216	-632.347

The statistical comparison of anticipated discharge by the GEP model (M7) with theoretical techniques like SCM, HDCM, VDCM, DDCM, and previously proposed methodology by Das et al. (2019) and Naik et al. (2017b) is represented in Table 4.6. Statistical analysis of many indices shows that the GEP model (M7) outperforms theoretical techniques and existing methodology in predicting discharge in nonprismatic compound channels. The GEP model (M7) is related to the highest R^2 value of 0.990, the lowest RMSE value of 0.094, and the lowest MAPE value of 3.511. The SI is a standardized unit used to quantify inaccuracies. A lower SI value suggests better model performance. The GEP model (M7) demonstrates a lower SI value of 0.043, suggesting little inaccuracy. The AIC is a commonly used criterion in the selection of statistical models. It is used to choose the most appropriate model by assessing the statistical likelihood function. The model with the lowest AIC score is considered the most optimal model. The GEP model (M7) has the lowest AIC score of -632.347 compared to the other techniques. Therefore, it is inferred that GEP model (M7) is the most effective and optimal model for discharge prediction in the nonprismatic compound channels.

The positive outcomes observed for both R^2 and AIC in our study are not coincidental, but rather highlight the strength of the model (M7). A high R^2 value demonstrates a strong agreement between the observed and predicted data, indicating that the model effectively captures the relationship among hydraulic and geometric parameters. In addition, the low AIC score suggests that the model strikes a balance between fitting the data well and minimizing complexity, making it a more efficient representation of the underlying data.

These results reflect the thorough development process and careful selection of variables, reinforcing the model's effectiveness and credibility for the study.

Table 4.6 Comparison of predicted discharge by different approaches

Parameters	GEP model (M7)	SCM	HDCM	VDCM	DDCM	Das et al. (2019) method	Naik et al. (2017b) method
R^2	0.990	0.470	0.590	0.740	0.780	0.833	0.905
RMSE	0.094	0.732	0.653	0.544	0.379	0.668	0.317
MAPE	3.511	43.570	32.501	30.670	26.205	18.702	13.512
SI	0.043	0.690	0.442	0.313	0.272	0.305	0.093
AIC	-632.347	1467.412	875.886	754.796	604.429	-212.888	-335.955

The GEP model (M7) for the predicted discharge as an expression tree (ET) is shown in Fig. 4.24. The input variables are represented as d0 to d6, and the constant value for gene one is represented as G1c3. An algebraic equation (Eq. 4.1) was created to decode this expression tree, connecting the output variables to the input variables.

In terms of the analytical form, the GEP model (M7) is modeled according to the following:

$$Q_r = \left[\frac{\beta n + 3.64\theta - 14.08}{3.83\theta - 14.82}\right] + \left[\frac{\beta n + \beta\theta + 5.27\beta}{\theta - 9.01\beta + 3.99}\right] + \left[(\alpha\beta + 12.28\beta + 12.28F_r + \alpha F_r) \times \left(\beta X_r S_{fp} + \beta^2 X_r\right)\right]$$

(4.1)

After simplification, the GEP model (M7) is represented as:

$$Q_r = \left[\frac{3.64\theta - 14.08}{3.83\theta - 14.82}\right] + \left[\frac{\beta\theta + 5.27\beta}{\theta - 9.01\beta + 3.99}\right]$$

(4.2)

Sub-ET 1
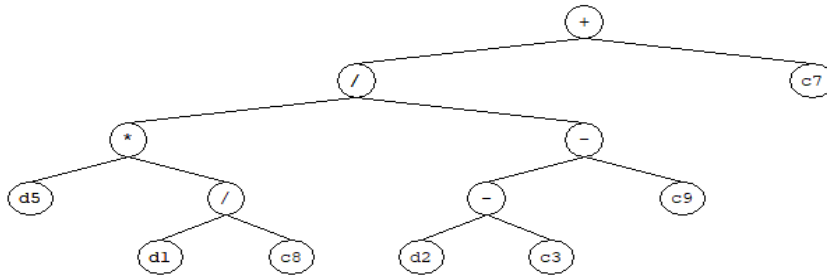
Sub-ET 2
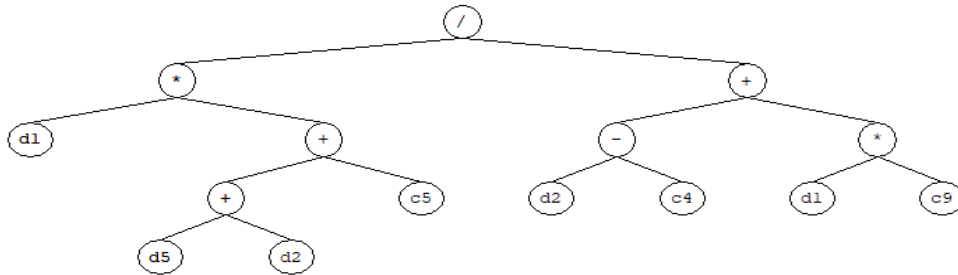
Sub-ET 3
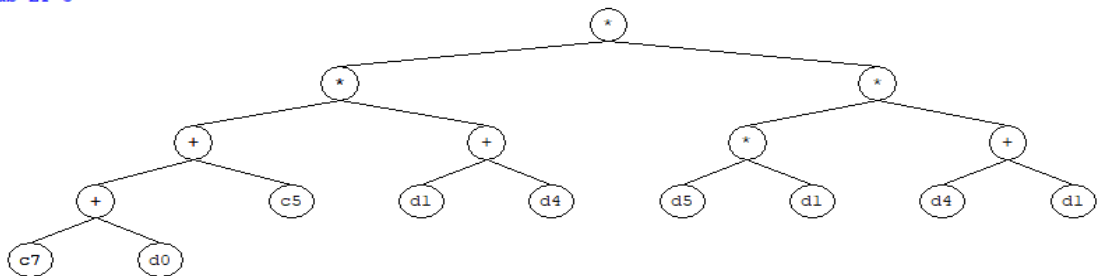
Fig. 4.24 GEP formulated expression tree

4.5 Practical application of the method

A thorough comprehension of the flow dynamics in both uniform and non-uniform parts of rivers is essential for mitigating the detrimental consequences of floods. This understanding is necessary in order to reduce the negative effects of floods. This understanding should include supplementary momentum transfer into flow models. Having this comprehension is essential for effectively building flood control and diversion structures. The proposed models in this study have practical implications for nonprismatic rivers, such as the River Main in Northern Ireland, the Brahmaputra River in India, and other comparable river systems.

The applicability of the equation developed using the GEP approach in a natural river system, namely the River Main in Northern Ireland, was assessed using data from Naik et al. (2017b). The river has a uniform and symmetrical cross-sectional configuration. The width ratio ranges from 1.2 to 2.5, while the relative flow depth value varies from 0.006 to 0.47, rendering it inferior to other natural rivers. The measured flow rate ranges from 18.34 to 57.7 cubic meters per second. The transverse profile of River Main, indicating the geometry of the channel as trapezoidal is depicted in Fig. 4.25. The experimental stretch refers to a specific 1 km segment of the River Main in Northern Ireland that has two-stage geometry. A top-down perspective of the reach illustrates that section 14 is considered to be upstream, section 6 is considered to be downstream, and the converging geometry is located in between these two sections as presented in Fig. 4.26. The measurements of the width and height of sections 14 and 6 at the borders of the reach are illustrated in Fig. 4.27. The top width of the composite waterway before convergence is 30.4 m and after convergence is 27.3 m, leading to a converging angle of 0.138°. Sand with a mean particle size that ranges from 1 to 2 mm will make up the bed material in the primary waterway. On the other hand, the banks of the primary waterway and flooded areas will be made up of grains with diameters that may reach up to 40 mm. It is estimated that the reach has a slope of bed in the longitudinal direction of 0.003. When it comes to principal waterways and flooding zones, the roughness coefficient that is taken into consideration is 0.025 and 0.035, respectively.

Utilizing the data obtained from River Main and applying it to the proposed equation using the GEP model (M7) yielded the following statistical metrics for the predicted discharge: R^2 (0.959), RMSE (2.633), MAE (2.337), and MAPE (10.467). The statistical analysis demonstrates the effectiveness of the GEP model (M7) in accurately estimating the flow rate of nonprismatic streams and its practical significance.
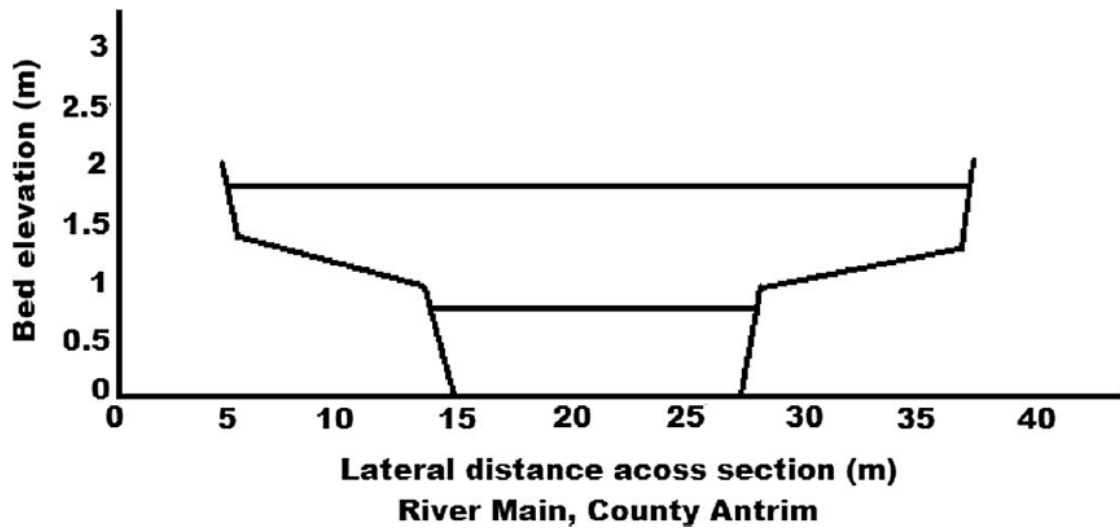
Fig. 4.25 Lateral cross-section of River Main (Naik et al. 2017b)
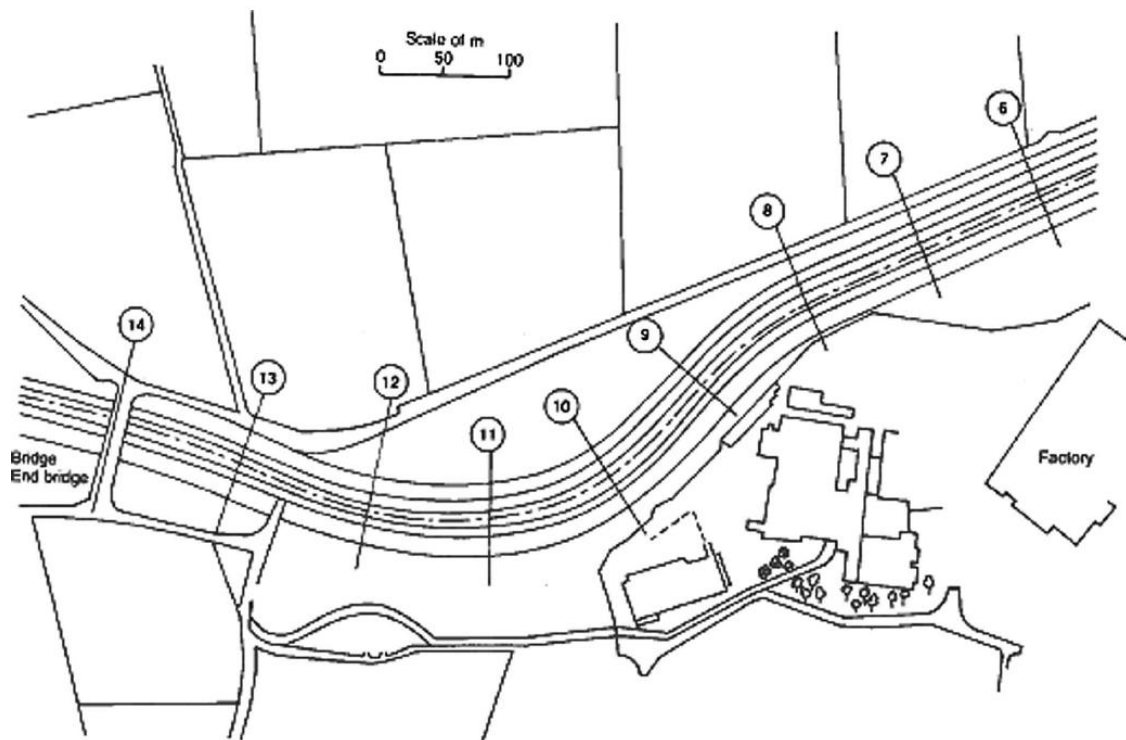
Fig. 4.26 Plan view of the experimental reach of River Main (Naik et al. 2017b)
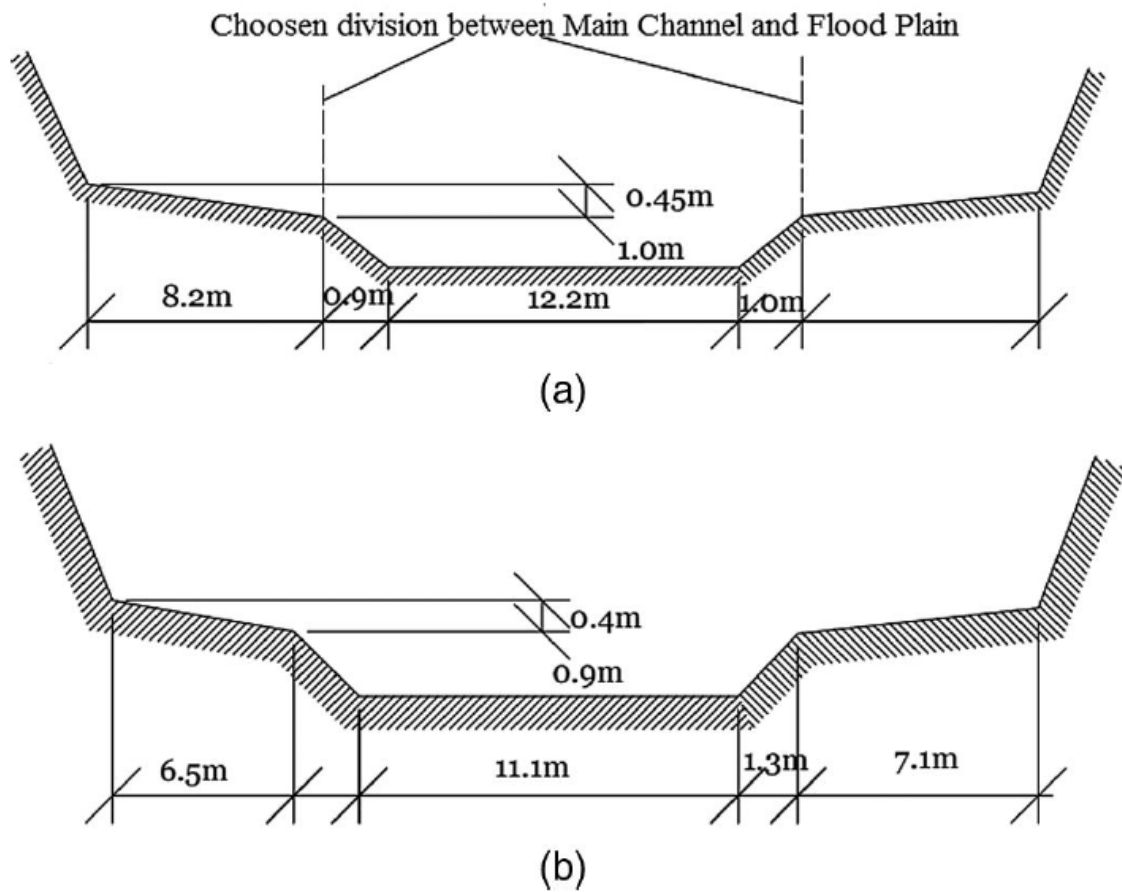
Fig. 4.27 Cross-sectional geometries of River Main at (a) upstream end of experimental reach (Section 14) (b) downstream end of experimental reach (Section 6) (Naik et al. 2017b)

CHAPTER 5

CONCLUSIONS AND SCOPE FOR FUTURE WORK

5.1 Conclusions

The investigation was carried out on a nonprismatic compound channel that consisted of a prismatic section followed by a converging section. The research examined five distinct relative flow depths, including 0.20, 0.30, 0.40, 0.50, and 0.60. The study conducted experiments on the following four different types of nonprismatic compound channels in a masonry flume:

(i) a compound channel with smooth converging floodplains,

(ii) a compound channel with rough converging floodplains,

(iii) a compound channel with sediment in the main channel and smooth converging floodplains,

(iv) a compound channel with sediment in the main channel and rough converging floodplains.

The findings of the study provide a variety of insights, such as:

❖ In nonprismatic compound channels with smooth and rough floodplains, without and with sediment, the stage-discharge relationship adheres to a power law ($H=CQ^n$). In both prismatic and nonprismatic sections of compound channels, the coefficient C is the same, whereas the exponent n is distinct.

❖ When comparing a nonprismatic compound channel with rough floodplains to smooth floodplains, it is seen that the exponent value of n (0.865) and (0.895) for rough floodplains is higher than (0.849) and (0.871) for smooth floodplains in the prismatic section and nonprismatic sections, respectively.

❖ When comparing a nonprismatic compound channel with sediment and rough floodplains to smooth floodplains, it is seen that the exponent value of n (0.739) and (0.785) for rough floodplains is higher than (0.732) and (0.761) for smooth floodplains in the prismatic section and nonprismatic sections, respectively.

❖ The water surface profile is decreased in nonprismatic compound channel with rough floodplains compared to smooth floodplains, correlating with increased head loss

resulting from the roughness of the floodplains. These findings validate the influence of channel geometry and floodplain roughness on flow dynamics.

❖ The findings validate that rough floodplains contribute to a greater energy slope compared to smooth floodplains, likely due to increased head loss attributed to channel shape and floodplain roughness. Further, the study revealed that the energy slope in the converging region of the compound channel experiences an abrupt rise as a result of the convergence of channel shape.

❖ The study concluded that in both prismatic and nonprismatic sections of the compound channel, the channel with rough floodplains exhibits lower velocities up to 5.5 percent and 16 percent when compared to the nonprismatic compound channel with smooth floodplains, without and with sediment, respectively.

❖ The velocity distribution across the width aligns with theoretical expectations when the relative depth is less than 0.20. Particularly, the maximum velocity is seen in the middle of the channel, while it tends to decrease towards the ends of the floodplain. Nevertheless, when the relative depth exceeds 0.30, the velocity in the interface region between the main channel and floodplains exhibits a decrease as it approaches the interface region. However, after reaching the interface region, there is an unexpected increase in velocity due to the transfer of momentum from the main channel to the floodplains. Following the interface region, the velocity diminishes as it moves towards the ends of the floodplain.

❖ The shear stress increases abruptly in the nonprismatic sections due to the resistance from converging boundaries. The shear stress is higher in nonprismatic compound channels with rough floodplains and the increase is found up to 70 percent and 94 percent as compared to nonprismatic compound channels with smooth floodplains, without and with sediment, respectively.

❖ The findings concluded that sediment transport rate is higher in nonprismatic compound channel with smooth floodplains up to 10 percent compared to rough floodplains. Due to the convergence of the channel geometry, the sediment transport rate in nonprismatic compound channel is found to be higher compared to prismatic compound channels.

❖ In a nonprismatic compound channels, sediment deposition occurs initially in the converging section. As the channel narrows further, increased flow velocity and shear stress lead to sediment degradation. Thus, changes in flow dynamics drive the sediment deposition and degradation patterns.

❖ Compared to smooth floodplains, rough floodplains enhance flow resistance (Manning's 'n') in nonprismatic compound channels without sediment and much more so in nonprismatic compound channels with sediment.

❖ The findings indicate that the values of 'n' decrease as the longitudinal distance increases in a compound channel, without sediment, with smooth and rough floodplains. This can be attributed to the converging geometry of the channel, which leads to flow acceleration.

❖ On the other hand, in a compound channel, with sediment in the main channel, with smooth and rough floodplains, the values of 'n' increase as the longitudinal distance increases. This can be attributed to the increased resistance provided by the sediment transport phenomenon.

❖ The increase in Manning's roughness coefficient 'n' in rough floodplains is up to 7 percent compared to a compound channel, without sediment, with smooth floodplains. The increase in roughness coefficient 'n' in rough floodplains in a compound channel with sediment is up to 20 percent compared to smooth floodplains in a compound channel with sediment.

❖ The findings suggest that the selection of variables for various model development should be based on the gamma test since models generated using the gamma test provide superior outcomes compared to models developed using correlation.

❖ A novel equation has been proposed to estimate the discharge in a nonprismatic compound channel with converging floodplains. The equation is created using several geometric and flow variables, using an expression tree approach that utilizes the GEP methodology.

❖ The GEP model (M7), which incorporates width ratio, relative flow depth, converging angle, relative distance, Froude number, Manning's roughness coefficient, and floodplain shear force, demonstrates superior performance across different statistical measures when compared to other GEP models for predicting discharge in nonprismatic compound channels. This is evident from its highest R^2 and lowest RMSE, MAPE, SI, and AIC values.

❖ The equation developed using the GEP method was applied to predict the discharge and compared the same for the River Main in Northern Ireland (Naik et al. 2017b), which has nonprismatic geometry. Statistical analysis revealed that the GEP method has the potential for predicting the discharge of nonprismatic river streams, with a mean error (MAPE) of 10%, making it suitable for practical applications.

5.2 Future scope of work

The possible extension of this study would be:

* ❖ To conduct experiments in nonprismatic compound channels with varying geometric shapes, such as trapezoidal channels.
* ❖ To analyze the flow characteristics in nonprismatic compound channels with vegetation.
* ❖ To analyze the sediment transport effects on flow characteristics in nonprismatic composite waterways with and without vegetation.
* ❖ Computational analysis of flow characteristics in nonprismatic compound channels with rough floodplains and sediment conditions using the finite element method.

References

Ackers, P. 1991. *Hydraulic design of straight compound channels*. Volume 1 - Summary and design method, Volume 2 - Appendices, Technical Report SR 281, Hydraulics Research Ltd, Wallingford, United Kingdom.

Ackers, P. 1992. "Hydraulic design of two-stage channels." *Proc. Inst. Civ. Eng. Waters, Maritime and Energy* 9988:247-257.

Ackers, P. 1993a. "Stage-discharge functions for two-stage channels." *J. Inst. Water & Environmental Management* 7 (1):52-61.

Ackers, P. 1993b. "Flow formulae for straight two-stage channels." *J. Hydraul. Res. IAHR* 31 (4):509-531.

Ali, M., G. Sterk, M. Seeger, M. Boersema, and P. Peters. 2012. "Effect of hydraulic parameters on sediment transport capacity in overland flow over erodible beds." *Hydrology and Earth System Sciences* 16 (2):591–601.

Atabay, S. A., and D. W. Knight. 2002. "The influence of floodplain width on the stage-discharge relationship for compound channels." *River Flow Proc. Int. Conf. on Fluvial Hydraulics*, Louvain-la-Neuve, Belgium, 1:197-204.

Atabay, S., and D. W. Knight. 2006. "1-D modelling of conveyance, boundary shear and sediment transport in overbank flow." *Journal of Hydraulic Research* 44(6):739-754.

Atabay, S., D. W. Knight, and G. Seckin. 2005. "Effects of overbank flow on fluvial sediment transport rates." *Proceedings of the Institution of Civil Engineers - Water Management* 158 (1):25-34.

Barman, J., and B. Kumar. 2023. "Flow in multi-layered vegetated compound channels with different bank slopes." *Physics of Fluids* 35 (3): article number 036601.

Bathurst, J. C., I. A. Benson, E. M. Valentine, and C. Nalluri. 2002. "Overbank sediment deposition patterns for straight and meandering flume channels." *Earth Surface Processes and Landforms* 27 (6):659–665.

Beaman, F. 2010. *Large eddy simulation of open channel flows for conveyance estimation*. Ph.D. Diss. University of Nottingham, UK.

Bijanvand, S., M. Mohammadi, and A. Parsaie. 2023. "Estimation of water's surface elevation in compound channels with converging and diverging floodplains using soft computing techniques." *Water Supply* 23 (4):1684–1699.

Bousmar, D., and Y. Zech. 1999. "Momentum transfer for practical flow computation in compound channels." *J. Hydraul. Eng. ASCE* 125 (7):696-706.

Bousmar, D., and Y. Zech. 2002. "Periodical turbulent structures in compound channels." *River flow* 1:177-185.

Bousmar, D., and Y. Zech. 2004. "Velocity distribution in non-prismatic compound channels." *Proceedings of the ICE-Water Management* 157 (2):99-108.

Branß, T., F. Núñez-González, and J. Aberle. 2022. "Fluvial levees in compound channels: a review on formation processes and the impact of bedforms and vegetation." *Environmental Fluid Mechanics* 22 (2–3):559–585.

Cassells, J. B. C., M. F. Lambert, and R. W. C. Myers. 2001. "Discharge prediction in straight mobile bed compound channels." *Proceedings of the Institution of Civil Engineers - Water and Maritime Engineering* 148 (3):177–188.

Cater, J. E., and J. J. R. Williams. 2008. "Large eddy simulation of a long asymmetric compound open channel." *Journal of Hydraulic Research* 46:445-453.

Chlebek et al. 2010. "A comparison of overbank flow conditions in skewed and converging/diverging channels." *River flow Proceedings of the international conference on fluvial hydraulics* 1:503-514.

Chunhong, Hu., Ji. Zuwen, and Guo. Qingchao. 2010. "Flow movement and sediment transport in compound channels." *Journal of Hydraulic Research* 48 (1):23-32.

Cokljat, D., and B. A. Younis. 1995. "Compound-channel flows a parametric study using a Reynolds-stress transport closure." *Journal of Hydraulic Research* 33 (3):307-320.

Conway, P., J. J. O'Sullivan, and M. F. Lambert. 2013. "Stage–discharge prediction in straight compound channels using 3D numerical models." *Water Management/Proceedings of ICE. Water Management* 166 (1):3–15.

Cunge, J. A., and M. Erlich. 1999. "Hydroinformatics in 1999: what is to be done?." *Journal of Hydroinformatics* 1:21-31.

Das, B. S., and K. K. Khatua. 2018. "Flow resistance in a compound channel with diverging and converging floodplains." *Journal of Hydraulic Engineering* 144 (8): article number 04018051.

Das, B. S., K. Devi, and K. K. Khatua. 2019. "Prediction of discharge in converging and diverging compound channel by gene expression programming." *ISH Journal of Hydraulic Engineering* 27 (4):385–395.

Devi, K., and K. K. Khatua. 2016. "Prediction of depth averaged velocity and boundary shear distribution of a compound channel based on the mixing layer theory." *Flow Measurement and Instrumentation* 50:147–157.

Elliott, S. C. A., and R. H. J. Sellin. 1990. "SERC flood channel facility: skewed flow experiments." *Journal of Hydraulic Research* 28 (2):197-214.

Fernandes, J. N. 2021. "Apparent roughness coefficient in overbank flows." *SN Applied Sciences* 3 (7):696.

Fernandes, J. N., J. B. Leal, and A. H. Cardoso. 2015. "Assessment of stage–discharge predictors for compound open-channels." *Flow Measurement and Instrumentation* 45:62–67.

Ferreira, C. 2001. "Gene expression programming: a new adaptive algorithm for solving problems." *Complex Systems* 13 (2):87-129.

Filonovich, M. 2015. *Numerical modelling of compound channel flow*. Ph.D. Diss. FCT (Fundaçãopara a Ciência e Tecnologia), Lisbon, Portugal.

Fraselle, Q., D. Bousmar, and Y. Zech. 2010. "Experimental investigation of sediment deposition on floodplains." *River Flow* 1:823-830.

Gadissa Kedir, E., C. S. P. Ojha, and K. S. H. Prasad. 2023. "Boundary shear stress and apparent shear forces in compound channels with different floodplain widths." *ISH Journal of Hydraulic Engineering* 30 (1):58–67.

Gamal Abdalla, M. 2016. "Effect of corrugated rough bed channels on sediment transport processes." *Journal of Water Resources and Ocean Science* 5 (6):114-121.

Gandhi, B. K., H. K. Verma, and B. Abraham. 2010. "Investigation of flow profile in open channels using CFD." *Proc. 8th Intl. Conference on Hydraulic Efficiency Measurement*.

Garcia, M., and Y. Niño. 1993. "Dynamics of sediment bars in straight and meandering channels: experiments on the resonance phenomenon." *Journal of Hydraulic Research* 31 (6):739–761.

Garde, R. J., and K. G. Ranga Raju. 1985. *Mechanics of sediment transportation and alluvial stream problems*. Wiley Eastern Ltd., 2nd Edition, New Delhi.

Gepsoft, GeneXproTools 5.0. 2014. *Data modeling & analysis software*. (n.d.). https://www.gepsoft.com/.

Ghosh, S., and S. B. Jena. 1971. "Boundary shear stress distribution in open channel compound." *Proc. Inst. Civil Eng.* 49:417–430.

Ibrahim, D. 2016. "An overview of soft computing." *Procedia Computer Science* 102:34–38.

Ikeda, S., T. Yamada, and Y. Toda. 2001. "Numerical study on turbulent flow and honami in and above the flexible plant canopy." *International journal of heat and fluid flow* 22 (3):252-258.

James, M., and R. J. Brown. 1977. "Geometric parameters that influence floodplain flow." *U.S. Army Engineer Waterways Experimental Station. Vicksburg Miss. June. Research report H-77*.

Jumain, M., Z. Ibrahim, Z. Ismail, M. F. Samsudin, M. Z. Tajol Anuar, S. Harun, and M. S. Rahman. 2016. "Flood flow characteristics and bed load transport in non-vegetated compound straight channels." *Jurnal Teknologi* 78:9-4.

Jumain, M., Z. Ismail, Z. Ibrahim, and N. A. Zaini. 2013. "Sediment transport rate and bed formation in straight compound channels." *Global Journal of Environmental Research* 7:40-44.

Kara, S., T. Stoesser, and T. W. Sturm. 2012. "Turbulence statistics in compound channels with deep and shallow overbank flows." *Journal of Hydraulic Research* 50 (5):482-493.

Karamisheva, R. D., J. F. Lyness, W. R. C. Myers, and J. J. O'Sullivan. 2006. "Sediment discharge prediction in meandering compound channels." *Journal of Hydraulic Research* 44 (5):603–613.

Kaushik, V., and M. Kumar. 2023b. "Assessment of water surface profile in nonprismatic compound channels using machine learning techniques." *Water Supply*, 23 (1): 356–378.

Kaushik, V., and M. Kumar. 2023a. "Sustainable gene expression programming model for shear stress prediction in nonprismatic compound channels." *Sustainable Energy Technologies and Assessments*, 57: 103229.

Kaushik, V., and M. Kumar. 2024. "Prediction of shear stress distribution in compound channel with smooth converging floodplains." *Journal of Hydrology and Hydromechanics*, 72 (2): 170–184.

Kaushik, V., B. Naik, M. Kumar, and V. K. Minocha. 2024a. "Prediction of the flow resistance in non-prismatic compound channels." *Water Practice and Technology*, 19 (5): 1822–1835.

Kaushik, V., M. Kumar, and B. Naik. 2024b. "Numerical Simulation of Flow Characteristics in Nonprismatic Compound Channels." *Water Practice and Technology*, 19 (7): 2532–2550.

Kaushik, V., M. Kumar, B. Naik, and A. Parsaie. 2023. "Modeling of water surface profile in non-prismatic compound channels." *Water Practice and Technology*, 18 (9): 2151–2167.

Khattab, N. I., A. Y. Mohammed, and A. A. Mala Obaida. 2023. "Discharge predicted in compound channels using adaptive neuro-fuzzy inference system (ANFIS)." *Open Engineering* 13 (1).

Khatua, K. K. 2008. *Interaction of flow and estimation of discharge in two-stage meandering compound channels*. Ph.D. Diss. National Institute of Technology, Rourkela, India.

Khatua, K. K., K. C. Patra, and P. K. Mohanty. 2012. "Stage-discharge prediction for straight and smooth compound channels with wide floodplains." *J. Hydraul. Eng. ASCE* 138 (1):93-99.

Khatua, K. K., K. C. Patra, and R. Jha. 2010. "Apparent shear stress in compound channels." *J. Hydraul. Res.* 16 (3):1-14.

Khazaee, I., and M. Mohammadiun. 2012. "Effect of flow field on open channel flow properties using numerical investigation and experimental comparison." *International Journal of Energy and Environment* 3 (4):617-628.

Khuntia, J. R., K. Devi, and K .K. Khatua. 2018. "Boundary shear stress distribution in straight compound channel flow using artificial neural network." *Journal of Hydrologic Engineering* 23 (5):04018014.

Knight, D. W., and A. Y. Shamseldin. 2005. *River basin modelling for flood risk mitigation*. Taylor & Francis, Netherlands.

Knight, D. W., and F. A. Brown. 2001. "Resistance studies of overbank flow in rivers with sediment using the flood channel." *Journal of Hydraulic Research* 39 (3):283-301.

Knight, D. W., and J. D. Demetriou. 1983. "Floodplain and main channel flow interaction." *J. Hydraul. Eng. ASCE* 109 (8):1073-1092.

Knight, D. W., and M. E. Hamed. 1984. "Boundary shear in symmetrical compound channels." *J. Hydraul. Eng. ASCE* 110 (10):1412-1430.

Lu, Y., N. S. Cheng, and M. Wei. 2021. "Formulation of bed shear stress for computing bed-load transport rate in vegetated flows." *Physics of Fluids* 33 (11).

Lyness, J. F., W. R. C. Myers, and J. J. O'Sullivan. 1998. "Hydraulic characteristics of meandering mobile bed compound channels." *Proceedings of the Institution of Civil Engineers - Water, Maritime and Energy* 130 (4):179 188.

Mihani, M. R., and B. Rezaei. 2023. "Experimental study of the flow field in compound channels with converging and inclined floodplains." *ISH Journal of Hydraulic Engineering* 29(sup1):83–91.

Minatti, L. 2015. "A well-balanced FV scheme for compound channels with complex geometry and movable bed." *Water Resources Research* 51 (8):6564–6585.

Mir, A. A., and M. Patel. 2023. "Machine learning approaches for adequate prediction of flow resistance in alluvial channels with bedforms." *Water Science & Technology* 89 (2):290–318.

Mohanta, A., and K. C. Patra. 2018. "LES modeling with experimental validation of a compound channel having converging floodplain." *Journal of the Institution of Engineers (India): Series A* 99 (3):519–537.

Mohanty, P. K., and K. K. Khatua. 2014. "Estimation of discharge and its distribution in compound channels." *Journal of Hydrodynamics* 26 (1):144-154.

Mohseni, M., and A. Naseri. 2023. "Water surface profile prediction in compound channels with vegetated floodplains." *Proceedings of the Institution of Civil Engineers - Water Management* 176 (5):235–246.

Moreta, P. J. M., and J. P. Martin-Vide. 2010. "Apparent friction coefficient in straight compound channels." *J. Hydraul. Res.* 48 (2):169-177.

Myers, W. R. C., and J. F. Lyness. 1997. "Discharge ratios in smooth and rough compound channels." *J. Hydraul. Eng. ASCE* 123 (3):182-188.

Myers, W. R. C., J. F. Lyness and J. Cassells. 2001. "Influence of boundary roughness on velocity and discharge in compound river channels." *Journal of Hydraulic Research* 39 (3):311–319.

Myers, W. R. C. 1987. "Velocity and discharge in compound channels." *J. Hydraul. Eng. ASCE* 113 (6):753-766.

Myers, W. R. C., and E. K. Brennan. 1990. "Flow resistance in compound channels." *Journal of Hydraulic Research* 28 (2):141–155.

Myers, W. R. C., and E. M. Elsawy. 1975. "Boundary shear in channel with flood plain." *J. Hydraul. Div. ASCE* 101 (7):933–946.

Myers, W. R. C., D. W. Knight, J. F. Lyness, J. B. Cassells, and F. Brown. 1999. "Manning and Darcy Weisbach resistance coefficients for inbank and overbank flow." *Proceedings of the Institution of Civil Engineers - Water, Maritime and Energy* 136 (2):105-115.

Naik, B., and K. K. Khatua. 2016. "Boundary shear stress distribution for a converging compound channel." *ISH Journal of Hydraulic Engineering* 22 (2):212-219.

Naik, B., and K. K. Khatua. 2017a. "Water surface profile computation for compound channels with narrow floodplains." *Arabian Journal for Science and Engineering* 42 (3):941–955.

Naik, B., E. Padhi, and K. K. Khatua. 2018a. "Flow prediction of boundary shear stress and depth average velocity of a compound channel with narrowing floodplain." *Iranian Journal of Science and Technology Transactions of Civil Engineering* 42 (4):415–425.

Naik, B., K. K. Khatua, E. Padhi, and P. Singh. 2018b. "Loss of energy in the converging compound open channels." *Arabian Journal for Science and Engineering* 43 (10):5119–5127.

Naik, B., K. K. Khatua, N. G. Wright, and A. Sleigh. 2017b. "Stage-discharge prediction for converging compound channels with narrow floodplains." *Journal of Irrigation and Drainage Engineering* 143 (8):04017017.

Naik, B., K. K. Khatua, N. Wright, A. Sleigh, and P. Singh. 2017c. "Numerical modeling of converging compound channel flow." *ISH Journal of Hydraulic Engineering* 24 (3):285–297.

Naik, B., V. Kaushik, and M. Kumar. 2022. "Water surface profile in converging compound channel using gene expression programming." *Water Supply*, 22 (5): 5221–5236.

Ozbek, T., and K. Cebe. 2003. "Comparison of methods for predicting discharge in straight compound channels using the apparent shear stress concepts." *Tr. Journal of Engineering and Environmental Science*, 101-109.

Panda, P. 2010. *Prediction of flow in compound open channel flows using artificial neural network*. Ph.D. Diss. National Institute of Technology, Rourkela, India.

Pang, B. 1998. "River flood flow and its energy loss." *J. Hydraul. Eng. ASCE* 124 (2):228-231.

Parsaie, A., S. Najafian, and Z. Shamsi. 2016. "Predictive modeling of discharge of flow in compound open channel using radial basis neural network." *Modeling Earth Systems and Environment* 2 (3):1-9.

Patel, V. C. 1965. "Calibration of the Preston tube and limitations on its use in pressure gradients." *J. Fluid Mech.* 231:85–208.

Prasad, B. S. S., A. Sharma, and K. K. Khatua. 2022. "Distribution and prediction of boundary shear in diverging compound channels." *Water Resources Management* 36 (13):4965–4979.

Proust et al. 2006b. "A methodology for computing non-uniform flows in compound channels." *River Flow Proceedings of the International Conference on Fluvial Hydraulics*, Lisbon, Portugal.

Proust, S., D. Bousmar, N. Rivière, A. Paquier, and Y. Zech. 2010. "Energy losses in compound open channels." *Advances in water Resources* 33 (1):1-16.

Proust, S., N. Rivière, D. Bousmar, A. Paquier, and Y. Zech. 2006a. "Flow in compound channel with abrupt floodplain contraction." *J. Hydraul. Eng.* 132 (9):958 970.

Rahim, A. S., H. A. Yonesi, H. R. Rahimi, B. Shahinejad, H. T. Podeh, and H. M. Azamathulla. 2023. "Effect of vegetation on flow hydraulics in compound open channels with non-prismatic floodplains." *AQUA — Water Infrastructure, Ecosystems and Society* 72 (5):781–797.

Rajaratnam, N., and R. M. Ahmadi. 1979. "Interaction between main channel and floodplain flows." *J. Hydraul. Div. ASCE* 105 (5):573-588.

Rezaei, B. 2006. *Overbank flow in compound channels with prismatic and non-prismatic floodplains*. Ph.D. Diss. The University of Birmingham, UK.

Rezaei, B. and D. W. Knight. 2009. "Application of the Shiono and Knight Method in compound channels with non-prismatic floodplains." *Journal of Hydraulic Research* 47 (6):716-726.

Rezaei, B. and D. W. Knight. 2010. "Overbank flow in compound channels with non-prismatic floodplains." *Journal of Hydraulic Engineering* 137 (8):815-824.

Sahu, M., S. Jana, S. Agarwal, K. K. Khatua, and S. S. Mahapatra. 2011b. "Point form velocity prediction in meandering open channel using artificial neural network." *Proceedings of International Conference on Environmental Science and Technology* (ICEST 2011).

Sahu, M., P. Singh, S. S. Mahapatra, and K. K. Khatua. 2012. "Prediction of entrance length for low Reynolds number flow in a pipe using neuro-fuzzy inference system." *Expert Systems with Applications* 39 (4):4545-4557.

Sahu, M., K. K. Khatua, and S. S. Mahapatra. 2011a. "A neural network approach for prediction of discharge in straight compound open channel flow." *Flow Measurement and Instrumentation* 22 (5):438-446.

Salvetti, M. V., Y. Zang, R. L. Street, and S. Banerjee. 1997. "Large-eddy simulation of free surface decaying turbulence with dynamic subgrid -scale models." *Physics of Fluids* 9 (8):2405-2419.

Scheuren, J. M., L. P. De, O. Waroux, and R. Below. 2008. "Annual disaster statistical review – the number and trends 2007." *Center for Research of the Epidemiology of Disasters (CRED)*, Jacoffsaet Printers, Melin, Belgium.

Selim, T., M. Hesham, and M. Elkiki. 2022. "Effect of sediment transport on flow characteristics in non-prismatic compound channels." *Ain Shams Engineering Journal* 13 (6):101771.

Sellin, R. H. J. 1964. "A laboratory investigation into the interaction between the flow in the channel of a river and that over its flood plain." *La Houllie Blanche*, 7:793-802.

Shiono, K., and D. W. Knight. 1988. "Refined modelling and turbulence measurements." *Proceedings of 3rd International Symposium*, IAHR, Tokyo, Japan, 26-28.

Shiono, K., and D. W. Knight. 1991. "Turbulent open-channel flows with variable depth across the channel." *Journal of Fluid Mechanics* 222:617-646.

Shiono, K., T. L. Chan, J. Spooner, P. Rameshwaran, and J. H. Chandler. 2009. "The effect of floodplain roughness on flow structures, bedforms and sediment transport rates in meandering channels with overbank flows: Part I." *Journal of Hydraulic Research* 47 (1):5-19.

Singh, P. K., X. Tang, and H. Rahimi. 2023. "Large-eddy simulation of compound channels with staged floodplains: flow interactions and turbulent structures." *Water* 15 (5):983.

Stephenson, D., and P. Kolovopoulos. 1990. "Effects of momentum transfer in compound channels." *J. Hydraul. Eng. ASCE* 116 (12):1512-1522.

Subramanya, K. 2015. *Flow in open channels*. McGraw Hill, Edition 4, India.

Tang, X. 2017. "An improved method for predicting discharge of homogeneous compound channels based on energy concept." *Flow Measurement and Instrumentation* 57:57–63.

Tang, X., and D. Knight. 2006. "Sediment transport in river models with overbank flows." *Journal of Hydraulic Engineering* 132 (1):77-86.

Tang, X., and D. W. Knight. 2008. "Lateral depth-averaged velocity distributions and bed shear in rectangular compound channels." *J. Hydraul. Eng. ASCE* 134 (9):1337 1342.

Thomas, T. G., and J. J. R. Williams. 1995. "Large eddy simulation of turbulent flow in an asymmetric compound open channel." *Journal of Hydraulic Research* 33:27- 41.

Thornton, C. I., S. R. Abt, C. E. Morris, and J. C. Fischenich. 2000. "Calculating shear stress at channel-overbank interfaces in straight channels with vegetated floodplains." *J. Hydraul. Eng.* 126:929–936.

Tominaga, A. and D. W. Knight. 2004. "Numerical evaluation of secondary flow effects on lateral momentum transfer in overbank flows." *River Flow*, Taylor and Francis Group, London.

Västilä, K., J. Järvelä, and H. Koivusalo. 2016. "Flow–vegetation–sediment interaction in a cohesive compound channel." *Journal of Hydraulic Engineering* 142 (1):04015034.

Wang, X., S. Li, Z. H. Yang, and W. X. Huai. 2022. "Incipient sediment motion in vegetated open-channel flows predicted by critical flow velocity." *Journal of Hydrodynamics* 34 (1):63–68.

WMO (World Meteorological Organization). 2003. "Manual on sediment management and measurement." *Operational hydrology report no. 47*, Geneva, Switzerland.

Wormleaton, P. R., and P. Hadjipanos. 1985. "Flow distribution in compound channels." *J. Hydraul. Eng. ASCE* 111 (7):1099-1104.

Wormleaton, P. R., J. Allen, and P. Hadjipanos. 1982. "Discharge assessment in compound channel flow." *J. Hydraul. Eng. ASCE* 108 (9):975-994.

Wu, W., L. Wang, X. Ma, R. Nie, and X. Liu. 2020. "Flow characteristics and bed morphology in a compound channel between two single channels." *Water* 12 (12):3544.

Xie, Z., B. Lin, and R. A. Falconer. 2013. "Large-eddy simulation of the turbulent structure in compound open-channel flows." *Advances in Water Resources* 53:66-75.

Yonesi, H. A., A. Parsaie, A. Arshia, and Z. Shamsi. 2022. "Discharge modeling in compound channels with non-prismatic floodplains using GMDH and MARS models." *Water Supply* 22 (4):4400–4421.

Yonesi, H. A., M. H. Omid, and S. A. Ayyoubzadeh. 2013. "The hydraulics of flow in nonprismatic compound channels." *J. Civ. Eng. Urbanism* 3 (6):342–356.

Zeng, R., and S. S. Li. 2023. "Large-eddy simulation of free-surface turbulent flow in a non-prismatic channel." *Journal of Hydroinformatics* 25 (5):1728–1746.

Zhang, W., Y. Xu, Y. Wang, and H. Peng. 2014. "Modeling sediment transport and river bed evolution in river system." *Journal of Clean Energy Technologies* 2 (2):175–179.

Zheleznyakov, G. V. 1965. "Relative deficit of mean velocity of unstable river flow: kinematic effect in river beds with floodplains." *Proc.14th Congress of IAHR* 5:144-148.

Annexure

PARA WISE RESPONSES BY MR. VIJAY KAUSHIK (2K20/PHDCE/01) TO FOREIGN EXAMINER

Thesis' weaknesses (not mandatory minor revisions) (as reported by foreign examiner)

The thesis does not have any significant weaknesses. However, I would like to provide a series of comments, some general and other editorial in nature, which could preserve the quality of the dissertation and, perhaps, offer some concern for discussion. When reading the thesis, I found the following points which would require further discussion:

(i) **Comment:** The results of this thesis are based on experiments at laboratory scale. It would be interesting to discuss scale effects mainly associated to the dimensions of the experimental channel and to the bed sediment used.

Response: Thank you for the valuable comment. Scale effects are crucial when considering the dimensions of the experimental channel and the bed sediment used. To address this, the proposed discharge equation was validated using nonprismatic river data from the River Main in Northern Ireland (as described in Section 4.5) to assess its applicability beyond laboratory conditions. This comparison helped counteract potential scale effects and demonstrated that the equation can reliably predict discharge in nonprismatic river streams. Additionally, since the equation effectively predicts discharge in nonprismatic rivers, it can also be applied to prismatic river channels with ease.

(ii) **Comment:** The ADV was employed to record instantaneous velocity components at a single-point of a channel section. However, a more explicit discussion on: sampling volume, sampling frequency, sampling time, denoising and despiking ADV velocity measurements would be desirable.

Response: Thank you for the valuable comment. In this study, instantaneous velocity measurements were taken at multiple points along the channel section, with a vertical interval of 2.5 cm and a horizontal interval of 10 cm, as shown in the grid

in Fig. 3.1. The depth-averaged velocity distribution across the width was then obtained by averaging the velocities over the flow depth. At a single point, ADV was operated at a sampling frequency of 25 Hz, with a sampling time of 1 minute per measurement point, resulting in 1500 velocity samples per location. To enhance data quality, a signal-to-noise ratio (SNR) threshold of 12 dB was used for denoising, and despiking techniques were applied to remove erroneous data points, ensuring reliable velocity measurements. The appropriate changes have been made in the methodology section.

(iii) Comment: When setting the models for prediction of the discharge in nonprismatic compound channels (e.g., Equation 3.26), both the Froude number and the Reynolds number are included. However, the similarity requirements posed by the Froude and Reynolds numbers can typically not be satisfied simultaneously. It would be desirable for this aspect to be clarified. In any case, it is interesting that the best GEP model (M7) would include the Froude number only!

Response: Thank you for the insightful comment. The functional relationship of the discharge ratio considers both the Froude number and the Reynolds number to account for the flow characteristics within the compound channel. However, achieving complete similarity between these two dimensionless numbers simultaneously is challenging due to their differing scaling requirements. In our study, the Froude number was prioritized to maintain dynamic similarity, as it governs free flows, while the Reynolds number remained within a turbulent flow regime to ensure representative flow conditions. Therefore, the GEP model (M7) incorporated the Froude number as a key parameter.

(iv) Comment: Still in regard to the model in Equation (3.26), the main channel and floodplain of rivers typically have different roughness; whereas, the candidate considers only one Manning's coefficient don't considering, therefore, the variation of roughness. This issue also would deserve a discussion.

Response: Thank you for the valuable suggestion. The discharge model in Equation (3.26) accounts for roughness variations by incorporating differential roughness (γ), which represents the ratio of the Manning's roughness coefficient of the floodplains to that of the main channel. Additionally, the model includes the composite

Manning's roughness coefficient (n), which represents the variation of overall resistance to flow due to the combined effects of the main channel and floodplains.

(v) Comment: I appreciated the systematic data processing with numerous diagrams, from Figure 4.1 to Figure 4.21, which also allow to extract the collected experimental data. However, I would have liked some more impactful plots like the contour plots of the velocity distributions and the bed morphology contour plots in case of the experiments with sediment. Similarly, in the description of the experiments I would have liked some more impactful photographs on the flow characteristics [see for instance the old paper by Sellin (La Houille Blanche, 1964)] and the bed morphologies in the main channel.

Response: Thank you for the insightful comment. As per your recommendation, contour plots depicting velocity distributions and bed morphology for experiments involving sediment have been presented.
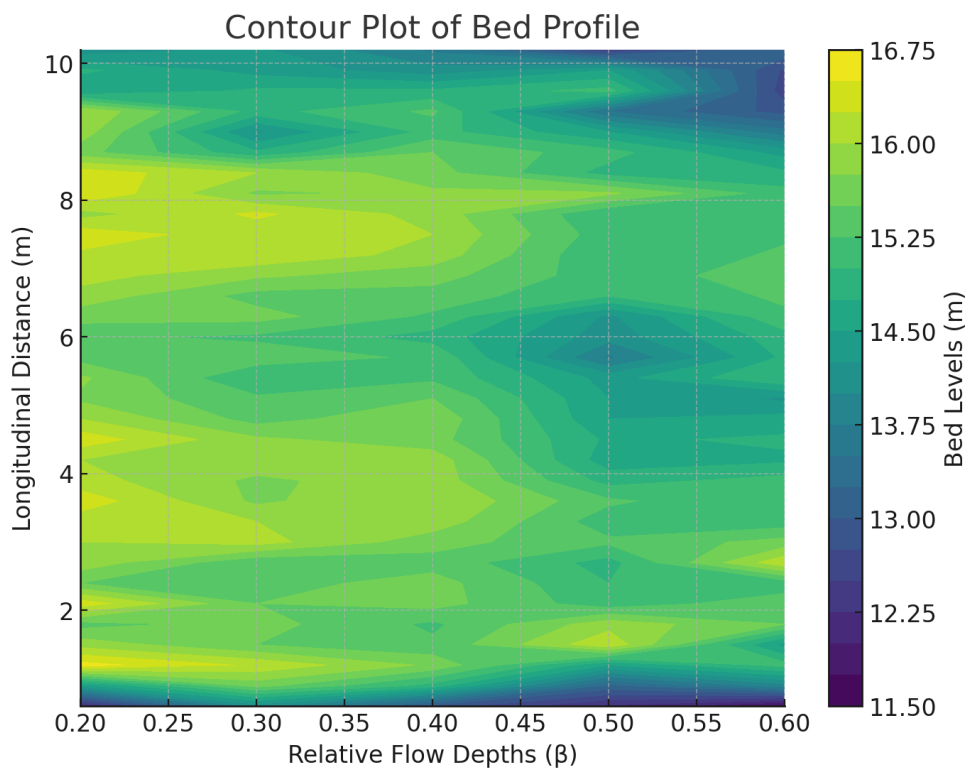
(a)
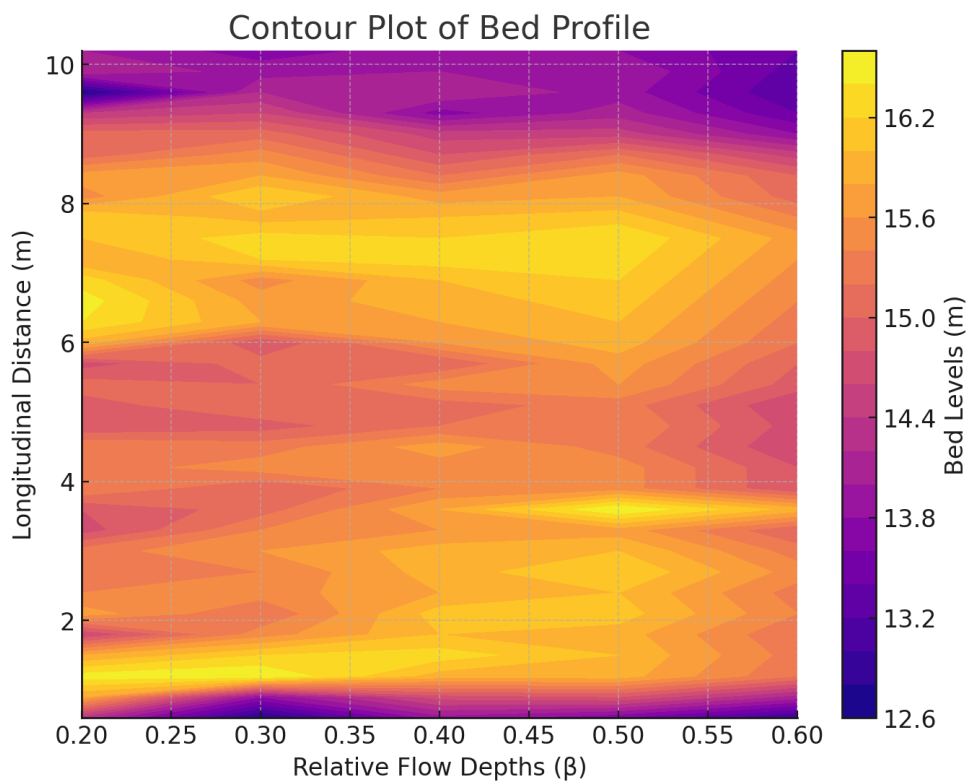
(b)

Fig. Contours of bed profile for the nonprismatic compound channels with (a) smooth floodplains (b) rough floodplains
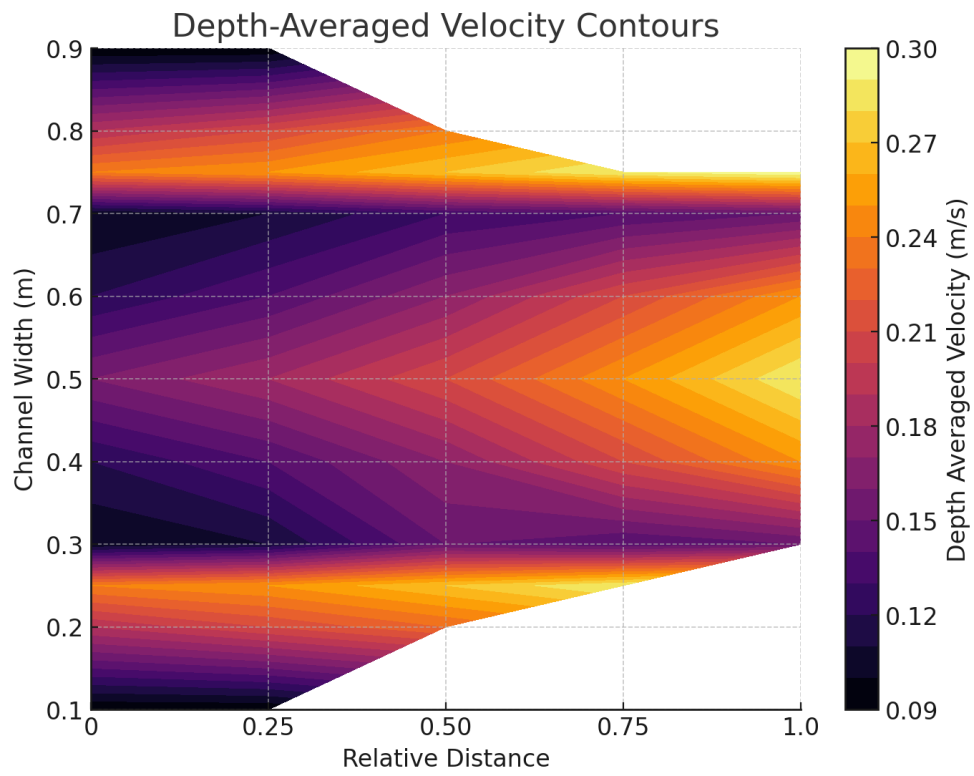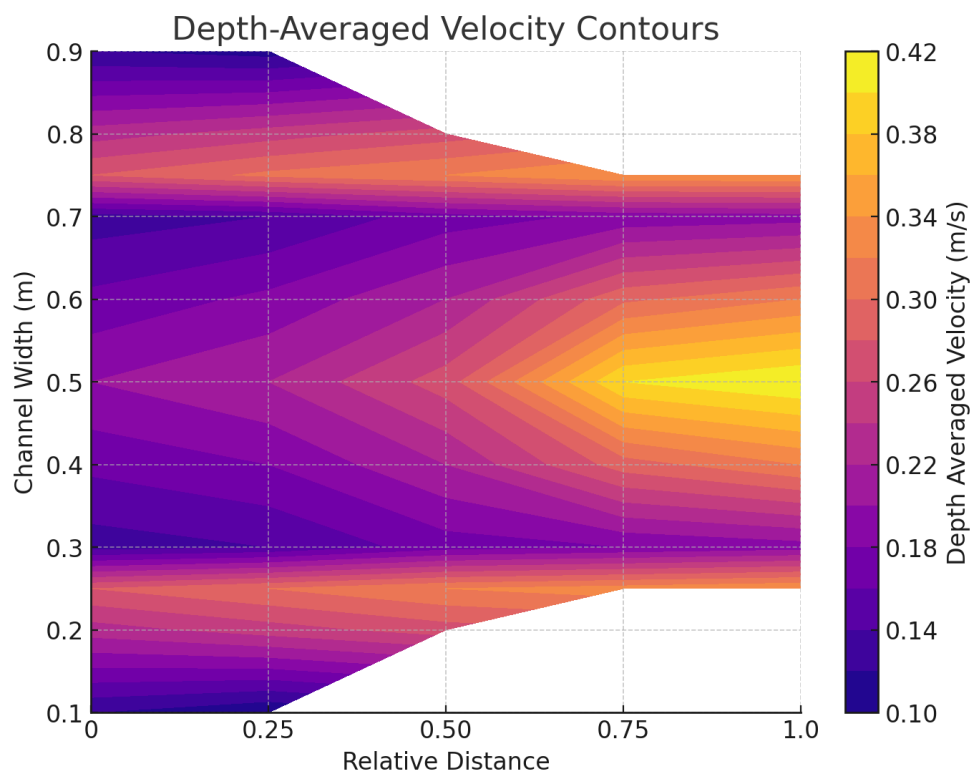
(a)

(b)

Fig. Contours of depth-averaged velocity distribution in nonprismatic compound channel with sediment and smooth floodplains for relative flow depth of (a) 0.20 (b) 0.60

(a)
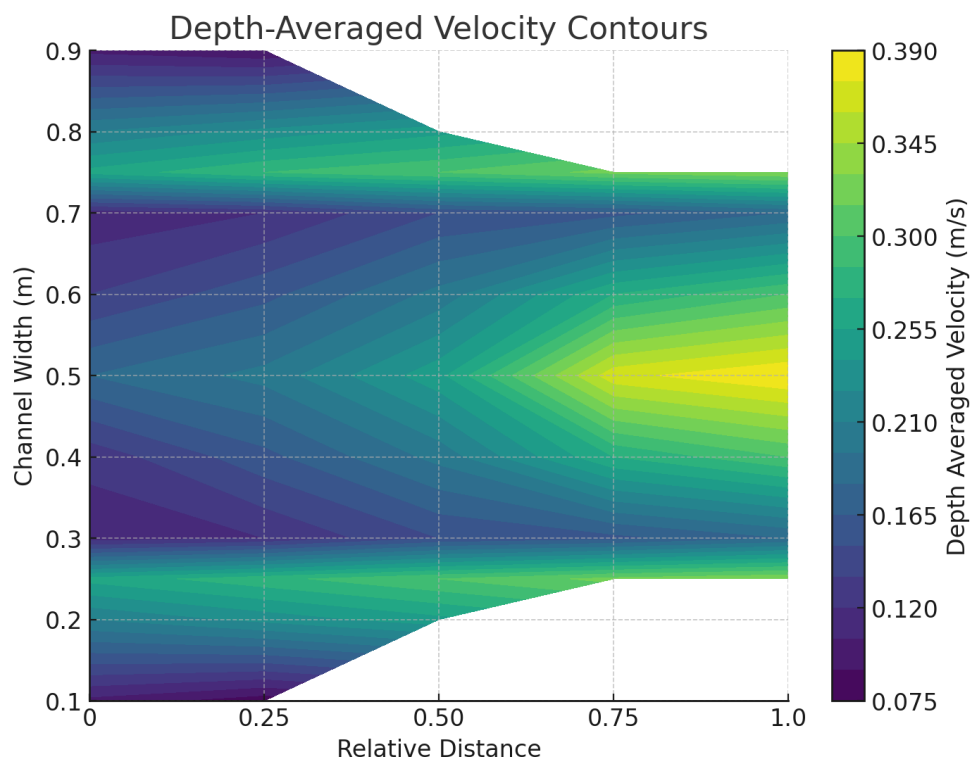
(b)

Fig. Contours of depth-averaged velocity distribution in nonprismatic compound channel with sediment and rough floodplains for relative flow depth of (a) 0.20 (b) 0.60

(vi) Comment: Diagrams are mainly provided in terms of dimensional variables. For instance, the stage-discharge diagram shows the stage H (m) as function of the Discharge Q (m³/s). I wonder how these diagrams, based on laboratory data, can be transferred into reality. In other terms, I would have liked dimensionless diagrams, perhaps with the identification of similarity laws.

Response: Thank you for the insightful comment. The dimensionless representation is important in enhancing the applicability of laboratory findings to real-world scenarios. As per your recommendation, dimensionless diagrams have been presented for the stage-discharge relationship in a nonprismatic compound channel with smooth and rough floodplains for different nonprismatic sections. In these diagrams, flow depth is expressed as the dimensionless term relative flow depth (β), which represents the ratio of overbank flow depth to the total flow depth. Similarly, discharge is represented by the discharge ratio (Q_r), defined as the ratio of discharge at any given depth to the bankfull discharge. The term X_r denotes the relative distance, which represents different nonprismatic sections and is defined as the ratio of the distance between two nonprismatic sections to the length of the converging section.

$$\beta = 0.126 \times Q^{1.619} \times 0.902^{X_r}$$

(a)

$$\beta = 0.127 \times Q^{1.638} \times 0.925^{X_r}$$
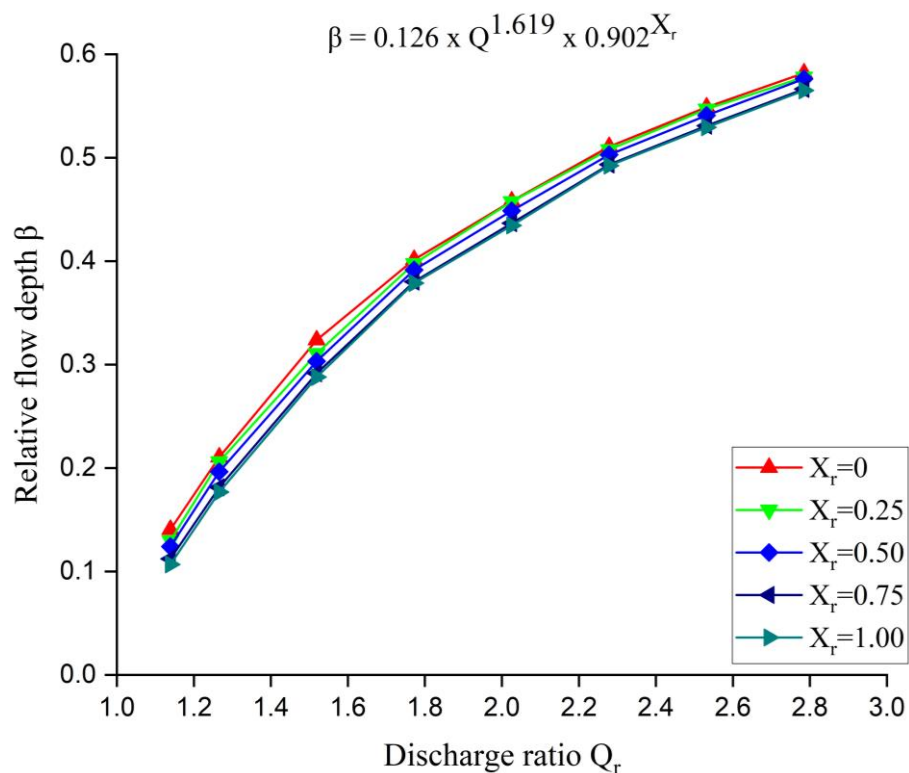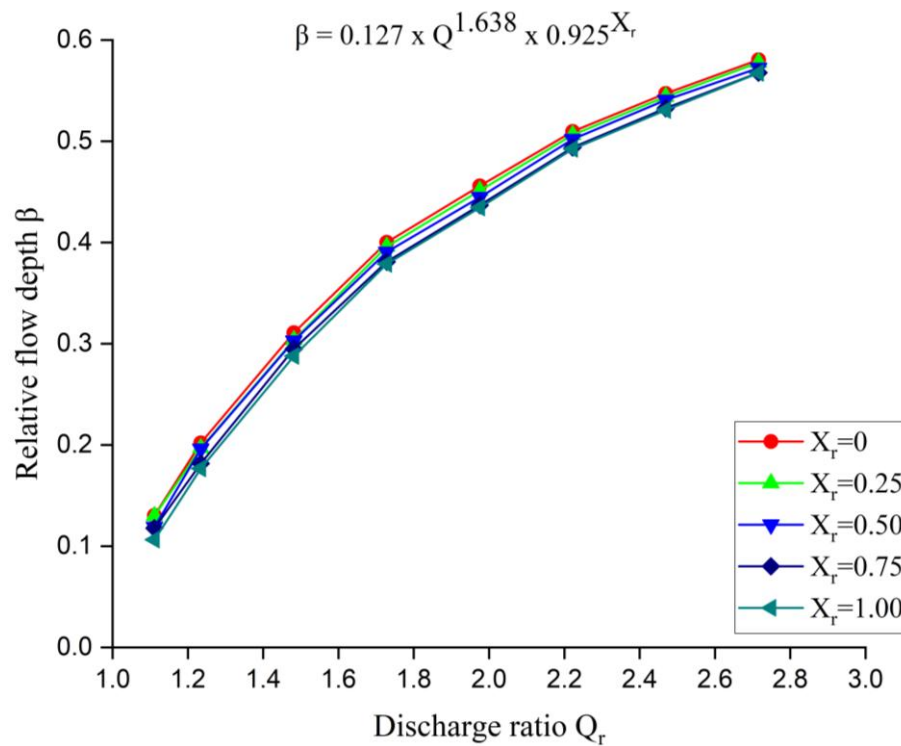
(b)

Fig. Stage-discharge relationship for nonprismatic compound channel with (a) smooth floodplains (b) rough floodplains

(vii) Comment: In regard to the Gene Expression Programming (GEP) models, it would be interesting to discuss: What is the reason for using GEP soft technique rather than other soft techniques? Could the best performance of GEP models be affected by overfitting? Did the candidate assess the physical consistency of the proposed GEP models?

Response: Thank you for the valuable suggestion. GEP was chosen over other soft computing techniques due to its ability to evolve mathematical expressions dynamically, making it highly effective for modeling complex nonlinear hydraulic behaviour's in nonprismatic compound channels. Unlike traditional machine learning methods, GEP offers explicit analytical equations, enhancing interpretability and applicability in hydraulic engineering. To address concerns regarding overfitting, the model's performance was rigorously evaluated using cross-validation techniques and by dividing the dataset into training and testing sets. The dataset, consisting of 630 data points for 14 variables from both past and present studies, representing sufficient data to avoid overfitting. The generalization

capability of the GEP model was further assessed by comparing its predictions with experimental and real river data. The GEP model was tested against both laboratory-scale experimental data and real-world field data from a river (e.g., River Main in Northern Ireland) to assess its predictive accuracy. The results demonstrated that the model provides reliable discharge predictions across varying flow conditions, reinforcing its physical relevance and practical applicability.

(viii) **Comment:** On the basis of the data acquired, elaborations aimed at a greater characterization of the turbulence would also be interesting. I'm thinking of the turbulence intensities, the turbulence kinetic energy (TKE), the Reynolds stress anisotropy. By the way, in regard to the experiments, was the approach flow a fully developed turbulent flow?

Response: Thank you for the valuable suggestion. The aspects of turbulence intensity, turbulence kinetic energy (TKE), and Reynolds stress anisotropy were not analyzed in the present study as measurements are inadequate to cover these aspects. However, I recognize their importance in providing a more detailed characterization of turbulence and will explore these aspects in our future research and publications. Regarding the approach flow, it was fully developed turbulent flow before entering the test section. This was verified through Reynolds number analysis, and ADV measurements, ensuring that the flow characteristics met the criteria for a fully developed turbulent regime.

(ix) **Comment:** Many refinements emerge as relevant from a careful reading of the text. Particular attention should be addressed to the definition of the symbols especially when equations are presented. Many equations/formulas are difficult to understand in their entirety mainly because the meaning of the symbols is not always explained.

Response: Thank you for the valuable suggestion. As per your recommendation, all symbols have now been explicitly defined immediately after each equation to enhance clarity and ensure a better understanding of the mathematical formulations. The necessary revisions have been incorporated throughout the thesis.

TYPOS/EDITORIAL CHANGES (#r#) (suggested by foreign examiner)

Here below, I have reported some additional editorial remarks. I hope the candidate would apply them as well as those similar but not reported here. The dissertation is valuable and quality and style are worth preserving.

[CHAPTER 2 - REVIEW OF LITERATURE]

[r1] At page 11 it reads "They provided", but it should read "He provided".
[r2] At page 12 it reads "Myers and Elswy (1975)", but it should read "Myers and Elsawy (1975)".
[r3] At page 19 it reads "Moreta and Vide (2010)", but it should read "Moreta and Martin-Vide (2010)".
[r4] At page 21 it reads "Conway et al. (2012)", maybe it should read "Conway et al. (2013)" according to the References section.

Response (r1 to r4): Thank you for the valuable suggestions. As per your recommendations, all necessary corrections have been incorporated into the literature review section.

[CHAPTER 3 - METHODOLOGY]

[r1] It reads "Utilizing observations collected from in-bank and over-bank flows in the flood and the primary pathway, a computational of Manning's roughness coefficient was carried out". However, it is unclear how the Manning's coefficient was computed!
Response: Thank you for the insightful comment. Manning's roughness coefficient has not been directly computed for the channel reach. Instead, it has been estimated inversely using Manning's equation based on section properties (flow area and hydraulic radius) and energy slope. The variation of Manning's roughness coefficient with flow depth has been analyzed and presented to provide a clearer understanding of its behavior.
[r2] At page 42 (and all over the thesis) it reads "v-notch", but I would write "V-notch".
Response: Thank you for the valuable suggestion. As per your recommendation, the necessary modifications have been made in the thesis.
[r3] At page 42 it reads "A gate was installed at the end of flume", but what type of gate is it (e.g. sluice gate, flap gate…)?

Response: Thank you for the insightful comment. The gate installed at the end of the flume is a sluice gate, which was used to regulate the water level and ensure a uniform flow depth throughout the entire length of the flume. This clarification has been incorporated into the thesis.

[r4] At page 46 the symbols in Equations (3.1) and (3.2) should be defined. Moreover, where was the head H measured?

Response: Thank you for the valuable suggestion. As per your recommendation, the symbols in Equations (3.1) and (3.2) have been explicitly defined in the thesis. Additionally, the head for the notch was measured from the crest of the notch to the undisturbed water surface upstream. The appropriate changes have been made in the thesis.

[r5] At page 49 the symbols in Equation (3.5) should be defined.

Response: Thank you for the valuable comment. The symbols in Equation (3.5) have been defined in the thesis for clarity.

[r6] At page 52 the symbols in Equations (3.12) and (3.13) should be defined.

Response: Thank you for the valuable comment. The symbols in Equations (3.12) and (3.13) have been defined in the thesis.

[r7] A more complete definition of the symbols in Equation (3.14) would allow a better comprehension of the Patel's (1965) technique.

Response: Thank you for the valuable comment. The symbols in Equation (3.14) have been defined in the thesis.

[r8] The text on pages from 54 to 60 appears quite general in nature. However, it can remain as it is.

Response: Thank you for the valuable suggestion. The text remains unchanged in the aforementioned section.

[r9] At page 61 the acronyms SCM & DCM should be spelled out.

Response: Thank you for the valuable comment. The acronyms SCM and DCM have been spelled out in their first appearance for clarity.

[r10] A more complete definition of the symbols in Equations from (3.19) to (3.25) would allow a better comprehension of the various methods.

Response: Thank you for the valuable comment. The symbols in Equations (3.19) to (3.25) have been defined in the thesis.

[r11] The functional relationship (3.26) includes both the Froude number and the Reynolds number. Is it correct? The similarity requirements set by the Froude and Reynolds numbers can typically not be satisfied simultaneously.

Response: Thank you for the insightful comment. The functional relationship of the discharge ratio considers both the Froude number and the Reynolds number to account for the flow characteristics within the compound channel. However, we acknowledge that achieving complete similarity between these two dimensionless numbers simultaneously is challenging due to their differing scaling requirements. In our study, the Froude number was prioritized to maintain dynamic similarity, as it governs free surface flows, while the Reynolds number remained within a turbulent flow regime to ensure representative flow conditions.

[r12] The sharpness of Table 3.2 should be improved.

Response: Thank you for the valuable comment. The sharpness and clarity of Table 3.2 have been improved in the thesis to enhance readability and presentation quality.

[r13] The symbols in equations from (3.24) to (3.28) should be defined.

Response: Thank you for the valuable comment. The symbols in Equations (3.24) to (3.28) have been defined in the thesis.

[CHAPTER 4 - RESULTS AND DISCUSSION]

[r1] Figures 4.3a and 4.3b look the same though they relate to smooth and rough floodplains respectively. Could the candidate check?

Response: Thank you for the valuable suggestion. As per your recommendation, I have carefully checked the figures illustrating the variation of the water surface profile for both smooth and rough floodplains. The trend of variation remains consistent in both cases. However, for the same discharge in a nonprismatic compound channel with rough floodplains, the flow depth is slightly lower compared to smooth floodplains. For relative flow depth of 0.60, the flow depth at the start of channel is 0.6250 m and 0.6230 m for nonprismatic compound channels with smooth and rough floodplains, respectively.

[REFERENCES]

Overall references are accurate. However, some refinements are needed. Here below some examples are provided.

[Ref. Ackers 1991] This reference should be slightly refined. It reads "Ackers, P. 1991. *Hydraulic design of straight compound channels.* Volume 1-summary and design method, volume 2-appendices", but I would write "Ackers, P. 1991. *Hydraulic design of straight compound channels.* Volume 1 - Summary and design method, Volume 2 - Appendices, Technical Report SR 281, Hydraulics Research Ltd, Wallingford, United Kingdom".

[Ref. Barman and Kumar 2023] It reads *Physics of Fluids 35 (3)*, but I would specify *Physics of Fluids 35 (3): article number 036601*.

[Ref. Das and Khatua 2018] It reads *Journal of Hydraulic Engineering 144 (8)*, but I would specify *Journal of Hydraulic Engineering 144 (8): article number 04018051*.

[Ref. Gamal Abdalla 2016] It reads "5 (6) :114", but it should read "5 (6): 114-121".

[Ref. Myer and Lyness 1997] It reads "Myer, W. R. C.", but it should read "Myers, W. R. C.".

[Ref. Myer et al. 2001] It reads "Myer, W. R. C.", but it should read "Myers, W. R. C.".

[Ref. Myers and Elsawy 1975] It reads "Boundary shears in channel with floodplain", but it should read "Boundary shear in channel with flood plain".

[Ref. Sahu et al. 2011b] Maybe the name of co-authors could be made explicit.

[Ref. Sahu et al. 2012] Similarly, maybe the name of co-authors could be made explicit.

[Ref. Sellin 1964] It reads "that over its floodplain", but it should read "that over its flood plain"; It reads *Houille Blanche*, Grenoble 7:793-802", but it should read *La Houille Blanche*, 7:793-802".

[Ref. Zhang et al. 2014] It reads "*Journal of Clean Energy Technologies 175-179*", but it should read *Journal of Clean Energy Technologies* 2 (2):175-179".

Response: Thank you for the valuable suggestions. As per your recommendations, all necessary refinements have been made in the references, and they have been thoroughly checked. The appropriate changes have also been implemented in the reference section.

PARA WISE RESPONSES BY MR. VIJAY KAUSHIK (2K20/PHDCE/01) TO INDIAN EXAMINER

General:

An excellent experimental study building a comprehensive understanding on a specific hydraulic aspect of sediment transport in prismatic, non-prismatic converging channels, as it is also evidenced by several quality research publications. Thesis is written well for English Grammar and style. The work presented is also sufficient in both quantity and quality and therefore strongly recommended for the award of PhD degree.

Specific:

1. **Comment:** Thesis title: Since the work relates to a specific topic, the same can be taken as title. For example, "SEDIMENT TRANSPORT IN PRISMATIC AND NONPRISMATIC CONVERGING CHANNELS."

   Response: Thank you for your valuable suggestion. Initially, the title proposed during my SRC was "Study of Sediment Transport in Prismatic and Nonprismatic Reaches of Compound Channels." It was suggested that while the title need to be broad and general in nature and the objectives should be specific to the study. Therefore, based on the recommendations of external experts, it was suggested to rename the title as "Sediment Transport in Prismatic and Nonprismatic Channels", as this approach ensures flexibility. Though your suggestions are apt and valuable, it may not be possible to change the title at this stage due to administrative reasons.

2. **Comment:** ABSTRACT: It begins with compound channels whereas the title does not include it. Further, the first two lines need revising or deleting or you need to explain how the compound channels affect the variables mentioned. Better, if the ABSTRACT is little more elaborated so that reader is able to comprehend that this study specifically deals with such aspects. The last line remains unsupported by the data.

   Response: Thank you for your valuable suggestion. Based on your recommendation, the first two lines have been removed from the abstract. Additionally, the abstract has been revised to provide a more comprehensive understanding of the aspects

under investigation. Furthermore, the last line has been substantiated with relevant data to ensure its validity and support the study's findings.

3. **Comment:** LITERATURE REVIEW: Thesis severely lacks in comprehending the review of literature appropriately. Looks like an MTech level review presented as it is from different research papers. This review needs to be discussed properly. May be, the whole can be comprehended in tabular form and discussed in text to arrive at a logical gap in research.

    Response: Thank you for your valuable suggestion. Based on your recommendation, I have restructured the literature review to ensure a more comprehensive synthesis of the existing research. The review is structured in a detailed tabular format and is supplemented by a discussion that highlights logical gaps in the existing body of research.

4. **Comment:** RESULTS AND DISCUSSIONS:

    a. It is always better for clarity in reading that the symbols are also described where they appear for the first time in text, besides their appearance in list of abbreviations.
    Response: Thank you for your valuable suggestion. Based on the recommendation, symbols have been defined at their first occurrence in the text to enhance clarity and understanding.

    b. How smooth or rough beds are described, just visual or some criteria followed?
    Response: In our study, the classification of smooth and rough beds was not solely based on visual assessment but the roughness characteristics of the beds were defined using Manning's n, as described by Subramanya (2015). A smooth surface was achieved through a trowel finish, while a rough surface was created using stone pitching to introduce roughness.

    c. While describing models or any other aspect, these should also be described in results and discussions so that one is able to follow the text. For example, at page 64, Model M7 appears all of a sudden without any reference to other models.

Response: Thank you for your valuable suggestion. Based on the recommendation, the models have been described within the results and discussion section. To address the concern that "Model M7 appears all of a sudden without any reference to other models," the text has been revised to include a clear definition of the characteristics of all models.

d. Units of depth, RMSE etc. not shown anywhere.

Response: Thank you for your valuable suggestion. The unit of flow depth (H) is measured in meters, whereas relative flow depth (β) and relative distance (X_r) are dimensionless parameters. The unit of RMSE is same as that of the considered parameter. Thus, RMSE for parameter depth is in meter and for discharge ratio, relative flow depth which are dimensionless parameters, and therefore it does not have any unit. Similarly, the units of all other terms have been provided for clarity and consistency.

e. Please describe beta (β) for its physical significance at its first appearance.

Response: Thank you for your valuable suggestion. Relative flow depth (β) is a dimensionless parameter and it is defined as the ratio of the overbank flow depth to the total flow depth. As the relative flow depth increases, a larger proportion of the water is found above the main channel, which can significantly affect the flow dynamics. This dimensionless parameter allows for a comparison across different channel designs and conditions, making it an essential factor in the analysis and design of compound channels.

f. Please describe which factor governs the momentum shift often mentioned in the text.

Response: In compound channels, momentum shift between the main channel and the floodplain is controlled by a combination of hydraulic and geometric factors. This includes the channel's shape and slope, the relative flow depths, the velocity distribution and the associated shear stresses at the interface. Surface roughness on both the main channel and floodplain also plays a crucial role, as it influences turbulence and energy dissipation, thereby affecting momentum transfer.

g. What is relative distance X_r, perhaps never explained in text. Similarly, others as well.

Response: Relative distance (X_r) is defined as the ratio of the distance between two converging sections to the length of a converging section. Relative distance (X_r) and other related parameters have now been explained in the thesis.

h. Page 120. Please explain if it is by chance that both R^2 and AIC are most favourable for the present study.

Response: The favourable results for both R^2 and AIC in our study are not by chance but rather a reflection of the robustness of the model (M7). The high R^2 value indicates a strong correlation between the observed and predicted values, suggesting that the model adequately captures the underlying relationship between the hydraulic and geometric parameters. Similarly, the low AIC value implies that our model achieves a balance between goodness-of-fit and model complexity, making it a more efficient representation of the data. These outcomes are a result of careful model development and appropriately chosen variables, and they enhance the utility and validity of the model for the study.

The marked thesis is attached herewith for numerous suggestions/typos. These may be addressed by the candidate and thesis need not to be sent for re-review.

Response: Thank you for your valuable suggestion. Based on the recommendations, marked suggestions/typos are incorporated in the thesis. Some of them are:

Comment: These factors…..which factors?

Response: Here factors written mistakenly, it should be compound channels.

Comment: How they are crucial for environmental, ecological, and design objectives.

Response: Compound channels play a crucial role in environmental, ecological, and design aspects. Environmentally, they help manage floodwaters by reducing flow velocity and minimizing erosion. Ecologically, they provide diverse habitats for aquatic and terrestrial species, maintaining ecosystem balance. From design aspects, it is essential for effective flood control, river engineering and sustainable infrastructure, ensuring that waterways function efficiently.

Comment: Converging sections have to be followed by diverging sections. Why not undertaken.

Response: Sir, this study specifically focuses on converging compound channels rather than both converging and diverging sections. Additionally, previous studies have examined flow behavior separately in converging and diverging sections. Therefore, the diverging section was not included in this study. However, in natural channels, a converging section may or may not be immediately followed by a diverging section, though all rivers eventually exhibit diverging sections as they discharge into the sea.

Comment: "Thus, computational analysis of flow characteristics in nonprismatic compound channels based on the finite element method/finite difference method may also be the future scope of the study." It can not be a research Gap for your study. If it is, then you have to work on it.

Response: Some of the identified research gaps were incorporated into the aims of the study. Literature is available on the computational analysis of flow characteristics in nonprismatic compound channels with smooth floodplains. Therefore, exploring the computational analysis of flow characteristics in nonprismatic compound channels with rough floodplains and sediment conditions using the finite element method may serve as a future research direction.

LIST OF PUBLICATIONS

❖ Kaushik, V., and M. Kumar. 2023. "Sustainable gene expression programming model for shear stress prediction in nonprismatic compound channels." *Sustainable Energy Technologies and Assessments*, 57: 103229. (IF: 7.1)
https://doi.org/10.1016/j.seta.2023.103229

❖ Kaushik, V., and M. Kumar. 2023. "Assessment of water surface profile in nonprismatic compound channels using machine learning techniques." *Water Supply*, 23 (1): 356–378. (IF: 1.9)
https://doi.org/10.2166/ws.2022.430

❖ Kaushik, V., and M. Kumar. 2024. "Prediction of shear stress distribution in compound channel with smooth converging floodplains." *Journal of Hydrology and Hydromechanics*, 72 (2): 170–184. (IF: 2.3)
https://doi.org/10.2478/johh-2024-0004

❖ Naik, B., V. Kaushik, and M. Kumar. 2022. "Water surface profile in converging compound channel using gene expression programming." *Water Supply*, 22 (5): 5221–5236. (IF: 1.9)
https://doi.org/10.2166/ws.2022.172

❖ Kaushik, V., M. Kumar, B. Naik, and A. Parsaie. 2023. "Modeling of water surface profile in non-prismatic compound channels." *Water Practice and Technology*, 18 (9): 2151–2167. (IF: 1.6)
https://doi.org/10.2166/wpt.2023.142

❖ Kaushik, V., B. Naik, M. Kumar, and V. K. Minocha. 2024. "Prediction of the flow resistance in non-prismatic compound channels." *Water Practice and Technology*, 19 (5): 1822–1835. (IF: 1.6)
https://doi.org/10.2166/wpt.2024.117

❖ Kaushik, V., M. Kumar, and B. Naik. 2024. "Numerical Simulation of Flow Characteristics in Nonprismatic Compound Channels." *Water Practice and Technology*, 19 (7): 2532–2550. (IF: 1.6)
https://doi.org/10.2166/wpt.2024.153

❖ Kaushik, V., and M. Kumar. 2023. "Water surface profile prediction in non-prismatic compound channel using support vector machine (SVM)." *AI In Civil Engineering*, 2 (1).

https://doi.org/10.1007/s43503-023-00015-1

❖ Kumar, R., V. Kaushik, and M. Kumar. 2023. "Application of Gene Expression Programming in Computation of Flow Resistance in Compound Channel with Converging Floodplains." *Civil Engineering and Architecture*, 11 (5): 2719–2730.
https://doi.org/10.13189/cea.2023.110535

❖ Kaushik, V., and M. Kumar. 2024a. "A Review of Different Approaches for Boundary Shear Stress Assessment in Prismatic Channels." *Lecture Notes in Civil Engineering*, 117–129.
https://doi.org/10.1007/978-981-99-3557-4_10

International Conferences

❖ Kaushik, V., and M. Kumar. "Water Surface Profile Prediction in Nonprismatic Compound Channels Using Support Vector Machine (SVM)." *International Conference on Advances in Civil Engineering*, held on 20-22 December 2022, organized by Technology Research and Innovation Centre, India and hosted by LSKBJ College of Engineering, Chanwad, Nashik, India.

❖ Kaushik, V., and M. Kumar. "A Review of Different Approaches for Boundary Shear Stress Assessment in Prismatic Channels." *1st International Conference on Innovations in Smart and Sustainable Infrastructure (ISSI-2022)*, held on 23-25 August 2022, organized by Civil Engineering Department, School of Technology, Pandit Deendayal Energy University, Gandhinagar, India.

❖ Kaushik, V., M. Kumar, and B. Naik. "A Review on Bed Morphology in Compound Channels: Processes, Patterns, and Implications." *28th International Conference on Hydraulics, Water Resources, River and Coastal Engineering (HYDRO 2023 International)*, held on 21st to 23rd December 2023, organized by Department of Civil Engineering, National Institute of Technology, Warangal, India.

Contents lists available at ScienceDirect

Sustainable Energy Technologies and Assessments

Sustainable gene expression programming model for shear stress prediction in nonprismatic compound channels

Vijay Kaushik [*], Munendra Kumar

Department of Civil Engineering, Delhi Technological University, Delhi 110042, India

ARTICLE INFO

ABSTRACT

Open channel flow resistance and channel stability can be determined from boundary shear stress distribution. Overbank floods cross the main channel and pours the floodplain. The momentum change between the main channel and floodplains creates complicated flow shapes in compound channels. This alters floodplain and main channel shear stress. River floodplains also support agriculture and development activities due to which floodplain shape changes along the flow length, creating a converging, diverging or skewed compound channels. Traditional empirical formulas cannot accurately estimate shear force distribution. Thus, creative and accurate methods remain in demand. Gene expression programming, an innovative approach, has been utilized in this study to develop a new equation for compound channel with converging floodplains in terms of nondimensional geometric and flow variables to estimate the boundary shear force carried by floodplains. The proposed GEP-based method is best when compared to previously developed methods. The findings indicate that the predicted percentage shear force carried by floodplains determined using GEP is in good agreement with the experimental data ($R^2 = 0.96$ and RMSE = 3.395 for the training data and $R^2 = 0.95$ and RMSE = 4.022 for the testing data).

Introduction

One or more adjacent floodplains usually surround the main channel in several natural rivers. Because these channels comprise more than one of the basic elementary configurations, they are referred to as compound channels. Numerous hydraulic phenomena, such as channel roughness, sedimentation, bed morphology, overbank flow conditions, etc., involve boundary shear stress as an essential parameter. Channel shape and secondary flow cell design affect boundary shear stress patterns in compound channels with smooth and rough floodplains. The hydraulic radius and longitudinal pressure gradient may be utilized to calculate compound channel average shear stress. These channels lose energy due to the high-velocity gradient and fluid viscosity resistance. Due to velocity field, secondary cell structures, cross-sectional geometry, and boundary roughness, boundary and local shear stresses are difficult to determine [1]. To better understand shear stress distribution, researchers performed various experiments [2,3]. Studies have examined wall shear stress distribution and flow resistance in two-stage and single-stage channels with varying sediment bed conditions in the main channel [4,5]. Sellin [6] studied momentum shift in experimental

flumes. Many scientists felt momentum transfer caused the non-uniform boundary shear stress patterns throughout the section perimeter [7,8]. Knight and Hamed [7] devised a boundary shear stress distribution model for homogeneous compound channels with a width ratio (α) up to 4. The work was carried forward by Khatua and Patra [9] based on the data collected during their experiments. They came up with a model suitable for channels with a width ratio (α) of 5. With $6.67 \leq \alpha \leq 11.96$, Mohanty and Khatua [10] have created another novel channel system model. Laboratory flumes explored prismatic and meandering compound channel shapes. Prismatic compound channels maintain shape, size, and longitudinal slope during the flow length. Flood control and diversion structures must examine these waterways' flow characteristics. Compared to nonprismatic compound channel data, prismatic compound channel data showed significant shear force estimation flaws [11–13]. Momentum shift must be considered in nonprismatic compound channel flow models. Cross-section shape and two-phase flow structure substantially impact boundary shear stress distribution. Therefore, new nonprismatic compound channel models are needed. Tests were performed on a two-stage channel with converging floodplains to find a unique expression for floodplain shear force [14].

Mathematical, analytical, or numerical models for wall shear stress

---

* Corresponding author.
  E-mail addresses: vijaykaushik_2k20phdce01@dtu.ac.in (V. Kaushik), munendrakumar@dtu.ac.in (M. Kumar).

Assessment of water surface profile in nonprismatic compound channels using machine learning techniques

Vijay Kaushik* and Munendra Kumar

Department of Civil Engineering, Delhi Technological University, Delhi, 110042, India.
*Corresponding author. E-mail: vijaykaushik_2k20phdce01@dtu.ac.in

ABSTRACT

Accurate prediction of water surface profile in an open channel is the key to solving numerous critical engineering problems. The goal of the current research is to predict the water surface profile of a compound channel with converging floodplains using machine learning approaches, including gene expression programming (GEP), artificial neural networks (ANNs), and support vector machines (SVMs), in terms of both geometric and flow variables, as past studies were more focused on geometric variables. A novel equation was also proposed using gene expression programming to predict the water surface profile. In order to evaluate the performance and efficacy of these models, statistical indices are used to validate the produced models for the experimental analysis. The findings demonstrate that the suggested ANN model accurately predicted the water surface profile, with coefficient of determination (R^2) of 0.999, root mean square error (RMSE) of 0.003, and mean absolute percentage error (MAPE) of 0.107%, respectively, when compared with GEP, SVM, and previously developed methods. The study confirms the application of machine learning approaches in the field of river hydraulics, and forecasting water surface profile of nonprismatic compound channels using a proposed novel equation by gene expression programming made this study unique.

Key words: geometric and flow parameters, machine learning techniques, nonprismatic compound channel, statistical analysis, water surface profile

HIGHLIGHTS

- The present study predicted the water surface profile in nonprismatic compound channels with the help of various machine learning approaches.
- The water surface profile is found to be affected by many nondimensional geometric and flow variables.
- The findings depict that the water surface profile predicted using ANN is in good agreement with the observed water surface profile.

sciendo   **Journal of Hydrology and Hydromechanics**   Institute of Hydrology SAS

Prediction of shear stress distribution in compound channel with smooth converging floodplains

Vijay Kaushik[1*], Munendra Kumar[2]

[1] Department of Civil Engineering, Delhi Technological University, Delhi, 110042, India. E-mail: vijaykaushik_2k20phdce01@dtu.ac.in
[2] Department of Civil Engineering, Delhi Technological University, Delhi, 110042, India. E-mail: munendrakumar@dtu.ac.in
* Corresponding author.

Abstract: Climate change can have a profound impact on river flooding, leading to increased frequency and severity of floods. To mitigate these effects, it is crucial to focus on enhancing early warning systems and bolstering infrastructure resilience through improved forecasting. This proactive approach enables communities to better plan for and respond to flood events, thereby minimizing the adverse consequences of climate change on river floods. During river flooding, the channels often take on a compound nature, with varying geometries along the flow length. This complexity arises from construction and agricultural activities along the floodplains, resulting in converging, diverging, or skewed compound channels. Modelling the flow in these channels requires consideration of additional momentum transfer factors. In this study, machine learning techniques, including Gene Expression Programming (GEP), Artificial Neural Networks (ANN), and Support Vector Machines (SVM), were employed. The focus was on a compound channel with converging floodplains, predicting the shear force carried by the floodplains in terms of non-dimensional flow and hydraulic parameters. The findings indicate that the proposed ANN model outperformed GEP, SVM, and other established approaches in accurately predicting floodplain shear force. This research underscores the efficacy of utilizing machine learning techniques in the examination of river hydraulics.

Keywords: Compound channel; Converging floodplains; Shear stress distribution; Non-dimensional parameters; Machine learning approaches.

INTRODUCTION

The dynamics of flow within a river are influenced by turbulence and the presence of three-dimensional objects. Consequently, selecting an appropriate modelling technique becomes a challenge when aiming to estimate various flow characteristics, including discharge, velocity, and shear stress. Mean velocities in both the main channel and floodplain fluctuate due to variations in hydraulic conditions. The determination of velocity profiles and fluid fields is contingent upon the presence of boundary shear stress. Beyond the bankfull stage, the flow within the primary channel exerts a propulsive or accelerating force on the flow across floodplains, inherently inducing a resistive or decelerating impact on the flow within the primary channel. The pioneering work on boundary shear distributions in open channels was conducted by Leighly (1932). Numerous scholars have conducted investigations on the resolution of boundary shear distributions in streams, using either direct or indirect methodologies. The analysis of shear forces at the bed helps elucidate the mechanism of bedload transfer, while the examination of shear forces at the walls offers a comprehensive perspective on variations in the channel pattern. Several researchers have conducted studies on the flow, velocity, and shear stress distribution on compound sections (Bhattacharya, 1995; Kar, 1977; Khatua et al., 2011a, b; Knight and Demetriou, 1983; Mohanty, 2013; Myers, 1987; Patra, 1999; Patra and Kar, 2000; Patra et al., 2004; Yang and Lim, 2005). Traditional channel division techniques are used for the assessment of discharge capacity in compound channels. It is postulated that the compound section is delineated by hypothetical interface planes located at the confluence of the main channel and the floodplain. The absence of shear stress in these regions suggests a lack of momentum transmission. The momentum transfer phenomena were first examined by Sellin (1964) via laboratory research. Subsequently, several researchers discovered that the uneven distribution of boundary shear stress along the perimeter of straight compound channels could be attributed to momentum transfer. As a result, they developed an empirical equation for quantifying shear stress, as evidenced by the works of Knight and Demetriou (1983), Knight and Hamed (1984), Myers (1987), Stephenson and Kolovopoulos (1990), Patra et al. (2004), and Yang and Lim (2005). In their seminal work, Knight and Hamed (1984) proposed a theoretical framework to analyse the distribution of boundary shear stress in a compound channel with homogenous characteristics. Their model specifically focused on width ratio (α) values ranging up to 4. In their work, Khatua and Patra (2007) further investigated the subject matter by conducting more experimental observations. They subsequently formulated a model that encompasses channels with width ratios (α) ranging up to 5.25. In their study, Mohanty and Khatua (2014) proposed a novel model for a channel characterized by values of α ranging from 6.67 to 11.96. Extensive investigations were conducted in laboratory flumes to study both prismatic and meandering compound channel designs. Nevertheless, a comparison between the compound section data of prismatic compound channels and non-prismatic compound channels revealed significant discrepancies in the estimation of shear force carried by floodplains. These errors can be attributed to the omission of additional mass and momentum transfer, as elucidated by Bousmar and Zech (2002), Bousmar et al. (2004), Rezaei (2006), and Rezaei and Knight (2009). The additional momentum exchange associated with this phenomenon must be considered when doing flow modelling for non-prismatic compound channels. The study conducted by Proust et al. (2006) investigated the phenomenon of asymmetric geometry,

Water Supply

Water surface profile in converging compound channel using gene expression programming

Bandita Naik [ID][a,*], Vijay Kaushik[b] and Munendra Kumar[b]

[a] Department of Civil Engineering, Methodist College of Engineering, Hyderabad, India
[b] Department of Civil Engineering, Delhi Technological University, Delhi, India
*Corresponding author. E-mail: banditanaik@methodist.edu.in

[ID] BN, 0000-0002-9488-2184

ABSTRACT

Assessment of water surface profile in compound channels is essential for flood defence systems. Agriculture and development activities in floodplains affect the floodplain shape over the length, leading in a converging compound channel. Few laboratory investigations proved overbank flow in converging floodplains. Therefore, innovative and precise approaches are still in great demand. In this paper, new approach has been proposed to forecast the water surface profile of various compound channels with converging floodplains using gene expression programming (GEP). The models are constructed utilising pertinent experimental data from past studies. A new equation is devised to compute water surface profile in such channels using non-dimensional geometric and flow parameters such as converging angle, width ratio, relative distance, relative depth, aspect ratio and bed slope. The findings demonstrate that the GEP-derived water surface profile is in good correlation with the experimental data and data from other studies ($R^2 = 0.99$ and $RMSE = 0.028$ for the training data and $R^2 = 0.99$ and $RMSE = 0.027$ for the testing data). According to the results of statistically based investigations, the GEP model created for the study of compound channel flow is reliable and can be used in this domain.

Key words: converging compound channel, error analysis, flow parameters, gene expression programming, water surface profile

HIGHLIGHTS

- In this paper, new approach has been proposed to forecast the water surface profile of various compound channels with converging floodplains using gene expression programming (GEP).
- The computed water surface profile using gene expression programming is found to be more accurate when compared to previous methods.

NOTATION

The following symbols are used in this paper:

B total width of compound channel
b total width of the main channel
H bank full depth
h total height of the main channel
L converging length
S longitudinal bed slope
Ψ non-dimensional water surface profile (H/h)
X_r relative distance(x/L)
x distance between two consecutive sections
α width ratio (B/b)
β relative flow depth [(H–h)/H]
δ aspect ratio (b/h)
θ converging angle

Check for updates

Modeling of water surface profile in non-prismatic compound channels

Vijay Kaushik [iD][a,*], Munendra Kumar[a], Bandita Naik[b] and Abbas Parsaie[c]

[a] Department of Civil Engineering, Delhi Technological University, Delhi 110042, India
[b] Department of Civil Engineering, Methodist College of Engineering, Hyderabad 500001, India
[c] Department of Hydraulic Structures, Faculty of Water and Environmental Engineering, Shahid Chamran University of Ahvaz, Ahvaz, Iran
*Corresponding author. E-mail: vijaykaushik_2k20phdce01@dtu.ac.in

[iD] VK, 0000-0002-7270-4520

ABSTRACT

Estimating the water surface elevation of river systems is one of the most complicated tasks in formulating hydraulic models for flood control and floodplain management. Consequently, utilizing simulation models to calibrate and validate the experimental data is crucial. HEC-RAS is used to calibrate and verify the water surface profiles for various converging compound channels in this investigation. Based on experimental data for converging channels ($\theta = 5°$, $9°$, and $12.38°$), two distinct flow regimes were evaluated for validation. The predicted water surface profiles for two relative depths ($\beta = 0.25$ and 0.30) follow the same variational pattern as the experimental findings and are slightly lower than the observed values. The MAPE for the simulated and experimental results is less than 3%, indicating the predicted HEC-RAS value performance and accuracy. Therefore, our findings imply that in the case of non-prismatic rivers, the proposed HEC-RAS models are reliable for predicting water surface profiles with a high generalization capacity and do not exhibit overtraining. However, the results demonstrated that numerous variables impacting the water surface profile should be carefully considered since this would increase the disparities between HEC-RAS and experimental data.

Key words: compound channel, converging floodplains, HEC-RAS modeling, water surface profile

HIGHLIGHTS

- In this article, research was conducted for the non-prismatic compound channel with converging floodplains, utilizing the HEC-RAS software.
- The findings depict the HEC-RAS models are accurate for forecasting the water surface profile of non-prismatic rivers, have a high capacity for generalization, and do not display any signs of overexertion.
- The usefulness of HEC-RAS tool for the design of flood control and diversion structures in the non-prismatic rivers.

Prediction of the flow resistance in non-prismatic compound channels

Vijay Kaushik [a],*, Bandita Naik[b], Munendra Kumar[a] and Vijay K. Minocha[a]

[a] Department of Civil Engineering, Delhi Technological University, Delhi 110042, India
[b] Department of Civil Engineering, Methodist College of Engineering, Hyderabad 500001, India
*Corresponding author. E-mail: vijaykaushik_2k20phdce01@dtu.ac.in

VK, 0000-0002-7270-4520

ABSTRACT

Achieving an accurate estimation of the flow resistance in open channel flows is crucial for resolving several critical engineering difficulties. In instances when there is excessive flow on both banks of a river, it results in the breach of the primary channel, leading to the discharge of water into the adjacent floodplain. The alteration of floodplain geometry occurs as a consequence of agricultural and developmental practises, leading to the emergence of compound channels that exhibit converging, diverging, or skewed characteristics throughout the course of the flow. The efficacy of conventional equations in accurately forecasting flow resistance is limited due to their heavy reliance on empirical approaches. As a result of this phenomenon, there persists a significant need for methodologies that possess both novelty and precision. The objective of this work is to use the support vector machine (SVM) technique for the estimation of the Manning's roughness coefficient in a compound channel with converging floodplains. Statistical indicators are used to validate the constructed models in the experimental investigation, enabling the assessment of their performance and efficacy. The findings indicate a significant correlation between the Manning's roughness coefficient predicted by SVM and both experimental data and prior research outcomes.

Key words: geometric and flow parameters, Manning's roughness coefficient, non-prismatic compound channel, statistical analysis, support vector machine

HIGHLIGHTS

- Flow resistance is crucial across various engineering contexts, such as planning irrigation systems, managing drainage networks, and constructing flood control structures.
- This study delved into assessing flow resistance in non-prismatic compound channels by employing support vector machines.
- The results indicate a strong alignment between the predicted Manning's roughness coefficient and the actual observed values.

Numerical simulation of flow characteristics in nonprismatic compound channels

Vijay Kaushik (iD)[a,*], Munendra Kumar[a] and Bandita Naik[b]

[a] Department of Civil Engineering, Delhi Technological University, Delhi 110042, India
[b] Department of Civil Engineering, Methodist College of Engineering, Hyderabad 500001, India
*Corresponding author. E-mail: vijaykaushik_2k20phdce01@dtu.ac.in

(iD) VK, 0000-0002-7270-4520

ABSTRACT

The assessment of the flow characteristics of river systems is a very intricate undertaking in the development of hydraulic models for the purposes of flood control and floodplain management. Therefore, it is essential to use simulation models in order to calibrate and verify the experimental results. In this study, the Hydrologic Engineering Centre's – River Analysis System (HEC-RAS) is used to calibrate and validate the distribution of velocity and shear stress for different converging compound channels. Two separate flow regimes were assessed for validation based on experimental data obtained from converging compound channels with angles of $\theta = 5°$, 9°, and 12.38°. The projected values for two relative depths ($\beta = 0.15$ and 0.20) exhibit a similar pattern of variation as the empirical observations and are marginally lower than the recorded values. This suggests that the HEC-RAS model accurately estimates the velocity and shear stress values. The disparity between the simulated and experimental outcomes shows a discrepancy of less than 10%. Hence, the implications of our results suggest that while dealing with nonprismatic rivers, it is advisable to take into account lower values. The used methodology and the outcomes focused on problem-solving might potentially inform the development of flood control infrastructure for nonprismatic watercourses.

Key words: converging floodplains, HEC-RAS modeling, nonprismatic compound channel, shear stress distribution, velocity distribution

HIGHLIGHTS

- This article presents a study that aimed to examine the flow characteristics in a nonprismatic compound channel with converging floodplains.
- The HEC-RAS software was used for this investigation.
- The findings demonstrate that the HEC-RAS models are precise in predicting the flow characteristics in nonprismatic channels, as well as replicate the experimental results.
- The implementation of the HEC-RAS tool is beneficial for designing flood mitigation and diversion structures in nonprismatic rivers.

ORIGINAL ARTICLE

Water surface profile prediction in non-prismatic compound channel using support vector machine (SVM)

Vijay Kaushik[1]* and Munendra Kumar[1]

Abstract

The process of estimating the level of water surface in two-stage waterways is a crucial aspect in the design of flood control and diversion structures. Human activities carried out along the course of rivers, such as agricultural and construction operation, have the potential to modify the geometry of floodplains, leading to the formation of compound channels with non-prismatic floodplains, thus possibly exhibiting convergent, divergent, or skewed characteristics. In the current investigation, the Support Vector Machine (SVM) technique is employed to approximate the water surface profile of compound channels featuring narrowing floodplains. Some models are constructed by utilizing significant experimental data obtained from both contemporary and previous investigations. Water surface profiles in these channels can be estimated through the utilization of non-dimensional geometric and flow parameters, including: converging angle, width ratio, relative depth, aspect ratio, relative distance, and bed slope. The results of this study indicate that the SVM-generated water surface profile exhibits a high degree of concordance with both the empirical data and the findings from previous research, as evidenced by its R^2 value of 0.99, RMSE value of 0.0199, and MAPE value of 1.263. The findings of this study based on statistical analysis demonstrate that the SVM model developed is dependable and suitable for applications in this particular domain, exhibiting superior performance in forecasting water surface profiles.

Keywords Non-prismatic compound channel, Non-dimensional parameter, Support vector machine (SVM), Water surface profile

1 Introduction

With growing population across the world, increasingly more people are living in and exploring the areas along rivers, leading to serious problems related to natural flooding, which often results in heavy life losses, in addition to economic damage. Trend analyses have shown that the proportion of both global losses and deaths attributable to flood disasters continue to rise rapidly (Berz, 2000). Given that flooding occurs when the volume of water flowing through a channel is greater than the channel's capacity, predicting the flow rate of natural streams is crucial for flood prevention. As a means to reduce casualties and salvage assets as much as possible, accurate flow parameter prediction in flood circumstances, therefore, has aroused the attention of academics and engineers over recent years, with various techniques and methodologies devised to precisely gauge and anticipate river discharge, velocity distribution, shear stress distribution, and water surface level in the event of overbank floods. Compound channels are a prevalent river feature during the period of overbank flows. The hydrodynamics of a river's discharge can induce alterations to the morphology of floodplains, leading to the development of a two-stage channel system that

*Correspondence:
Vijay Kaushik
vijaykaushik_2k20phdce01@dtu.ac.in
[1] Department of Civil Engineering, Delhi Technological University, Delhi 110042, India

Application of Gene Expression Programming in Computation of Flow Resistance in Compound Channel with Converging Floodplains

Rahul Kumar[*], Vijay Kaushik, Munendra Kumar

Department of Civil Engineering, Delhi Technological University, India

Abstract   It is essential to the resolution of a large number of pressing engineering issues to have an accurate estimate of the flow resistance in an open channel flow. When there is an overbank flow on both sides of the river, it breaks through the main channel and pours out into the floodplain. The flow structure in such compound channels may become rather convoluted because of the transfer of momentum that occurs between the principal channel and the floodplains. This has a significant bearing on the flow resistance in the different subsections of the floodplain and the main channel. In addition, activities such as agriculture and construction have been carried out in the floodplain areas of a river system. Because of this, the geometry of the floodplain changes over the length of the flow, which ultimately results in the formation of a converging, diverging or skewed compound channel. Conventional formulae, which are too reliant on empirical methods, are not successful in predicting flow resistance with a high degree of accuracy. As a direct consequence of this, there is a continued high need for methods that are both original and exact. The purpose of this study is to use Gene Expression Programming to make a prediction about the manning's roughness coefficient in a compound channel with converging floodplains. The prediction will be made in terms of the geometric factors as well as the flow variables. Statistical indices are utilized to verify the created models for the experimental study so that the performance and effectiveness of these models can be evaluated. The results show that the GEP-derived manning's roughness coefficient has a strong connection both with the data from experiments and with the results of previous investigations. The GEP model that was developed for the purpose of analyzing compound channel flow has been shown to be credible by the findings of statistically sound research, and as a consequence, it is applicable to this field of study.

Keywords   Compound Channel, Converging Floodplains, Manning's Roughness Coefficient, Geometric and Flow Parameters, Statistical Analysis, Gene Expression Programming

1. Introduction

The prediction of an accurate discharge in flooded rivers is one of the most significant challenges in river engineering. This challenge arises from the fact that the geometry and hydraulic parameters of a river may change over time. The quantification of the impediment posed by channels and floodplains to the flow of floodwaters is accomplished by means of the roughness coefficient. In 1D flow analysis, it is common practice to select an appropriate roughness coefficient value to evaluate a channel's conveyance capacity. This particular value of the roughness coefficient is assumed to be constant over the whole of the flow surface and at each and every depth. If

A Review of Different Approaches for Boundary Shear Stress Assessment in Prismatic Channels

Vijay Kaushik and Munendra Kumar

Abstract The stress range of shear at the channel's boundaries has a direct bearing on the flow of fluid inside the channel. Hence, understanding it is critical for defining the fluid field and velocity profile. Many engineering issues, such as design of flood control structures, energy loss calculation, and sedimentation, require shear stress computation. The proportion analysis between width and depth has strong influence over the stress distribution at shear in direct channels. Sinuosity, aspect ratio, and meander length affect shear stress distribution in meandering channels. Henceforth, the necessity of scrutinizing the methods used to determine the stress distribution in the channels. This paper analyzes the pros and cons of several methodologies that helps to estimate the allocating the stress ranges of shear via the prismatic channels. The review states that the vertical depth method, the normal depth method, the Guo and Julien method, the Prasad and Manson method, the Knight et al. method, the merged perpendicular method, and the Preston tube technique are the most popular methods that assist to estimate the distribution of boundary shear passing through the channels. This is due to the fact that these methods are straightforward, reliable, and easy to implement. After examining a number of other approaches, it was determined that the Preston tube technique was by far the most effective way in order to determine the stress range for boundary shear in all different kinds of channel sections.

Keywords Open channel flow · Prismatic channels · Boundary shear stress distribution

V. Kaushik (✉) · M. Kumar
Department of Civil Engineering, Delhi Technological University, Delhi 110042, India
e-mail: vijaykaushik_2k20phdce01@dtu.ac.in

M. Kumar
e-mail: munendrakumar@dtu.ac.in

International Conference on Advances in Civil Engineering 2022

ICACE
20-22 DEC 2022

Certificate

This is to certify that the paper entitled

Water Surface Profile Prediction in Nonprismatic Compound Channel Using Support Vector Machine (SVM)

authored by

Vijay Kaushik, Munendra Kumar

is presented in the International Conference on Advances in Civil Engineering 2022 held on 20-22 December 2022, organized by Technology Research and Innovation Centre, India and hosted by LSKBJ College of Engineering, Chandwad, Nashik, India

Dr. Sandip A. Kale
Technical Committee Chair

LSKBJ College of Engineering,
Chandwad, Nashik, India

Chaitanya Bharathi Institute of
Technology (A), Hyderabad, India

Dr. Yuvaraj L. Bhirud
Chairperson
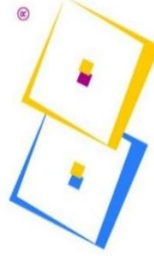
Technology Research and
Innovation Centre, India

Dr. K Jagannadha Rao
Chairperson

Academy of Nanotechnology and
Waste Water Innovations, SA

Dr. Mahadeo D. Kokate
Principal, LSKBJ COE Chandwad, India

Accra Technical
University, Ghana

SGM College of Engineering,
Mahagaon, India

8418

PANDIT DEENDAYAL ENERGY UNIVERSITY · A RESERVOIR OF KNOWLEDGE

INNOVATION IN SMART AND SUSTAINABLE INFRASTRUCTURE (ISSI2022)

CERTIFICATE
OF APPRECIATION

PRESENTED TO

Vijay Kaushik ; Munendra Kumar

for presenting a paper titled

A Review of Different Approaches for Boundary Shear Stress Assessment in Prismatic Channels

at the 1st International Conference on "INNOVATIONS IN SMART AND SUSTAINABLE INFRASTRUCTURE (ISSI-2022)" organized by Civil Engineering Department, School of Technology, Pandit Deendayal Energy University – Gandhinagar during 23rd to 25th August 2022.

Dr. Dhruvesh Patel
Convener

Dr. Tejas Thakker
Chair, HOD Civil

Prof. Surendra Singh Kachhwaha
Director – SOT

HYDRO-2023 INTERNATIONAL

CERTIFICATE

This is to certify that Mr./Ms./Prof./Dr.

Vijay Kaushik

has presented paper on

A Review on Bed Morphology in Compound Channels: Processes, Patterns, and Implications by Vijay Kaushik, Munendra Kumar and Bandita Naik in the 28th Conference on Hydraulics, Water Resources, River and Coastal Engineering (HYDRO 2023 INTERNATIONAL), Organized by the Department of Civil Engineering, National Institute of Technology, Warangal, under the aegis of The Indian Society for Hydraulics (ISH), Pune, during December 21-23, 2023.

Dr. Manish Pandey
Organizing Secretary

Prof. N.V. Umamahesh
Co-Ordinator

DELHI TECHNOLOGICAL UNIVERSITY

(Formerly Delhi College of Engineering)

Shahbad Daulatpur, Main Bawana Road, Delhi-42, India

PLAGIARISM VERIFICATION

Title of the Thesis: **Sediment Transport in Prismatic and Nonprismatic Channels**

Total Pages: **144**

Name of the Scholar: **Vijay Kaushik (2K20/PHDCE/01)**

Supervisor(s): **Prof. Vijay K. Minocha**

Department: **Civil Engineering**

This is to report that the above thesis was scanned for similarity detection. Process and outcome is given below:

Software used: **Turnitin**   Similarity Index: **7%**   Total Word Count: **30090**

Date: 05/03/2025

Candidate's Signature

Signature of Supervisor(s)

Curriculum Vitae

Vijay Kaushik

Email: vijaykaushik_2k20phdce01@dtu.ac.in
        vijaykaushik220795@gmail.com

Educational Qualifications

- Ph.D. in Civil Engineering (Water Resources Engineering) from Delhi Technological University.

- Completed M.Tech in Hydraulics and Water Resources Engineering from Delhi Technological University with 88.9% in the year 2020.

- Completed B.Tech in Civil Engineering from Galgotias University, Uttar Pradesh with 94% in the year 2016.

- Completed 12th Standard in Science Stream from Air Force Sr. Sec. School, Race Course (Central Board of Secondary Education) securing 81% in the year 2012.

- Completed 10th standard from Air Force Sr. Sec. School, Race Course (Central Board of Secondary Education) securing 63% in the year 2010.

Thesis

- **Ph.D. thesis title:** Sediment Transport in Prismatic and Nonprismatic Channels
  Supervisor: Prof. Vijay K. Minocha, Professor, Delhi Technological University

- **M.Tech thesis title**: Study of Sediment Transport on Sharp Crested Triangular Weir
  Supervisor: Prof. Munendra Kumar, Professor, Delhi Technological University

- **B.Tech thesis title**: A Comparative Study of Compressive Strength of Cube with Steel Fibre, Glass Fibre and Nominal Mix Concrete.
  Supervisor: Mohd. Nadeem, Associate Professor, Galgotias University, Uttar Pradesh

Certification & Achievements

- First prize in Science Fair at zonal level and second prize at state level
- Won Volleyball championship in G-Olympia
- Certificate of participation in NCC Camps
- Won NCC Marching Competition at state level
- **Gate qualified**
- **M.Tech Vice Chancellor's Gold Medallist**
- **Research Excellence award**

Publications

- **Kaushik, V.**, & Kumar, M. (2024). Prediction of shear stress distribution in compound channel with smooth converging floodplains. Journal of Hydrology and Hydromechanics, 72(2), 170–184.
- **Kaushik, V.**, & Kumar, M. (2023). Sustainable gene expression programming model for shear stress prediction in nonprismatic compound channels. Sustainable Energy Technologies and Assessments, 57, 103229.
- **Kaushik, V.**, & Kumar, M. (2023). Assessment of water surface profile in nonprismatic compound channels using machine learning techniques. Water Supply, 23(1), 356 – 378.
- **Kaushik, V.**, Kumar, M., Naik, B., & Parsaie, A. (2023). Modeling of water surface profile in non-prismatic compound channels. Water Practice & Technology, 18(9), 2151–2167.
- **Kaushik, V.**, Naik, B., Kumar, M., & Minocha, V. K. (2024). Prediction of the flow resistance in non-prismatic compound channels. Water Practice and Technology, 19 (5), 1822–1835**.**
- **Kaushik, V.**, Kumar, M., & Naik, B. (2024). Numerical simulation of flow characteristics in nonprismatic compound channels. Water Practice & Technology, 19 (7), 2532–2550.
- Naik, B., **Kaushik, V.**, & Kumar, M. (2022). Water surface profile in converging compound channel using gene expression programming. Water Supply, 22(5), 5221–5236.
- **Kaushik, V.**, & Kumar, M. (2023). Water surface profile prediction in non-prismatic compound channel using support vector machine (SVM). AI Civ. Eng. 2, 6.

- **Kaushik, V.**, & Kumar, M. (2024). A Review of Different Approaches for Boundary Shear Stress Assessment in Prismatic Channels. Lecture Notes in Civil Engineering, 117–129.

- Pujari, S., **Kaushik, V.**, & Kumar, S. A. (2024). A review of energy dissipation on different types of spillways. AIP Conf. Proc., 3010, 030015-1–030015-7.

- Pujari, S., **Kaushik, V.**, Awasthi, N., Gupta, S. K., & Kumar, S. A. (2023). Application of machine learning approaches in the computation of energy dissipation over rectangular stepped spillway. H2Open Journal, 6(3), 433–448.

- Kumar, R., **Kaushik, V.**, Kumar, M. (2023). Application of Gene Expression Programming in Computation of Flow Resistance in Compound Channel with Converging Floodplains. Civil Engineering and Architecture, 11(5), 2719-2730.

- Pujari, S., **Kaushik, V.**, Kumar, S. Anbu. (2023). Prediction of Energy Dissipation over Stepped Spillway with Baffles Using Machine Learning Techniques. Civil Engineering and Architecture, 11(5), 2377-2391.

- Pujari, S., **Kaushik, V.**, & Kumar, S. A. (2023). Prediction of energy dissipation over stepped spillway. Journal of the Balkan tribological association, 29(2), 186–198.

- **Kaushik, V.**, Awasthi, N., Gupta, S.K., Singh, D., Kumar, M. (2023). A Review of Sedimentation on Different Types of Weirs. In: Pandey, M., Azamathulla, H., Pu, J.H. (eds) River Dynamics and Flood Hazards. Disaster Resilience and Green Growth. Springer, Singapore.

- **Kaushik, V.**, & Awasthi, N. (2023). Simulation of reservoir outflows using regression tree and support vector machine. AI Civ. Eng. 2, 2.

- Satapathy, A., Naik, B., Awasthi, N., **Kaushik, V.** (2023). Estimation of Surface Runoff Using SWAT Model and ArcGIS Approach. International journal of COMADEM, 26(2), 37-45.

- Mishra, S., Kumar, M., **Kaushik, V.** (2022). Numerical modelling of Flow characteristics over sharp crested triangular and W-shaped weirs for establishing downstream scour behavior. International journal of COMADEM, 25(1), 63-70.

- **Kaushik, V.**, Kumar, M., Naik, B. (2022). Modeling of Water Distribution Network Using WATERGEMS. International journal of COMADEM, 25(4), 53-60.

- **Kaushik, V.**, Singh, D., & Kumar, M. (2021). Effects of Fibers on Compressive Strength of Concrete. Materials Today: Proceedings, 80, 3281–3285.

- **Kaushik, V.**, Kumar, M. (2020). Analysis of the Sediment Laden Flows by Flow Measuring Weirs. International Journal of Advanced Science and Technology, 29(8s), 3040-3048.

International Conferences

- **Kaushik, V.**, Kumar, M. Water Surface Profile Prediction in Nonprismatic Compound Channels Using Support Vector Machine (SVM). International Conference on Advances in Civil Engineering, held on 20-22 December 2022, organized by Technology Research and Innovation Centre, India and hosted by LSKBJ College of Engineering, Chanwad, Nashik, India.

- Gupta, S. K., **Kaushik, V.**, Kumar, M. Estimation of Volume of Total Sediments of Reservoir and Useful Life of Reservoir. International Conference on Advances in Civil Engineering, held on 20-22 December 2022, organized by Technology Research and Innovation Centre, India and hosted by LSKBJ College of Engineering, Chanwad, Nashik, India.

- Pujari, S., **Kaushik, V.**, Kumar, S. Anbu. A Review of Energy Dissipation on Different Types of Spillways. International Conference on Advances in Civil Engineering, held on 20-22 December 2022, organized by Technology Research and Innovation Centre, India and hosted by LSKBJ College of Engineering, Chanwad, Nashik, India.

- Kumar, R., **Kaushik, V.**, Kumar, M. Prediction of Flow Resistance in Compound Channel with Converging Floodplains Using Gene Expression Programming. International Conference on Advances in Civil Engineering, held on 20-22 December 2022, organized by Technology Research and Innovation Centre, India and hosted by LSKBJ College of Engineering, Chanwad, Nashik, India.

- **Kaushik, V.**, Kumar, M. A Review of Different Approaches for Boundary Shear Stress Assessment in Prismatic Channels. 1st International Conference on Innovations in Smart and Sustainable Infrastructure (ISSI-2022), held on 23-25 August 2022, organized by Civil Engineering Department, School of Technology, Pandit Deendayal Energy University, Gandhinagar, India.

- **Kaushik, V.**, Kumar, M. A Review on Bed Morphology in Compound Channels: Processes, Patterns, and Implications. 28th International Conference on Hydraulics, Water Resources, River and Coastal Engineering (HYDRO 2023 International), held

on 21st to 23rd December 2023, organized by Department of Civil Engineering, National Institute of Technology, Warangal, India.

Short Term Courses/FDPs

- Participated in Faculty Development Program on Disaster Preparedness and Risk Reduction organized by Geo-Meteorological Risk Management Division Through India Universities and Institutions Network for Disaster Risk Reduction of National Institute of Disaster Management, Ministry of Home Affairs, Govt. of India in collaboration with Department of Civil Engineering, Delhi Technological University, from 11th to 15th December 2023.

- Participated in Faculty Development Program on Applications of Artificial Intelligence and Machine Learning in Civil Engineering organized by Department of Civil Engineering, R. V. R. & J. C College of Engineering, Chowdavaram, Guntur, Andra Pradesh in association with Indian Geotechnical Society, Guntur chapter from 27th October 2022 to 25th November 2022.

- Participated in webinar on Applications of Artificial Intelligence in Civil Engineering organized by Department of Civil Engineering, R. V. R. & J. C College of Engineering, Chowdavaram, Guntur, Andra Pradesh in association with Indian Geotechnical Society, Guntur chapter on 27th October 2022.

- Participated in webinar on Vision Based Damage Monitoring of Structures Using Deep Learning organized by Department of Civil Engineering, R. V. R. & J. C College of Engineering, Chowdavaram, Guntur, Andra Pradesh in association with Indian Geotechnical Society, Guntur chapter on 28th October 2022.

- Participated in webinar on Neural Network and Fuzzy Applications in Traffic Flow Modeling organized by Department of Civil Engineering, R. V. R. & J. C College of Engineering, Chowdavaram, Guntur, Andra Pradesh in association with Indian Geotechnical Society, Guntur chapter on 3rd November 2022.

- Participated in webinar on Evolutionary Algorithms for Optimal Reservoir Operation organized by Department of Civil Engineering, R. V. R. & J. C College of Engineering, Chowdavaram, Guntur, Andra Pradesh in association with Indian Geotechnical Society, Guntur chapter on 10th November 2022.

- Participated in webinar on AI and ML: Future of Construction organized by Department of Civil Engineering, R. V. R. & J. C College of Engineering, Chowdavaram, Guntur, Andra Pradesh in association with Indian Geotechnical Society, Guntur chapter on 17th November 2022.

- Participated in webinar on Applications of Hybrid AI in Civil Engineering organized by Department of Civil Engineering, R. V. R. & J. C College of Engineering, Chowdavaram, Guntur, Andra Pradesh in association with Indian Geotechnical Society, Guntur chapter on 24th November 2022.

- Participated in webinar on AI and ML in Geospatial Technology with Few Water Resources Engineering Applications organized by Department of Civil Engineering, R. V. R. & J. C College of Engineering, Chowdavaram, Guntur, Andra Pradesh in association with Indian Geotechnical Society, Guntur chapter on 25th November 2022.

- Participated in training programme on River Sediment and Hydrological Extreme Causes, Impacts and Management from 07th March 2022 to 11th March 2022 organized by National Institute of Disaster Management, Ministry of Home Affairs, Govt. of India in collaboration with NIT Warangal.

- Participated in Faculty Development Program on Artificial Intelligence and Deep Learning Applications conducted by the Department of Computer Science and Engineering, National Institute of Technology, Warangal, from 25th to 29th October 2021.

Software Knowledge

- HEC-RAS
- Ansys Fluent
- MATLAB
- GeneXpro Tools
- Origin pro

References

1. Prof. Vijay K. Minocha
    Professor
    Department of Civil Engineering
    Delhi Technological University
    Email: vminocha@rediffmail.com

2. Prof. Munendra Kumar
    Professor
    Department of Civil Engineering
    Delhi Technological University
    Email: munendrakumar@dtu.ac.in

3. Prof. S. Anbu Kumar
    Professor
    Department of Civil Engineering
    Delhi Technological University
    Email: sanbukumar@dce.ac.in

4. Dr. Bandita Naik
    Professor
    Department of Civil Engineering
    Methodist College of Engineering & Technology
    Osmania University
    Email: banditanaik1982@gmail.com

5. Dr. Ritu Raj
    Assistant Professor
    Department of Civil Engineering
    Delhi Technological University
    Email: rituraj.ahirwar@gmail.com